

**SYNTHESIS AND CHARACTERISATION OF  
A NOVEL HYDROXYLATED POLYESTER  
RESIN SYSTEM FOR COIL COATINGS**

**By**

**Ali NIKNAFS**

**Submitted in accordance with the  
requirements for the degree of  
Doctor of Philosophy**

**The University of Leeds  
Department of Colour Science,  
School of Chemistry  
August 2011**

**The candidate confirms that the work submitted is his own and that  
appropriate credit has been given where reference has been made to  
the work of others.**

**To my beloved ones:**

**My wife, Monireh  
my parents  
and my brother, Amir**

## **ACKNOWLEDGEMENTS**

I hereby would like express my gratitude to all who advised, encouraged, and supported me during this study as following:

- **Professor Long Lin**, for his considerate visit to Goharfam Industrial and Manufacturing Company's plant complex on 22.12.2005 and under whose supervision, invaluable advice and full support this study was carried out.
- **Goharfam Industrial and Manufacturing Company**, for providing the facilities for the synthesis and evaluation of the coil coating saturated polyester resin systems and the resulting coil coating films.
- **Iran Polymer and Petrochemical Institute**, for providing the equipment for the analysis of  $^{13}\text{C}$  NMR,  $^1\text{H}$  NMR and SEC.
- **Iran Colour Research Center**, for providing the equipment for the analysis of FTIR and DSC.
- **Dr. Chris Gabbutt**, for his kind advice on the interpretation of  $^{13}\text{C}$  NMR and  $^1\text{H}$  NMR spectra.
- **My parents**, for their support and patience.
- **My wife**, for her love, support, care and priceless patience throughout this effort.

## ABSTRACT

The continuous coating of steel and galvanised steel coils is referred to as coil coating. Coil coating is considered the most efficient coating method with regard to the amount of coated area per unit of time. Coil coatings include primer coating, top coating and backside coating. In general, the primer coating and top coating need to balance effectively among flexibility, adhesion, and film hardness. As such, saturated polyester resins with the capability of being molecularly engineered have found applications in coil coatings as the key binder. Nowadays, a combination of up to five polyester resins with different molecular structures are employed in coil primer coatings and coil top coat coatings to derive hard yet flexible coatings. The aim of this study was to synthesise and characterise a novel and standalone polyester resin system that would provide multiple properties simultaneously, thus, eliminating the need to use mixtures of polyesters in coil coatings. The multiple properties concerned included high flexibility, excellent adhesion and sufficient chemical resistance. For development of the polyester resin system concerned, a variety of polyols and dicarboxylic acids were polymerised to form polymeric polyester binders. Direct esterification polymerisation technique was employed for synthesis of the polyesters. The results obtained at an early stage indicated that in order to develop such a single resin system, achievement of an optimum balance among flexibility, adhesion and glass transition temperature was essential. Differential scanning calorimetry (DSC) showed that the augmentation or reduction of the glass transition temperature of the saturated polyester led to the augmentation or reduction of the film hardness of the resulting coil coating. Thus, a unique blend of neopentyl glycol, 1,4 cyclohexanedimethanol, 1,6 hexanediol, adipic acid, isophthalic acid, and terephthalic acid was polymerised. The resulting product performed efficiently as a standalone binder system in a coil primer coating and a coil top coating, providing all of the required properties. Molecular structures of the saturated polyesters synthesised were confirmed by carbon-13 and proton ( $^1\text{H}$ ) nuclear magnetic resonance (NMR) and Fourier transformed infrared (FTIR). Alterations made to molecular structure of the polyesters through partial replacement of their diols with new ones were visible in expected frequency ranges of the resulting  $^{13}\text{C}$ NMR and  $^1\text{H}$ NMR spectra. According to size exclusion chromatography (SEC), molecular weight characteristics of the pilot scale and the industrial scale reproductions of the novel, single component coil coating polyester resin system developed were comparable with the initial product synthesised at the lab scale.

## TABLE OF CONTENTS

<b>ACKNOWLEDGEMENTS.....</b>	<b>II</b>
<b>ABSTRACT.....</b>	<b>III</b>
<b>TABLE OF CONTENTS.....</b>	<b>IV</b>
<b>LIST OF SCHEMES.....</b>	<b>X</b>
<b>LIST OF FIGURES.....</b>	<b>XII</b>
<b>LIST OF TABLES.....</b>	<b>XVII</b>
<b>LIST OF ABBREVIATIONS AND DEFINITIONS.....</b>	<b>XXII</b>
<b>CHAPTER 1 – INTRODUCTION.....</b>	<b>1</b>
<b>1.1 Saturated polyester resin manufacturing technology, properties and applications in surface coatings.....</b>	<b>1</b>
<b>1.2 Application of saturated polyester resins in coil coatings.....</b>	<b>3</b>
<b>1.3 Synthesis of saturated polyester resins via direct esterification.....</b>	<b>8</b>
<b>1.3.1 Externally catalysed direct esterification.....</b>	<b>10</b>
<b>1.3.2 Equipment for synthesis of polyester via direct esterification and issues involved in such syntheses.....</b>	<b>11</b>
<b>1.4 Recent advances in polyester synthesis.....</b>	<b>15</b>
<b>1.5 Molecular structure of linear and branched polyesters.....</b>	<b>17</b>
<b>1.5.1 Molecular chain growth of linear polyesters during synthesis.....</b>	<b>17</b>
<b>1.5.2 Molecular chain growth of branched polyesters during synthesis.....</b>	<b>19</b>
<b>1.6 Monomers for synthesis of saturated polyester resins via direct esterification.....</b>	<b>20</b>
<b>1.6.1 Polyols.....</b>	<b>21</b>

1.6.2 Polyacids.....	26
1.7 Curing agents of stoving polyester coil coatings.....	31
1.7.1 Amine curing agents.....	31
1.7.2 Curing agents investigated recently .....	35
1.8 Techniques for characterisation of saturated polyester resins.....	37
1.8.1 Differential scanning calorimetry (DSC) .....	37
1.8.2 Size exclusion chromatography (SEC).....	40
1.8.3 Infrared (IR) spectroscopy.....	44
1.8.4 Nuclear magnetic resonance (NMR) spectroscopy.....	47
1.9 Project objective.....	54
CHAPTER 2 – EXPERIMENTAL.....	57
2.1 Chemicals and lab equipment.....	57
2.1.1 Chemicals used for the synthesis of saturated polyester resins for coil coating.....	57
2.1.2 Lab equipment used for the synthesis of saturated polyester resins for coil coating.....	59
2.1.3 Chemicals used for the determination of solid content, acid value and hydroxyl value of the synthesised polyester resins.....	61
2.1.4 Apparatus used for the determination of solid content, acid value, hydroxyl value and density of the synthesised polyester resins.....	62
2.2 Theoretical evaluation of the designed polyester formulations prior to polymerisation.....	64
2.3 Procedure of polyester synthesis and its establishment in the lab, pilot plant, and large scale production facilities.....	69
2.3.1 General method of synthesis.....	69
2.3.2 Lab scale polyester synthesis.....	71
2.3.3 Pilot scale polyester synthesis.....	74

2.3.4	Industrial scale polyester synthesis.....	79
2.3.5	Examples of lab, pilot, and industrial scale polymerisation details for a single saturated polyester.....	89
2.3.5.1	Procedure of polymerisation.....	89
2.3.5.2	Theoretical evaluation of the lab scale formulation and the relevant polymerisation details.....	91
2.3.5.3	Theoretical evaluation of the pilot scale reproduction formulation and the relevant polymerisation details.....	94
2.3.5.4	Theoretical evaluation of the industrial scale reproduction formulation and the relevant polymerisation details.....	96
2.3.5.5	Diluent solvent composition.....	98
2.3.5.6	Characteristics of the same polyester after synthesis in the lab, pilot and industrial scales in terms of the acid value, viscosity and hydroxyl value.....	99
2.4	Equipment used for DSC, NMR, IR and SEC analysis of the saturated polyester resins synthesised and the relevant test parameters.....	100
2.4.1	DSC instrument.....	101
2.4.2	NMR instrument.....	101
2.4.3	FTIR instrument.....	102
2.4.4	SEC instrument.....	102
2.5	Tests of coil coating films and procedures for preparation of coil coatings from the saturated polyester resins synthesised.....	103
2.5.1	Crucial mechanical tests and chemical resistance tests for coil top coatings.....	103
2.5.1.1	Resistance to cracking on bending or the T-bend test.....	104
2.5.1.2	Resistance of the coil top coating to MEK solvent.....	108
2.5.1.3	Resistance to cracking after rapid deformation by impact.....	109
2.5.1.4	Resistance to salt spray.....	110
2.5.1.5	Konig pendulum film hardness.....	111
2.5.2	Basis of selection with respect to the properties desired to be achieved by the standalone and universal resin to be developed....	113

<b>2.5.3 Preparation procedures for the coil coatings and coil coated substrates.....</b>	<b>116</b>
<b>2.5.3.1 Equipment used for preparation, application, and curing of the coil coatings .....</b>	<b>116</b>
<b>2.5.3.2 Method of preparation for coil top coatings derived from the saturated polyester resins synthesised.....</b>	<b>117</b>
<b>2.5.3.3 Method of preparation for the coil primer coating to be derived from the standalone universal saturated polyester resin to be developed.....</b>	<b>118</b>
<b>2.5.3.4 Substrates used, pre-treatment of the substrates and method of application and curing schedule for coil primer coatings .....</b>	<b>118</b>
<b>2.5.3.5 Method of application and curing schedule for the coil top coatings derived from the saturated polyester resins synthesised.....</b>	<b>119</b>
<b>2.5.3.6 Method of application and curing schedule for the coil primer coating and the coil top coating to be derived from the standalone saturated polyester resin to be developed.....</b>	<b>119</b>

**CHAPTER 3 – RESULTS AND DISCUSSION.....120**

<b>3.1 Saturated polyester resins synthesised during the early stages of the study and their defect.....</b>	<b>120</b>
<b>3.1.1 Composition of the saturated polyesters synthesised during the early stages of the study and properties of the resulting coil top coatings.....</b>	<b>120</b>
<b>3.1.2 Cracking resistance of the coil top coating after the T-bend test.....</b>	<b>122</b>
<b>3.1.3 Resistance of the coil top coating to MEK solvent.....</b>	<b>127</b>
<b>3.1.4 Resistance of the coil top coating to cracking after deformation by 15 Joules impact.....</b>	<b>129</b>
<b>3.1.5 Suitability of the early polyesters as flexibilisers for coil coatings..</b>	<b>129</b>
<b>3.1.5.1 Pendulum film hardness of the coil top coating derived from the control polyesters and the coil top coatings derived from samples M and N.....</b>	<b>130</b>
<b>3.1.5.2 Similarity of the mechanical and pendulum film hardness properties of the control flexibiliser polyester resin with samples M and N.....</b>	<b>130</b>
<b>3.1.5.3 Employment of samples M and N as flexibiliser polyester resins in the control coil top coating.....</b>	<b>131</b>



<b>3.2 Development of a novel and standalone saturated polyester resin system for coil primer coating and coil top coating and the relevant characterisation.....</b>	<b>133</b>
<b>3.2.1 Incorporation of high level of flexibility, adequate adhesion, and suitable glass transition temperature into a saturated polyester resin.....</b>	<b>133</b>
<b>3.2.1.1 Glass transition temperature of the saturated polyester resins synthesised during the early stages of the study.....</b>	<b>134</b>
<b>3.2.1.2 Effect of the aliphatic diol on the glass transition temperature, pendulum film hardness and flexibility of the saturated polyester resins synthesised.....</b>	<b>136</b>
<b>3.2.1.3 Stages of development for a saturated polyester resin with suitable glass transition temperature, excellent flexibility and adequate adhesion.....</b>	<b>142</b>
<b>3.2.2 Moieties present in the molecular structure of the copolyesters synthesised.....</b>	<b>155</b>
<b>3.2.2.1 <sup>13</sup>C NMR spectra.....</b>	<b>155</b>
<b>3.2.2.2 <sup>1</sup>H NMR spectra.....</b>	<b>190</b>
<b>3.2.2.3 FTIR spectra.....</b>	<b>215</b>
<b>3.2.3 Composition of the saturated polyester resins synthesised and the overall properties of the resulting coil coatings.....</b>	<b>219</b>
<b>3.2.3.1 Resistance of the coil top coating to MEK solvent.....</b>	<b>221</b>
<b>3.2.3.2 Resistance of the coil top coating to cracking after deformation by 15 Joules impact.....</b>	<b>223</b>
<b>3.2.3.3 Resistance to salt spray.....</b>	<b>225</b>
<b>3.2.4 Characteristics of the pilot scale and the industrial scale reproductions of the novel and standalone coil coating polyester resin developed.....</b>	<b>226</b>
<b>3.2.4.1 Size exclusion chromatography of the pilot scale and the industrial scale reproductions of sample T.....</b>	<b>226</b>
<b>3.2.4.2 Properties of the coil coatings derived from the pilot scale and the industrial scale reproductions of sample T.....</b>	<b>228</b>
<b>CHAPTER 4 – CONCLUSIONS.....</b>	<b>230</b>

<b>CHAPTER 5 – FUTURE WORK.....</b>	<b>236</b>
<b>REFERENCES.....</b>	<b>241</b>

## LIST OF SCHEMES

<b>Scheme 1.1</b> Schematic illustration of the structure of a polyester backbone formed by the reaction between a diol and a diacid.....	1
<b>Scheme 1.2</b> Reaction scheme of a diol and a diacid leading to formation of ester.....	8
<b>Scheme 1.3</b> Polyester formation through reaction of a (x+1) moles of diol and (x) moles of diacid.....	9
<b>Scheme 1.4</b> Typical structural composition of a polyester resin .....	10
<b>Scheme 1.5</b> Mechanism of direct proton-catalysed esterification.....	11
<b>Scheme 1.6</b> Chemical structure of $\epsilon$ -caprolactone.....	16
<b>Scheme 1.7</b> Ring opening polymerisation of lactones in presence of nucleophiles and through catalysis by organometallics.....	16
<b>Scheme 1.8</b> Idealised polymerisation of bifunctional polyols and polyacids leading to linear polyesters.....	18
<b>Scheme 1.9</b> Idealised polymerisation of tri-functional polyols and diacids leading to a branched polyester.....	19
<b>Scheme 1.10</b> Chemical structure of neopentyl glycol .....	21
<b>Scheme 1.11</b> Chemical structure of trimethylol propane .....	22
<b>Scheme 1.12</b> Chemical structure of 1,6 hexanediol .....	23
<b>Scheme 1.13</b> Chemical structure of 1,4 cyclohexanedimethanol .....	24
<b>Scheme 1.14</b> Chemical structures of ethylene glycol, diethylene glycol and propylene glycol .....	25
<b>Scheme 1.15</b> Chemical structure of isophthalic acid .....	26
<b>Scheme 1.16</b> Chemical structure of terephthalic acid .....	27
<b>Scheme 1.17</b> Chemical structure of 1,4 cyclohexanedicarboxylic acid.....	28
<b>Scheme 1.18</b> Chemical structures of adipic acid and azelaic acid.....	29
<b>Scheme 1.19</b> Dimer acid formation from conjugated linoleic acid .....	30
<b>Scheme 1.20</b> Chemical structures of the amines primarily used in the preparation of amine curing agents.....	31

<b>Scheme 1.21</b> Methylation reaction stage of aminoplast preparation.....	32
<b>Scheme 1.22</b> Alkylation reaction stage of aminoplast preparation.....	32
<b>Scheme 1.23</b> Idealised reaction of a hydroxyl functional polyester backbone with an amino curing agent.....	33
<b>Scheme 1.24</b> Bonds potentially formed during the reaction of a hydroxyl functional polyester backbone and an aminoplast .....	33
<b>Scheme 1.25</b> Monomeric structure of hexamethoxy methyl melamine.....	35
<b>Scheme 1.26</b> Reactive moieties of fatty acid methyl esters.....	36
<b>Scheme 1.27</b> Chemical structure of succinic acid.....	50
<b>Scheme 1.28</b> Chemical structure of <i>p</i> -hydroxy benzoic acid.....	54
<b>Scheme 1.29</b> Proposed reaction scheme for grafting of <i>p</i> -hydroxy benzoic acid to a linear and hydroxyl functional polyester via direct esterification.....	55
<b>Scheme 2.1</b> General molecular structure of aliphatic hydrocarbon organic solvents.....	99
<b>Scheme 2.2</b> General molecular structure of ester organic solvents.....	99
<b>Scheme 3.1</b> Central methylene carbon in the moiety of 1,3 propanediol .....	161
<b>Scheme 3.2</b> Terminal methylene carbons in the moieties of 1,3 propanediol and ethylene glycol .....	167
<b>Scheme 3.3</b> Terminal methylene carbons in the moieties of 1,4 butanediol.....	167
<b>Scheme 3.4</b> Carbonyl carbons in the succinic moiety.....	189
<b>Scheme 3.5</b> Protons that could have given rise to the peaks in the <sup>1</sup> H NMR spectra in the range of 6.5-7.2 ppm.....	210
<b>Scheme 3.6</b> Protons that could have given rise to the peaks in the <sup>1</sup> H NMR spectra in the range of 8.0-8.5 ppm.....	213
<b>Scheme 5.1</b> Molecular structure of hydroxy pivalic acid neopentyl glycol ester.....	237
<b>Scheme 5.2</b> Molecular structure of hexahydrophthalic anhydride.....	237
<b>Scheme 5.3</b> Reaction of hexahydrophthalic anhydride and a diol.....	238

## LIST OF FIGURES

<b>Figure 1.1</b> Consumption share of 592 kt of coil coatings in 2007 of various regions.....	3
<b>Figure 1.2</b> Application of pre-coated steel coils in 2007 in different European industries....	4
<b>Figure 1.3</b> Process flow diagram of a typical coil coating line.....	5
<b>Figure 1.4</b> Diagram of direct roll coating as used in coil coating application lines.....	6
<b>Figure 1.5</b> Picture of a coil coating application line .....	6
<b>Figure 1.6</b> Diagram of a typical polyester resin manufacturing reactor.....	12
<b>Figure 1.7</b> Typical graph of refractive indices vs. glycol percent in azeotrope for neopentyl glycol and cyclohexanedimethanol .....	14
<b>Figure 1.8</b> Schematic of a heat-flux DSC instrument.....	38
<b>Figure 1.9</b> Typical DSC curve of a polymer.....	38
<b>Figure 1.10</b> Schematic of a basic gel permeation chromatograph.....	42
<b>Figure 1.11</b> An illustration of particle separation in size exclusion chromatography.....	43
<b>Figure 1.12</b> IR stretching and bending vibration types of a -CH <sub>2</sub> group.....	44
<b>Figure 1.13</b> Various types of vibrational bands in the infrared spectra.....	45
<b>Figure 1.14</b> Schematic of a typical infrared spectrometer.....	46
<b>Figure 1.15</b> Infrared spectra of poly(ester amide) derived from 1,4-butanediol, adipic acid and 6-aminohexanoic acid.....	46
<b>Figure 1.16</b> Schematic of a basic NMR spectrometer.....	47
<b>Figure 1.17</b> Proton chemical shifts of various structures in ppm.....	48
<b>Figure 1.18</b> Carbon-13 NMR chemical shifts of various structures in ppm.....	49
<b>Figure 1.19</b> <sup>1</sup> H NMR spectrum of polydiethylene glycol succinate and related assignments.....	50
<b>Figure 1.20</b> <sup>1</sup> H NMR spectrum of polyneopentyl glycol succinate and related assignments.....	51
<b>Figure 1.21</b> <sup>13</sup> C NMR spectrum of polydiethylene glycol succinate and related assignments.....	52

<b>Figure 1.22</b> $^{13}\text{C}$ NMR spectrum of polyneopentyl glycol succinate and related assignments.....	53
<b>Figure 2.1</b> Equipment and glassware assembly used for the synthesis of saturated polyester resins at the lab scale.....	71
<b>Figure 2.2</b> Position of partial condenser's thermometer .....	72
<b>Figure 2.3</b> Pilot plant reactor.....	74
<b>Figure 2.4</b> Pilot plant's oil heating chamber and pump.....	74
<b>Figure 2.5</b> Positions of the inlet and outlet of the hot oil on the pilot plant's reactor.....	75
<b>Figure 2.6</b> Inlets and outlets of the cooling water of the pilot plant's reactor.....	75
<b>Figure 2.7</b> Control panel of the pilot plant's reactor.....	76
<b>Figure 2.8</b> Twelve metric ton reactor of the resin plant.....	79
<b>Figure 2.9</b> Resin plant's hot oil boiler room.....	80
<b>Figure 2.10</b> Resin plant's water reservoir and cooling tower.....	80
<b>Figure 2.11</b> Pumps of the resin plant's water reservoir.....	81
<b>Figure 2.12</b> Baelz MBA 340 pneumatic 3-way hot oil valve.....	81
<b>Figure 2.13</b> Temperature monitoring diagram of the resin plant's reactors.....	82
<b>Figure 2.14</b> Temperature monitoring and process control room of the resin plant.....	82
<b>Figure 2.15</b> Hot oil inlets of the jacket of the twelve metric ton reactor.....	83
<b>Figure 2.16</b> Inlet and outlet valves of the hot oil of the jacket of the twelve metric ton reactor.....	84
<b>Figure 2.17</b> Secondary hot oil pump of the twelve metric ton reactor.....	84
<b>Figure 2.18</b> Main pipelines of the inlet and outlet water of the resin plant.....	86
<b>Figure 2.19</b> Solvent storage tanks of the resin plant.....	87
<b>Figure 2.20</b> Pneumatic pumps of the solvent storage tanks of the resin plant.....	88
<b>Figure 2.21</b> Solvent collector and solvent meter of the resin plant's twelve metric ton reactor.....	88
<b>Figure 2.22</b> 7000 litre reactor used for the industrial scale reproduction of sample T.....	97

<b>Figure 2.23</b>	Schematic illustration of ECCA T-bends-1.....	104
<b>Figure 2.24</b>	Schematic illustration of ECCA T-bends-2.....	105
<b>Figure 2.25</b>	Schematic illustration of apparatus forming bends through folding-1.....	106
<b>Figure 2.26</b>	Schematic illustration of apparatus forming bends through folding-2.....	106
<b>Figure 2.27</b>	Schematic illustration of forming bends with vice and thumbs.....	107
<b>Figure 2.28</b>	T-bend test apparatus and procedure.....	107
<b>Figure 2.29</b>	MEK solvent rubbing test on a coil coated steel substrate.....	108
<b>Figure 2.30</b>	Elcometer 1615 impact tester.....	109
<b>Figure 2.31</b>	Inside of the salt spray cabinet.....	110
<b>Figure 2.32</b>	Schematic illustration of the cut profile and dimensions of primer and top coated specimen to be exposed to salt spray.....	111
<b>Figure 2.33</b>	Schematic illustration of Elcometer 3034 pendulum hardness tester.....	112
<b>Figure 2.34</b>	Schematic illustration of the position of the pendulum's agate balls on the coating film.....	112
<b>Figure 3.1</b>	DSC thermograms of sample M and sample N.....	135
<b>Figure 3.2</b>	DSC thermograms of samples O and P.....	137
<b>Figure 3.3</b>	DSC thermogram of sample Q.....	138
<b>Figure 3.4</b>	DSC thermogram of sample R.....	145
<b>Figure 3.5</b>	DSC thermogram of sample S.....	147
<b>Figure 3.6</b>	DSC thermogram of sample T.....	149
<b>Figure 3.7</b>	<sup>13</sup> C NMR spectra in the range of 21-22 ppm.....	157
<b>Figure 3.8</b>	<sup>13</sup> C NMR spectra in the range of 24-29 ppm.....	159
<b>Figure 3.9</b>	<sup>13</sup> C NMR spectra in the range of 33-37 ppm.....	162
<b>Figure 3.10</b>	<sup>13</sup> C NMR spectra of samples O, P and Q in the range of 62-66 ppm.....	165
<b>Figure 3.11</b>	<sup>13</sup> C NMR spectra of samples R, S and T in the range of 62-66 ppm.....	166
<b>Figure 3.12</b>	<sup>13</sup> C NMR spectra of samples O, P and Q in the range of 67-71 ppm.....	169

<b>Figure 3.13</b>	$^{13}\text{C}$ NMR spectra for samples R, S and T in the range of 67-71 ppm.....	170
<b>Figure 3.14</b>	$^{13}\text{C}$ NMR spectra in the range of 77-78 ppm.....	172
<b>Figure 3.15</b>	$^{13}\text{C}$ NMR spectra of samples O, P and Q in the range of 124-130 ppm.....	172
<b>Figure 3.16</b>	$^{13}\text{C}$ NMR spectra of samples R, S and T in the range of 124-130 ppm.....	173
<b>Figure 3.17</b>	$^{13}\text{C}$ NMR spectra of samples O and Q in the range of 130-132 ppm.....	175
<b>Figure 3.18</b>	$^{13}\text{C}$ NMR spectra of samples P, R and S in the range of 130-132 ppm.....	177
<b>Figure 3.19</b>	$^{13}\text{C}$ NMR spectrum of sample T in the range of 130-132 ppm.....	178
<b>Figure 3.20</b>	$^{13}\text{C}$ NMR spectra in the range of 164-168 ppm.....	181
<b>Figure 3.21</b>	$^{13}\text{C}$ NMR spectra in the range of 171-175 ppm.....	187
<b>Figure 3.22</b>	$^1\text{H}$ NMR spectra in the range of 0.0-1.3 ppm.....	191
<b>Figure 3.23</b>	$^1\text{H}$ NMR spectra in the range of 1.3-2.0 ppm.....	195
<b>Figure 3.24</b>	$^1\text{H}$ NMR spectra in the range of 2.0-2.5 ppm.....	198
<b>Figure 3.25</b>	$^1\text{H}$ NMR spectrum of polyneopentyl glycol adipate.....	199
<b>Figure 3.26</b>	$^1\text{H}$ NMR spectra in the range of 3.20-3.70 ppm.....	200
<b>Figure 3.27</b>	$^1\text{H}$ NMR spectra of samples O and Q in the range of 3.8-4.5 ppm.....	202
<b>Figure 3.28</b>	$^1\text{H}$ NMR spectra of samples P, R and S in the range of 3.8-4.5 ppm.....	205
<b>Figure 3.29</b>	$^1\text{H}$ NMR spectrum of sample T in the range of 3.8-4.5 ppm.....	207
<b>Figure 3.30</b>	$^1\text{H}$ NMR spectra in the range of 6.5-7.2ppm.....	209
<b>Figure 3.31</b>	$^1\text{H}$ NMR spectra in the range of 8.0-8.5 ppm.....	212
<b>Figure 3.32</b>	FTIR spectra of the synthesised copolyesters .....	216
<b>Figure 3.33</b>	Appearance of the coil top coating film derived from the developed standalone polyester resin system after completion of the salt spray test. ....	225
<b>Figure 3.34</b>	GPC chromatogram of sample T.....	226
<b>Figure 3.35</b>	GPC chromatograms of the pilot scale and the industrial scale reproductions of sample T.....	227



## LIST OF TABLES

<b>Table 1.1</b> General technical data and curing conditions of major coil coatings .....	7
<b>Table 1.2</b> General film properties of coil coatings .....	8
<b>Table 2.1</b> Chemicals used for the synthesis of saturated polyester resins for coil coating.....	58
<b>Table 2.2</b> Monomer, dimer, and trimer content of Pripol 1022 dimer acid.....	59
<b>Table 2.3</b> Lab equipment used for the synthesis of saturated polyester resins for coil coating.....	59
<b>Table 2.4</b> Chemicals used for the determination of solid content according to ISO 3251...61	
<b>Table 2.5</b> Chemicals used for the determination of acid value according to ISO 3682.....61	
<b>Table 2.6</b> Chemicals used for the determination of hydroxyl value according to ISO 4629.....	62
<b>Table 2.7</b> Apparatus used for the determination of solid content according to ISO 3251...62	
<b>Table 2.8</b> Apparatus used for the determination of acid value according to ISO 3682 .....	63
<b>Table 2.9</b> Apparatus used for the determination of hydroxyl value according to ISO 4629.....	63
<b>Table 2.10</b> Apparatus used for the determination of density according to ISO 2811.....	63
<b>Table 2.11</b> Formulation and theoretical evaluation of a saturated polyester resin.....	65
<b>Table 2.12</b> Formulation of the saturated polyester resin synthesised as sample T throughout the course of the study.....	90
<b>Table 2.13</b> Theoretical evaluation of the lab scale formulation of sample T.....	92
<b>Table 2.14A</b> Lab scale polymerisation details of sample T.....	92
<b>Table 2.14B</b> Lab scale polymerisation details of sample T.....	93
<b>Table 2.15</b> Theoretical evaluation of the scaled up formulation of sample T for pilot synthesis.....	94
<b>Table 2.16</b> Pilot scale polymerisation details of Sample T.....	95
<b>Table 2.17</b> Theoretical evaluation of the scaled up formulation of sample T for synthesis in the 7000 litre reactor.....	96

<b>Table 2.18A</b> Industrial scale polymerisation details of sample T.....	97
<b>Table 2.18B</b> Industrial scale polymerisation details of sample T.....	98
<b>Table 2.19</b> Characteristics of sample T after synthesis in the lab, pilot, and industrial scales in terms of acid value, viscosity and hydroxyl value.....	100
<b>Table 2.20</b> Details of the <sup>13</sup> C NMR and <sup>1</sup> H NMR analysis carried out on the saturated polyester resins synthesised.....	102
<b>Table 2.21</b> Specifications of the saturated polyester resins employed in the control coil top coating.....	113
<b>Table 2.22</b> Specifications of Cymel 303.....	114
<b>Table 2.23</b> Specifications of the saturated polyesters employed in the control coil primer coating.....	114
<b>Table 2.24</b> Mechanical and chemical resistance properties of the control coil primer coating and control coil top coating.....	115
<b>Table 2.25</b> Lab equipment used for the preparation, application, and curing of the coil coatings.....	116
<b>Table 3.1</b> Composition and hydroxyl values of the coil coating saturated polyester resins synthesised during the early stages of the study.....	121
<b>Table 3.2</b> Properties of the resulting coil top coating films of the saturated polyester resins synthesised during the early stages of the study.....	121
<b>Table 3.3</b> Chemical structures and molar contents of the polyols and polyacids used in the preparation of samples A and M.....	125
<b>Table 3.4</b> Pendulum film hardness of the control coil top coating and the coil top coatings derived from samples M and N.....	123
<b>Table 3.5</b> Properties of the coil top coating derived from the competitor flexibiliser polyester resin and the coil top coatings derived from samples M and N.....	131
<b>Table 3.6</b> Properties of the coil top coating solely derived from the semi-branched control polyester resin and the coil top coatings derived from the mixture of the same control resin with samples M and N .....	132
<b>Table 3.7</b> Composition of sample M and sample N.....	134
<b>Table 3.8</b> Composition of samples O, P and Q.....	136
<b>Table 3.9</b> Glass transition temperatures of samples O, P and Q and the results of the tests of T-bend and pendulum hardness for the resulting coil top coating films.....	138

<b>Table 3.10</b> Glass transition temperatures of samples M, N, O, P and Q and the pendulum hardness of their resulting coil top coating films.....	139
<b>Table 3.11</b> Glass transition temperatures of samples N and Q and the results of the tests of T-bend and pendulum hardness for the resulting coil top coating films.....	143
<b>Table 3.12</b> Combination of the formulations of samples N and Q into a single formulation according to their mixing ratio in the coil top coating.....	143
<b>Table 3.13</b> Composition of sample R.....	144
<b>Table 3.14</b> Glass transition temperature of sample R and the results of the tests of T-bend and pendulum hardness for the resulting coil top coating film.....	145
<b>Table 3.15</b> Composition of sample S.....	146
<b>Table 3.16</b> Glass transition temperature of sample S and the results of the tests of T-bend and pendulum hardness for the resulting coil top coating film.....	147
<b>Table 3.17</b> Composition of sample T.....	149
<b>Table 3.18</b> Glass transition temperature of sample T and the results of the tests of T-bend and pendulum hardness for the resulting coil top coating film.....	150
<b>Table 3.19</b> Composition of samples R, S, and T.....	150
<b>Table 3.20</b> Glass transition temperatures of samples R, S and T and the results of the tests of T-bend and pendulum hardness for the resulting coil top coating films.....	151
<b>Table 3.21</b> Feed composition and free hydroxyl content of the synthesised copolyester samples that were examined by NMR spectroscopy NMR.....	156
<b>Table 3.22</b> Assignments for the $^{13}\text{C}$ NMR spectra in the range of 21-22 ppm.....	157
<b>Table 3.23</b> Assignments for the $^{13}\text{C}$ NMR spectra in the range of 24-29 ppm.....	160
<b>Table 3.24</b> Assignments for the $^{13}\text{C}$ NMR spectra in the range of 33-37 ppm.....	163
<b>Table 3.25</b> Assignments for the $^{13}\text{C}$ NMR spectra in the range of 62-66 ppm.....	166
<b>Table 3.26</b> Assignments for the $^{13}\text{C}$ NMR spectra of samples O, P and Q in the range of 67-71 ppm.....	169
<b>Table 3.27</b> Assignments for the $^{13}\text{C}$ NMR spectra of samples R, S and T in the range of 67-71 ppm.....	170
<b>Table 3.28</b> Assignments for the $^{13}\text{C}$ NMR spectra of samples O, P and Q in the range of 124-130 ppm.....	173

<b>Table 3.29</b> Assignments for the $^{13}\text{C}$ NMR spectra of samples R, S and T in the range of 124-130 ppm.....	174
<b>Table 3.30</b> Assignments for the $^{13}\text{C}$ NMR spectra of samples O and Q in the range of 130-132 ppm.....	176
<b>Table 3.31</b> Assignments for the $^{13}\text{C}$ NMR spectra of samples P, R and S in the range of 130-132 ppm.....	177
<b>Table 3.32</b> Additional assignments for the $^{13}\text{C}$ NMR spectra of samples P, R and S in the range of 130-132 ppm.....	178
<b>Table 3.33</b> Assignments for the $^{13}\text{C}$ NMR spectrum of sample T in the range of 130-132 ppm.....	179
<b>Table 3.34</b> Additional assignments for the $^{13}\text{C}$ NMR spectrum of sample T in the range of 130-132 ppm.....	180
<b>Table 3.35</b> Assignments for the $^{13}\text{C}$ NMR spectra of samples O and Q in the range of 164-168 ppm.....	182
<b>Table 3.36</b> Assignments for the $^{13}\text{C}$ NMR spectra of samples P, R and S in the range of 164-168 ppm.....	184
<b>Table 3.37</b> Assignments for the $^{13}\text{C}$ NMR spectrum of sample T in the range of in the range of 164-168 ppm.....	185
<b>Table 3.38</b> Additional assignments for the $^{13}\text{C}$ NMR spectrum of sample T in the range of in the range of 164-168 ppm.....	186
<b>Table 3.39</b> Assignments for the $^{13}\text{C}$ NMR spectra of samples O and Q in the range of 171-175 ppm.....	187
<b>Table 3.40</b> Assignments for the $^{13}\text{C}$ NMR spectra of samples P, R, S and T in the range of 171-175 ppm.....	188
<b>Table 3.41</b> Assignments for the $^1\text{H}$ NMR spectra in the range of 0.0-1.3 ppm.....	192
<b>Table 3.42</b> Assignments for the $^1\text{H}$ NMR spectra in the range of 1.3-2.0 ppm.....	196
<b>Table 3.43</b> Assignments for the $^1\text{H}$ NMR spectra in the range of 2.0-2.5 ppm.....	198
<b>Table 3.44</b> Assignments for the $^1\text{H}$ NMR spectrum of polyneopentyl glycol adipate.....	200
<b>Table 3.45</b> Assignments for the $^1\text{H}$ NMR spectra in the range of 3.20-3.70 ppm.....	201
<b>Table 3.46</b> Assignments for the $^1\text{H}$ NMR spectra of samples O and Q in the range of 3.8-4.5 ppm.....	203

<b>Table 3.47</b> Additional assignments for the $^1\text{H}$ NMR spectrum of sample O in the range of 3.8-4.5 ppm.....	204
<b>Table 3.48</b> Additional assignments for the $^1\text{H}$ NMR spectra of samples P, R and S in the range of 3.8-4.5 ppm.....	206
<b>Table 3.49</b> Additional assignments for the $^1\text{H}$ NMR spectrum of sample T in the range of 3.8-4.5 ppm.....	208
<b>Table 3.50</b> Frequencies of the singlet, doublet and triplet peaks in the $^1\text{H}$ NMR spectra of samples O, P and Q in the range of 6.50-7.20 ppm .....	210
<b>Table 3.51</b> Frequencies of the singlet, doublet and triplet peaks in the $^1\text{H}$ NMR spectra of samples R, S and T in the range of 6.50-7.20 ppm .....	211
<b>Table 3.52</b> Assignments for the $^1\text{H}$ NMR spectrum of sample O in the range of 6.5-7.2 ppm.....	211
<b>Table 3.53</b> Assignments for the $^1\text{H}$ NMR spectra of samples P, Q, R, S and T in the range of 6.5-7.2 ppm.....	212
<b>Table 3.54</b> Frequencies of the doublet peaks in the $^1\text{H}$ NMR spectra in the range of 8.0-8.50 ppm .....	214
<b>Table 3.55</b> Assignments for the $^1\text{H}$ NMR spectra in the range of 8.0-8.5 ppm.....	214
<b>Table 3.56</b> Assignments for the FTIR spectra.....	217
<b>Table 3.57</b> Composition, glass transition temperature and free hydroxyl content of the synthesised saturated polyester resins .....	220
<b>Table 3.58</b> Properties of the coil coatings derived from the synthesised saturated polyester resins .....	220
<b>Table 3.59</b> $M_n$ , $M_w$ , and polydispersity indices of sample T and its pilot scale and industrial scale reproductions.....	228
<b>Table 3.60</b> Properties of the coil coatings derived from the pilot scale and the industrial scale reproductions of sample T.....	229
<b>Table 4.1</b> Composition of the novel and standalone coil coating saturated polyester resin system developed .....	230
<b>Table 5.1</b> Proposed formulation for a coil coating polyester resin with enhanced resistance to UV radiation.....	238

## LIST OF ABBREVIATIONS AND DEFINITIONS

<b>NPG</b>	<b>Neopentyl glycol</b>
<b>TMP</b>	<b>Trimethylol propane</b>
<b>1,6HD</b>	<b>1,6 hexanediol</b>
<b>1,4 CHDM</b>	<b>1,4 cyclohexanedimethanol</b>
<b>IPA</b>	<b>Isophthalic acid</b>
<b>TPA</b>	<b>Terephthalic acid</b>
<b>1,4 CHDA</b>	<b>1,4 cyclohexanedicarboxylic acid</b>
<b>ADA</b>	<b>Adipic acid</b>
<b>HPN</b>	<b>Hydroxy pivalic acid neopentyl glycol ester</b>
<b>HHPA</b>	<b>Hexahydrophthalic anhydride</b>
<b>HMMM</b>	<b>Hexamethoxy methyl melamine</b>
<b>DSC</b>	<b>Differential scanning calorimetry</b>
<b>SEC</b>	<b>Size exclusion chromatography</b>
<b>GPC</b>	<b>Gel permeation chromatography</b>
<b>FT</b>	<b>Fourier transformed</b>
<b>IR</b>	<b>Infrared</b>
<b>NMR</b>	<b>Nuclear magnetic resonance</b>
<b>T<sub>g</sub></b>	<b>Glass transition temperature</b>
<b>T<sub>m</sub></b>	<b>Melting temperature</b>
<b>M<sub>n</sub></b>	<b>Number average molecular weight</b>

$M_w$	<b>Weight average molecular weight</b>
$\bar{\nu}$	<b>Wave number</b>
$\lambda$	<b>Wave length</b>
$w_i$	<b>Total raw material weight input</b>
$m_i$	<b>Total number of moles of raw materials</b>
$e_{COOH}$	<b>Total number of equivalent weights of acid</b>
$e_{OH}$	<b>Total number of equivalent weights of hydroxyl</b>
$w_{H_2O}$	<b>Total theoretical liberated water of reaction</b>
$Y_A$	<b>Theoretical yield of a polyester formulation at acid value=A</b>
$H$	<b>Theoretical hydroxyl value of a polyester formulation</b>
$M_A$	<b>Theoretical yield at acid value=A of a polyester formulation</b>
$P$	<b>Degree of reaction</b>
$P_{gel}$	<b>Degree of reaction at gel point</b>
$X_p$	<b>Degree of polymerisation</b>
$F$	<b>Average functionality</b>
$K$	<b>Patton's constant</b>


## CHAPTER 1- INTRODUCTION

### 1.1 Saturated polyester resin manufacturing technology, properties and applications in surface coatings

Polyester resins have been known and applied as polymeric binders in surface coatings for many years. These polymers are obtained by reacting multi-functional acids or anhydrides with multi-functional alcohols to form a polymeric backbone containing reacted polyols and polyacids linked to each other by ester groups.<sup>1-4</sup>

In the case of a diol and a diacid reacted together to form such a backbone, the structure can be schematically shown in Scheme 1.1;



Where  represents an ester linkage  
 ---- represents the reacted diol  
 \_\_\_\_\_ represents the reacted diacid

**Scheme 1.1 Schematic illustration of the structure of a polyester backbone formed by the reaction between a diol and a diacid<sup>5</sup>**

Saturated polyesters can be produced from a wide range of di- or multifunctional alcohols and acids. As such, polyester resins can be molecularly engineered to give a wide range of chemical and physical properties.<sup>1,2</sup> Due to this, saturated polyesters can be designed to provide similar or even better mechanical properties and outdoor durability than acrylic resins.<sup>6</sup> Therefore, saturated polyester resins are widely applied in coatings for outdoor applications.<sup>6</sup>

Saturated polyester resins are widely supplied as solutions in organic solvents which are typically aromatic hydrocarbons, aliphatic hydrocarbons, alcohols, glycols and esters. These conventional resins are still being widely used. They have been and are still being developed with a wide range of reactivity, flexibility, hardness, and durability suitable for a variety of industrial applications. A wide range of relatively cost effective raw materials are



available to formulate tailor-made polyesters for a variety of industrial coating applications. This has attributed to the success of polyesters as a major binder system for industrial coatings.<sup>1,2,4</sup> Some of the properties which can be achieved are summarised as follows;<sup>1,2</sup>

- 1) Thermoset or ambient curable coatings can be manufactured.
- 2) Pale coloured resins can be produced. This enables the production of colorless lacquers or brilliant white shades.
- 3) Highly flexible coatings can be achieved.
- 4) Efficient pigment dispersibility can be achieved. This results in high gloss and colour stability of the derived coating film.
- 5) Coatings with excellent weathering properties can be formulated.

In addition, saturated polyester resins can be formulated for a variety of coating systems and coating application methods. The coating application methods and the coating systems concerned are as follows;<sup>1,2</sup>

- 1) Roller coating; (liquid coatings).
- 2) Conventional spraying; (low viscosity material).
- 3) High pressure airless spraying; (high viscosity materials).
- 4) Fluidised bed and electrostatic fluidised bed; (powder coatings).
- 5) Electrostatic spraying; (liquid coatings).
- 6) Electrostatic spraying; (powder coatings).

The difference between saturated and unsaturated polyester resins comes from the incorporation of unsaturated dicarboxylic acid compounds in unsaturated polyesters. The more important unsaturated compounds used in the preparation of unsaturated polyesters include maleic acid, maleic anhydride and fumaric acid. Inclusion of such compounds in unsaturated polyesters provides them with the ability to copolymerise with unsaturated compounds such as styrene.<sup>4</sup> Thermosetting saturated polyester resins are either formulated with excess hydroxyl or acid groups which can then be crosslinked with suitable curing agents. The curing agents that are mostly used for hydroxyl terminated polyester resins are aminoplasts. Melamine formaldehyde resins are among the more important aminoplasts. Saturated polyester resins in combination with melamine formaldehyde resins are specifically designed for stoving finishes applied on industrial articles. Curing temperatures range from 120°C to 300°C. These polyesters generally find applications in coil coating, automotive, architectural, and major appliance industries.<sup>1,2,4</sup>

## 1.2 Application of saturated polyester resins in coil coatings

The continuous coating of metal coils, normally with liquid coatings, is referred to as coil coating. This technology is well established and is constantly gaining interest and market share.<sup>7,8</sup> Coil coating substrates include steel, galvanised steel and aluminium.<sup>9,10</sup>

The consumption share of coil coatings of various regions in the year 2007 is provided in Figure 1.1.

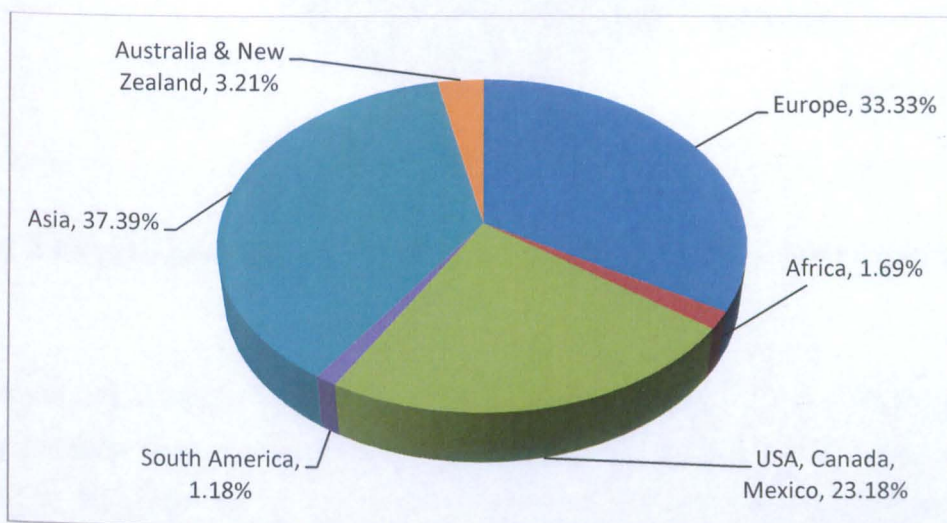
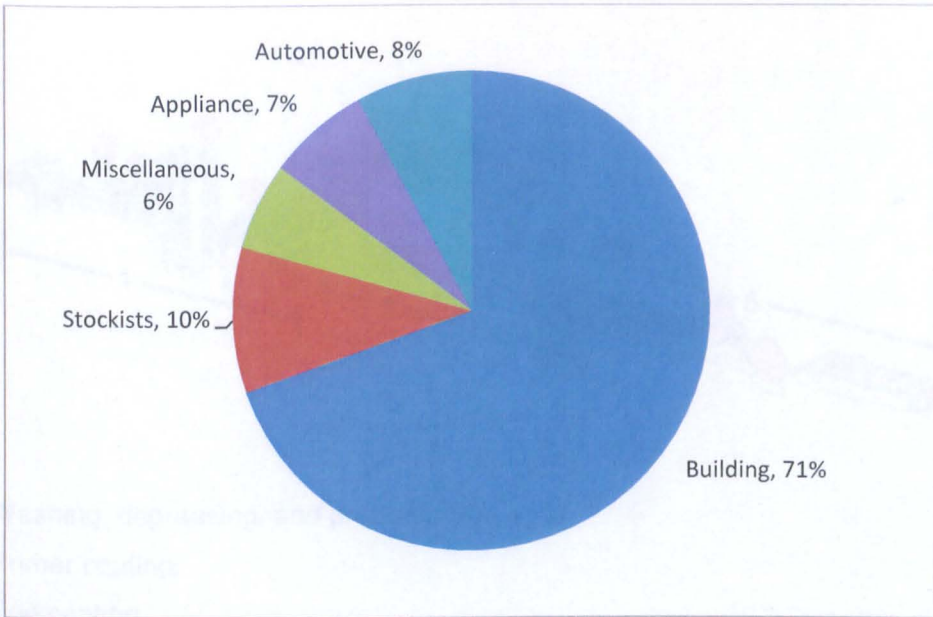


Figure 1.1 Consumption share of 592 kt of coil coatings in 2007 of various regions<sup>11</sup>

It has been claimed that currently almost all industrial sections use coil coatings. The major users of coated coils are as follows;<sup>12-15,19</sup>

- a) Construction industry; indoor and outdoor panels;
- b) Manufacturers of household appliances;
- c) Commercial vehicles; manufacturers of trailers and caravans; and
- d) Manufacturers of industrial lighting systems.

Consumption shares of coated coils in the above mentioned sections are shown in Figure 1.2.



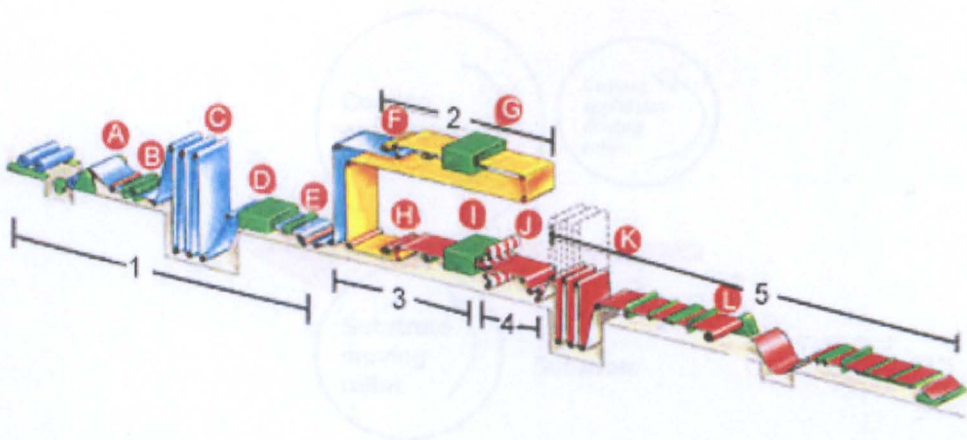
**Figure 1.2 Application of pre-coated steel coils in 2007 in different European industries<sup>11</sup>**

The process of coil coating, in which the coating is applied by rollers, is quite similar to a giant printing press. The process runs at a constant speed with metal coils continuously joined together. However, there is a major difference between a coil coating process and a printing press, and that is the need for pre-treatment, coating, and curing of the metal coils.<sup>14-17</sup>

On typical coil coating lines, metal coils with thicknesses of 0.2mm to 2mm are processed. Rolled coils of soft grade steel, general purpose structural steel, galvanized thin sheet, hot-dip galvanized aluminium and its alloys are amongst the materials used. Maximum coil widths are 1.8 meters for steel coils and 2.0 meters for aluminium coils.

Line speed can be between 60-150 m/min for steel coils.<sup>8,18</sup> For aluminium coils however, the speed goes beyond 200 m/min.<sup>14,16</sup>

Figure 1.3 shows the components of a typical coil coating line;



**Section 1:** Washing, degreasing, and pretreatment

**Section 2:** Primer coating

**Section 3:** Top coating

**Section 4:** Laminating station

**Section 5:** Winding, strip storage, and recoiling for shipment

**Figure 1.3 Process flow diagram of a typical coil coating line** <sup>16</sup>

During the coating process, bare metal is uncoiled (A). The coil is spliced (B) and goes through the accumulator stack (C). Then, the cleaning, degreasing and chemical pretreatment are carried out (D). After the coil is cleaned and pretreated, it goes through a drying oven (E). The pre-treated and dried coil is primer coated on one or both sides in the primer unit (F). The primer is cured in the first oven (G). A top coat is applied on the front and a protective coat is applied on the back of the primer coated coil in the coating unit (H), after which it enters the second curing oven (I). The coated coils are then laminated on one or both sides or embossed (J) and enter the exit accumulator stack (K). Finally the finished metal coils are recoiled and stored for shipment. (L) <sup>14,16,17,19</sup>

Curing of the wet coated coils takes place in high temperature convection ovens with the peak metal temperature (PMT) reaching approximately 230°C. <sup>8,18</sup>

The coil coating process is considered as the most efficient coating method with regard to the amount of coated area per unit of time. The majority of the primers and top coats are nowadays applied by direct roll coating <sup>14</sup> as shown in Figure 1.4.

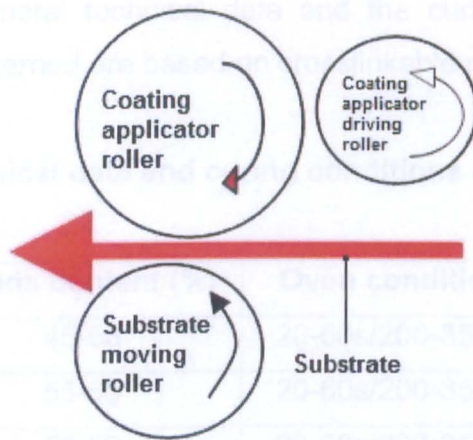


Figure 1.4 Diagram of direct roll coating as used in coil coating application lines <sup>14</sup>

The picture of a typical coil coating application is shown in Figure 1.5

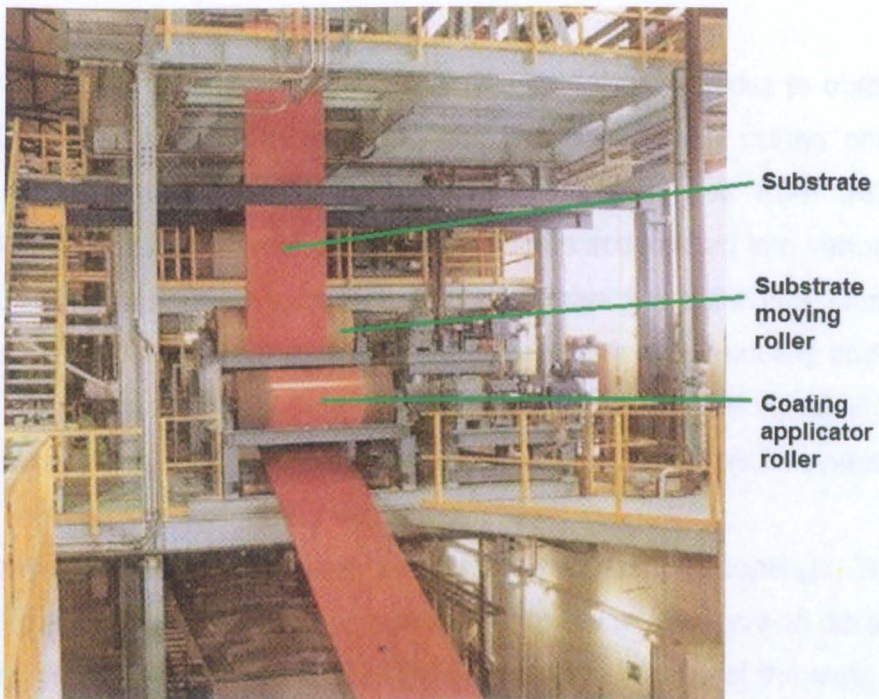


Figure 1.5 Picture of a coil coating application line<sup>14</sup>

The technology of coil coating has led to the reduction of costs, economic advantages, productivity and high quality. In addition, it has reduced the emission of volatile organic compounds (VOC). Therefore, this technique can limit environmental impact in comparison with other coating application technologies.<sup>12,19,20</sup>

Table 1.1 provides the general technical data and the curing conditions of major coil coatings. The coatings concerned are based on crosslinkable materials.

**Table 1.1 General technical data and curing conditions of major coil coatings <sup>14</sup>**

Layer	Solids content (%)	Oven conditions	Film thickness
Primer	45-55	20-60s/200-350°C	5-8 µm
Top coat	55-65	20-60s/200-350°C	20-25 µm
Back coat	50-60	20-60s/200-350°C	8-10 µm

The curing of the coatings based on crosslinkable materials takes place in specially designed induction, forced air, and several zone ovens. These ovens are sometimes extremely long in order to allow a curing time of 20-60 seconds at the coating line speed.

Coil coatings have to meet fundamental technical requirements. In order to obtain a good final product at the rapid curing processes mentioned, an efficient curing chemistry is required.<sup>7,8</sup> The coating must have a good leveling and be free from frothing and sagging.<sup>8,18</sup> In addition, the coated and coiled metal sheets are formed into various shapes by the customers. The forming processes include cutting, bending, punching, stamping and roll forming. These processes put an extremely high demand on the flexibility and adhesion of the coating.<sup>7,8,18,19</sup> Due to this, saturated polyester resins with the capability of being molecularly engineered, find application in coil coatings as the major binder system.

European Coil Coating Association has defined test methods for coil coatings. These tests evaluate the performance of coil coatings in terms of flexibility, adhesion and durability. The tests concerned are universally known as ECCA test methods. Amongst the tests, the most critical are resistance to cracking on bending known as the T-bend test, and methyl ethyl ketone solvent double rub resistance.<sup>14,15</sup> Table 1.2 provides coating film properties that are commonly expected from coil coatings.

**Table 1.2 General film properties of coil coatings**<sup>14</sup>

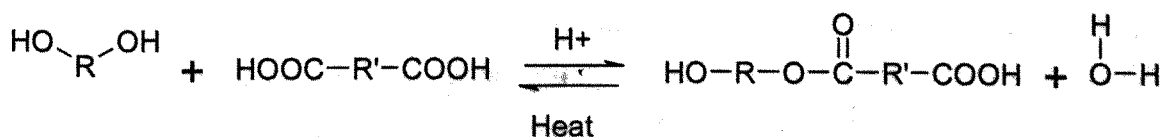
Property	Unit	Total coating
Film thickness	µm	7-40
Flexibility	T-bends	0T-2T
MEK solvent resistance	Double rubs	50-100
Exposure in Florida (5°)	Years	<3

The T-bend test is described in ECCA-T7 test method. It is a variation of the mandrel bending test and involves bending the test panel. A variety of devices can be employed for bending. The bending takes place within 1-2 seconds. The result is the value of the bending radius at which no cracks occur. The smallest bending radius is stated as 0T.<sup>14,15</sup>

ECCA test methods for coil coatings and the relevant paint film requirements are discussed in detail in Section 2.5.

### 1.3 Synthesis of saturated polyester resins via direct esterification

One of the more important preparation routes of saturated polyester resins is the direct esterification synthesis. Direct esterification is a step growth polymerisation technique. In this method, the polyester is prepared by the condensation reaction of polyols with diacids or multifunctional anhydrides.<sup>21-25</sup> A typical esterification reaction scheme for a diol and a diacid is shown in Scheme 1.2.

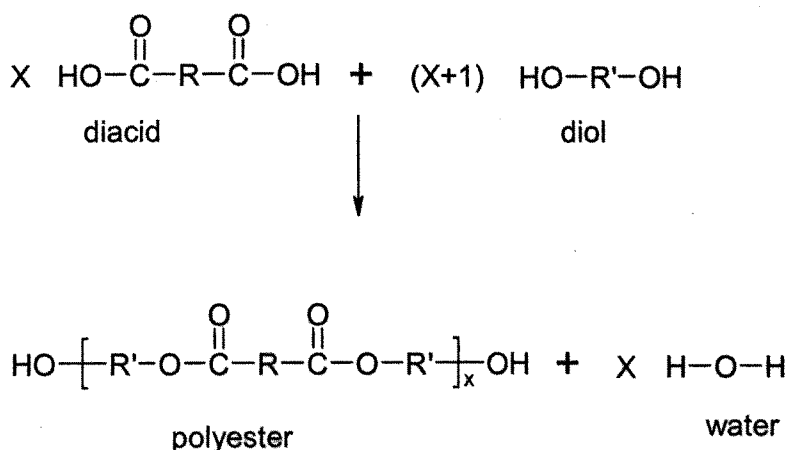


**Scheme 1.2 Reaction scheme of a diol and a diacid leading to formation of ester**<sup>6,21-26</sup>

Several factors affect the rate by which the ester is formed. These are as follows;<sup>21,22,24,25</sup>

- 1) Temperature;
- 2) Concentration and ratio of reactants;
- 3) Incorporation of catalysts; and
- 4) Removal of water created by the reaction. This would prevent the hydrolysis of the ester as well as the reverse reaction.

In terms of polymer production, the reaction of a diol and a diacid can be shown in Scheme 1.3.



**Scheme 1.3 Polyester formation through reaction of (x+1) moles of diol and (x) moles of diacid<sup>21,24,27-29</sup>**

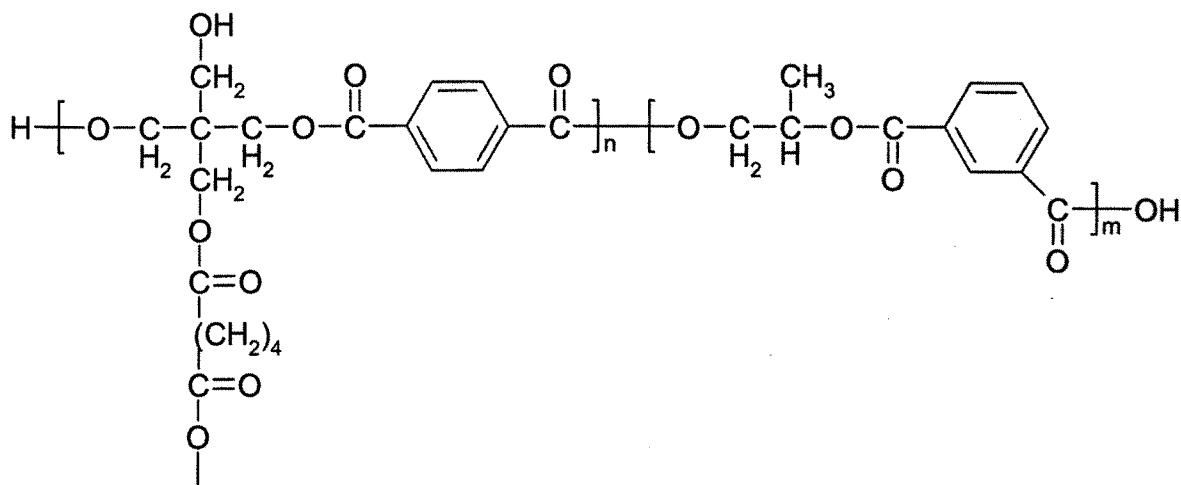
The excess of diol within the reaction systems, leads to hydroxyl functionality and low molecular weights. When equimolar quantities of reactants are used, a high molecular weight polyester resin is generally obtained.

The direct esterification of polyols by polyacids is a general method for preparation of polyesters.<sup>21-25</sup> This method has been widely used in a variety of recent studies which involved polyester synthesis. Malanowski et al<sup>6</sup> synthesised poly (neopentyl glycol isophthalate) through direct esterification of neopentyl glycol and isophthalic acid according to Scheme 1.3. Vahteristo et al<sup>22</sup> prepared a polyester from neopentyl glycol and propionic acid through direct esterification. Umare et al<sup>27</sup> used direct esterification to synthesise a series of aliphatic copolyesters from 1,3 propandiol, adipic acid, and succinic acid. Soni et al<sup>30</sup> employed direct esterification to prepare a copolyester from lactic acid, terephthalic acid, and ethylene glycol. Wang et al<sup>31</sup> prepared copolyesters via direct esterification from



dimethyl terephthalate, 1,4 butandiol, ethylene glycol and 1,4 cyclohexanedicarboxylic acid. Boyes et al<sup>29</sup> used direct esterification to react a hydroxyl functional polyester resin with *p*-hydroxybenzoic acid.

A typical structural composition of a polyester resin is shown in Scheme 1.4.



**Scheme 1.4** Typical structural composition of a polyester resin<sup>32</sup>

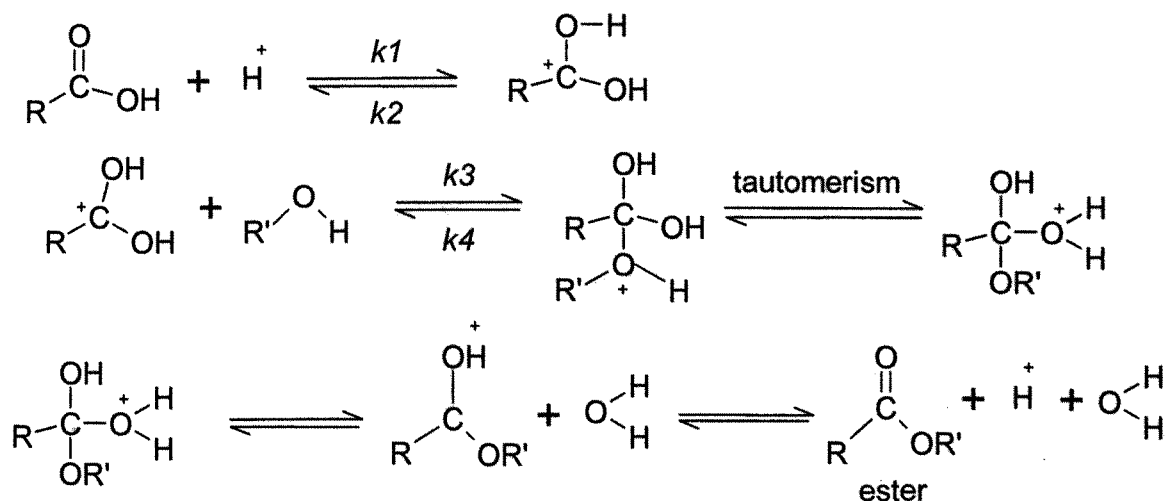
### 1.3.1 Externally catalysed direct esterification

In order to increase the reaction rate during polymerisation, small amounts of external catalysts (0.05-0.5 % weight) are added to the reaction mixture. These catalysts include strong mineral acids, oxides or salts of heavy metals, and organometallic compounds of tin, titanium, zirconium and lead. The most popular of the mineral acids include sulphuric acid and para-toluene sulphonic acid.<sup>22,33</sup>

Although mineral acids can be of a high efficiency for direct esterification, they have been shown to be effective in side reaction catalysis, leading to poor quality polyesters. As replacement for mineral acids, metal based catalysts and ion exchange resins have nowadays gained importance.<sup>22,33</sup>

Amongst metal catalysts, tin compounds have so far been found to be the most effective.<sup>33</sup> Ion exchange resins that are typically employed include sulfonic acid cation exchangers and quaternary ammonium anion exchangers.<sup>22</sup>

The generally accepted mechanism of direct proton-catalysed esterification is illustrated in Scheme 1.5.



**Scheme 1.5 Mechanism of direct proton-catalysed esterification**<sup>33,34</sup>

The above reaction pathway may be extended to include proton-catalysed direct polyesterification.

The kinetics and mechanism of metal derived catalysts are far from being well understood. If an analogy with proton catalysis is considered, it can be assumed that metal compounds introduce a positive charge on the carbonyl group through forming a complex with the substrate. Based on experimental data however, there are plenty of results suggesting more complex behaviour of these catalysts in the reacting system.<sup>33</sup>

### 1.3.2 Equipment for synthesis of polyester via direct esterification and issues involved in such syntheses

The diagram of a typical reactor for synthesis of polyester via direct esterification is shown in Figure 1.6.

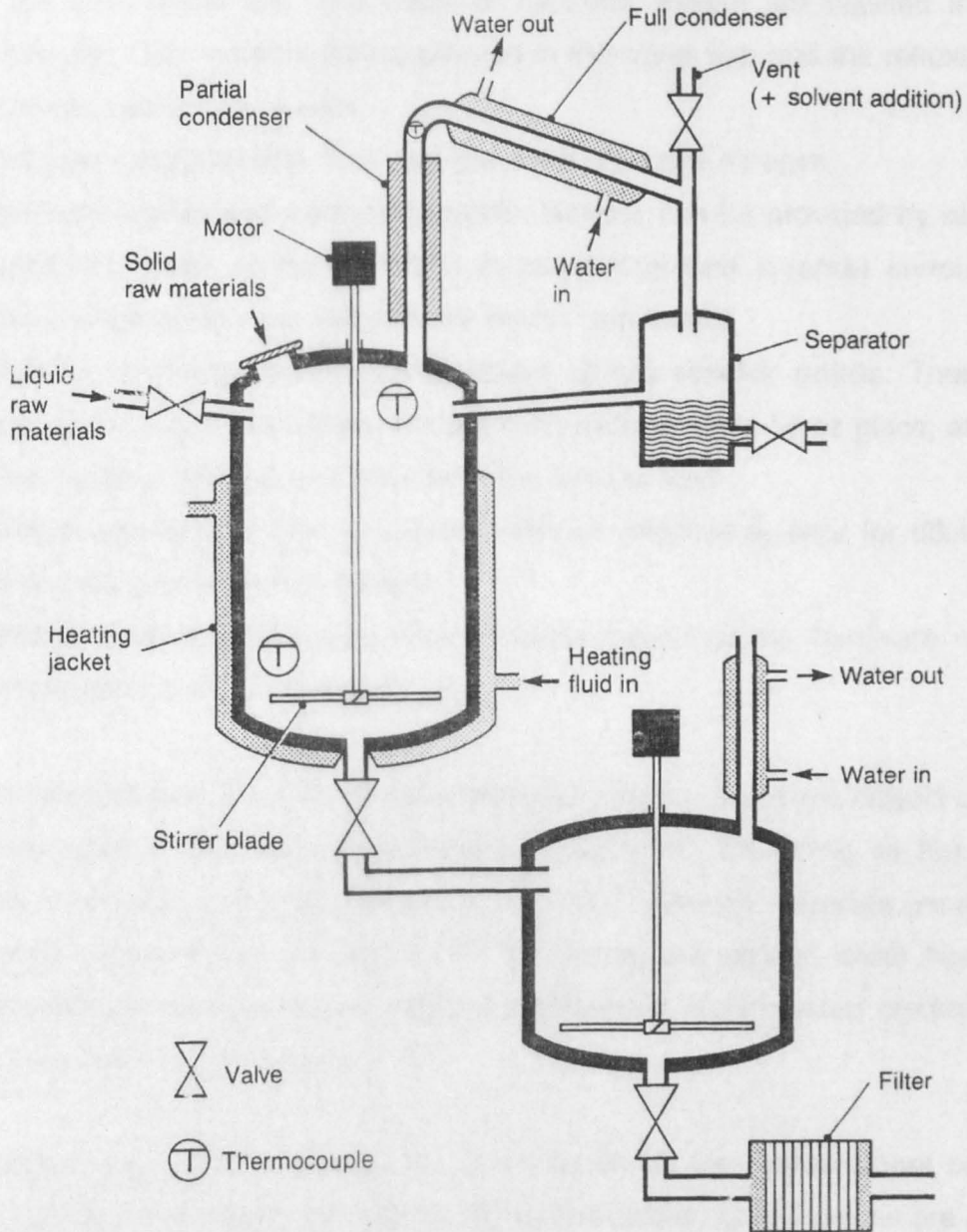


Figure 1.6 Diagram of a typical polyester resin manufacturing reactor <sup>35</sup>

A polyester resin manufacturing plant consists mainly of the following equipment, <sup>35</sup>

- 1) **Reaction equipment:** These include a heated reactor with an efficient stirrer. The reactor is equipped with a vapour release at the top leading to partial and total condensers. The total condenser leads to a water trap separator which enables the collection and measurement of the water produced as a result of the esterification process. The partial condenser directs the water of reaction or the refluxing solvent

to the total condenser. The water or refluxing solvent are liquified in the total condenser. The water is then separated in the water trap and the refluxing solvent is passed back to the reactor.

- 2) **Inert gas supply facility:** The inert gas used is usually nitrogen.
- 3) **Thermal heating and cooling circuits:** Heating can be provided by steam, or a heated fluid such as hot oil which is pumped around a jacket surrounding the reactor. Cooling coils are built into the reactor separately.
- 4) **Facilities for temperature measurement at key reactor points:** These include those inside the reactor where the polymerisation reaction takes place, at the head of the partial condenser and the inlet of the heating fluid.
- 5) **Dilution equipment:** This is a vessel with an effective agitator for dilution of the resins to the desired solids content.
- 6) **Process control equipment:** These include control board, hardware controllers, and computer and software controllers.

In a typical production process of saturated polyester resins, usually the polyols are initially added to the reactor and heated until complete meltdown. Depending on the nature of polyols, this initial heat up can be between 50-130 °C.<sup>35</sup> Then the polyacids are added and the mixture is heated up to 200-250°C.<sup>27,29,36,37</sup> During the second stage heat up, the polycondensation or the esterification reaction commences and the water produced by the reaction is separated from the batch.<sup>27,35,36</sup>

The progress of this so-called resin cook is monitored via the measurement of the *acid value* and *viscosity* of the reaction mixture. When the desired specifications are achieved, the resin is cooled. As the acid value of the mixture decreases, the molecular weight of the resin increases. This leads to the increase of the viscosity.<sup>25,35</sup>

When using diols such as neopentyl glycol in the preparation of saturated polyester resins, significant polyol losses can occur during the polymerisation process. The polyol vapours are carried over with the water vapour and separated from the batch. This leads to disruption of the polymer structure. In order to minimise glycol losses, normally a packed condenser which fractionates and returns glycols to the reactor is used. This packed condenser, which is often referred to as the partial condenser, allows the water vapours or refluxing solvent to pass through. The temperature of the top of the partial condenser

should also never exceed 102°C. These measures would minimise glycol losses. However, glycol loss can never be totally avoided no matter how much careful control is incorporated. Nevertheless, there are methods for determination of the amount of the glycol loss so that appropriate compensation can be made. This is done by measuring how much glycol is in the azeotrope liberated as the result of the esterification reaction. The refractive index of the azeotrope liberated is measured. For each polyol, published standard graphs of refractive index vs. glycol percent in azeotrope exists. Figure 1.7 provides an example of the said graphs.

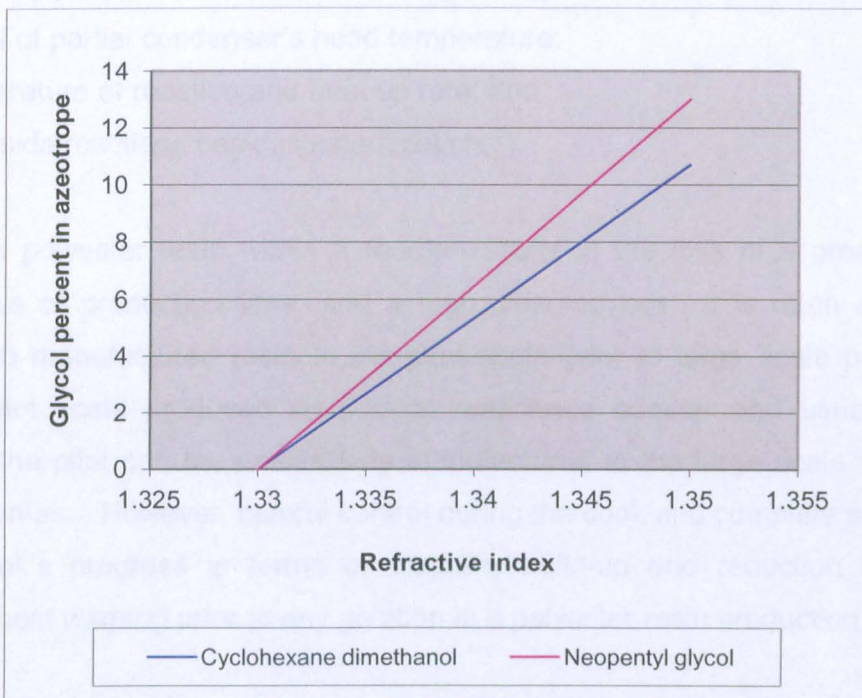


**Figure 1.7 Typical graph of refractive indices vs. glycol percent in azeotrope for neopentyl glycol and cyclohexanedimethanol<sup>25</sup>**

By measuring the refractive index of the azeotrope liberated, knowing its recovered quantity, and comparing it with the appropriate graph, the amount of glycol loss can be calculated and compensated as follows: <sup>25,35</sup>

$$\text{Glycol loss} = (\% \text{ glycol in separated azeotrope}) \times (\text{Total expected azeotrope of reaction})$$

When a mixture of volatile polyols is used however, determination of exact glycol losses becomes extremely difficult.<sup>25</sup>

One of the more severe phenomena which may occur during a polyester cook is gelation. If the equivalents of acid are greater than those of the hydroxyl in the initial formulation of a polyester resin, the resin will gel. Therefore, polyesters are usually formulated with hydroxyl excess. There are also a number of extremely useful approaches that enables the determination of the safe cook of a polyester formulation. However, even by putting in place these measures, unexpected gelation of a safe formulation can often happen as a result of the following;<sup>38</sup>

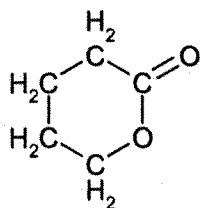
- 1) Loss of glycol or other volatile material through inefficient condensers or inefficient control of partial condenser's head temperature;
- 2) Temperature of reaction and heat up rate; and
- 3) Other side reactions besides esterification.

Gelation of a polyester resin within a reactor results in the loss of a great deal of raw materials, loss of production time, and a high clean-up cost. It is often a necessity to produce a lab manufactured resin at the pilot scale prior to large scale production in a reactor. A pilot scale produced resin is a confidence booster and usually the resins produced at the pilot can be successfully manufactured in the large scale with the same desired properties. However, careful control during the cook and complete awareness of a particular cook's progress in terms of viscosity build-up and reduction of acid value provides the best warning prior to any gelation in a polyester resin production.

## 1.4 Recent advances in polyester synthesis

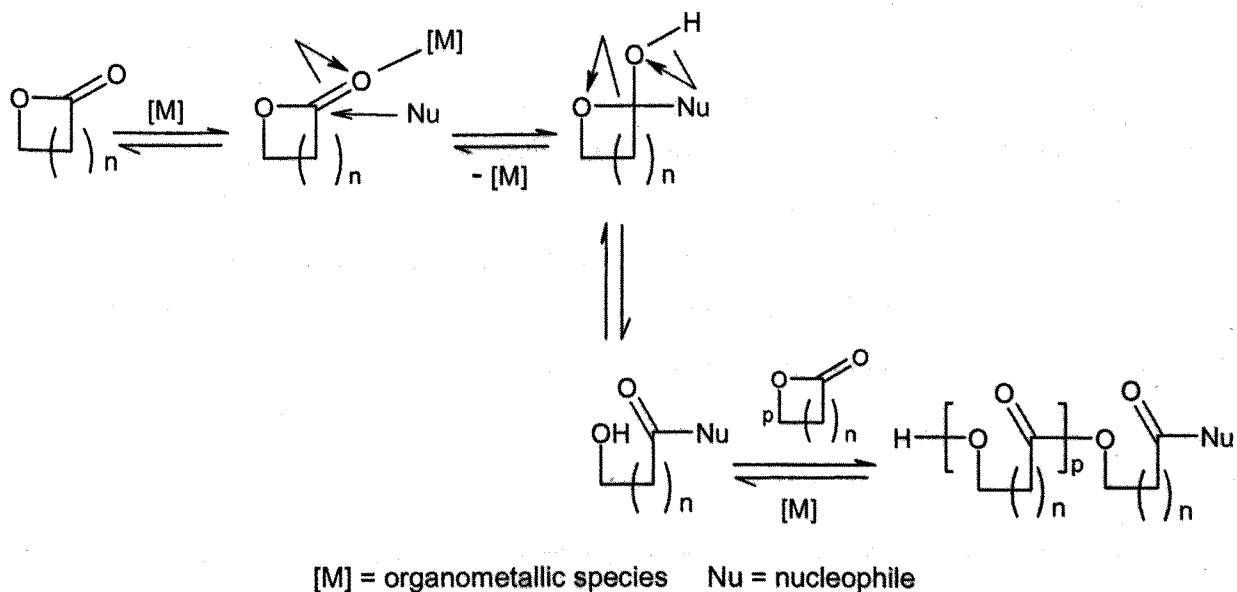
Preparation of polyesters by ring opening polymerisation (ROP) has recently gained interest. Lactones constitute the basis for the ring opening polymerisation method. At the moment, ring opening polymerisation is largely employed to prepare aliphatic polyesters from lactones.<sup>21,39</sup>

$\epsilon$ -caprolactone is one of the more important lactones widely employed for the synthesis of polyesters by ring opening polymerisation. The chemical structure of  $\epsilon$ -caprolactone is shown in Scheme 1.6



**Scheme 1.6 Chemical structure of  $\epsilon$ -caprolactone<sup>21</sup>**

Ring-opening polymerisation is a chain polyaddition polymerisation technique.<sup>21,39</sup> Similar to other addition polymerisation methods, a variety of initiators and catalysts have been used for the ring-opening polymerisation. These include ionic initiators and organometallic catalysts. Organometallics are metal derivatives. One of the major mechanisms by which ring opening polymerisation of lactones proceeds is through complexation of the carbonyl group by the organometallic catalyst. The polymerisation is then initiated by a nucleophile such as water or alcohol present.<sup>21</sup> This mechanism is shown in Scheme 1.7.



**Scheme 1.7 Ring opening polymerisation of lactones in presence of nucleophiles and through catalysis by organometallics<sup>21</sup>**

Absence of by-product during the reaction and rapid process are the major advantages of ring opening polymerisation.<sup>21,39</sup> Ring opening polymerisation has to be carried out in particular mediums such as organic solvents. Super critical fluids are also employed. Jerome et al<sup>21</sup> prepared poly( $\epsilon$ -caprolactone) in super critical carbon dioxide.

Aliphatic polyesters prepared by ring opening polymerisation are mainly used as biodegradable polymers for drug delivery purposes.<sup>21</sup> Polyesters prepared from lactones by ring opening polymerisation have a limited application in industrial coatings. As mentioned in Section 1.2, the mechanical and chemical resistance properties of industrial coatings such as coil coatings must be exceptional. Polyesters prepared from lactones are basically unable to meet the properties required by industrial coatings. Polyesters for industrial coatings are primarily prepared from a variety polyols and dicarboxylic acids that are polymerised through direct esterification. The more important polyols and dicarboxylic acids used in the preparation of polyesters for industrial coatings will be discussed in Section 1.6.

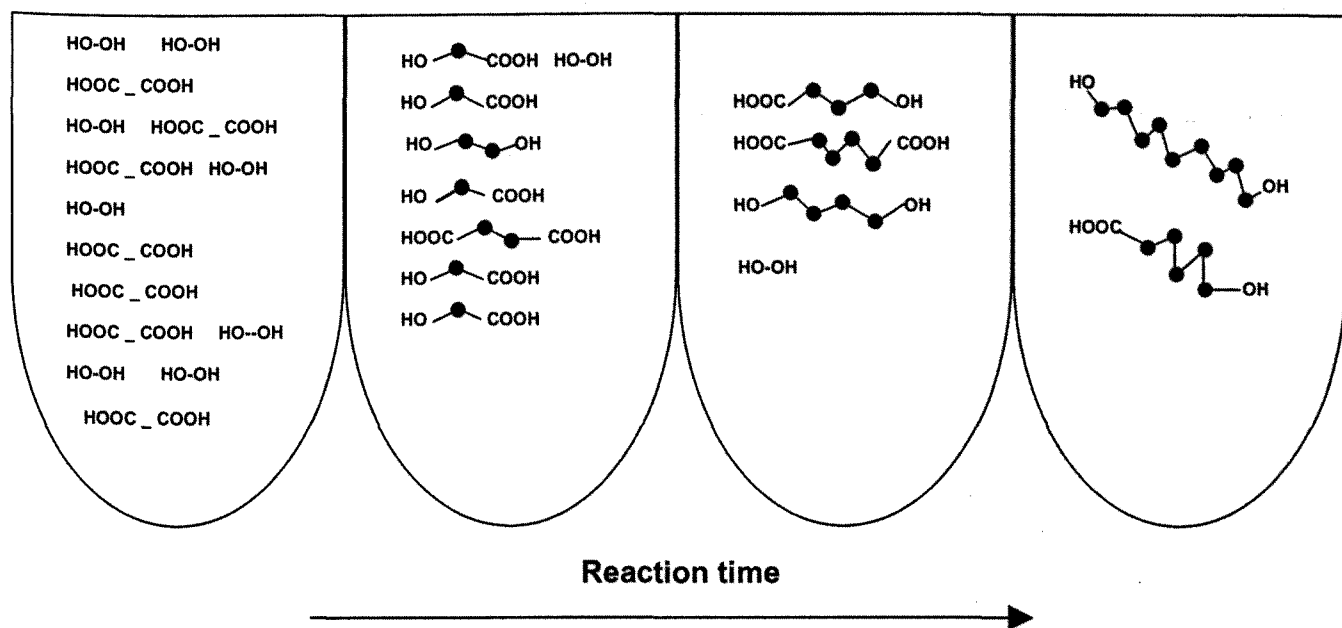
## **1.5 Molecular structure of linear and branched polyesters**

The properties of a polyester coating film are strongly dependant on the molecular structure of the base polyester resin. Therefore, it is of great importance to be aware of the criteria that are available to control the chain growth of polyesters and their resultant molecular architecture. The achievement of a desired polyester structure, either linear or branched, vitally depends on the structure and functionality of the original monomers. The monomers used for direct esterification step polymerisation of polyester resins usually contain at least two different types of functional groups. These are either  $-OH$  or  $-COOH$  functionalities, which are able to react with each other, but not with themselves. Sections 1.5.1 and 1.5.2 provide an idealistic illustration of the chain build-up of linear and branched polyesters.

### **1.5.1 Molecular chain growth of linear polyesters during synthesis**

When bifunctional monomers containing  $-OH$  and  $-COOH$  functionalities are incorporated in an initial polyester resin's formulation, the resulting polyester will be linear as illustrated in Scheme 1.8;<sup>40</sup>





Where ● represents an ester linkage  
 HO-OH represents the diol reactant  
 HOOC - COOH represents the diacid reactant

### Scheme 1.8 Idealised polymerisation of bifunctional polyols and polyacids leading to linear polyesters

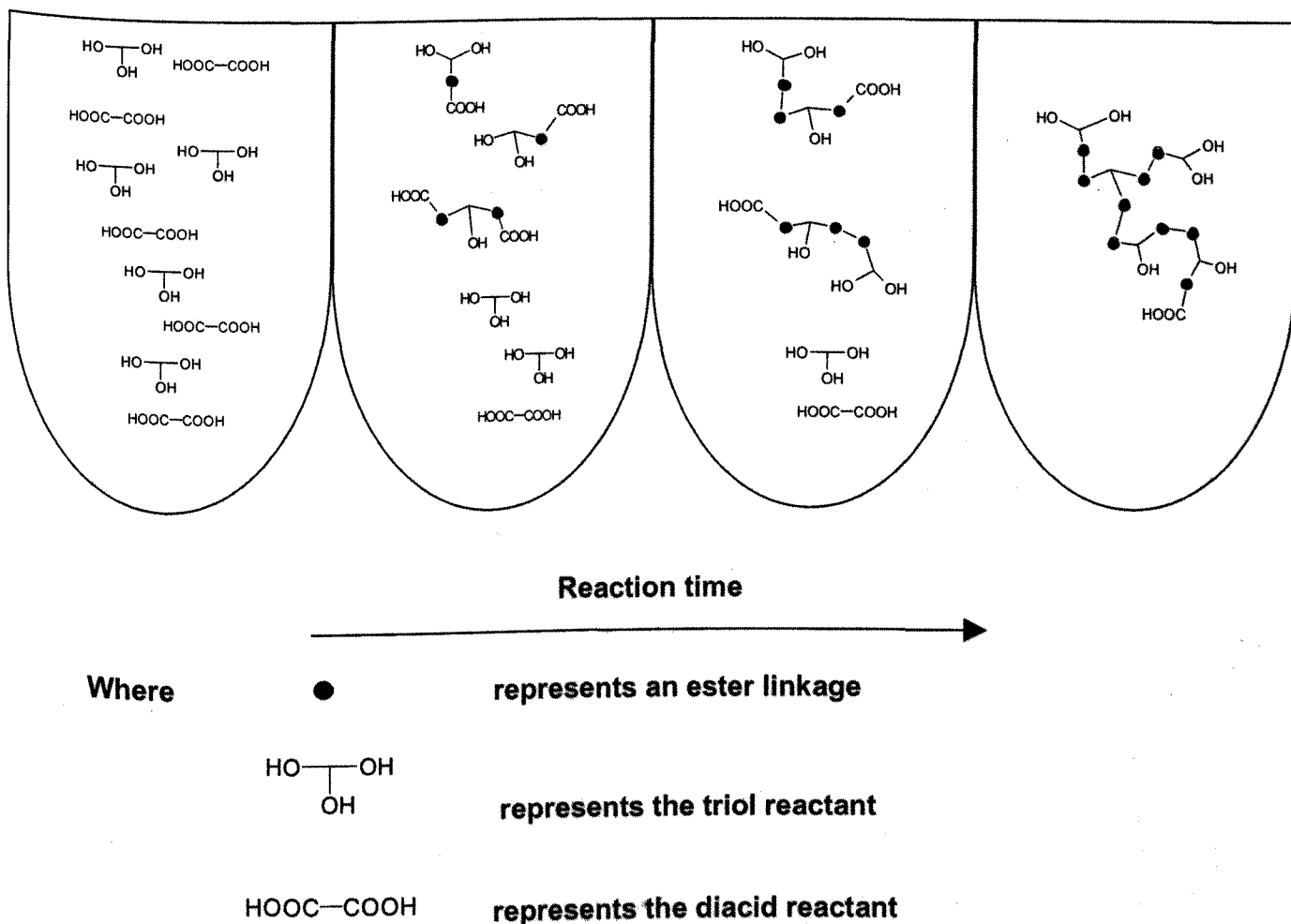
Although Scheme 1.8 is strictly applicable for ideal systems in which no  $-OH$  or  $-COOH$  consuming side reactions occur and also no cyclic molecules are formed, it can be extended to include practical polymerisation systems as long as the impact of side reactions and cyclisation is insignificant.<sup>40</sup>

Various sized molecules are present at any moment with two functional groups at their ends which are inclusive of  $-OH$  and  $-COOH$ . If it is assumed that  $-OH$  can only react with  $-COOH$  and vice versa, the number of  $-OH$  and  $-COOH$  functionalities which have reacted at any one time will be similar. If the initial concentration of  $-COOH$  is less than  $-OH$ , which is usually the case as mentioned in Section 1.3.2, then once  $-COOH$  has completely reacted, all the succeeding molecules will contain  $-OH$  functionality at both ends. In addition, when  $[OH] > [COOH]$ , the resulting molecular weight of the polyester will be limited.<sup>40</sup>

### 1.5.2 Molecular chain growth of branched polyesters during synthesis

When monomers with functionalities of higher than two, such as a triol, are incorporated in an initial polyester resin's formulation, the resulting polyester will be of a branched structure. Branching agents commonly employed are tri- or tetrafunctional. <sup>41</sup>

Scheme 1.9 illustrates the reaction of triols and bifunctional diacids leading to a branched polyester;



**Scheme 1.9 Idealised polymerisation of tri-functional polyols and diacids leading to a branched polyester**

In order to obtain long chain branched polyesters, multifunctional comonomer branching agents are employed. <sup>41</sup> The multifunctional monomer determines the number of bonds at a

branched point of a polyester. In the polyester shown in Scheme 1.9, three bonds are attached to each branched point. These points are due to the triols which originally possessed three –OH functionalities. Polymerisation of mixtures of bifunctional monomers and multifunctional monomers with functionalities of greater than three cannot only lead to branching, but also to crosslinked molecular structures. In such cases, the chain build-up starts with the stepwise formation of linear and branched oligomers and proceeds. The chain length then increases with the stepwise reaction of these oligomers. The more branched a molecule is, the greater is the probability of its reaction, for the probability of the reaction of a certain molecule depends on the number of its functional groups. Therefore, molecules having a greater number of branches grow faster than linear molecules with fewer functional groups. At a given value of conversion, the gel point is attained, at which a giant molecule whose moieties occupy the whole reaction vessel is formed accompanied by rapid increase in the polyester's viscosity. If the reaction of the functional groups is allowed to continue beyond gel point, crosslinking density would increase so far as to obtain a rock solid material.<sup>42</sup>

It is broadly acknowledged that a high degree of branching in a polymer backbone results in improved solubility and lower crystallinity. Crystallinity occurs for symmetrical chains that are regularly available in linear polymers.<sup>41</sup>

## **1.6 Monomers for synthesis of saturated polyester resins via direct esterification**

For formulating and synthesising a polyester resin through the direct esterification reaction pathway, a wide range of monomers or raw materials are available. Each of the monomers concerned hold unique properties. By being able to incorporate a variety of raw materials, it can be imagined that an infinite number of polyesters can be formulated. However, the value of any formulation lies in its ability to meet the requirements of the final application. Therefore, it is extremely important to try to know the contribution of these raw materials to the final performance of each formulation. To this day, this has remained a challenge, for even by incorporating the right monomer or at least, what is thought to be the right monomer for a specific application, completely different results are sometimes obtained. This is due to the fact that the polymers obtained are of extremely complex structure and it

is not possible to be in possession of a clear and complete picture of the polymer backbone that is obtained by a formulation.

In general, three major property considerations exist for polyester resin raw materials. These considerations are based on the molecular structure of these raw materials and are as follows;<sup>43</sup>

- 1) **Functionality:** This normally relates to –OH functionality and commonly, in order to incorporate –OH functionality to the polyester backbone, a tri- or tetrafunctional polyol is used.
- 2) **Hardness:** Raw materials with branched structures, aromatic rings, or short chains are regarded as *hard* materials.
- 3) **Flexibility:** Raw materials with aliphatic long chains are regarded as *flexible* materials.

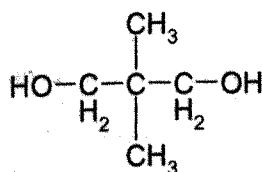
In addition to the monomers used for the preparation of a polyester resin, the hardness and flexibility of the resulting polyester coating would also highly depend on the nature of the curing agent employed.<sup>43</sup>

Some of the more important polyols and polyacids used in the preparation of polyester resins are discussed in Sections 1.6.1 and 1.6.2.

### 1.6.1 Polyols

#### I. Neopentyl glycol (NPG)

The chemical structure of neopentyl glycol is shown in Scheme 1.10



Molecular weight : 104

Equivalent weight : 52

**Scheme 1.10 Chemical structure of neopentyl glycol<sup>6,22,44</sup>**

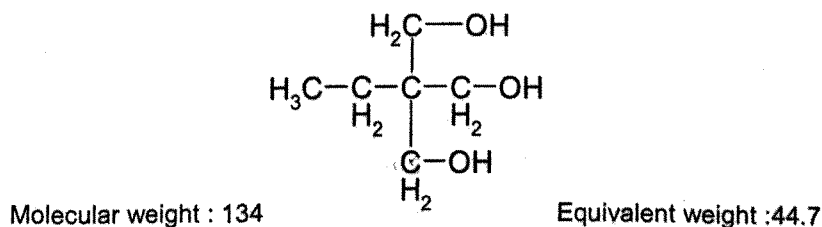
Neopentyl glycol has primary application in polyester resins intended for industrial coatings.<sup>45</sup>

This diol is considered as a hard raw material. It has two primary hydroxyl functionalities that provide good reactivity during both the esterification process and also during the subsequent crosslinking of the prepared polyester. Neopentyl glycol provides chemical resistance, corrosion protection, and stability towards hydrolysis through the increase of the steric hindrance caused by the presence of methyl groups. In addition, these methyl groups also improve the solubility of the prepared polyester as they prevent the chains from being too close to one another.<sup>43,44,46</sup> Moreover, neopentyl glycol has no labile  $\beta$  hydrogens which results in excellent exterior durability.<sup>6,44</sup>

The resins formulated with neopentyl glycol are of pale colour and low viscosity. The properties mentioned depend on the incorporation amount of neopentyl glycol. However, there is a major drawback regarding high level of incorporation of neopentyl glycol in a polyester formulation. During the esterification process, neopentyl glycol readily distills with the water of reaction and can lead to structure disruption or even gelation.<sup>43,44,46</sup> The latter may occur unless neopentyl glycol corrections are made during the synthesis according to the procedures mentioned in Section 1.3.2.

## II. Trimethylol propane (TMP)

The chemical structure of trimethylol propane is shown in Scheme 1.11



**Scheme 1.11 Chemical structure of trimethylol propane<sup>41,44</sup>**

Trimethylol propane is a triol with three primary hydroxyl functionalities. It is employed to provide hydroxyl functionality on the polyester backbone for subsequent crosslinking of the polyester resin with curing agents. It is assumed that the three  $-\text{OH}$  groups have similar

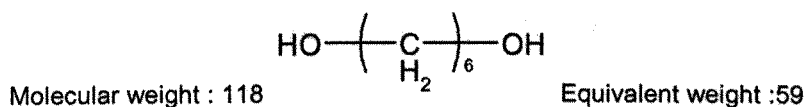
reactivities since they are primary.<sup>43,44</sup> "As a general rule, reactivity decreases as we pass from primary to secondary to tertiary"<sup>43</sup>. Therefore, the primary –OH groups left in the polyester backbone as a result of the incorporation of trimethylol propane will result in a relatively high level of reactivity of the polyester. This triol also improves the exterior durability of the polyester coating due to unavailability of labile β hydrogens.<sup>43,44</sup> More important triols used in the preparation of polyesters include glycerol and trimethylol ethane.

As stated by McKee et al<sup>41</sup>, trimethylol propane and other triols are also used as branching agents for the synthesis of high molecular weight branched polyesters (p.511). Weisskopf<sup>47</sup> used trimethylol propane as a branching agent to synthesise high molecular weight poly(ethylene terephthalate)s. Yoon et al<sup>48</sup> also synthesised branched poly(ethylene terephthalate)s through incorporation of trimethylol ethane.

Inclusion of triols in polyester preparation affects the thermal properties of the polyester as well. Tang et al<sup>28</sup> showed that the increase in the content of glycerol resulted in the increase of the glass transition temperature of the polyester through formation of a molecular structure with a compact network (p.3363).

### III. 1,6 hexanediol (1,6 HD)

The chemical structure of 1,6 hexanediol is shown in Scheme 1.12



**Scheme 1.12 Chemical structure of 1,6 hexanediol** <sup>44,50</sup>

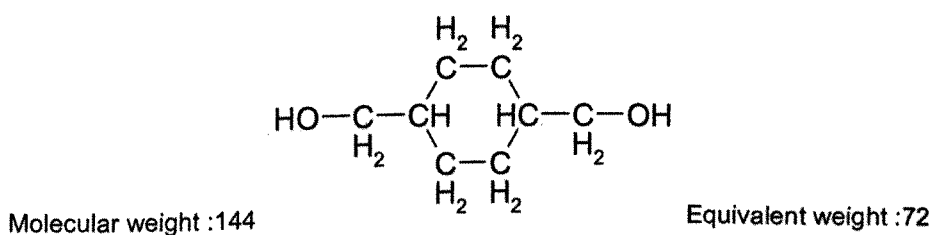
1,6 hexanediol is a linear diol and imparts flexibility to the polyester resin. It is primarily used in applications that demand high performance in terms of bending and impact resistance. Generally, this diol is combined with hard polyacids such as isophthalic acid or terephthalic acids in order to compensate for the loss of hardness while maintaining a good level of flexibility.<sup>43,44</sup>

As stated by McKee et al<sup>41</sup>, increase of the number of carbons in alkyl chains would result in the reduction of the glass transition temperature of the polyester (p.531). The fractional volume in polyesters increases with the increase of alkyl length which leads to the drop of the glass transition temperature.<sup>41</sup> Based on this, it can be assumed that inclusion of 1,6 hexanediol in a polyester formulation could result in the decrease of the glass transition temperature. Mehdipour-Ataie<sup>49</sup> concluded that introduction of flexible units such as 1,6 hexanediol moiety into a polyester would enhance the solubility.

1,6 hexanediol has also been used for preparation of biodegradable aliphatic polyesters. A number of recent research involving 1,6 hexanediol pertain to biodegradable aliphatic polyesters. Liu et al<sup>50</sup>, synthesised biodegradable aliphatic polyesters from 1,6 hexanediol,  $\epsilon$ -caprolactone, and adipic acid. Gesti et al<sup>51</sup> synthesised aliphatic biodegradable polyesters from 1,6 hexanediol and dodecanodioic acid.

#### IV. 1,4 cyclohexanedimethanol (1,4 CHDM)

The chemical structure of 1,4 cyclohexanedimethanol is shown in Scheme 1.13



**Scheme 1.13 Chemical structure of 1,4 cyclohexanedimethanol** <sup>44,52-54</sup>

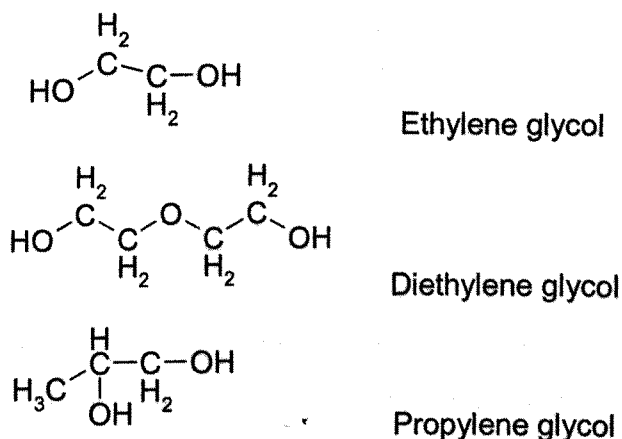
1,4 cyclohexanedimethanol is an alicyclic glycol.<sup>52</sup> The cycloaliphatic structure of 1,4 cyclohexanedimethanol imparts particular conformational transitions and molecular structure to polyesters.<sup>53</sup> Ni et al<sup>54</sup> stated that polyesters containing cyclic moieties in their backbone are of transitional mechanical properties in comparison to aromatic and linear polyesters (p.50). 1,4 cyclohexanedimethanol could provide an excellent compromise between hardness and flexibility.<sup>44,55</sup> The two primary hydroxyl functionalities provide excellent reactivity during both the esterification process and the subsequent crosslinking reaction. Although the cyclohexyl ring is completely saturated, the presence of labile  $\beta$  hydrogens lowers the exterior durability of polyesters based on this diol.<sup>44</sup> Generally, this

diol is used for its excellent contribution to hardness and backbone rigidity.<sup>44,53</sup> Amongst recent research into polyesters for surface coatings involving 1,4 cyclohexanedimethanol, those of Ni et al<sup>54</sup> and Awasthi and Agrawal<sup>56</sup> can be considered. In both works, 1,4 cyclohexanedimethanol was used for the synthesis of hydroxylated polyesters for high solids polyurethane coatings. Awasthi and Agrawal<sup>56</sup> showed that polyesters containing cycloaliphatic moieties such as 1,4 cyclohexanedimethanol, provided better mechanical and chemical resistance properties in comparison to linear and aromatic polyesters.

1,4 cyclohexanedimethanol has also been used for preparation of biodegradable aliphatic / alicyclic polyesters. In the most recent research in this regard, Tsai et al<sup>52</sup> synthesised biodegradable aliphatic / alicyclic copolyesters from 1,4 cyclohexanedimethanol, 1,4 butanediol, and sebacic acid.

## V. Miscellaneous glycols

There is a wide range of glycol compounds which can be used in polyester preparation. The more important of such glycols are shown in Scheme 1.14.



**Scheme 1.14 Chemical structures of ethylene glycol, diethylene glycol and propylene glycol<sup>30,44</sup>**

With respect to polyesters for industrial surface coatings, the glycols shown in Scheme 1.14 impart flexibility to the system. This is done at the cost of hardness. Flexibility increases with the chain length of the glycol while hardness decreases. A major drawback



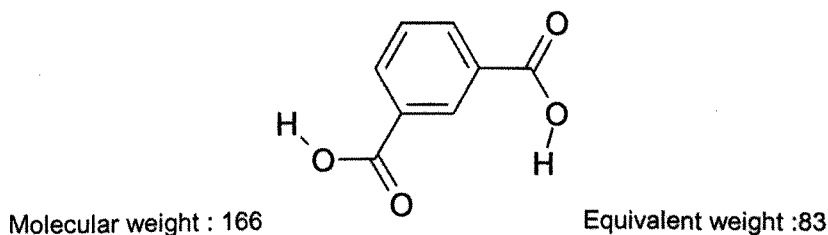
exists for the synthesis of polyesters with the glycols shown in Scheme 1.14. These compounds are water soluble. Therefore, heavy glycol losses can occur during the preparation of polyesters via polycondensation.<sup>43,44,57,58</sup>

Recent research into polyesters indicates that biodegradable aliphatic polyesters are now being mostly prepared from the glycols shown in Scheme 1.14. In this regard, the work of Soni et al<sup>30</sup> can be considered as one in which biodegradable copolyesters from ethylene glycol, lactic acid and terephthalic acid were synthesised.

## 1.6.2 Polyacids

### I. Isophthalic acid (IPA)

The chemical structure of isophthalic acid is shown in Scheme 1.15.

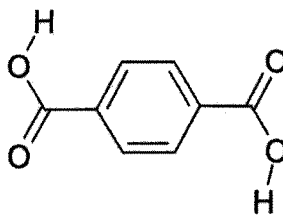


**Scheme 1.15 Chemical structure of isophthalic acid**<sup>6,39,44</sup>

Isophthalic acid is one of the more important dicarboxylic acids and is widely used in the preparation of polyesters.<sup>54</sup> The aromatic isophthalic acid is considered as a hard raw material.<sup>43,44</sup> It is principally used to enhance chemical resistance, hardness and glass transition temperature.<sup>54,56</sup> Isophthalic acid also provides increased resistance against hydrolysis.<sup>54</sup> However, isophthalic acid limits the photo-oxidative stability of the polyester as the phenyl ring absorbs UV-light.<sup>54</sup> In addition, the flexibility and impact resistance are adversely affected by isophthalic acid.<sup>59</sup> Wang et al<sup>23</sup> stated that incorporation of aromatic moieties in a polyester backbone improves mechanical and physical properties and provides heat stability (p.3020).

### II. Terephthalic acid (TPA)

The chemical structure of terephthalic acid is shown in Scheme 1.16.



Molecular weight :166

Equivalent weight :83

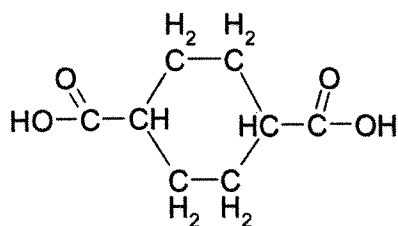
### Scheme 1.16 Chemical structure of terephthalic acid <sup>30,39,44</sup>

Terephthalic acid has similar properties as isophthalic acid. Wang et al<sup>31</sup>, who synthesised copolyesters from dimethyl terephthalate, 1,4 butanediol and cyclohexanedicarboxylic acid concluded that the presence of aromatic repeat units would enhance the thermal stability of the resulting polyester (p.2225). Danick<sup>59</sup> acknowledged that the reaction of terephthalic acid with glycols resulted in long chains that would impart flexibility to the system. Lozano et al<sup>60</sup> synthesised a series of polyesters that contained terephthalic acid and showed that the increase in the content of terephthalic acid resulted in the augmentation of chain stiffness and glass transition temperature. Muller et al<sup>61</sup> concluded that polyesters with high content of aromatic constituents such as terephthalic acid are quite resistant to hydrolytic degradation.

Experimental data has shown that in comparison to isophthalic acid, the incorporation of terephthalic acid further improves the mechanical and heat resistance properties of a polyester resin. However, there are some drawbacks with respect to polyester synthesis when terephthalic acid is employed. Terephthalic acid is less reactive than isophthalic acid and requires the use of esterification catalysts and high reaction temperatures. It also has a strong tendency towards crystallisation and reduces the solubility of the polyesters containing it. In polyesters that are designed for surface coatings applications, terephthalic acid is not usually incorporated solely and is often mixed with isophthalic acid. <sup>43,44,62</sup>

### III. 1,4 cyclohexanedicarboxylic acid (1,4 CHDA)

The chemical structure of 1,4 cyclohexanedicarboxylic acid is shown in Scheme 1.17.



Molecular weight :172

Equivalent weight :86

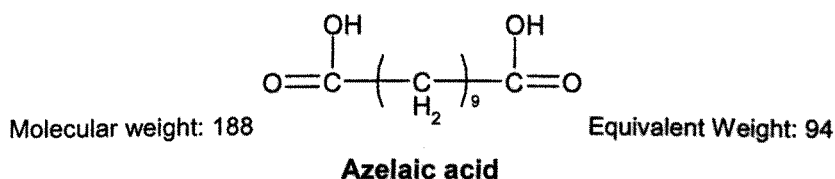
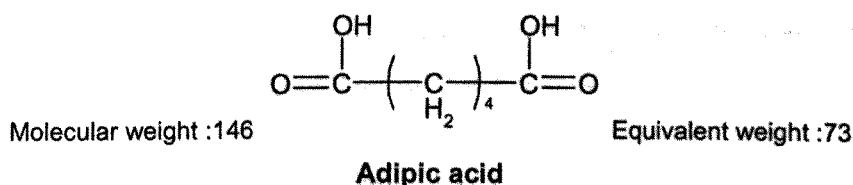
### Scheme 1.17 Chemical structure of 1,4 cyclohexanedicarboxylic acid <sup>31,54,56</sup>

1,4 cyclohexanedicarboxylic acid has similar properties as its diol homologue cyclohexanedimethanol.<sup>44,63</sup> In comparison to aromatic diacids of isophthalic acid and terephthalic acid, the cycloaliphatic structure of 1,4 cyclohexanedicarboxylic acid provides a lower glass transition temperature.<sup>54</sup> However, 1,4 cyclohexanedicarboxylic acid contributes to a higher glass transition temperature than linear diacids.<sup>54,56</sup> In terms of mechanical properties, the cycloaliphatic structure of 1,4 cyclohexanedicarboxylic acid provides an intermediate flexibility between aromatic and linear structures.<sup>44,54</sup> Ni et al<sup>54</sup> concluded that cycloaliphatic diacids provide intermediate mechanical and tensile properties between aromatic and linear diacids. In some cases, similar contribution to flexibility as linear diacids have been reported for 1,4 cyclohexanedicarboxylic acid. Heidt and Elliot<sup>64</sup> modified isophthalic acid based polyesters with 1,4 cyclohexanedicarboxylic acid and the linear adipic acid. They concluded that 1,4 cyclohexanedicarboxylic acid resulted in the same flexibility as adipic acid with the advantage of not diminishing hardness or glass transition temperature.

Biodegradable aliphatic/alicyclic polyesters have also been prepared from 1,4 cyclohexanedicarboxylic. Wang et al<sup>31</sup> prepared biodegradable polyesters from 1,4 cyclohexanedicarboxylic and concluded that similar to aromatic units, cyclic units can also enhance the thermal stability of the polyester.

#### IV. Linear diacids

A variety of aliphatic dicarboxylic acids are used for the synthesis of polyesters. The difference between these aliphatic diacids is the number of carbons in the chain. The more important aliphatic diacids used in polyester preparation include adipic acid and azelaic acid. The chemical structures of adipic acid and azelaic acid are shown in Scheme 1.18.



**Scheme 1.18 Chemical structures of adipic acid and azelaic acid<sup>44,60</sup>**

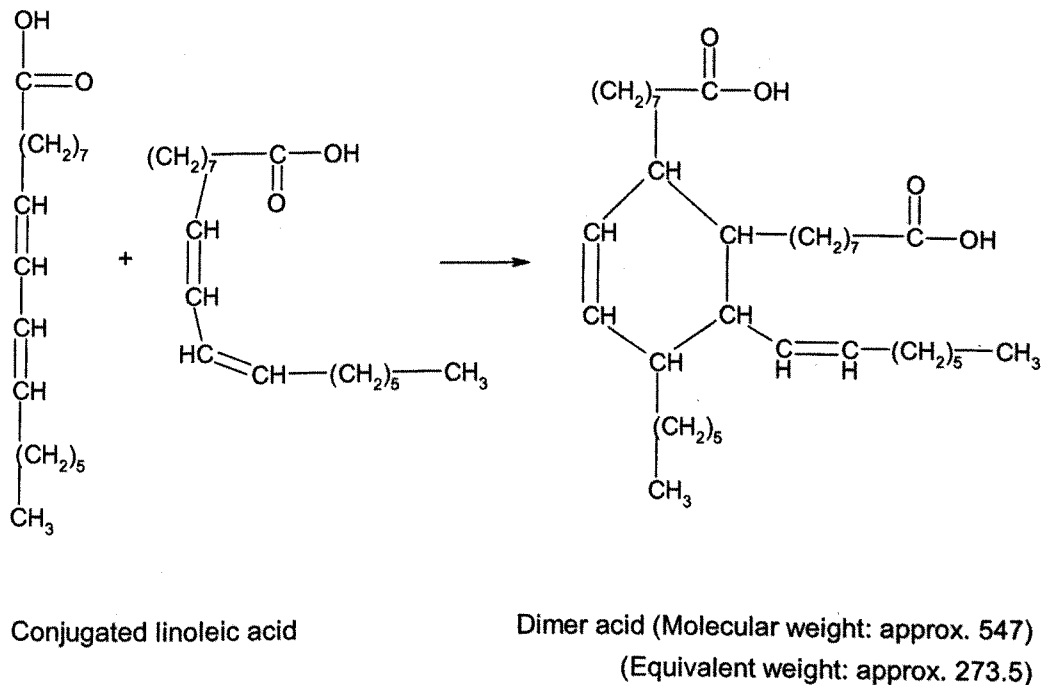
The linear dicarboxylic acids shown in Scheme 1.18 provide flexibility. However, they result in the reduction of hardness.<sup>43,44</sup> Lozano et al<sup>60</sup> concluded that replacement of adipic acid units by terephthalic acid units in a series of synthesised biodegradable polyesters resulted in the augmentation of the glass transition temperature. Ferré et al<sup>37</sup> synthesised poly(ester amide)s that contained adipic acid and concluded that the increase in the content of adipic acid resulted in the decrease of the polymer's melting point and glass transition temperature. Linear diacids also reduce the chemical resistance. Awasthi and Agrawal<sup>56</sup> synthesised a hydroxylated saturated polyester resin from 1,4 cyclohexanedimethanol, azelaic acid and adipic acid. They showed that its resistance to acids, alkalis and solvents was poor in comparison to polyesters based on isophthalic acid and 1,4 cyclohexanedicarboxylic acid. To compensate for the loss of hardness, glass transition temperature and chemical resistance, aliphatic diacids have to be incorporated alongside hard polyacids and polyols.<sup>44</sup>

## V. Dimer acids

In the preparation of polyesters, dimer fatty acids are also employed. Dimer acids can lead to extreme flexibility and a significant drop in the level of hardness.<sup>43,65</sup> Dimer acids are manufactured by catalytically polymerising fatty acids to form a mixture of monomer, dimer, and trimer acids. These mixtures, which are commercially available as Pripols or equivalent products, are generally referred to as dimer acids. Usually, two moles of C18 fatty acids are polymerised. The resulting dimer acid will probably be of a C6 core and a variety of

isomers. Fatty acids used in dimerisation are triglyceride oils of natural origin, varying in structure. A substantial proportion of these fatty acids is composed of linoleic acid.<sup>65-67</sup>

Scheme 1.19 illustrates an idealised dimerisation process.



**Scheme 1.19 Dimer acid formation from conjugated linoleic acid<sup>66</sup>**

Typically, the composition of available dimer acids in terms of monomer, dimer, and trimer is in the following range:<sup>66</sup>

Monomeric fatty acid: 1%-10%

Dimerised fatty acid: 60%-85%

Trimerised fatty acid: 10%-20%

The overall functionality of the dimer acid is greatly affected by the trimer content. Trimer content is usually greater than the monomer content, thus affecting the functionality of the dimer acid by increasing it over two.<sup>66</sup> This means that if a dimer acid with a greater trimer content is incorporated in a polyester formulation along with diols and diacids, the resulting backbone could contain free carboxyl functionality.

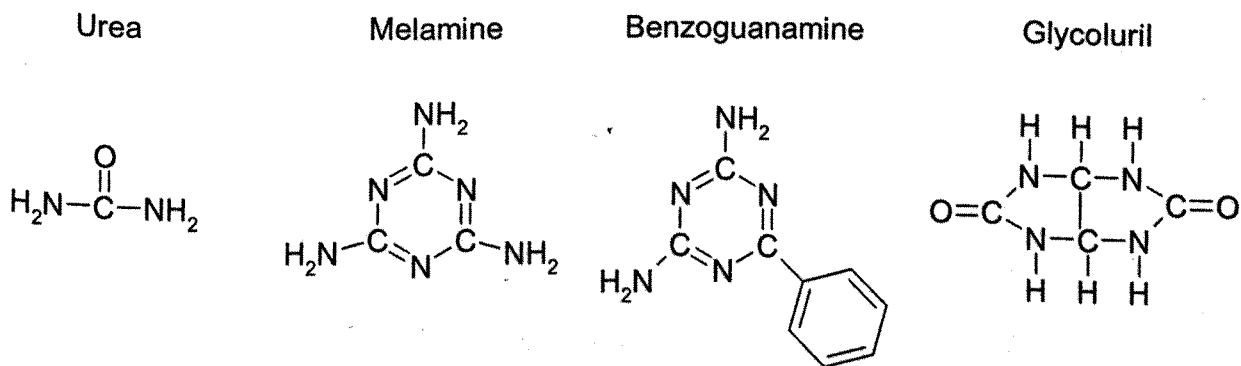
The long aliphatic chains available in the oligomeric dimer acid provide high flexibility to the resulting coating film. However, similar to aliphatic diacids, hard diols and diacids have to be incorporated alongside the dimer acid in order to maintain the balance between hardness and flexibility.

## 1.7 Curing agents of stoving polyester coil coatings

Saturated polyester resins have no curing mechanism on their own. Therefore, proper curing agents are incorporated in polyester coatings. The properties of the final polyester coating are dramatically affected by the nature of the curing agent and the type of cross-linking achieved. The more important curing agents employed in polyester coatings include amine, isocyanate, and epoxide. Polyesters designed to be cross-linked with amine or isocyanate curing agents are formulated with hydroxyl excess, while polyester backbones designed to be cross-linked with epoxides must contain free carboxyl functionality sites.<sup>68</sup>

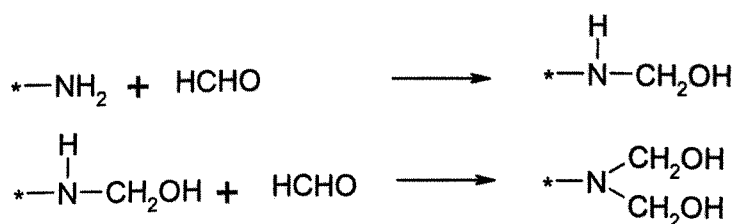
### 1.7.1 Amine curing agents

Amine curing agents are primarily used in stoving industrial polyester coatings. Amine curing agents, or aminoplasts, are modified products from the condensation reaction between amines and formaldehyde.<sup>68,69</sup> Scheme 1.20 provides the chemical structures of the major amines that are used in the preparation of aminoplasts.



Scheme 1.20 Chemical structures of the amines primarily used in the preparation of amine curing agents<sup>68,69</sup>

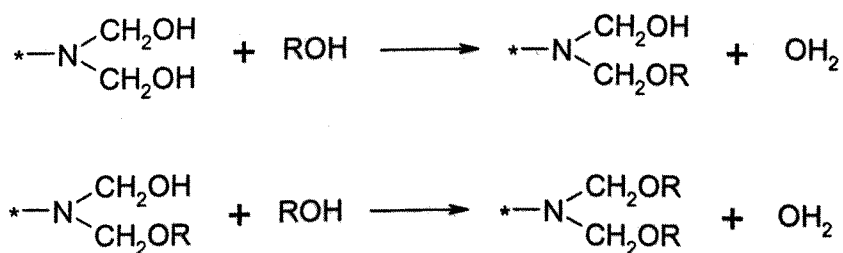
Aminoplasts are prepared via two reactions of methylation and alkylation. The first reaction is methylation. During methylation the  $-\text{NH}_2$  group of the amine is methylated through the reaction of the amine with formaldehyde.<sup>70</sup> The methylation reaction is shown in Scheme 1.21.



\* represents an amine residue

**Scheme 1.21 Methylation reaction stage of aminoplast preparation<sup>70</sup>**

The methylated amine is hydroxyl rich with extreme polarity and can't be used with the hydrocarbon solvents commonly used in polyester resin systems.<sup>68</sup> During the second reaction, the hydroxyl groups are alkylated with an alkylation alcohol along with simultaneous polymerisation of the methylated amine through methylol groups.<sup>68,70</sup> The alkylation reaction is shown in Scheme 1.22.



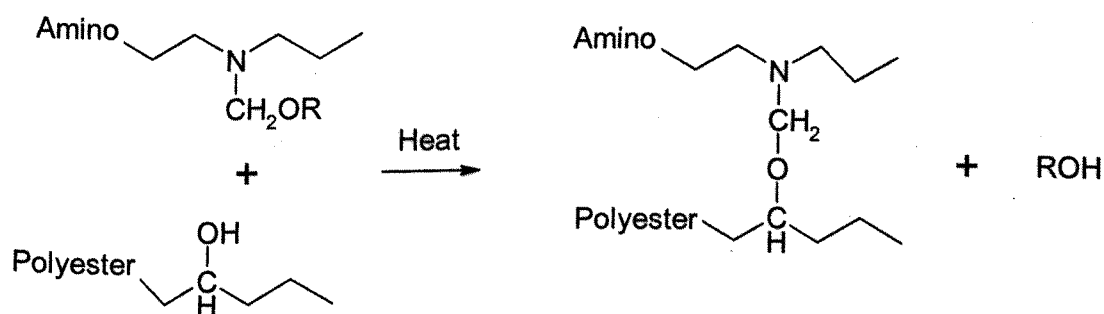
\* represents an amine residue

**Scheme 1.22 Alkylation reaction stage of aminoplast preparation<sup>70</sup>**

The final alkylated and polymerised product is effectively soluble in hydrocarbon solvents. The reactivity of an amino crosslinking agent, is determined by the alkyl (R) group. Polarity,

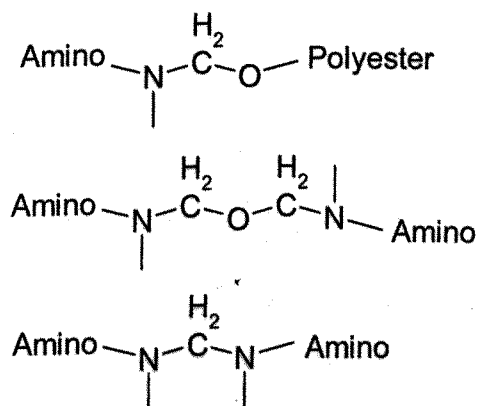
compatibility and solubility, are determined by the degree of alkylation. Generally, normal butanol, isobutanol and methanol are used as alkylation alcohols.<sup>68</sup>

The terminal end-groups of hydroxyl-excess formulated saturated polyester resins have hydroxyl functionality. The hydroxyl groups react with an aminoplast to form a crosslinked network and the final coating film. The reaction of an hydroxylated saturated polyester resin with an amine curing agent is shown in Scheme 1.23.



**Scheme 1.23 Idealised reaction of a hydroxyl functional polyester backbone with an amino curing agent<sup>68</sup>**

Potential bonds which may form as a result of the reaction of an aminoplast with an hydroxyl functional polyester are shown in Scheme 1.24.<sup>69</sup>



**Scheme 1.24 Bonds potentially formed during the reaction of a hydroxyl functional polyester backbone and an aminoplast<sup>69</sup>**

Depending on the curing time, hydroxyl content of the polyester resin and the type of aminoplast used, the curing temperature of amine curing agents with hydroxyl functional

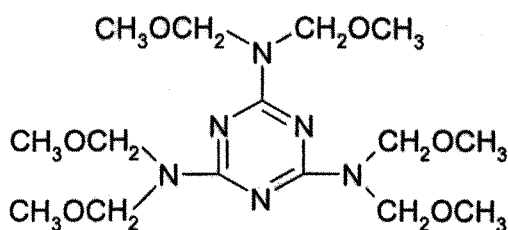


polyester resins may range from 120-350°C. Catalysis by acid is often used in order to lower the curing temperature. The ratio of polyester/aminoplast in a coating formulation is often practically derived after the evaluation of the cured paint film.<sup>68</sup> This is due to the fact that the chemistry of aminoplast crosslinking with a hydroxyl functional polymer backbone is not totally known and is still being studied.

The film forming reactions are those reactions between either the polyester resin and the amino resin or the amino resin and the amino resin. There are many possible different reactions which can take place between different functional groups of an aminoplast. Some of these reactions are those between the methylol ( $\text{CH}_2\text{OH}$ ) and the alkylated methylol groups ( $\text{CH}_2\text{OR}$ ). The self-reactions of the amino resins lead to practical determination of the amount of amino resin used against a polyester resin in a coating formulation. Typically, 25-30% of the aminoplast and 70-75% of the polyester resin are used in coating formulations in order to achieve a suitable balance between the desired properties. However, if a single polyester resin is cured by different classes of aminoplasts, the final coating properties inclusive of hardness and flexibility will also be different. Besides reaction time and temperature and presence or absence of a catalyst, the functional groups of the aminoplast also affect the final film properties of a polyester coating.<sup>68,69</sup>

The choice of the aminoplast highly depends on the coating system, the final application, and the curing schedule. Urea formaldehyde resins are cost effective with a fast cure response. However, since the durability and weathering resistance of melamine formaldehyde cured systems are far more superior, most industrial top coat systems are formulated with melamine formaldehyde resins.

Amongst alkylated melamine formaldehyde resins, highly methylated melamine formaldehyde curing agents have a low tendency for self-condensation reactions.<sup>68,69</sup> The molecular structure of hexamethoxy methyl melamine (HMMM) which is one of the more important methylated melamine formaldehyde curing agents is shown in Scheme 1.25.



**Scheme 1.25 Monomeric structure of hexamethoxymethyl melamine<sup>68</sup>**

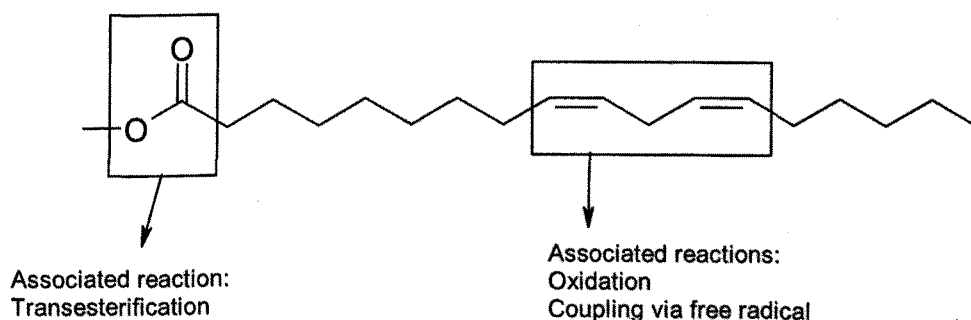
The low self condensation tendency of HMMM during the curing reaction, leads to the achievement of maximum performance by a tailor-made and molecularly engineered saturated polyester resin. Linear saturated polyester resins crosslinked with HMMM produce flexible coating films that are suitable for the requirements of coil coatings. As it is alkylated with methanol, HMMM is universally compatible with water-based or solvent based resins. However, HMMM crosslinkers have a slow cure response and require the use of high curing temperatures as well as strong acid catalysis.<sup>68,69</sup>

### 1.7.2 Curing agents investigated recently

Nowadays, the majority of the coil coatings are solvent based. 50% or more of the coil coatings are comprised of solvents. Increased environmental concerns and imminent legislations have resulted in an industrial interest to reduce the emission of volatile organic compounds (VOC). To eliminate the solvent content, the use of waterborne, powder and UV curable coil coating systems have been suggested. However, these technologies have not yet proven to be practicable industrially. In terms of coating performance, they are still inferior in comparison to solvent based systems. In addition, the use of waterborne, powder and UV curable coil coatings would involve extreme clean-up difficulties. The application of these coating systems would also require high cost production facilities that are currently not feasible.<sup>7,8,18</sup>

Johansson and Johansson<sup>7,8,18</sup> suggested the use of reactive diluents to reduce the solvent content in coil coatings. The reactive diluent acts as a solvent in the coil coating and reduces its viscosity. During the cure, the reactive diluent would be incorporated into the coil coating film instead of evaporating. It is supposed that similar to a curing agent, the reactive diluent would chemically react with the polyester resin of the coil coating and

would be incorporated into the crosslinked network of the coating film. Based on these assumptions, fatty acid methyl esters were investigated as reactive diluents in coil coatings.<sup>7,8,18</sup> Fatty acid methyl esters are long chain molecules containing an average of 18 carbons.<sup>18</sup> Reactive moieties of fatty acid methyl esters and the reactions that they can presumably undergo are shown in Scheme 1.26.



**Scheme 1.26 Reactive moieties of fatty acid methyl esters<sup>18</sup>**

It was shown that under the curing conditions of coil coatings, the ester moiety present in fatty acid methyl esters could react with the hydroxyl groups of the coil coatings' polyester resin.<sup>7,8</sup> The fatty acid methyl esters studied for the purpose concerned included rape seed methyl ester, tall oil methyl ester and linseed oil methyl ester.<sup>7,8,18</sup> In comparison to other thermally cured coating systems, the curing process in a coil coating is highly complex which is due to the rapid rate of cure.<sup>8,71</sup> Therefore, only the final cured films of the coil coatings in which fatty acid methyl esters were incorporated could be evaluated.<sup>8</sup> It was concluded that fatty acid methyl esters would be reactive in a thermally cured coil coating system and could result in the reduction of the emission of VOC.<sup>7</sup>

However, drawbacks were observed if fatty acid methyl esters were used as reactive diluents in coil coatings. It was found that the evaporation and oxidation of fatty acid methyl esters competed with their reaction with the hydroxyl groups of the polyester resin.<sup>7,18</sup> Fatty acid methyl esters resulted in the reduction of the glass transition temperature of the final coating film.<sup>18</sup> The large molecules of fatty acid methyl esters plasticised and lowered the crosslink density of the cured film.<sup>8,18</sup> In addition, introduction of fatty acid methyl esters altered the appearance and mechanical properties of the cured coil coating film.<sup>8,18</sup> The final coil coating film properties must remain intact. Thus, the incorporation of reactive

diluents as novel curing agents and VOC reducers in coil coatings is subject to further study and cannot be practiced for the moment.

## **1.8 Techniques for characterisation of saturated polyester resins**

In this section, the main analytical techniques used for characterisation of thermal properties, chemical structure, and molecular weight of saturated polyester resins are introduced.

### **1.8.1 Differential scanning calorimetry (DSC)**

Differential scanning calorimetry or DSC is a thermal analytical technique. DSC measures the amount of heat absorbed or released by a sample as it is heated, cooled, or held at a constant temperature relative to an inert reference. Studying physical transformations or phase transitions is the main purpose of DSC. Melting, glass transitions, or exothermic decompositions are examples of phase transitions. Energy changes or heat capacity changes are involved in phase transitions. These changes can be detected by DSC with great sensitivity. When a sample undertakes a phase transition, more, or less heat will need to flow into it. This phenomenon is the basic principle that underpins the DSC technique. Requirement of more or less heat flow will depend on the process being exothermic or endothermic. By observing the differences in the heat flow between the sample and the inert reference, DSC instruments are able to measure the amount of heat absorbed or released during phase changes.<sup>72,73</sup>

The majority of DSC instruments are of a heat-flux design. Heat flux is sometimes referred to as heat flow rate intensity. In other words, heat flux is the rate of heat flow through a unit of area per unit of time.<sup>74</sup>

The schematic of a heat flux DSC instrument is shown in Figure 1.8 as follows.

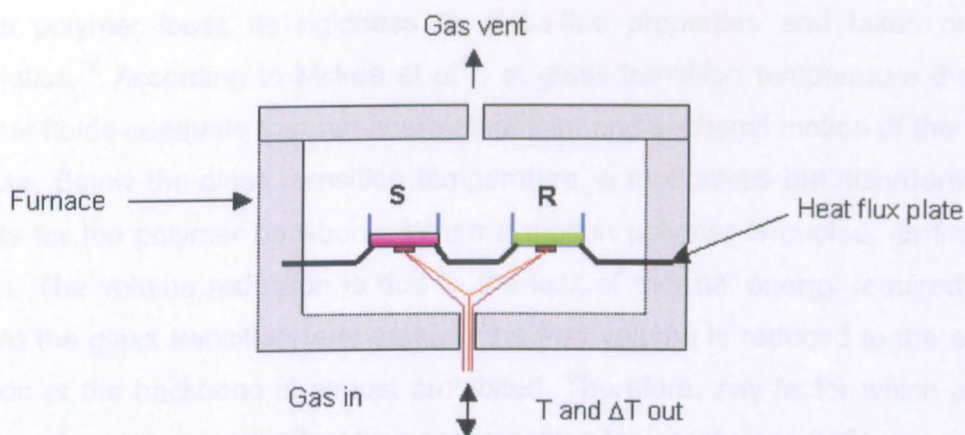


**Figure 1.8 Schematic of a heat-flux DSC instrument<sup>74</sup>**

In order to make a good thermal contact between the sample and the heat flux plate, flattened and small samples are contained in shallow pans. Balanced heating of the sample and the reference is achieved by using a metal of high thermal conductivity for construction of the furnace. A gas flow is also established in the cell containing the sample and the reference to assist in heat transfer and sweep the volatiles away. The control of the furnace, acquisition of the signal, and data processing are computer handled.<sup>74</sup> The result of a DSC experiment is a curve of heat flow versus temperature as shown in Figure 1.9;

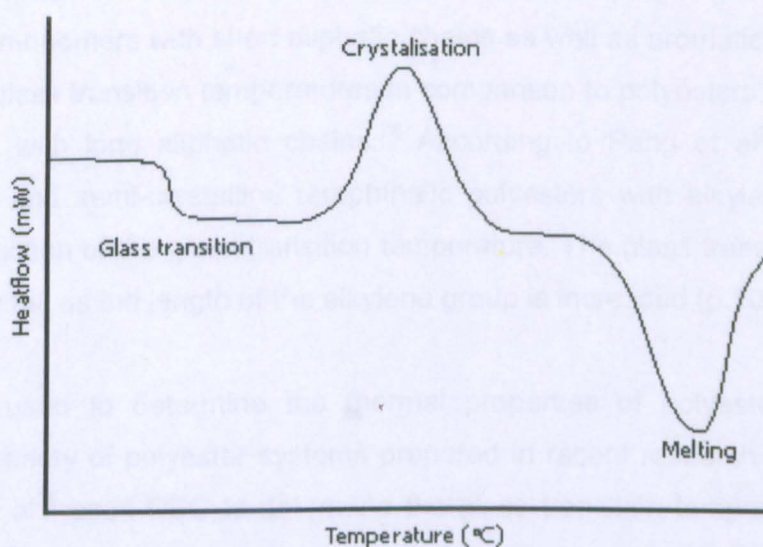


**Figure 1.9 Typical DSC curve of a polymer<sup>72</sup>**

In terms of polymers, DSC is widely employed to determine the melting point ( $T_m$ ) and the glass transition temperature ( $T_g$ ). The glass transition temperature is the temperature at

which the polymer loses its rigidity or glass-like properties and takes on rubbery characteristics.<sup>75</sup> According to Mckee et al<sup>41</sup>, at glass transition temperature the chain of the polymer holds adequate thermal energy that joint and sectional motion of the backbone could occur. Below the glass transition temperature, a motionless but disordered state of melt exists for the polymer backbone. When a molten polymer is cooled, its free volume decreases. The volume reduction is due to the lack of thermal energy required for chain mobility. At the glass transition temperature, the free volume is reduced to the extent that joint motion of the backbone is almost prohibited. Therefore, any factor which affects the free volume of a polymer, will affect its glass transition temperature (p.350).

The peak areas in a DSC curve are proportional to the amount of heat emitted from or taken up by the sample. Integration of the peak area corresponding to a specific transition gives the amount of the relevant heat energy. It can be seen, from the schematic DSC curve in Figure 1.9, that in addition to the crystallisation and melting point peaks, there is a base line shift. This shift corresponds to the glass transition temperature and is due to the change in the heat capacity of the sample.<sup>72,76</sup>

In terms of polyesters, the more important properties affected by the glass transition temperature include flexibility, hardness, and resistance properties.<sup>77</sup> Preparation of polyesters from monomers with short aliphatic chains as well as aromatic rings is known to result in higher glass transition temperatures in comparison to polyesters that are prepared from monomers with long aliphatic chains.<sup>78</sup> According to Pang et al<sup>39</sup> modification of aromatic, tough and semi-crystalline terephthalic polyesters with alkylene groups would result in the reduction of the glass transition temperature. The glass transition temperature would constantly fall as the length of the alkylene group is increased (p.1030).

DSC is widely used to determine the thermal properties of polyesters. The thermal properties of a variety of polyester systems prepared in recent research were determined by DSC. Tsai et al<sup>36</sup> used DSC to determine the glass transition temperature of a series of copolyesters synthesised from succinic acid, ethylene glycol and 1,3 propanediol. Wang et al<sup>31</sup> employed DSC to thermally characterise a series of biodegradable polyesters prepared from dimethyl terephthalate, 1,4 butanediol, and 1,4 cyclohexanedicarboxylic acid. Mehdipour-Ataie<sup>49</sup> and Ferré et al<sup>37</sup> determined the glass transition temperatures and melting points of polyester(amide)s by DSC.

With respect to industrial polyester coatings such as coil coatings, it is almost impossible to understand their performance without an appreciation of the physical state transitions that can occur in their base polyester resin. The relative values of glass transition temperature and melting point are the most important features in determining the eventual behaviour of polyesters. Other transitions may be present below the glass transition temperature or between the glass transition temperature and the melting point, but their effects are known to be little and less obvious.<sup>79</sup>

### 1.8.2 Size exclusion chromatography (SEC)

Among the factors which greatly influence the properties of polymeric materials inclusive of saturated polyester resins are molecular weight and molecular weight distribution. For a surface coating resin, sufficient strength and mechanical properties might favor a high molecular weight. But high molecular weights often lead to high melt viscosities which in turn cause drawbacks during both polymerisation and application. By correlation, molecular weight distribution can have a strong effect on the properties of molten polymers from a rheological point of view, with a broader molecular weight distribution leading to a higher melt viscosity.<sup>80</sup>

The molecules of a polymeric material, even those of a homopolymer with the same repeating unit, come in a variety of sizes with different weights. For linear polymers, the comprising molecules are of different chain lengths.<sup>81</sup> The molecular weight and the molecular weight distribution of a polymer are determined and described in certain terms. The most important of these include number average molecular weight ( $M_n$ ), weight average molecular weight ( $M_w$ ), and polydispersity index which is a measure of the molecular weight distribution.

The values of  $M_n$  and  $M_w$  and the polydispersity index are of great importance, "since they affect many of the characteristic physical properties of a polymer. Subtle batch-to-batch differences in these measurable values can cause significant differences in the end-use properties of a polymer"<sup>82</sup> inclusive of a surface coating resin. Some of these properties, applicable to surface coating resins include tensile strength, modulus of elasticity, hardness, impact strength, toughness, adhesive strength, cure time, stress-crack resistance, and as mentioned, the melt viscosity.<sup>82</sup>

The number average molecular weight is a common method for determination of the molecular weight of polymers. It is determined by measuring the molecular weight of  $N$  polymer molecules. The weights are then summed and divided by  $N$  <sup>81,83</sup>

$$M_n = \frac{\sum_i N_i M_i}{\sum_i N_i}$$

An alternative approach towards the molecular weight determination of a polymer is the weight average molecular weight. This is calculated from <sup>81,83</sup>

$$M_w = \frac{\sum_i N_i M_i^2}{\sum_i N_i M_i}$$

where  $N_i$  is the number of molecules of molecular weight  $M_i$ . <sup>83,84</sup>

A measure of the molecular weight distribution of a certain polymer is called polydispersity index. The polydispersity index designates the distribution of individual molecular weights in a batch of polymers. The term polydisperse, applies to a polymer which exists over a wide range of molecular weights. <sup>85,86</sup>

The polydispersity index ( $D$ ) is calculated from <sup>85</sup>

$$D = \frac{M_w}{M_n}$$

where  $M_w$  is the weight average molecular weight and  $M_n$  is the number average molecular weight. The value of  $D$  is greater than one in the majority of cases, but as the polymer chains approach uniform chain length, the value of  $D$  draws near unity. The polydispersity index mainly depends on the mechanism of polymerisation, the number of reactants present, and the reactant ratio. The values of  $D$  are in the region of two for typical step growth polymerisations. <sup>82</sup>



Today, the only proven technique for characterising the complete molecular weight distribution of a polymer is gel permeation chromatography or GPC. GPC can determine  $M_n$ ,  $M_w$ , and the fundamental molecular weight distribution.<sup>82</sup> GPC is a size exclusion chromatographic (SEC) technique in which particles are separated based on their effective solution size which is technically referred to as the hydrodynamic volume.<sup>87,88</sup>

The different elution or filtration rates of variously sized molecules through a stationary phase constitutes the principle of molecule separation on size basis. For the achievement of such separation, all the molecules have to be simultaneously loaded, so that the same size molecules are eluted together. In apparatus terms, size exclusion chromatography takes place in a column packed with extremely small polymeric porous beads with pores of different sizes. This packing is the stationary phase and is known as a gel.<sup>87-89</sup>

The mobile phase is a solvent which is continuously pumped into the system by means of a solvent delivery system.<sup>88</sup> A basic gel permeation chromatograph is schematically shown in Figure 1.10.

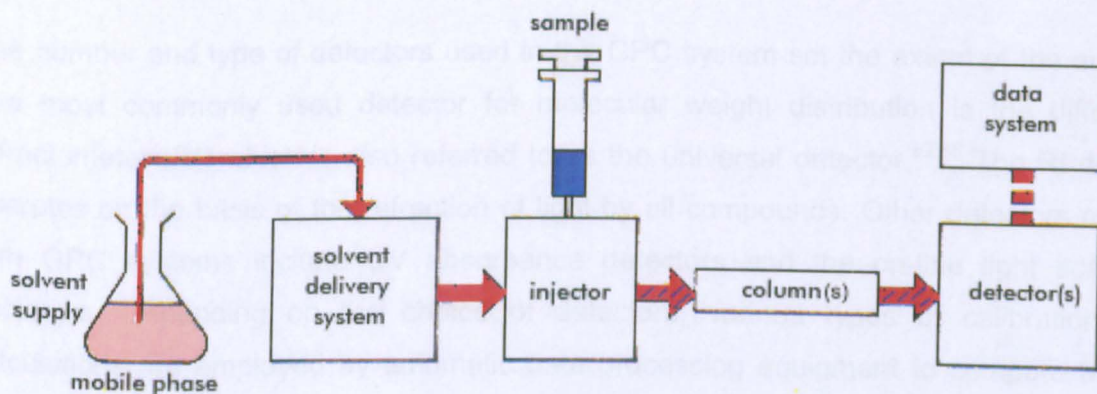


**Figure 1.10 Schematic of a basic gel permeation chromatograph<sup>82</sup>**

The sample is then injected into the mobile phase. The sample solution is carried through the GPC column by the flow of the mobile phase. The larger molecules, cannot fit into the gel pores and are therefore eluted faster than the smaller molecules.<sup>88</sup> The said separation process is shown in Figure 1.11.

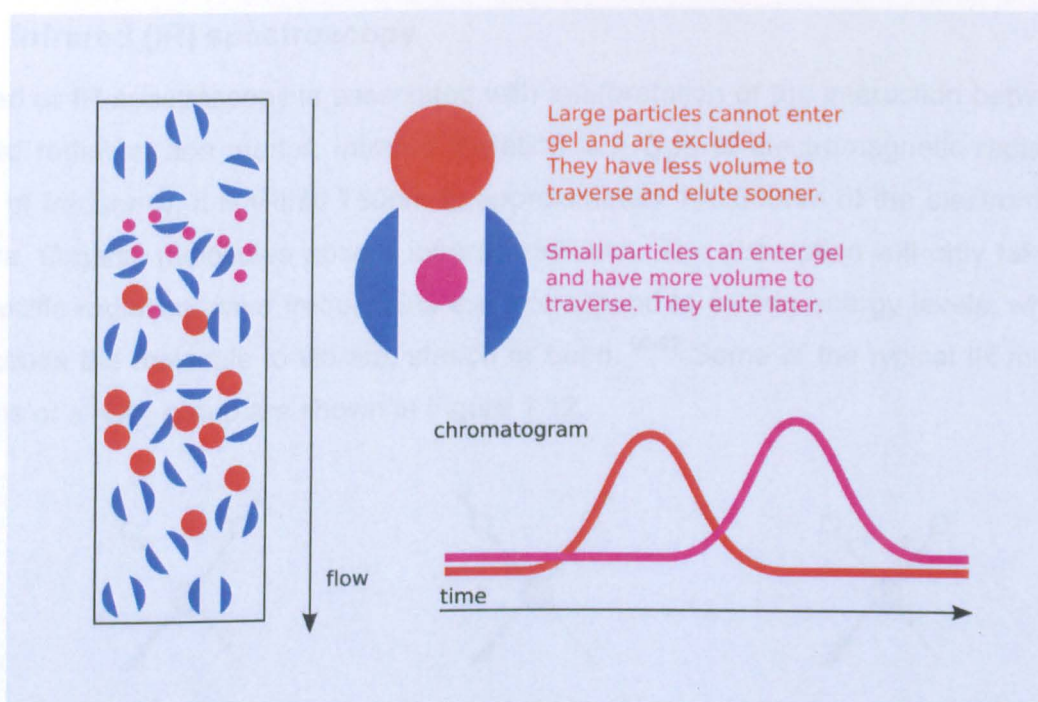


**Figure 1.11 An illustration of particle separation in size exclusion chromatography<sup>87</sup>**

The number and type of detectors used in the GPC system set the extent of the analysis. The most commonly used detector for molecular weight distribution is the differential refractometer (RI) which is also referred to as the universal detector.<sup>82,88</sup> The RI detector operates on the basis of the refraction of light by all compounds. Other detectors coupled with GPC systems include UV absorbance detectors and the on-line light scattering detectors. Depending on the choice of detectors, various types of calibrations and calculations are employed by automatic data processing equipment to compute  $M_n$ ,  $M_w$ , and polydispersity index.<sup>82,88</sup>

Polyesters are commonly characterised by size exclusion chromatography. Amongst recent research in which polyesters were characterised by size exclusion chromatography, those of Wang et al<sup>23,31</sup>, Tsai et al<sup>36</sup> and McKee et al<sup>41</sup> worth mentioning. McKee et al<sup>41</sup> studied molecular weight of polyesters with respect to the content of multifunctional monomers. According to the results of size exclusion chromatography, McKee et al<sup>41</sup> showed that both the molecular weight distribution and the weight average molecular weight of polyesters could be increased through the introduction of trifunctional monomers such as trimethylol propane (p.513).

### 1.8.3 Infrared (IR) spectroscopy

Infrared or IR spectroscopy is associated with interpretation of the interaction between the infrared radiation and matter. Infrared radiation is a type of electromagnetic radiation. In terms of frequency, it is within 780nm to approximately 100,000nm of the electromagnetic spectra. Organic molecules absorb infrared radiation. The absorption will only take place for specific radiation wave frequencies that correspond to certain energy levels, which will then cause the molecule to vibrate, stretch or bend.<sup>90-92</sup> Some of the typical IR molecular motions of a  $-\text{CH}_2$  group are shown in Figure 1.12.

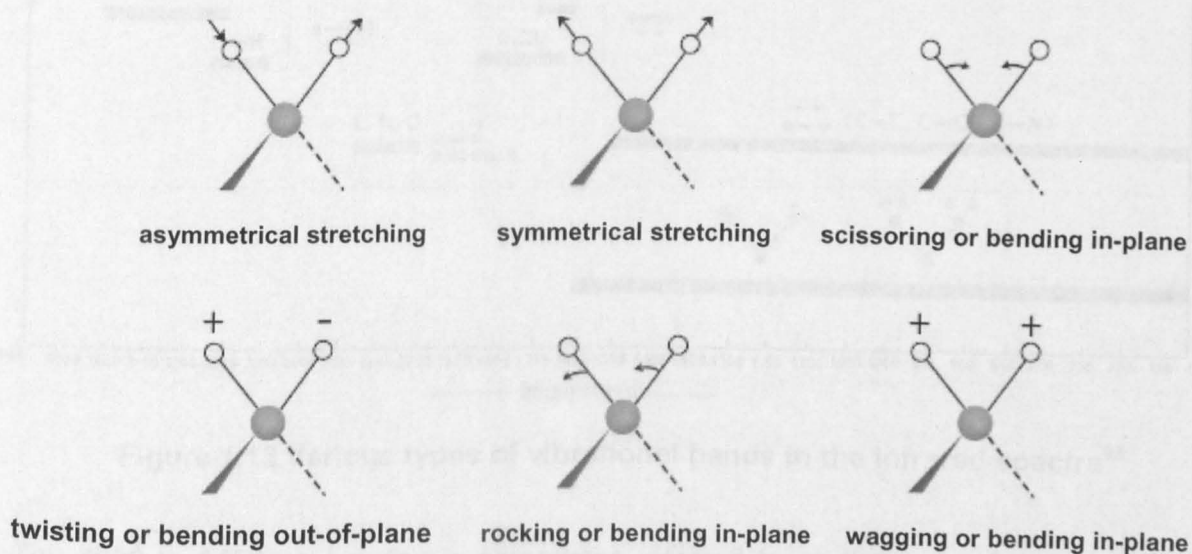


**Figure 1.12 IR stretching and bending vibration types of a  $-\text{CH}_2$  group<sup>90,91</sup>**

The vibrating bond of a radiated molecule will absorb the energy only if both the frequency of the light and that of the bond itself are the same. When the infrared radiation is absorbed, the magnitude of the vibrations matching that of the infrared light will increase. As a consequence, the bond connecting the two atoms will compress or stretch to a greater extent. By knowing the fact that each infrared radiation frequency corresponds to a certain molecular motion, interpretation of both molecular motions and types of bonds or functional groups present from a molecule's IR spectra is possible.<sup>90-92</sup> Correlation charts are available in this regard.

In infrared spectroscopy, the radiation wave frequencies are often expressed as wave-numbers ( $\text{cm}^{-1}$ ), which is the inverse of the wavelength as shown in the following;<sup>90</sup>

$$\bar{\nu} \text{ (wave number in cm}^{-1}\text{)} = \frac{1}{\lambda \text{ (wavelength in cm)}}$$

A summary of general regions of the infrared spectra in which various types of vibrational bands are observed is provided in Figure 1.13.

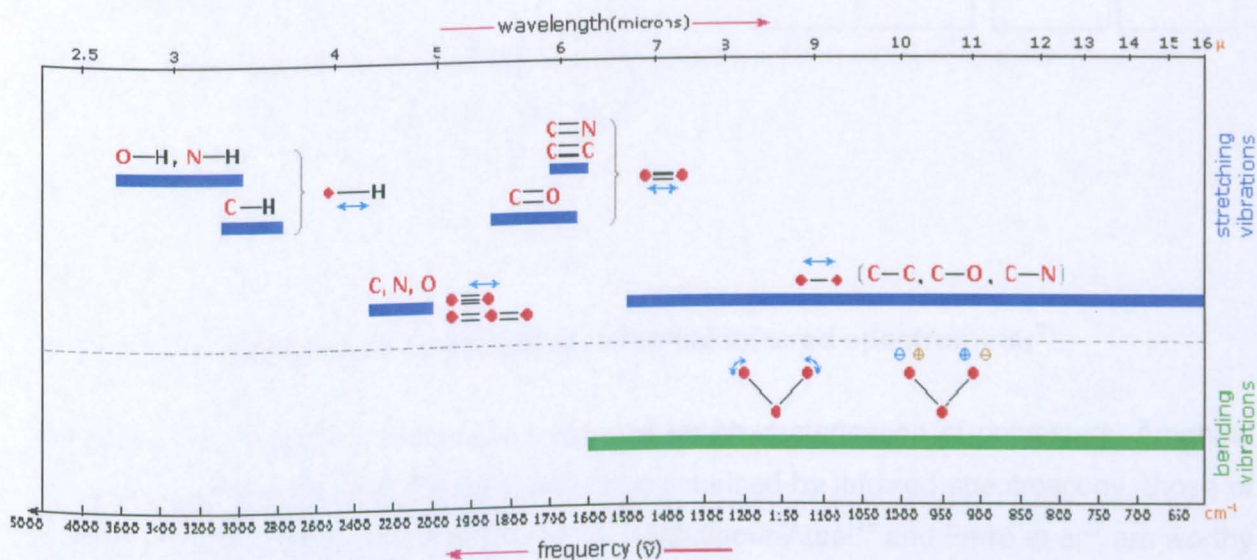


Figure 1.13 Various types of vibrational bands in the infrared spectra<sup>93</sup>

The 4000 to 1450  $\text{cm}^{-1}$  region is sometimes referred to as the group frequency region. Absorption bands in this region are usually due to stretching vibrations of diatomic units. The infrared spectra in the 1450 to 600  $\text{cm}^{-1}$  is often called the fingerprint region due to unique patterns that are observed there.<sup>93</sup>

During the operation of a typical IR spectrometer, a beam of infrared light is produced. This beam is split into two beams with one passing through the sample and the other passing through the reference. The reference is often the solvent in which the sample is dissolved in. Both beams are reflected back to the splitter. The splitter alternates the beams prior to their entrance to the detector. After the detection is done, signals are compared and Fourier transformed in the processor and a spectra is obtained. The data is Fourier transformed to collect the data over the whole spectral range simultaneously.<sup>91,92</sup> A typical infrared spectrometer is schematically shown in Figure 1.14.

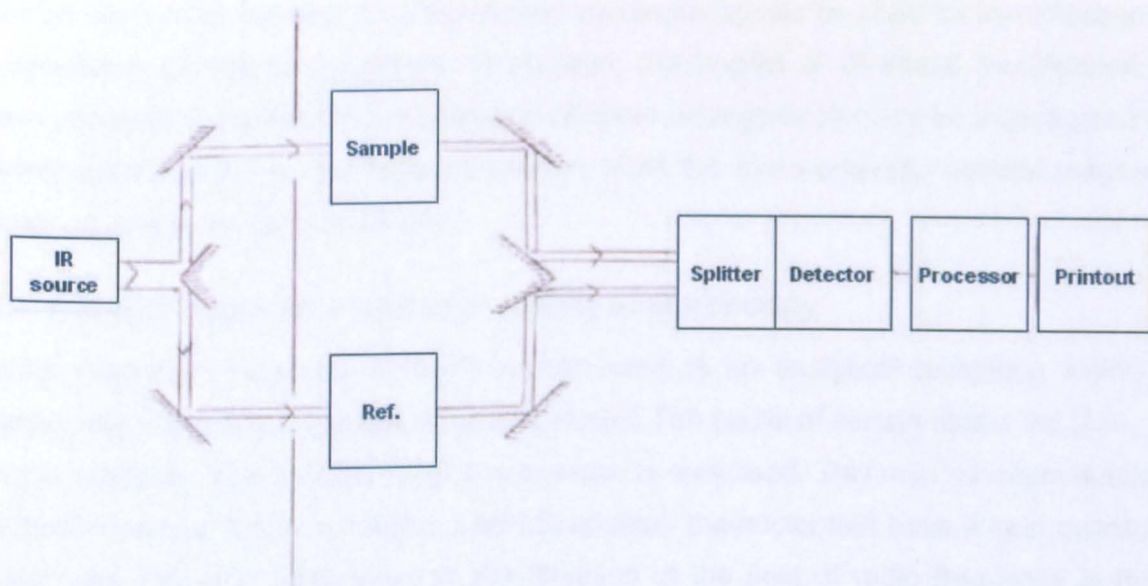


Figure 1.14 Schematic of a typical infrared spectrometer<sup>91</sup>

Infrared spectroscopy is commonly employed for characterisation of polyesters. Amongst recent research in which polyesters were characterised by infrared spectroscopy, those of Johansson and Johansson<sup>7</sup>, Wang et al<sup>23,31</sup>, Mehdipour-Ataei<sup>49</sup> and Ferré et al<sup>37</sup> are worthy of a mention. The infrared spectra of a poly(ester amide) synthesised by Ferré et al<sup>37</sup> from 1,4-butanediol, adipic acid and 6-aminohexanoic acid is shown in Figure 1.15.

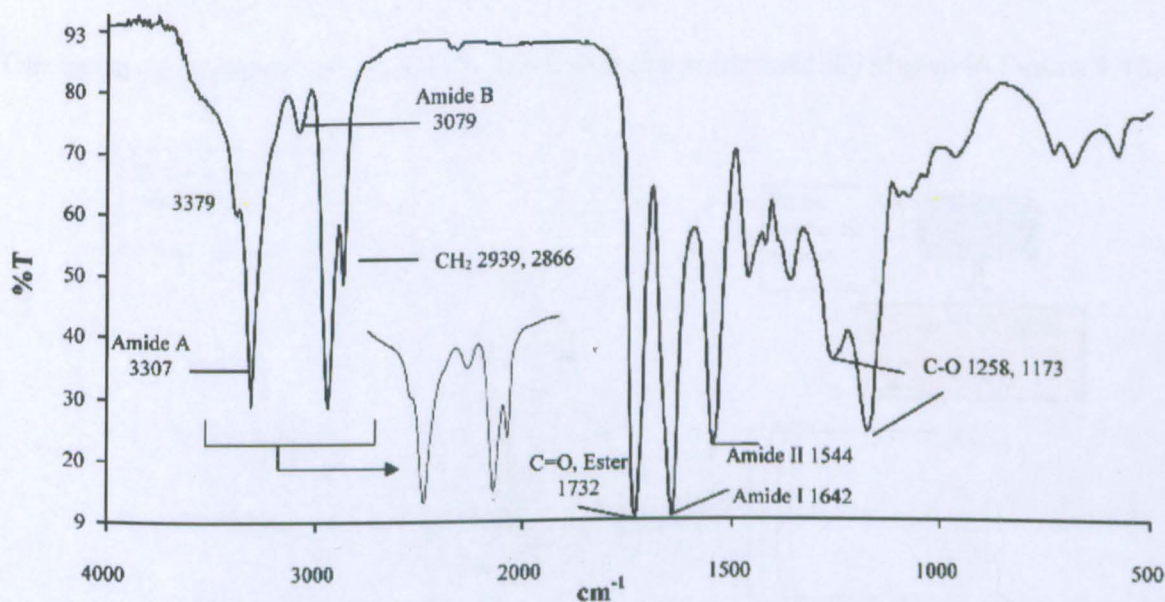


Figure 1.15 Infrared spectra of poly(ester amide) derived from 1,4-butanediol, adipic acid and 6-aminohexanoic acid<sup>37</sup>

It can be seen, from Figure 1.15, that infrared spectroscopy can be used for identification of the functional groups of polyesters. In addition, the impact of chemical modification of known polyester compositions on alteration of chain arrangements may be investigated by infrared spectroscopy. In this regard however, often the more powerful nuclear magnetic resonance spectroscopy is employed.

#### 1.8.4 Nuclear magnetic resonance (NMR) spectroscopy

Nuclear magnetic resonance or NMR spectroscopy is an analytical technique which is based on the magnetic properties of specific nuclei. The nuclei of certain atoms act like mini bar magnets. These nuclei have a spin which is quantised. This spin quantum number has distinct values. When a magnetic field is applied, the nuclei that have a spin quantum number of over zero will align themselves in the direction of the field. If radio frequency is then applied, the nuclei will turn over 180 degrees and align themselves in the opposite direction. The radio frequency at which the turn over takes place depends on the electronic environment of the nucleus.<sup>94,95</sup>

Some of the more important NMR active nuclei include protons (i.e. hydrogen), carbon-13, fluorine-19, and nitrogen-15. Oxygen-16 and carbon-12 are NMR inactive. The extent of the sensitivity of each type of nuclei to NMR is defined in its gyromagnetic ratio. Nuclei with larger gyromagnetic ratio have higher sensitivity to NMR.<sup>94,95</sup>

The basic components of a NMR spectrometer are schematically shown in Figure 1.16.

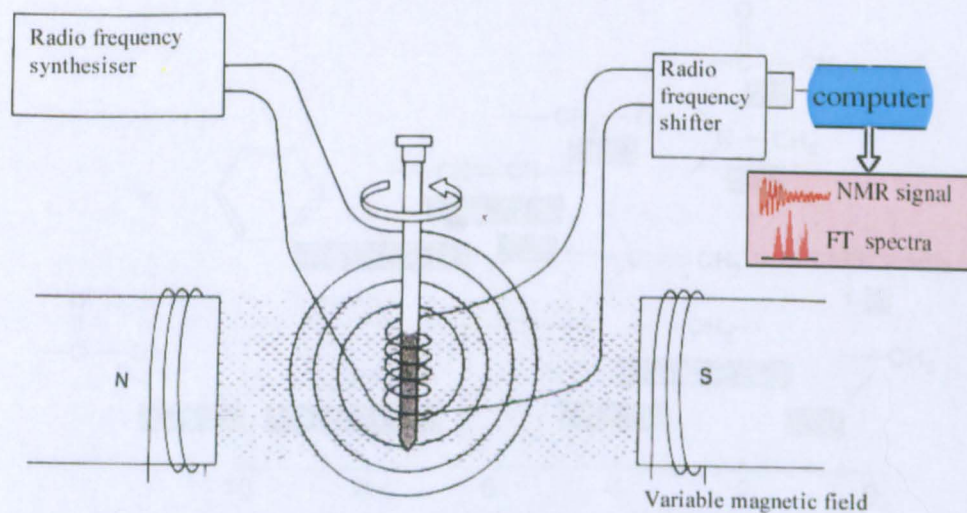


Figure 1.16 Schematic of a basic NMR spectrometer<sup>96,97</sup>

The sample to be investigated by the NMR spectrometer is dissolved in a proton free solvent. Deuterated solvents such as deuterated chloroform ( $\text{CDCl}_3$ ) are usually employed. The sample is placed in a cell, which is a tiny glass tube. The cell is placed in the spectrometer's magnetic field which is produced by a superconducting magnet. In order to obtain a uniform magnetic field, the sample is shimmed along its own axis. The magnetic field polarises the nuclei and aligns them parallel to the field axis. Within the magnetic field, a coil exists which is attached to the radio frequency synthesiser. This coil provides the required energy for turning over and changing the direction of the polarised nuclei. The sample is pulsed with multiple radio frequencies at certain times. For a normal sample, sixteen pulses are usually applied. The time taken for the nuclei to turn back to the original magnetic field direction is recorded by the radio frequency shifter. The data in the time domain are then Fourier transformed into the frequency domain in parts per million (ppm) and displayed as resonance signals or peaks in a spectrum.<sup>96,97</sup>

Interpretation of NMR spectra is done in a number of ways and is based on the fact that only the nuclei in different electronic environments give rise to different signals. The more important interpretation methods include spectral shift, spin-spin coupling, and integration.<sup>94</sup> Spectral shift provides information about the location of the nucleus that is giving rise to the signal or peak. Proton ( $^1\text{H}$ ) NMR chemical shifts of various structures are provided in Figure 1.17.

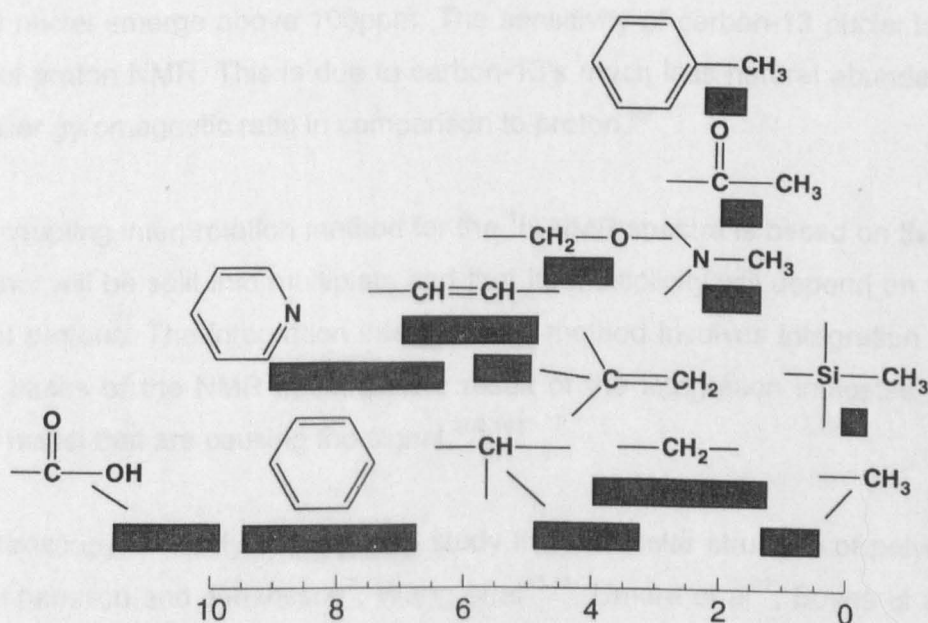


Figure 1.17 Proton NMR chemical shifts of various structures in ppm<sup>98</sup>

Aliphatic protons give rise to signals below 6ppm. Signals from aromatic protons emerge between 6 and 9ppm. Above 15ppm, no signals usually appear in a proton NMR spectrum.<sup>98</sup> Carbon-13 NMR chemical shifts of various structures are shown in Figure 1.18.

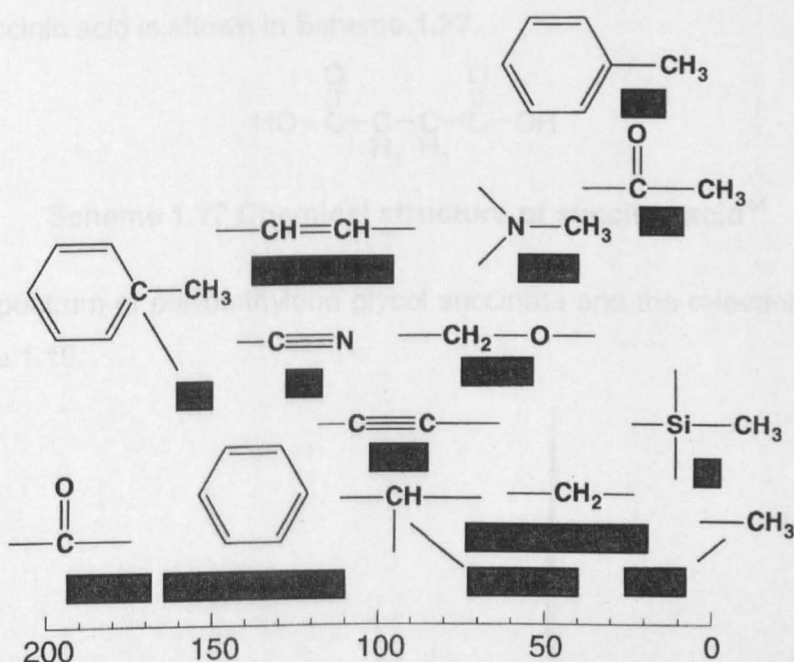


Figure 1.18 Carbon-13 NMR chemical shifts of various structures in ppm<sup>99</sup>

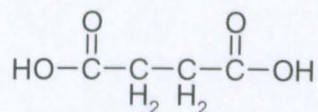
Aliphatic carbon-13 nuclei give rise to peaks below 100ppm. The peaks of aromatic carbon-13 nuclei emerge above 100ppm. The sensitivity of carbon-13 nuclei is much less than that of proton NMR. This is due to carbon-13's much less natural abundance as well as its smaller gyromagnetic ratio in comparison to proton.<sup>99</sup>

Spin-spin coupling interpretation method for the  $^1\text{H}$  NMR spectra is based on the fact that a proton signal will be split into multiplets and that its multiplicity will depend on the number of adjacent protons. The integration interpretation method involves integration of the area under the peaks of the NMR spectra. The result of the integration indicates the relative number of nuclei that are causing the signal.<sup>100,101</sup>

NMR spectroscopy is widely employed to study the molecular structure of polyesters. The works of Johansson and Johansson<sup>7</sup>, Wang et al<sup>23,31</sup>, Umare et al<sup>27</sup>, Boyes et al<sup>29</sup>, Tsai et al<sup>36</sup>, Ferré et al<sup>37</sup>, Yoon et al<sup>48</sup>, Mehdipour-Ataie<sup>49</sup> and Oh and Kim<sup>102</sup> are some of the recent research in which polyesters were characterised by NMR spectroscopy. In what

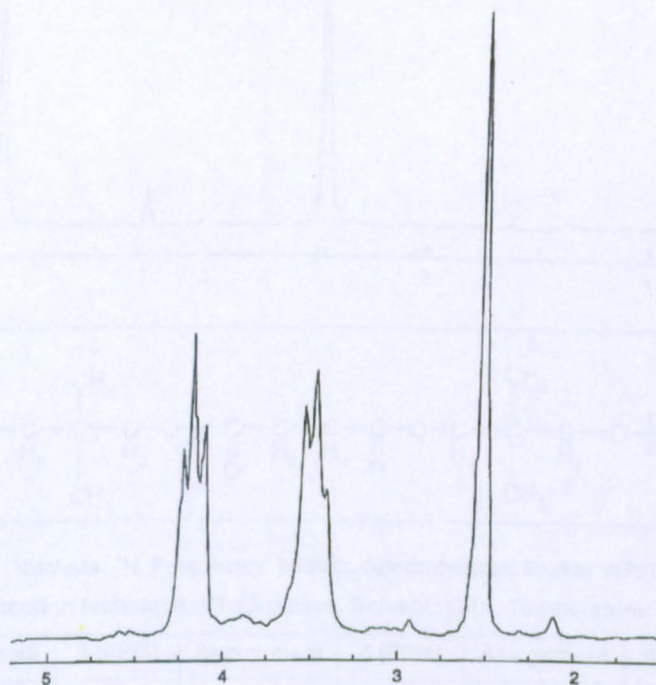


follows, the  $^1\text{H}$  NMR and  $^{13}\text{C}$  NMR spectra of two polyester systems and the relevant interpretation are provided. The polyesters concerned are polydiethylene glycol succinate and polyneopentyl glycol succinate. The chemical structures of neopentyl glycol and diethylene glycol were shown in Schemes 1.10 and 1.14 respectively. The chemical structure of succinic acid is shown in Scheme 1.27.



**Scheme 1.27 Chemical structure of succinic acid<sup>44</sup>**

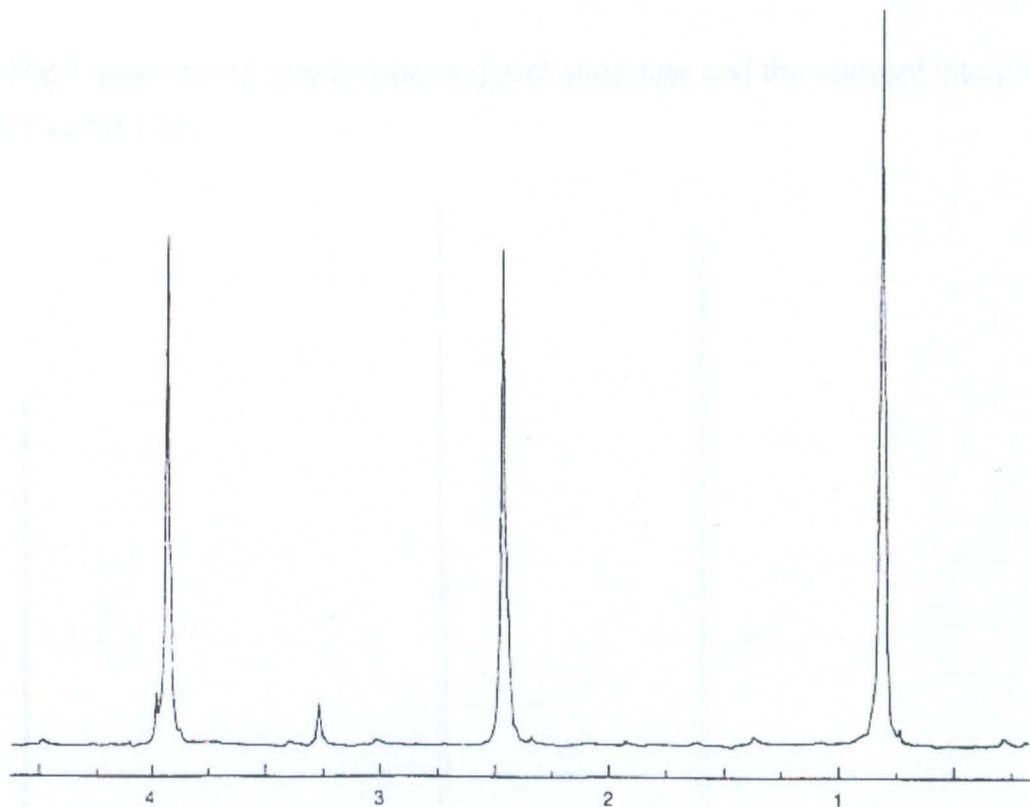
The  $^1\text{H}$  NMR spectrum of polydiethylene glycol succinate and the relevant interpretation is shown in Figure 1.19.



$-\text{O}-\left[ \overset{\text{O}}{\parallel}{\text{C}}-\underset{\text{H}_2}{\text{C}}-\underset{\text{H}_2}{\text{C}}-\overset{\text{O}}{\parallel}{\text{C}}-\text{O}-\underset{\text{H}_2}{\text{C}}-\underset{\text{H}_2}{\text{C}}-\text{O}-\underset{\text{H}_2}{\text{C}}-\underset{\text{H}_2}{\text{C}}-\text{O}- \right]_n-\overset{\text{O}}{\parallel}{\text{C}}-$					
<span style="color: red;">1</span> <span style="color: red;">2</span> <span style="color: red;">3</span> <span style="color: red;">4</span> <span style="color: red;">4</span> <span style="color: red;">3</span>					
<b>Analysis details</b>					
Nucleus: $^1\text{H}$ , Frequency: 80MHz, Spectrometer: Bruker WP80,					
Detection technique: FT-10 pulses, Solvent: $\text{C}_6\text{D}_6$ , Temperature: $80^\circ\text{C}$					
$\delta$ (PPM)	Assignment	$\delta$ (PPM)	Assignment	$\delta$ (PPM)	Assignment
2.50	1,2	3.45	4	4.15	3

**Figure 1.19  $^1\text{H}$  NMR spectrum of polydiethylene glycol succinate and related assignments<sup>103</sup>**

The  $^1\text{H}$  NMR spectrum of polyneopentyl glycol succinate and the relevant interpretation is shown in Figure 1.20.



$\delta$ (PPM)	Assignment	$\delta$ (PPM)	Assignment	$\delta$ (PPM)	Assignment	$\delta$ (PPM)	Assignment
0.85	3,6	2.48	1	3.25	5	3.92	2,4

Analysis details							
Nucleus: $^1\text{H}$ , Frequency: 80MHz, Spectrometer: Bruker WP80,							
Detection technique: FT-10 pulses, Solvent: $\text{C}_6\text{D}_6$ , Temperature: 80°C							

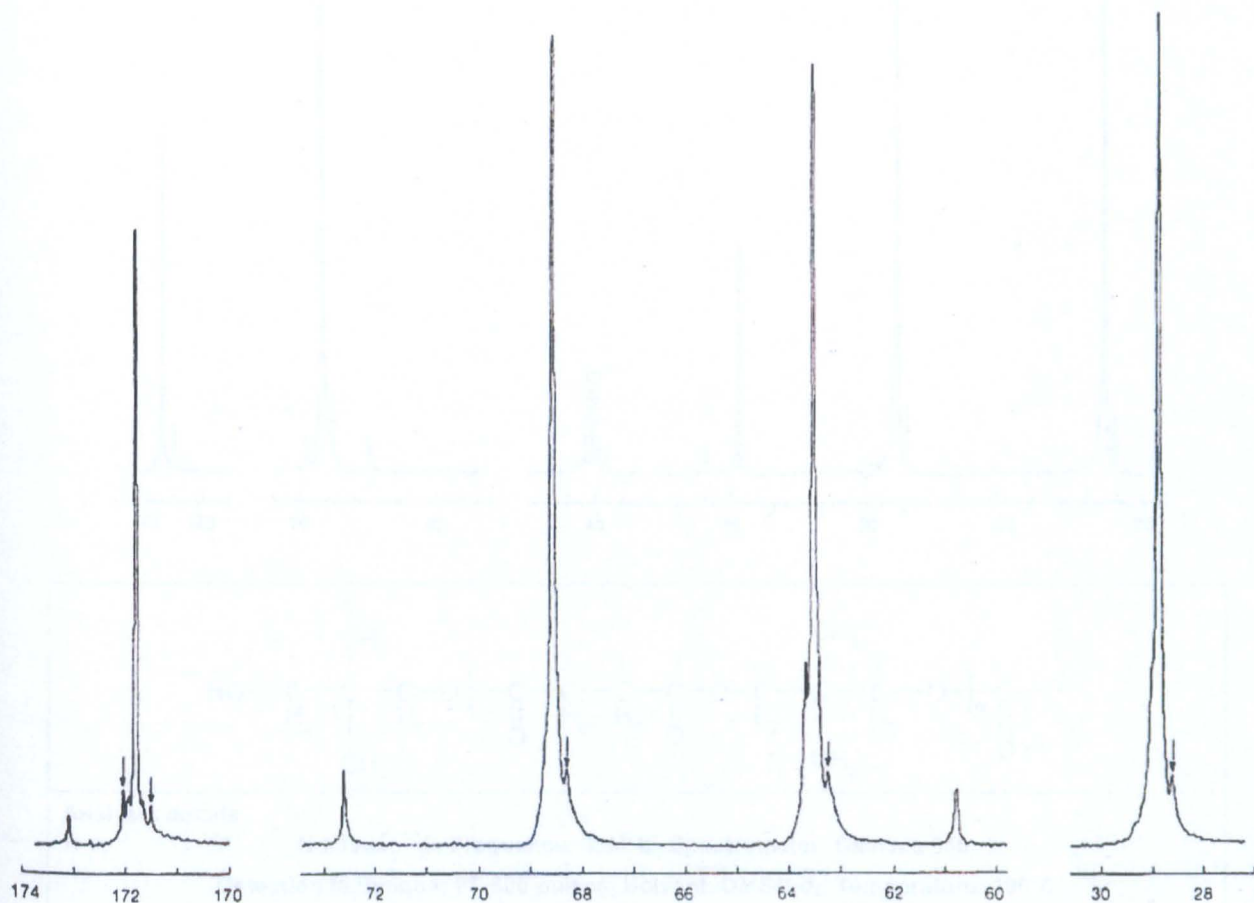
Chemical structure with assignments							
6	$\text{HO}-\text{C}(\text{H}_2)-\text{C}(\text{CH}_3)_2-\text{C}(\text{H}_2)-\text{O}-$		$\left[ \text{C}(=\text{O})-\text{C}(\text{H}_2)-\text{C}(\text{H}_2)-\text{C}(=\text{O})-\text{O}-\text{C}(\text{H}_2)-\text{C}(\text{CH}_3)_2-\text{C}(\text{H}_2)-\text{O} \right]_n$		$-\text{C}(=\text{O})-$		3
	5	4	1	1	2	2	

Figure 1.20  $^1\text{H}$  NMR spectrum of polyneopentyl glycol succinate and related assignments<sup>104</sup>

It can be seen, from the  $^1\text{H}$  NMR spectra in Figures 1.19 and 1.20, that only the peaks that emerged in the region of 2.48-2.50ppm were similar in terms of frequency and intensity. The said peaks pertained to the specified protons of succinic acid that was common in both of the polyesters concerned. Replacing diethylene glycol with neopentyl glycol had resulted in the emergence of peaks with different frequencies in the spectrum of polyneopentyl

glycol succinate. This phenomenon was definitely due to the different electronic environment of the specified protons of neopentyl glycol in Figure 1.20.

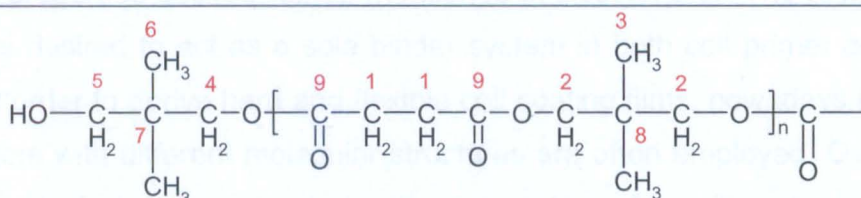
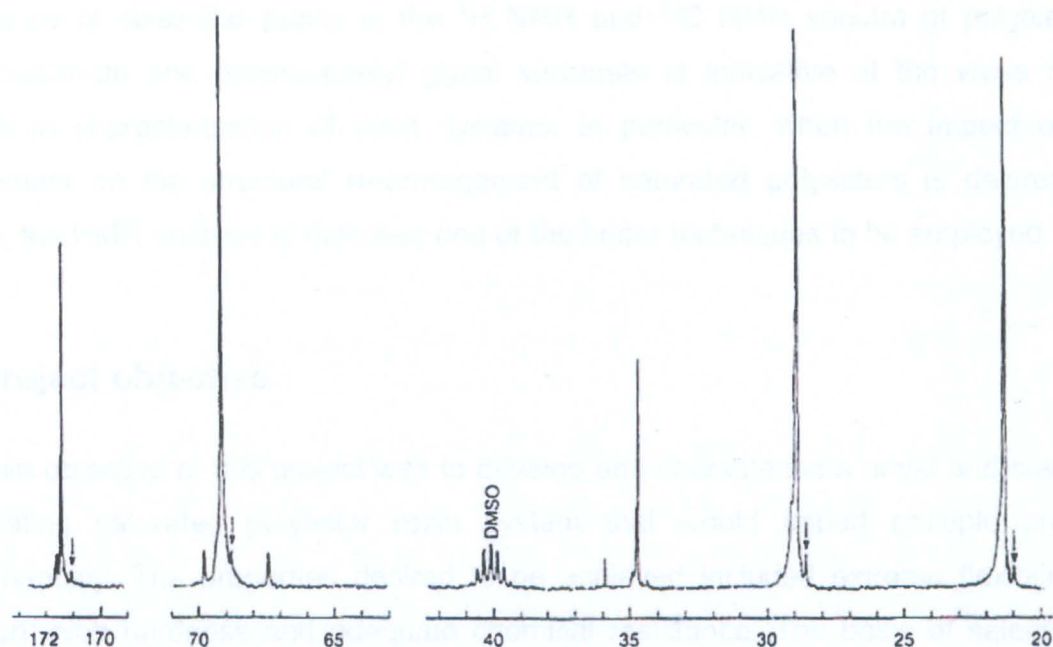
The  $^{13}\text{C}$  NMR spectrum of polydiethylene glycol succinate and the relevant interpretation is shown in Figure 1.21.



$\delta$ (PPM)	Assignment	$\delta$ (PPM)	Assignment	$\delta$ (PPM)	Assignment	$\delta$ (PPM)	Assignment
28.92	1,2	60.74	6	63.62	3	68.53	4
72.53	5	171.82	7	173.15	-COOH	-----	-----

Figure 1.21  $^{13}\text{C}$  NMR spectrum of polydiethylene glycol succinate and related assignments<sup>105</sup>

The  $^{13}\text{C}$  NMR spectrum of polyneopentyl glycol succinate and the relevant interpretation is shown in Figure 1.22.



#### Analysis details

Nucleus:  $^{13}\text{C}$ , Frequency: 88MHz, Spectrometer: Caméca 350,  
 Detection technique: FT-500 pulses, Solvent: DMSO- $d_6$ , Temperature: 100°C

$\delta$ (PPM)	Assignment	$\delta$ (PPM)	Assignment	$\delta$ (PPM)	Assignment	$\delta$ (PPM)	Assignment
21.07	3,6	28.68	1	34.44	8	35.85	7
67.35	5	68.88	2	69.6	4	171.15	9

**Figure 1.22**  $^{13}\text{C}$  NMR spectrum of polyneopentyl glycol succinate and related assignments<sup>106</sup>

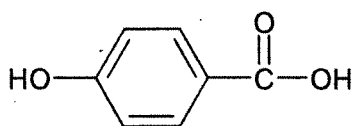
Similar to the  $^1\text{H}$  NMR spectra of the polyesters concerned, the relevant  $^{13}\text{C}$  NMR spectra were also of different patterns because of replacement of diethylene glycol with neopentyl glycol. Signals pertaining to the specified carbons of succinic acid, common in both of the polyesters, had appeared in the regions of 28.68-28.92ppm and 171.15-173.15ppm.

However, due to the different magnetic properties of carbons of diethylene glycol and neopentyl glycol, dissimilar signals were present in the related spectra.

Emergence of dissimilar peaks in the  $^1\text{H}$  NMR and  $^{13}\text{C}$  NMR spectra of polydiethylene glycol succinate and polyneopentyl glycol succinate is indicative of the value of NMR analysis in characterisation of such systems. In particular, when the impact of glycol replacement on the structural re-arrangement of saturated polyesters is desired to be studied, the NMR analysis is definitely one of the better techniques to be employed.

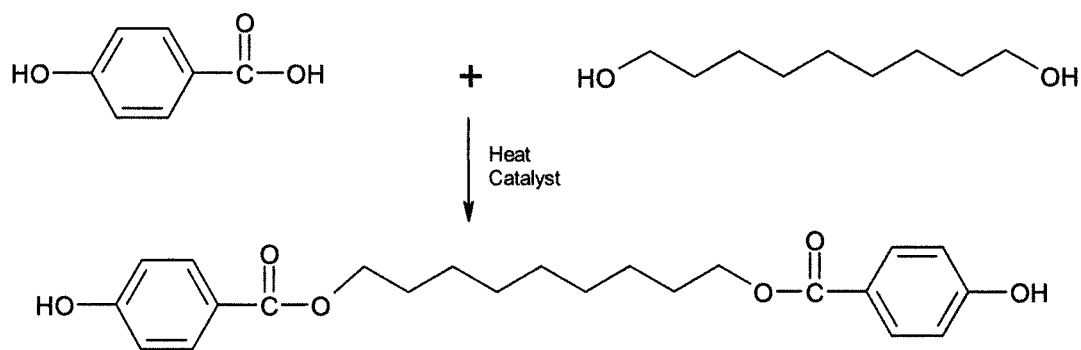
## 1.9 Project objective

The main objective of this project was to develop and characterise a novel and standalone coil coating saturated polyester resin system that would impart multiple properties simultaneously. The properties desired to be achieved included extreme flexibility, high adhesion, high hardness and adequate chemical resistance. The basis of selection with respect to the properties desired will be mentioned in Section 2.6. The resin system to be developed was desired to act as a sole binder system in both coil primer coating and coil top coating. In order to derive hard and flexible coil coating films, nowadays a mixture of up to five polyesters with different molecular structures are often employed. Overall, research into development of singular saturated polyester systems for coil coatings with balanced hardness, flexibility and chemical resistance appears to be limited. Amongst the works published in this regard, that of Boyes et al<sup>29,107</sup> was found to be more relevant and has been considered. Boyes et al<sup>29,107</sup> made an effort to promote the hardness of a linear and flexible hydroxyl functional coil coating polyester. Thus, *p*-hydroxybenzoic acid was grafted to a hydroxyl functional polyester through direct esterification. The chemical structure of *p*-hydroxy benzoic acid is shown in Scheme 1.28.



**Scheme 1.28 Chemical structure of *p*-hydroxy benzoic acid<sup>107</sup>**

Based on relevant  $^1\text{H}$  NMR and  $^{13}\text{C}$  NMR spectra, Boyes et al<sup>29</sup> showed that *p*-hydroxy benzoic acid did react with the hydroxyl functionalities of the polyester, but the reaction did not proceed to completion (p.139). The proposed reaction scheme is shown as follows;



**Scheme 1.29 Proposed reaction scheme for grafting of *p*-hydroxy benzoic acid to a linear and hydroxyl functional polyester via direct esterification<sup>29</sup>**

Boyes et al<sup>107</sup> concluded that grafting of *p*-hydroxy benzoic acid to the hydroxyl functional polyester resulted in the simultaneous augmentation of both hardness and flexibility. It can be assumed that the aromatic moiety of *p*-hydroxy benzoic acid in the backbone could have resulted in increased hardness. However, this effect could only be seen at low bake conditions for the coil coating. The coil coating derived from the *p*-hydroxy benzoic acid grafted polyester had to be cured at 175°C for 40 minutes to compensate between hardness and flexibility effectively. As mentioned in Section 1.2, coil coatings are generally cured at 200-350°C for 20-60 seconds. Thus, the resin system developed by Boyes et al<sup>29,107</sup> could not be employed as a sole binder system for coil coatings. Boyes et al<sup>107</sup> reported that the melting and sublimation of the unreacted portion of *p*-hydroxy benzoic acid at coil coating curing conditions, resulted in a significant drop in the performance of the coil coating (p.150).

In this project, approaches that would involve the modification of hydroxylated aliphatic polyesters through grafting of aromatic moieties will not be taken. Instead, effort will be made to develop a saturated polyester resin system that would compromise between hardness and flexibility in the first place and at coil coating curing conditions. The effort will focus on deriving the standalone coil coating saturated polyester resin from the polyols and dicarboxylic acids introduced in Section 1.6. Synthesis would be through direct esterification. The direct esterification synthesis method was introduced in Section 1.3. It was envisaged that the project would take the following route.

- 1- Formulation design and lab-scale synthesis of a saturated polyester resin.

- 2- The polyester synthesised would be incorporated as the sole binder system in a particular coil top coating system. The polyester concerned would act as a replacement for two competitor polyester resins. The coil top coating containing the two competitor saturated polyesters would be set as control.
- 3- The coil top coating film derived from the polyester synthesised would be evaluated in comparison to control. Procedures for coating film evaluation will be discussed in detail in Section 2.5.1.
- 4- If the resulting coil top coating film of the polyester prepared was not adequately hard and flexible, particularly in comparison to control, a new polyester formulation would be designed and synthesised.
- 5- Steps 2-4 would be repeated until a polyester system was obtained that could contribute to an efficient balance between hardness and flexibility in the coil top coating.
- 6- If a polyester was derived that could act as a singular binder system in the coil top coating, it would then be incorporated as the sole binder system in a particular coil primer coating. The polyester concerned would act as a replacement for three competitor polyester resins in the primer coating. The coil primer coating containing three competitor saturated polyesters would be set as control.
- 7- The coil primer coating and the coil top coating films derived solely from the polyester concerned would be evaluated in comparison to the controls.
- 8- If the resulting coil primer coating and coil top coating films were found to be inefficient in terms of hardness and flexibility in comparison to the controls, a new polyester formulation would be designed and synthesised.
- 9- Steps 6-8 would be repeated until a polyester system was obtained that could contribute to an efficient balance between hardness and flexibility in both of the coil primer coating and coil top coating.
- 10- The standalone coil top coating and coil primer coating saturated polyester to be developed and other precursors to be synthesised in the course of the project would be characterised through determination of the following :
  - a) Glass transition temperature by differential scanning calorimetry
  - b) Molecular structure by  $^{13}\text{C}$  NMR,  $^1\text{H}$  NMR, and FTIR
  - c) Molecular weight characteristics by size exclusion chromatography for lab, pilot, and industrial scale reproductions of the standalone universal resin to be developed.

## CHAPTER 2 - EXPERIMENTAL

### 2.1 Chemicals and lab equipment

Information regarding the chemicals and the lab equipment used are provided in Sections 2.1.1 to 2.1.4.

#### 2.1.1 Chemicals used for the synthesis of saturated polyester resins for coil coating

A list of the chemicals used for the synthesis of saturated polyester resins for coil coating is provided in Table 2.1.

**Table 2.1 Chemicals used for the synthesis of saturated polyester resins for coil coating (continued on page 58)**

MATERIAL	SUPPLIER	FUNCTION
Pripol 1022	<u>Croda Europe</u> PO Box 2 2800 AA Gouda Buurtje 1 2802 BE Gouda The Netherlands Tel +31 (0)182 542911 Fax +31 (0)182 542250 email: <a href="mailto:polymers.eu@croda.com">polymers.eu@croda.com</a>	Dimer fatty acid
Adipic acid	<u>Radici Chimica SpA</u> Via G. Fauser, 50 IT - 28100 Novara- Italy Phone +39 0321 693111 Fax +39 0321 693201	Aliphatic diacid
Isophthalic acid	<u>KP Chemical Corp.</u> International public company 427-3 Sanggae-dong, Nam-gu, Ulsan, 680 180, South Korea Tel +82 052 278 3400, Fax +82 052 272 3800, web: <a href="http://www.kpchem.co.kr">http://www.kpchem.co.kr</a>	Aromatic diacid
Terephthalic acid	<u>Shahid Tondgooyan Petrochemical Company (STPC)</u> Site 4, Imam Khomeini Port, Mahshahr, Iran Tel +98-65-22652048 Fax +98-65-22652000 e-mail: <a href="mailto:site@stpc.ir">site@stpc.ir</a> , web: <a href="http://www.stpc.ir">www.stpc.ir</a>	Aromatic diacid
Phthalic anhydride	<u>DC Chemical</u> 50, Sogong-dong, Jung-gu, Seoul, 100-718, Korea Tel +82-2-727-9500 Fax +82-2-756-9565	Acid anhydride



MATERIAL	SUPPLIER	FUNCTION
Maleic anhydride	<u>TCL Industries (Malaysia) Sdn. Bhd.</u> Plot No. 4248 Teluk Kalong Industrial Estate 24007 Kemaman, Terengganu, MALAYSIA Tel +60-9-8633029 Fax +60-9-8633085 e-mail: <a href="mailto:tcli@po.jaring.my">tcli@po.jaring.my</a>	Acid anhydride
Mono propylene glycol	<u>SKK</u> Kyobo Tower, 1303-22, Seocho 4-dong, Seocho-gu Seoul 137-070, Korea Tel +82-2-3787-1993 Fax +82-2-537-3142	Aliphatic diol
Trimethylol propane	<u>Mitsubishi Chemical</u> 14-1 Shiba 4-chome, Minato-ku, Tokyo 108-0014, Japan Tel [+81] (0)3-6414-3000 Fax [+81] (0)3-6414-3671	Triol
Neopentyl glycol	<u>Mitsubishi Chemical</u>	Branched diol
1,6 Hexanediol	<u>LANXESS España</u> Moll de Barcelona, s/n - WTC Nord 7ª Planta E 08039 Barcelona Tel +34 93 341 52 00 Fax +34 93 341 52 95 e-mail: <a href="mailto:infochemicals@lanxess.com">infochemicals@lanxess.com</a>	Aliphatic diol
Cyclohexane-dimethanol	<u>Eastman Chemical B.V.</u> Europe, Middle East & Africa Fascinatio Boulevard 602-614 2909 VA Capelle aan den IJssel The Netherlands Statutory seat The Hague Chamber of Commerce Rotterdam 27150948 Tel +31 10 2402 111 Fax +31 10 2402 111	Cycloaliphatic diol
TIBKAT 256 [Mono butyl oxide (C <sub>4</sub> H <sub>9</sub> )SnOOH]	<u>Goldschmidt TIB GmbH</u> Muelheimer Strasse 16-22 68219 Mannheim / Germany Tel +49-(0)6218-901-0 Fax +49-(0)6218-902 e-mail: <a href="mailto:info@goldschmidttib.co">info@goldschmidttib.co</a>	Tin based esterification catalyst
Xylene	<u>Bandar Imam Petrochemical Company (BIPC)</u> Bandar Imam P.O.Box: 138 Iran Tel & Fax : +98-21-33130277	Azeotropic solvent
Solvesso-100	<u>Shell Chemicals Europe BV</u> PO Box 8610 3009 AP Rotterdam The Netherlands Tel.+31 10 231 7000	Diluting solvent
Solvesso-150	<u>Shell Chemicals Europe BV</u>	Diluting solvent
Methoxy propyl acetate	<u>BASF SE</u> Operating Division Petrochemicals Regional Business Unit Plasticisers and Solvents Europe, 67056 Ludwigshafen, Germany web: <a href="http://www.basf.de/solvents">www.basf.de/solvents</a>	Diluting solvent

The materials shown in Table 2.1 were used as received. Specifications of Pripol 1022 dimer acid are shown in Table 2.2;

**Table 2.2 Monomer, dimer, and trimer content of Pripol 1022 dimer acid <sup>108</sup>**

Dimer acid	Monomeric fatty acid (%)	Dimerised fatty acid (%)	Trimerised fatty acid (%)	Acid value (mgKOH/g)
Pripol 1022	2	76	22	193.5

### 2.1.2 Lab equipment used for the synthesis of saturated polyester resins for coil coating

A list of the lab equipment employed for the synthesis of polyester resins is provided in Table 2.3.

**Table 2.3 Lab equipment used for the synthesis of saturated polyester resins for coil coating (continued on page 60)**

EQUIPMENT	QUANTITY	FUNCTION
2-litre round bottom glass kettle (with 4 necks)	1	Reaction vessel
3-litre round bottom glass kettle (with 4 necks)	1	Reaction vessel
4-litre round bottom glass kettle (with 4 necks)	1	Reaction vessel
Mechanical agitator	1	Mixing
Partial condenser	1	Vapour riser
Total condenser	1	Vapour condenser
Water trap	1	Separating the water of reaction
Open column	1	Separating the water of reaction during azeotropic distillation in case an azeotrope solvent was used during the resin cook

<b>EQUIPMENT</b>	<b>QUANTITY</b>	<b>FUNCTION</b>
2-litre heating mantle	1	Heating the reaction vessel
4-litre heating mantle	1	Heating the reaction vessel
Calibrated 0-400°C Thermometer	1	Monitoring the temperature of the reaction vessel
Calibrated 0-150°C Thermometer	1	Monitoring the temperature at the top of the partial condenser
Nitrogen gas supply	1 complete set inclusive of nitrogen gas tank, appropriate piping, pressure gauges and valves	Providing nitrogen gas blanket inside the reaction vessel at a typical flow rate of 0.022 m <sup>2</sup> /h
Pressurised air supply	1 complete set with appropriate facilities	Cooling the reaction vessel, controlling top of partial condenser's temperature
0.001 g accuracy balance	1	Weighing raw materials
250 cm <sup>3</sup> glass beaker	1	Weighed material container
500 cm <sup>3</sup> glass beaker	1	Weighed material container
Plastic funnel	1	Pouring weighed raw materials into the reaction kettle
50 cm <sup>3</sup> graduated pipette	1	Sampling the resin throughout the cook for the determination of acid value and viscosity
100 cm <sup>3</sup> beaker	3	Sampling the resin throughout the cook
MEK solvent wash bottle	1	Cleansing used apparatus
10 µm paper filter	available accordingly	Filtering the cooked resin after dilution
4-litre metal cans	available accordingly	Container for the synthesised resin

The equipment specified in Table 2.3 are standard apparatus for the lab scale synthesis of polyester systems. Similar equipment were used for the synthesis of a variety of polyester systems in the recent works of Vahteristo et al<sup>22</sup>, Boyes et al<sup>29</sup>, Tsai et al<sup>36</sup>, Soni et al<sup>30</sup>, Ferré et al<sup>37</sup> and Lozano et al<sup>60</sup>.

### 2.1.3 Chemicals used for the determination of solid content, acid value and hydroxyl value of the synthesised polyester resins

The polyester resins synthesised were diluted in appropriate solvents. The solvents used will be mentioned in Section 2.3.5.5. After dilution, the solid contents of the polyesters were tested according to the test method defined by ISO 3251<sup>109</sup>. The reagents required for the determination of the solid content according to ISO 3251 are specified in Table 2.4.

**Table 2.4 Chemicals used for the determination of solid content according to ISO 3251<sup>109</sup>**

Reagent	Function
Toluene	Solvent for the resin sample
Acetone	Solvent for the resin sample
n-Butanol	Solvent for the resin sample

The acid values of the polyester resins synthesised were tested according to the test method defined by ISO 3682<sup>110</sup>. The reagents required for the determination of the acid value according to ISO 3682 are specified in Table 2.5.

**Table 2.5 Chemicals used for the determination of acid value according to ISO 3682<sup>110</sup>**

Reagent	Function
0.5 N methanolic potassium hydroxide	Titration solution
Phenolphthalein indicator 1% in ethanol	Indicator
Toluene	Solvent for the resin sample
Diacetone alcohol	Solvent for the resin sample

The hydroxyl value of the polyester resins synthesised were tested according to the test method defined by ISO 4629<sup>111</sup>. The reagents required for the determination of the hydroxyl value according to ISO 4629 are specified in Table 2.6.

**Table 2.6 Chemicals used for the determination of hydroxyl value according to ISO 4629<sup>111</sup>**

Reagent	Function
Acetic anhydride	Acetylating agent component
Pyridine	Acetylating agent component/ solvent
Cyclo hexanone	Solvent for the resin sample
Tetra hydrofuran	Solvent for the resin sample
Distilled water	Solvent for the resin sample
Acetone	Washing solvent
0.5N ethanolic potassium hydroxide solution	Titrating solution
Phenolphthalein indicator solution (10 g/l in ethanol)	Indicator of the end of titration

#### 2.1.4 Apparatus used for the determination of solid content, acid value, hydroxyl value and density of the synthesised polyester resins

The apparatus that are listed in Table 2.7 were used for the determination of solid content according to the test method defined by ISO 3251<sup>109</sup>.

**Table 2.7 Apparatus used for the determination of solid content according to ISO 3251<sup>109</sup>**

Apparatus	Quantity	Function
0.0001 g accuracy balance	1	Weighing
Oven, controllable at specified temperatures	1	Vapouriser of the resin sample's volatile matter
Metal dishes	2	Sample container
Dessicator filled with silica gel	1	Keeping the sample dry after oven drying

The apparatus that are listed in Table 2.8 were used for the determination of acid value according to the test method defined by ISO 3682<sup>110</sup>.

**Table 2.8 Apparatus used for the determination of acid value according to ISO 3682<sup>110</sup>**

Apparatus	Quantity	Function
0.01 g accuracy balance	1	Weighing
Wide neck conical flask, 300 ml	1	Test material container
50 ml burette graduated to 0.1 ml	1	Titration apparatus
Hot plate	1	Heating the resin sample and test solvents mixture in order to facilitate homogenisation
Mortar and pestle	1	Mixing test materials

The apparatus that are listed in Table 2.9 were used for the determination of hydroxyl value according to ISO 4629<sup>111</sup>.

**Table 2.9 Apparatus used for the determination of hydroxyl value according to ISO 4629<sup>111</sup>**

Apparatus	Quantity	Function
250 ml flat bottomed flask	2	Test material container
0.001 g accuracy balance	1	Weighing
2 ml measuring cylinder	1	Sampling
Partial condenser	2	Reflux cooler
10.00 ml pipette	1	Sampling

The apparatus that are listed in Table 2.10 were used for the determination of density according to the test method defined by ISO 2811<sup>112</sup>.

**Table 2.10 Apparatus used for the determination of density according to ISO 2811<sup>112</sup>**

Apparatus	Quantity	Function
100 ml metal pycnometer	1	Density determination apparatus
0.001 g accuracy balance	1	Weighing
Water bath, controlled at 23°C	1	Maintaining the pycnometer's temperature at 23°C ( $\pm 5^\circ\text{C}$ )

## 2.2 Theoretical evaluation of the designed polyester formulations prior to polymerisation

Prior to synthesis of any polyester system, it is extremely helpful and important to theoretically evaluate the considered formulation by calculating certain parameters. These parameters are calculated from the molecular and equivalent weights of the formulation components and include the following;

- 1) Hydroxyl excess
- 2) Theoretical hydroxyl value
- 3) Theoretical amount of liberated water
- 4) Theoretical yield at acid value=0
- 5) Theoretical yield at acid value=A
- 6) Theoretical molecular weight at a given acid value
- 7) Indication of the tendency of the considered formulation to gel

For the theoretical calculation of the above mentioned parameters for a designed polyester formulation, the following definitions have to be considered; <sup>113</sup>

$w_i$  = Total raw material weight input

$m_i$  = Total number of moles of raw materials

$e_{\text{COOH}}$  = Total number of equivalent weights of acid

$e_{\text{OH}}$  = Total number of equivalent weights of hydroxyl

$w_{\text{H}_2\text{O}}$  = Total theoretical liberated water of reaction

A typical saturated polyester resin formulation is provided in Table 2.11 and theoretically evaluated. The theoretical parameters calculated include the amount of liberated water, hydroxyl excess, yield at acid value=0, yield at acid value=8, hydroxyl value, molecular weight at acid value=8 and the tendency to gel.

**Table 2.11 Formulation and theoretical evaluation of a saturated polyester resin**

Raw Material	Molecular weight	Equivalent weight	Charged weight (g)	Moles	Equivalents hydroxyl ( $e_{OH}$ )	Equivalents acid ( $e_{COOH}$ )	Theoretical weight of liberated water (g)
Adipic Acid	146	73	247.92	1.6981	-----	3.3962	61.131
Isophthalic acid	166	83	350	2.1084	-----	4.2169	75.9036
Terephthalic acid	166	83	175	1.0542	-----	2.1084	37.9518
Trimethylol propane	134	44.7	87.5	0.653	1.9575	-----	-----
Neopentyl glycol	104	52	437.5	4.2067	8.4135	-----	-----
1,6 Hexanediol	118	59	102.08	0.8651	1.7302	-----	-----
Total			1400	10.586	12.101	9.7215	174.986

Based on the total weight input, molecular and equivalent weights of the formulation's polyols and polyacids, the following can be calculated as

$$w_i = 1400, m_i = 10.586, e_{OH} = 12.101, e_{COOH} = 9.7215$$

The theoretical weight of liberated water is calculated based on polyacids, since in saturated polyester formulations the hydroxyl equivalents are usually in excess.<sup>113</sup> The liberated water is calculated according to the basic esterification reaction and the number of moles of each acidic component. The esterification reaction concerned was shown in Scheme 1.2. It can be seen, from Scheme 1.2, that each equivalent of acid or each carboxyl functionality reacts with one hydroxyl group and liberates one mole (18 g) of water. Two carboxyl functionalities are capable of liberating two moles (36 g) of water. In other words, one mole of a diacid liberates two moles of water. Thus, Y moles of a diacid would liberate (Yx2x18) grams of water. The theoretical liberated amount of water of the example polyester resin formulation is therefore  $w_{H_2O} = 174.986$  g.

Hydroxyl excess is obtained from  $e_{OH} / e_{COOH}$ <sup>113</sup>. Therefore, hydroxyl excess for the example resin will be:  $e_{OH} / e_{COOH} = 12.101/9.7215 = 1.2448$  (i.e. hydroxyl excess of 24.48%)



As mentioned in Section 1.3.2, the progress of polyester polymerisation is monitored by measuring the acid value of the reaction mixture. As the polymerisation proceeds, the acid value decreases. The acid value (A) "is the number of mgKOH equivalent to carboxyl groups in 1g of the resin."<sup>113</sup> In practice, polyester polymerisations are stopped prior to reaching acid value zero.

Theoretical yield at acid value=0 ( $Y_0$ ) is calculated from  $Y_0 = w_i - w_{H_2O}$ .<sup>113</sup> For the example resin,  $Y_0 = 1400 - 174.986 = 1225.014$ .

The theoretical yield at acid value=A ( $Y_A$ ) is calculated from

$$Y_A = \frac{56100}{56100 - (18 \times A)} \times Y_0 \quad .^{113}$$

The number 56100 in the above equation is the molecular weight of potassium hydroxide (KOH) in mg/mole. Thus, the theoretical yield at acid value=8 for the example polyester resin would be

$$@ A=8, \quad Y_8 = \frac{56100}{56100 - (18 \times 8)} \times 1225.014 = 1228.166g.$$

Obviously, the yield would be higher prior to reaching acid value=0. This is due to the smaller amount of liberated water.

The hydroxyl value of a resin is "the number of mgKOH equivalent to the hydroxyl groups in 1g of the resin."<sup>113</sup> The theoretical hydroxyl value of a designed polyester resin formulation can be calculated from

$$H = \frac{(e_{OH} - e_{COOH}) \times 56100}{Y_0} \quad .^{113}$$

Thus, the hydroxyl value of the example saturated polyester resin would be;

$$H = [(12.101 - 9.7215) \times 56100] / 1225.014 = 108.9775 \text{ mgKOH/g.}$$

The following expression can be used to calculate the theoretical molecular weight of a polyester resin cooked to acid value A;

$$M_A = \frac{Y_A}{(m_i - e_{COOH}) + \frac{Y_A \times A}{56100}} \cdot 113$$

For the example polyester resin, the theoretical molecular weight at acid value 8 would be

$$M_8 = \frac{1228.166}{(10.586 - 9.7215) + \frac{(1228.166 \times 8)}{56100}} = 1181.8247 \frac{g}{mol}$$

With regard to the theoretical hydroxyl value and the theoretical molecular weight, it must be stressed that these are only theoretical amounts and are just an indication. The actual hydroxyl value can be determined by standard methods such as ISO 4629. As mentioned in Section 1.8.2, actual molecular weights are determined by size exclusion chromatography.

For a newly considered formulation, it is extremely important to have an initial indication of its tendency to gel. There are two common methods for the determination a safe polyester cook. These are the Extension of the Carother's equation or Patton's Constant.<sup>113</sup>

### 1) Extension of the Carother's equation:

$$\text{Degree of reaction} = P = \frac{2}{F} - \frac{2}{X_p \times F} \quad 113$$

Where F is the average functionality;  $F = \frac{\text{Total number of effective groups}}{\text{Total number of molecules}}$ .<sup>113</sup>

Hydroxyl groups are usually in excess in polyester formulations. These excess hydroxyl groups do not take part in the esterification reaction. Therefore "the number of effective groups is assumed to be twice the number of acid equivalents"<sup>113</sup> and the above equation will be

$$F = \frac{2 \times e_{COOH}}{m_i} \quad .^{113}$$

F for the example polyester formulation will be  $F = (2 \times 9.7215)/10.586 = 1.8367$ .

$X_p$  is the degree of polymerisation and is calculated from the following equation.

$$X_p = \frac{\text{Number of moles initially}}{\text{Number of moles at the degree of reaction } P} \quad .^{113}$$

Since there are no reacting moles available at the gel point,  $X_p$  will be infinite. Therefore, P at gel point will be;

$$P_{gel} = 2/F. \quad .^{113}$$

This equation is known as the Extension of the Carother's equation. Although not producing absolutely accurate results, the Extension of the Carother's equation is still widely used as a rule of thumb for development of new experimental polyester formulations.  $P_{gel}$  for a polyester formulation must be greater than one ( $P_{gel} > 1$ ) in order to ensure that the degree of reaction is in excess of 100% and that the formulation is safe.<sup>113</sup>

For the example formulation;  $P_{gel} = 2/1.8367 = 1.0889$ . Therefore the formulation can be considered to be safe for synthesis.

$P_{gel}$  becomes 1 or below when the average functionality F becomes 2 or greater. Thus calculating F can be another way of determining the safe cook of a polyester resin formulation by considering that F should always be lower than 2 ( $F < 2$ ).

## 2) Patton's Constant

Patton's constant (K) is also used widely for the determination of the safe cook of a polyester resin. The Patton's constant is given as

$$K = \frac{m_i}{e_{COOH}} \quad .^{113}$$

K for the example polyester formulation will be:  $K = 10.586 / 9.7215 = 1.0889$

K in this approach must be 1 or greater. As can be seen  $K = P_{gel}^{80,81}$

Either of the Carother's or Patton's approach would be extremely useful and efficient in formulating polyesters. However and as mentioned in section 1.3.2, during a polyester resin polymerisation, much depends on the process control capability provided by the plant equipment as well as the characteristics of the raw materials. A supposed safe polyester formulation can easily gel during synthesis due to inadequate process control. Theoretical evaluation of a polyester resin formulation by the above mentioned approaches provides an extremely useful aid for development of new polyester systems. Theoretical evaluation of a new formulation as such would provide a preview of the formulation's basic characteristics prior to lab synthesis, particularly with regard to hydroxyl value, molecular weight and  $P_{gel}$ . Hydroxyl value has a significant influence on the final film performance of a polyester coating and needs to be tailor-made for specific applications. Polyester formulations can be designed with either high or low hydroxyl functionalities. Theoretical molecular weights can be an indication of the viscosity of the polyester. High theoretical molecular weights often result in high final viscosities. The saturated polyester resins synthesised for this study were theoretically evaluated using the same approaches prior to synthesis.

## **2.3 Procedure of polyester synthesis and its establishment in the lab, pilot plant, and large scale production facilities**

In this section, the methods employed for the synthesis of the saturated polyesters in this study are described. The general method of polyester synthesis via direct esterification is explained in Section 2.3.1. In Sections 2.3.2, 2.3.3, and 2.3.4, design of the process for the synthesis of polyester in the lab scale, pilot scale and large scale production facilities is discussed. In Section 2.3.5, reaction details of a particular polyester formulation in the lab, pilot plant and industrial scale reactor are provided.

### **2.3.1 General method of synthesis**

As mentioned in Section 1.3.2, for the synthesis of polyesters via direct esterification, the solid polyols are initially added to the reactor and heated until complete meltdown. The melting point of the polyols commonly used in the preparation of saturated polyester resins

is within 50-130°C. After the polyols have been melted, the polyacids are added to the reaction vessel. Depending on the reaction temperature, the mixture is heated up to 200-250°C. During the second stage heat up, the esterification reaction initiates and the water generated by the reaction is separated. At a certain point, the reacting mixture becomes clear and the generation of water of reaction usually diminishes. From this point onwards, the polymerisation or cooking progress of the polyester resin is monitored by the determination of the acid value and the viscosity of the clear resin. When the desired specifications are achieved, the resin is cooled and diluted to the desired solids content with the appropriate solvents.

Synthesis of polyester systems via direct esterification according to the procedure mentioned has been carried out in a variety of recent research. In the works of Umare et al<sup>27</sup>, Boyes et al<sup>29</sup>, Tsai et al<sup>36</sup> and Ferré et al<sup>37</sup>, different polyesters were synthesised by using the same method of synthesis.

As such, the following polymerisation or cooking procedure was generally used for the synthesis of saturated polyester resins in this study.

- 1- Solid polyols were charged to the reactor and heated until complete meltdown;** Depending on the type of polyol incorporated in the designed polyester formulations, the maximum temperature at this stage varied between 80-130 °C.
- 2- Polyacids and the esterification catalyst (mono butyl oxide) were charged to the reactor.**
- 3- The mixture was heated up to 235-250°C under nitrogen blanket while keeping the temperature of the top of the partial condenser below 103°C;** The temperature of the partial condenser's outlet was controlled below 103°C. This was done to avoid the loss of glycol and to ensure that only the vapour of the water generated by the reaction was being removed from the reaction vessel.
- 4- The mixture was kept between 235-250°C until it became clear. After it became clear, the resin was esterified to the lowest possible acid value (mgKOH/g).**

5- After completion of the cook, the resin was cooled to 170°C and diluted to 65% solid content with appropriate solvents.

This general procedure of polyester synthesis was used for the lab, pilot, and industrial scale polymerisations.

### 2.3.2 Lab scale polyester synthesis

The equipment and the glassware assembly that were used for the synthesis of saturated polyester resins at the lab scale are shown in Figure 2.1.

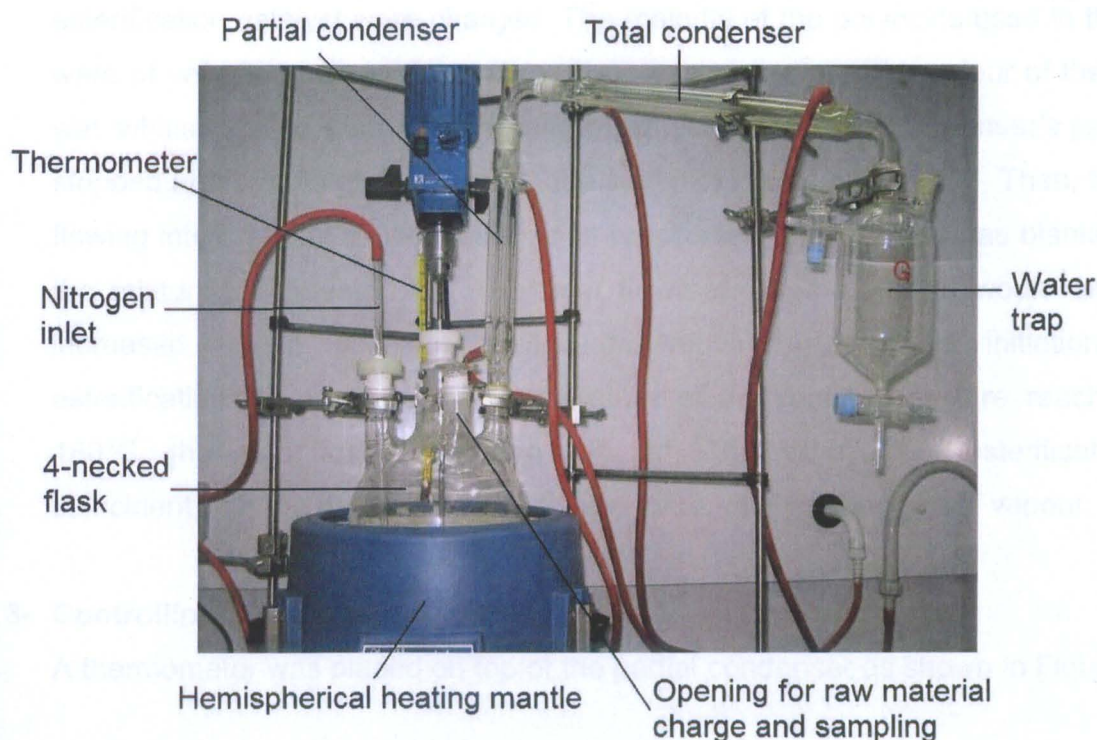


**Figure 2.1 Equipment and glassware assembly used for the synthesis of saturated polyester resins at the lab scale**

In the recent works of Umare et al<sup>27</sup>, Boyes et al<sup>29</sup>, Tsai et al<sup>36</sup> and Ferré et al<sup>37</sup> similar equipment as those shown in Figure 2.1 were used for the synthesis of a variety of polyester systems.

In order to synthesise saturated polyester resins at the lab scale, the equipment that is shown in Figure 2.1 was operated according to the following procedure in order to simulate the general method of synthesis mentioned in Section 2.3.1;

### 1- Melting the polyols:

The polyols were charged from the opening of the flask (Figure 2.1). The heating mantle was turned on. The rate of heating was adjusted as such so that it could effectively melt the charged polyols. As mentioned in Section 2.3.1, this temperature varied between 50-130°C. Cooling water was allowed to flow in the partial condenser's jacket to condense glycol vapours during the melting process.

### 2- Charging the polyacids and initiating the esterification reaction:

After complete meltdown of the polyols, the polyacids and the tin based esterification catalyst were charged. The majority of the polyacids used in this study were of very fine powder form. The mixer was turned on. The colour of the mixture was whitish at this stage. The flowing of water in the partial condenser's jacket was stopped and the water remaining in the said jacket was discharged. Then, the water flowing into the total condenser's jacket was turned on. Nitrogen was blanketed and the mixture was heated up. The heat flow rate of the mantle would always be increased at this point to provide the required energy for initiation of the esterification reaction. As the temperature of the reaction mixture reached 160-180°C, the esterification reaction initiated. The initiation of esterification was coincident with the generation of the water of reaction in the form of vapour.

### 3- Controlling the temperature at the top of the partial condenser:

A thermometer was placed on top of the partial condenser as shown in Figure 2.2.

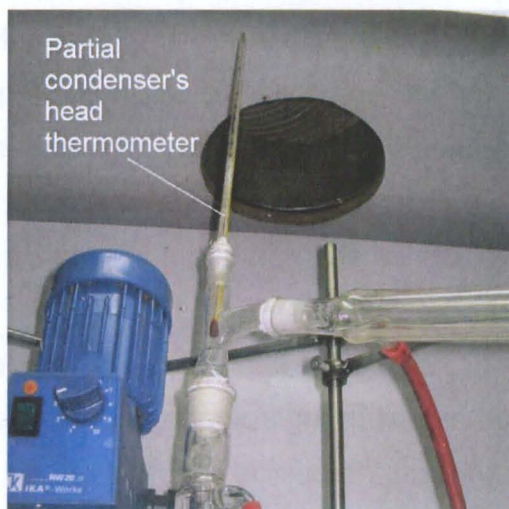


Figure 2.2 Position of partial condenser's thermometer

As the vapour of the water generated by the reaction passed through the top of the partial condenser, the temperature at the top of the partial condenser rapidly increased from room temperature to 95-103°C. The temperature of the vapour at the top of the partial condenser was maintained between 100-103°C in order to prevent the loss of glycol. This was also done to ensure that only the vapour of the water generated by the reaction was being separated from the reacting mixture. If the temperature of the vapour at the top of the partial condenser exceeded 103°C, water was allowed to gently flow into the partial condenser's jacket. This led to a drop of the vapour temperature at the top of the partial condenser and thus, prevented glycol loss.

#### **4- Increasing the kettle's temperature to 230-250°C:**

As generation of the water of reaction began to slow down, the kettle was heated further. The temperature of the reacting mixture was gradually increased. Simultaneously, the temperature at the top of the partial condenser was maintained within 100-103°C. As the temperature of the kettle reached 230-250°C, the resin became clear and the generation of the esterification water was diminished.

#### **5- Esterifying to the lowest possible acid value and ending the polymerisation:**

After the appearance of the resin became clear, samples were taken from the kettle for the determination of the acid value and the viscosity. The resin was polymerised to the lowest possible acid value. Effort was made to obtain the lowest possible acid value by not exceeding 250°C. Exceeding 250°C during such polymerisations often resulted in the development of colour in the cooking resin. After the acid value of the resin ceased to drop any further, the kettle was cooled by pressurised air to 140°C. The nitrogen blanket was then removed and the appropriate solvent was added for dilution of the resin to 65% solid content. After dilution, the resin was mixed at high speed for 15 minutes and discharged from the kettle.

The resin was allowed to cool down for one day before it was used for analysis and application in the coil coatings. It often took eight to twelve hours to synthesise saturated polyesters at the lab scale according to the procedure described.



### 2.3.3 Pilot scale polyester synthesis

The pilot plant included a 50 litre stainless steel reactor, variable speed agitator, heating jacket, cooling coils, packed partial condenser, total condenser, water trap, facilities for blanketing the nitrogen gas, and the relevant thermocouples and piping connections for a standard reactor. The pilot plant reactor concerned is shown in Figure 2.3.

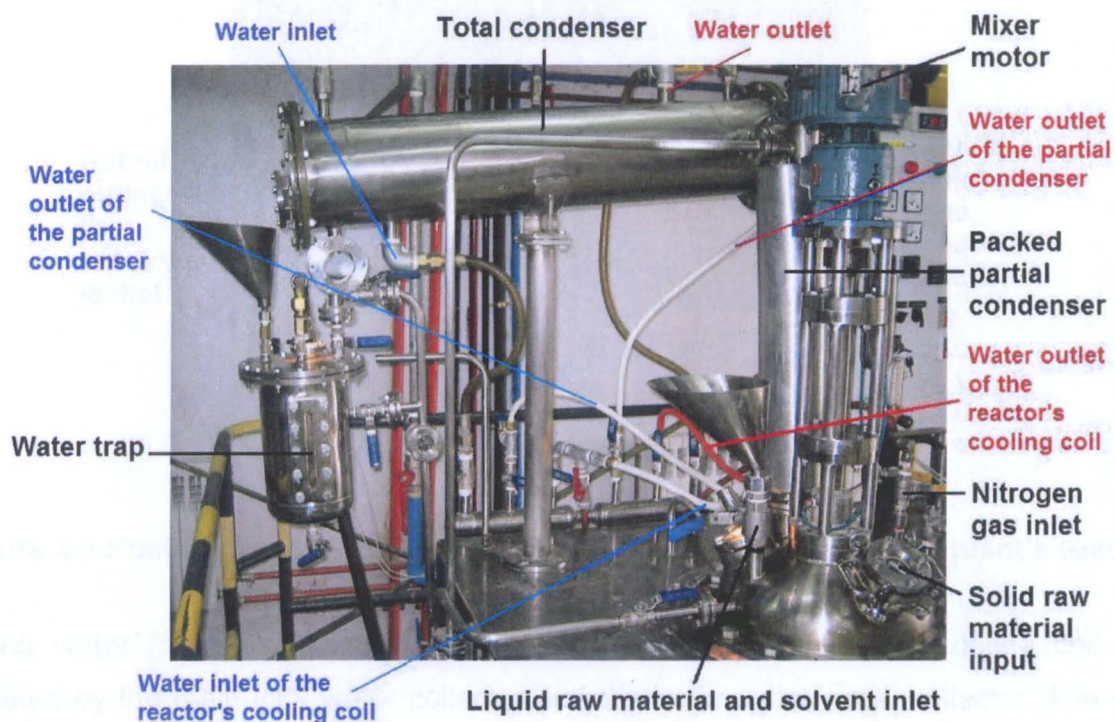


Figure 2.3 Pilot plant reactor

For heating, oil was heated by means of electrical heating elements and pumped to the reactor's jacket. The oil heating chamber and the hot oil pump are shown in Figure 2.4.

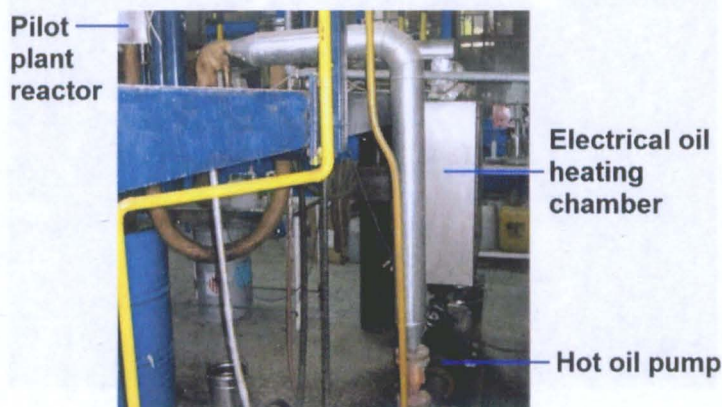
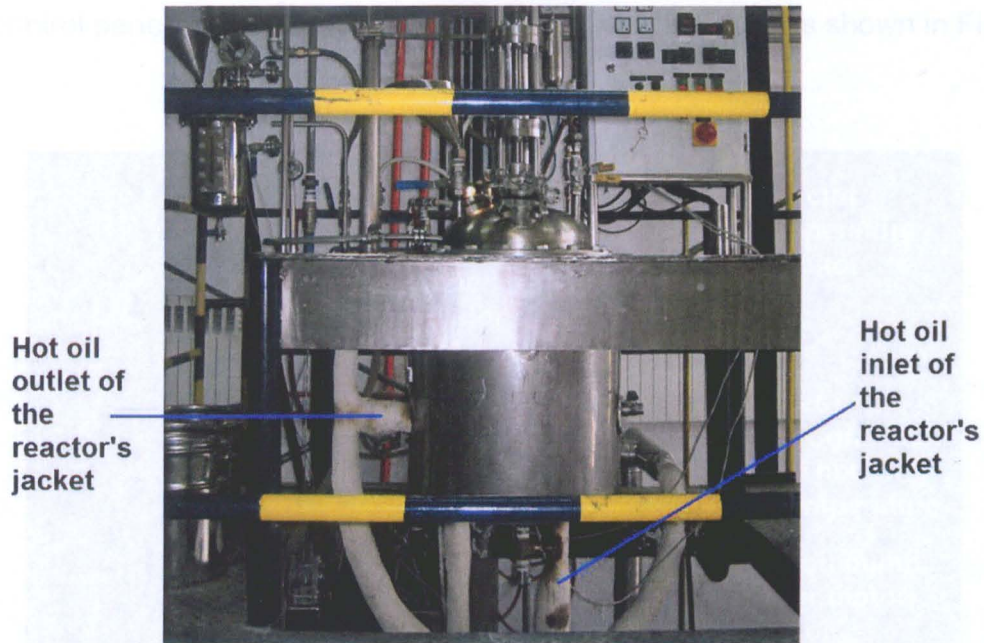


Figure 2.4 Pilot plant's oil heating chamber and pump

Hot oil inlet and outlet of the reactor's jacket are shown in Figure 2.5.



**Figure 2.5** Positions of the inlet and outlet of the hot oil on the pilot plant's reactor

Cooling water for the jackets of the condensers and the reactor's cooling coil were circulated by the main inlet water collector and the main outlet water collector. The water collectors concerned are shown in Figure 2.6.

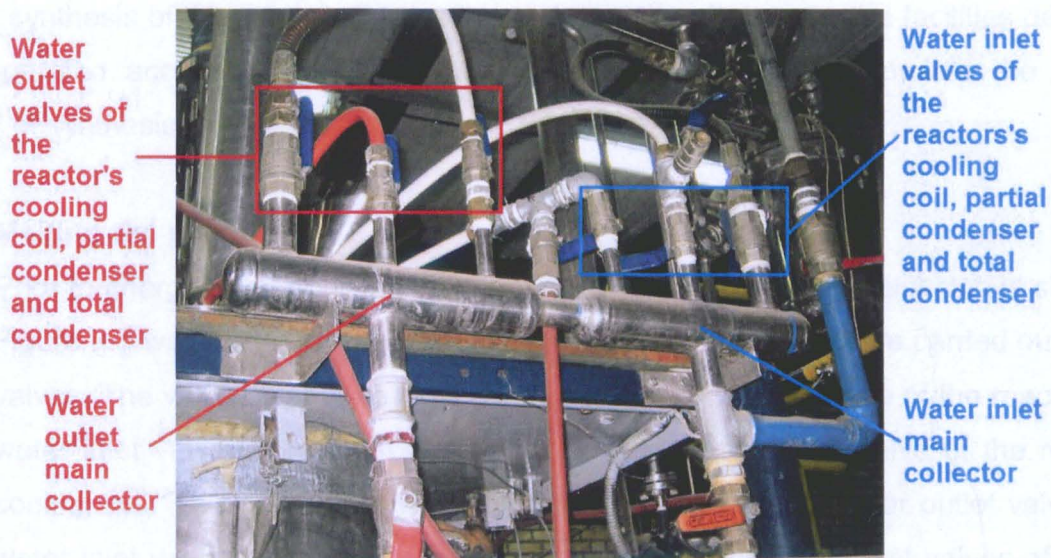


**Figure 2.6** Inlets and outlets of the cooling water of the pilot plant's reactor

The hot oil temperature, the reactor mixture temperature and the temperature at the top of the partial condenser were electronically monitored, adjusted and controlled via the reactor's control panel. The control panel of the pilot plant's reactor is shown in Figure 2.7.

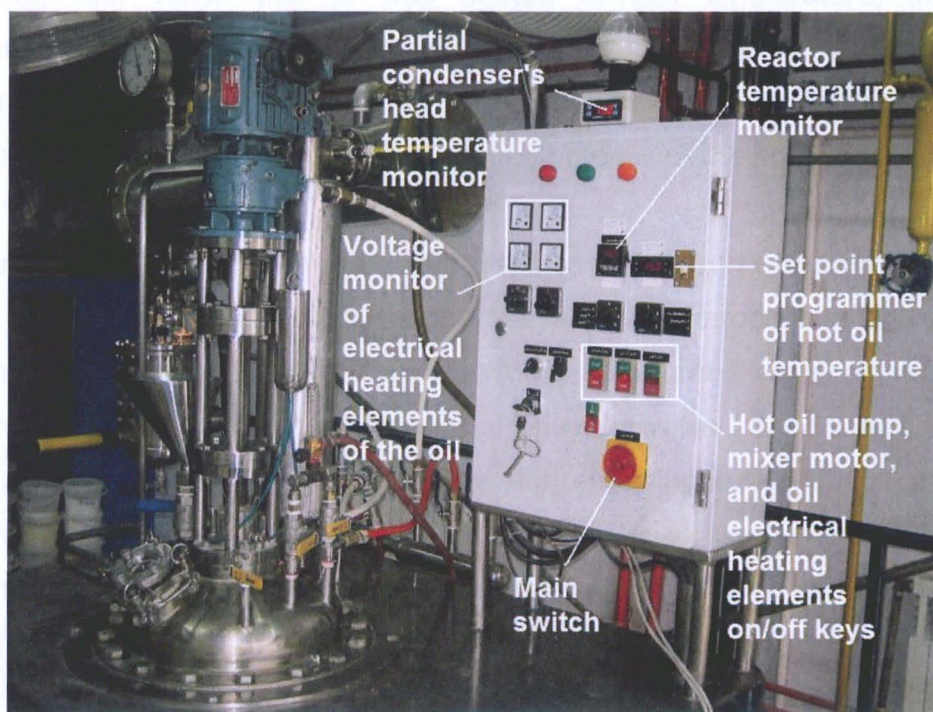


**Figure 2.7 Control panel of the pilot plant's reactor**

For the synthesis of the saturated polyester resins at the pilot scale, the facilities described were operated according to the following procedure in order to simulate the general method of synthesis mentioned in Section 2.3.1.

### 1- Melting the polyols:

Prior to charging the polyols, the main switch of the control panel which is shown in Figure 2.7 was turned on. A series of closures and openings were carried out for the valves. The valves that were closed included the discharge valve of the reactor, the water inlet valve of the total condenser, and the water inlet valve of the reactor's cooling coil. The valves that were left open included all the water outlet valves, the water inlet valve of the partial condenser, and the inlet and outlet valves of the hot oil of the reactor's jacket. The polyols were charged from the opening specified in Figure 2.3. Nitrogen gas was blanketed on the upper part of the reactor. The hot oil

pump was turned on. The hot oil temperature was set on 150°C by the relevant set point programmer on the control panel (Figure 2.7). The set point programmer of the hot oil temperature was coupled to the electrical oil heating elements. It automatically turned on the heating elements as the new temperature was programmed. When the oil was heated to that temperature, the set point programmer automatically turned off the electrical heating elements. As mentioned in Section 2.3.2, cooling water was allowed to flow in the partial condenser's jacket to condense the vapours during the melting process of the polyols.

## **2- Charging the polyacids and initiating the esterification reaction:**

The polyacids and the esterification catalyst were charged after the polyols were melted and liquefied. The motor of the mixer was turned on for homogenisation of the mixture of the polyols and polyacids. The inlet valve for the water of the packed partial condenser was closed and the water remaining in its jacket was discharged. Then, the inlet valve of the water of the total condenser was opened. The blanketing of nitrogen gas on the upper part of the reactor was stopped. It was then blanketed on the lower part of the reactor and through the mixture. The hot oil temperature was set on 185°C to provide the required energy for the initiation of the esterification reaction. Similar to the lab-scale polyester synthesis, the temperature at which the esterification reaction initiated in the pilot reactor was within 160-180°C.

## **3- Controlling the temperature at the top of the packed partial condenser:**

The rise of the temperature at the top of the packed partial indicated the start of the esterification reaction in the pilot reactor. As the partial condenser was baffled, the temperature of the vapour at the top of the partial condenser hardly exceeded 103°C. However, if the temperature of the vapour at the top of the partial condenser exceeded 103°C, the inlet valve for the water of the jacket of the partial condenser was opened to some degree. This valve was placed on the main water inlet collector. The water collector concerned was shown in Figure 2.6. After the vapour temperature at the top of the partial condenser had dropped below 103°C, the said water valve was closed to allow the separation of the vapour of the water generated by the reaction.

**4- Increasing the temperature of the pilot reactor to 230-250°C:**

Similar to the lab-scale process, as generation of the water of reaction began to slow down, the reactor was heated further. The decrease of the vapour temperature at the top of the partial condenser indicated that the rate of the generation of the water of reaction had decreased. At this point, the reactor's temperature was increased by 5°C. This was done by setting the temperature of the circulating hot oil above the desired reactor temperature by 10°C i.e. If the pilot reactor's temperature was desired to be 205°C, the hot oil temperature was set on 215°C. By using this scheme, the temperature of the reacting mixture was gradually increased to 230-250°C. At the same time, the temperature at the top of the partial condenser was maintained between 95-103°C.

**5- Esterifying to the lowest possible acid value and ending the polymerisation:**

After the appearance of the resin became clear and generation of the water of reaction diminished, samples were taken from the reactor for the determination of the acid value and the viscosity. The pilot reactor was equipped with a valve for sampling. After the acid value of the resin did not decrease any further, the reaction was stopped by cooling the resin inside the reactor. First, the hot oil heating elements were turned off. The hot oil inlet valve of the pilot reactor's jacket was closed and the circulating hot oil was bypassed back to the heating chamber. The inlet valve of the water of the partial condenser was opened. Then the inlet valve of the reactor's cooling coil on the main water inlet collector (Figure 2.6) was opened. When the temperature of the resin inside the reactor fell to 140°C, the lower nitrogen blanket was removed. Finally, the diluting solvent was added from the inlet specified in Figure 2.3. After the addition of the solvent, the speed of the mixer was increased to obtain homogeneity. The diluted resin was mixed for 30 minutes. Samples were taken from the reactor for the determination of solid content. If the solid content was above the desired range, it would be adjusted through further addition of solvent to the diluted resin. The resin was then discharged from the reactor.

It often took ten to fourteen hours to synthesise saturated polyesters at the pilot scale according to the procedure described.

### 2.3.4 Industrial scale polyester synthesis

The value of any newly developed polyester resin system would be in its reproducibility in the industrial scale. Therefore, the novel and standalone coil coating polyester resin system to be developed during the course of this study was desired to be reproducible at the industrial scale. In this regard, a significant amount of time during this study was dedicated to establishing polyester synthesis in the large scale production facilities that were available. By doing as such, the industrial scale reproducibility of the novel and standalone coil coating polyester resin system to be developed could be evaluated.

Establishing polyester synthesis in the large scale required detailed knowledge of the plant facilities, their method of operation and their order of operation. In this section, the plant facilities and the method by which they had to be operated to be able carry out large scale polyester synthesis are described.

The production facilities included four reactors with different production capacities and two blenders for diluting the resins. The plant's twelve metric ton reactor is shown in Figure 2.8

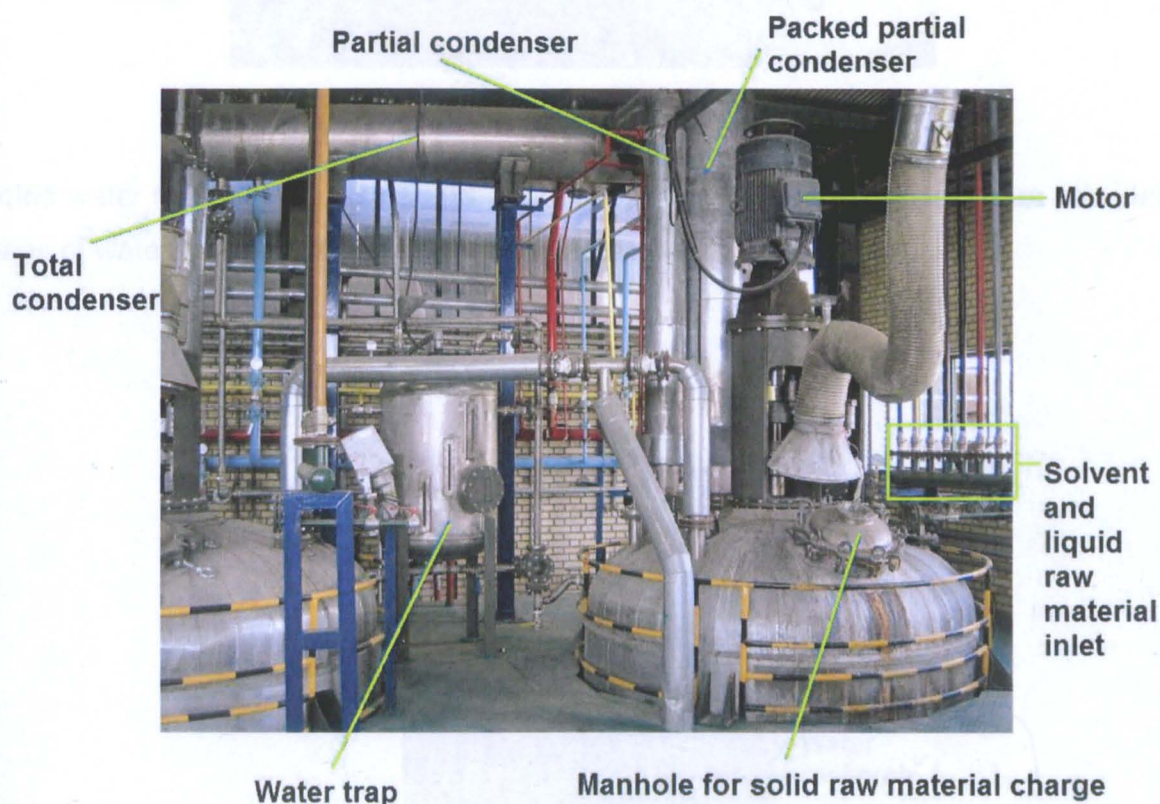
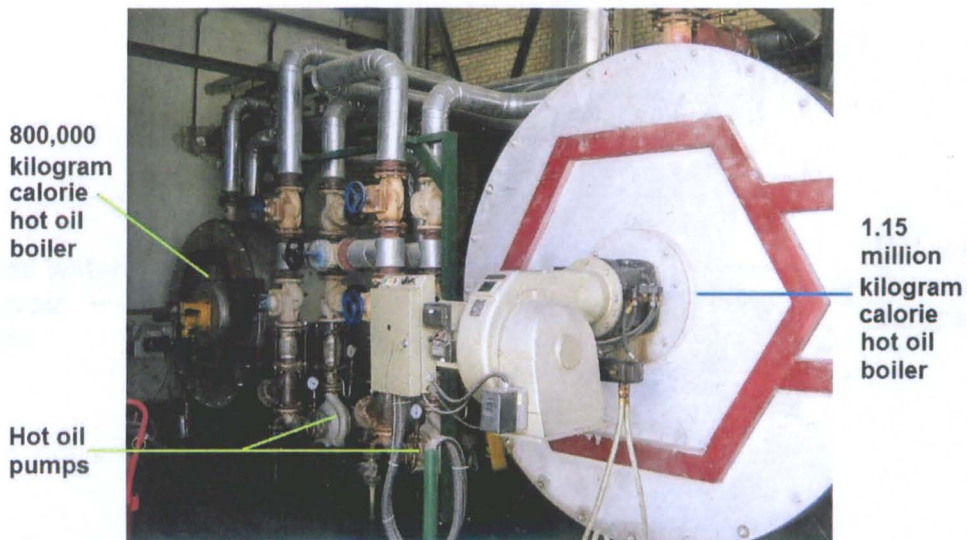


Figure 2.8 Twelve metric ton reactor of the resin plant

The reactors were designed for the synthesis of polyester resins via direct esterification. They were equipped with the equipment mentioned earlier in Section 1.3.2 and shown in Figure 1.6. The plant had a production capacity of 30 metric tons per day. The reactors were heated through their heating jacket in which the hot oil was circulated. Oil could be heated up to 300°C in the boiler room of the plant. The boiler room included two boilers with different capacities and two hot oil pumps. Each boiler fed two reactors and one dilution blender. The boiler room of the plant is shown in Figure 2.9.



**Figure 2.9 Resin plant's hot oil boiler room**

Cooled water for the condensers and the cooling coils inside the reactors was provided by means of water reservoir and cooling tower as shown in Figure 2.10.

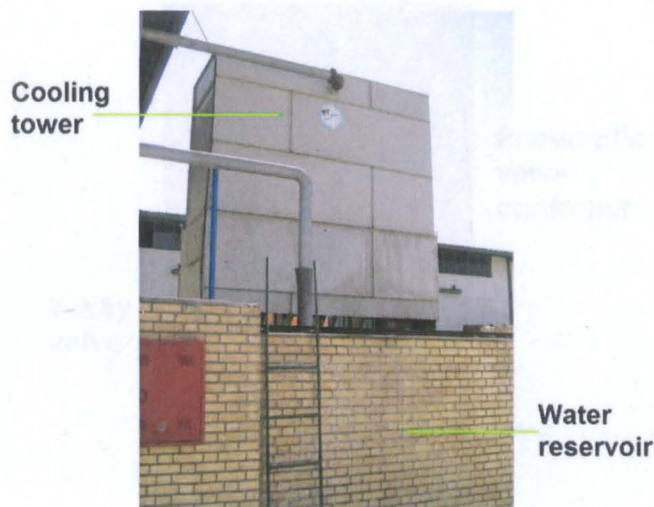


**Figure 2.10 Resin plant's water reservoir and cooling tower**

The cooling water was circulated by means of appropriate pumps. The water reservoir contained two chambers. The first chamber contained the hot water circulated back from the outlets of the condensers and cooling coils of the reactors. The hot water in this chamber was pumped to the top of the cooling tower. The cooling tower itself was placed on top of the second water chamber. The second chamber collected the water cooled by the cooling tower. The cooled water was then pumped back to the inlets of the condensers and cooling coils of the reactors. The pumps of the plant's water reservoir are shown in Figure 2.11.



**Figure 2.11 Pumps of the resin plant's water reservoir**

The reactors' temperatures were adjusted by pneumatic 3-way valves. These pneumatic 3-way valves had been installed on the hot oil circuit as shown in Figure 2.12.

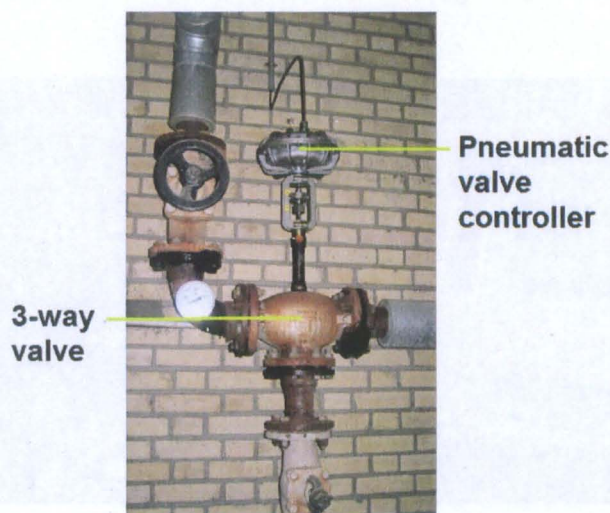


**Figure 2.12 Baelz MBA 340 pneumatic 3-way hot oil valve**



The 3-way valves opened and closed the hot oil circuit automatically based on the electronically provided instructions from the process control room. High accuracy thermocouples were installed at key reactor positions. These positions included the top of the packed vapour riser, inside the reactor, and hot oil inlets. The thermocouples were connected to the electronic monitoring equipment in the process control room. The temperature monitoring diagram of the resin plant's reactors is shown in Figure 2.13.

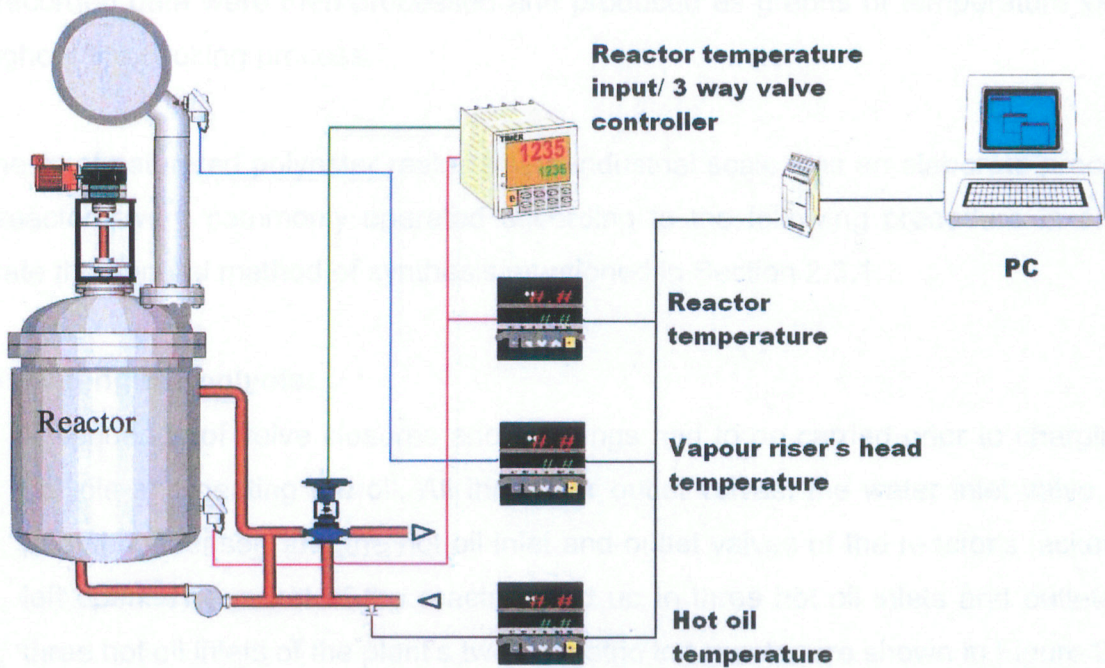


Figure 2.13 Temperature monitoring diagram of the resin plant's reactors

Process control facilities of the resin plant are shown in Figure 2.14



Figure 2.14 Temperature monitoring and process control room of the resin plant

In addition to the electronic temperature monitoring, analogue monitoring had also been employed in order to cope with any electronic equipment failure. This had been done by installing analogue thermometers at the same positions where the electronic temperature sensors were installed. Strict computer based process-control monitoring had also been employed. The reactor mixture temperature, packed vapour risers' temperature and hot oil inlet temperature of each reactor were recorded by means of specially developed software. The recorded data were then processed and produced as graphs of temperature vs. time throughout the cooking process.

Synthesis of saturated polyester resins at the industrial scale was an elaborate procedure. The reactors were commonly operated according to the following procedure in order to simulate the general method of synthesis mentioned in Section 2.3.1;

#### 1- Melting the polyols:

A sequence of valve closures and openings had to be carried prior to charging the polyols and heating the oil. All the water outlet valves, the water inlet valve of the partial condenser, and the hot oil inlet and outlet valves of the reactor's jacket were left open. The jacket of the reactors had up to three hot oil inlets and outlets. The three hot oil inlets of the plant's twelve metric ton reactor are shown in Figure 2.15.

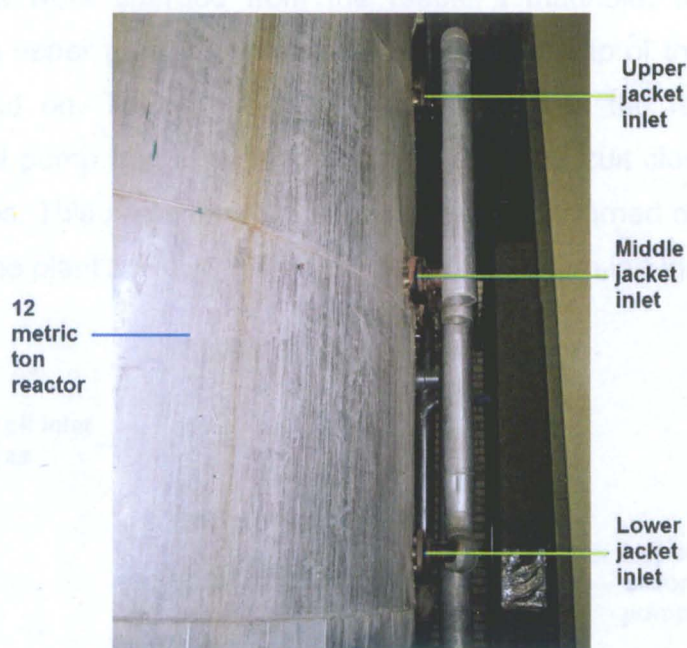
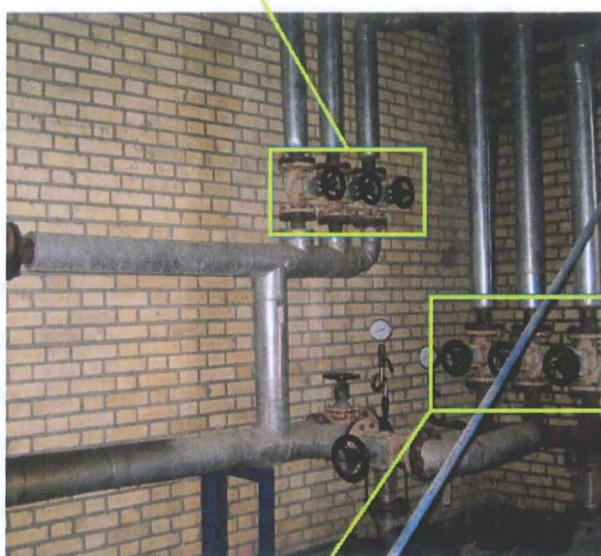


Figure 2.15 Hot oil inlets of the jacket of the twelve metric ton reactor

The valves of the inlets and outlets of the hot oil of the plant's twelve metric ton reactor are shown in Figure 2.16.

Lower, middle, and upper outlet valves



Lower, middle, and upper inlet valves

**Figure 2.16 Inlet and outlet valves of the hot oil of the jacket of the twelve metric ton reactor**

The valves that were closed included the discharge valve of the reactor, the water inlet valve of the total condenser, and the water inlet valve of the reactor's cooling coil. The polyols were charged from the reactor's manhole. Nitrogen gas was blanketed on the upper part of the reactor. The hot oil pump of the reactor's hot oil boiler was turned on. To aid the flow of the hot oil in the reactor's jacket, a secondary hot oil pump had also been installed on the circuit close to the reactor's hot oil inlet valves. This secondary hot oil pump was also turned on. The secondary hot oil pump of the plant's twelve metric ton reactor is shown in Figure 2.17.

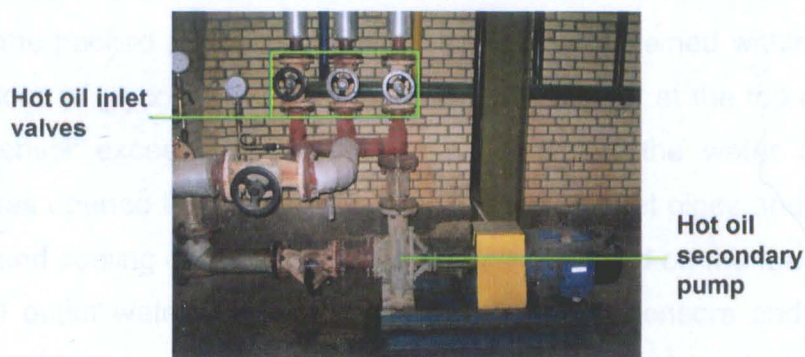


**Figure 2.17 Secondary hot oil pump of the twelve metric ton reactor**

The pumps of the hot and cooled water reservoirs were turned on. The air blowing fans of the cooling tower were turned on. The reactor's hot oil boiler was turned on and it was programmed to heat the oil to 180°C. Finally, the hot oil temperature of the 3-way valve controller was programmed on 150°C. By doing so, the valve would be shut after the temperature of the reactor had reached 150°C. In other words, the reactor temperature would not exceed 150°C throughout the procedure of polyol melting.

## **2- Charging the polyacids and initiating the esterification reaction:**

After the polyols were melted, the polyacids and the esterification catalyst were charged from the reactor's manhole. To homogenise the mixture of the polyols and polyacids, the motor of the mixer was turned on. The inlet valve of the water of the total condenser was opened. Then, the inlet valve of the water of the packed partial condenser was closed and the water remaining in its jacket was discharged. The nitrogen blanket on the upper part of the reactor was removed. Nitrogen was then blanketed in the lower part of the reactor and through the mixture. The boiler was programmed to heat the oil up to 270°C. The electronic controller of the 3-way hot oil valve was programmed on 185°C. This was done to allow the temperature of the reactor to reach 185°C. Therefore, the required energy for initiation of the esterification reaction was provided. As mentioned in Sections 2.3.2 and 2.3.3, the esterification reaction of the polyesters of this study initiated within 160-180°C.

## **3- Controlling the temperature at the top of the packed partial condenser:**

Similar to the pilot plant process at this point, the rise of the temperature at the top of the packed partial condenser indicated the start of the esterification reaction in the large scale reactor. As mentioned in Sections 2.3.2 and 2.3.3, the temperature at the head of the packed partial condenser had to be maintained within 95-103°C to prevent the loss of glycol. If the temperature of the vapour at the top of the packed partial condenser exceeded 103°C, the inlet valve of the water of the partial condenser was opened to some extent. The inlet and outlet pipes and valves of the condensers and cooling coils of the reactors were all placed on the main pipelines of the inlet and outlet water. The water outlets of the condensers and cooling coils were all directed to the main water outlet pipeline. The main water outlet pipeline directed the outlet water to the hot water reservoir. Similarly, the water inlet pipes

and valves of the condensers and cooling coils of the reactors were placed on the main water inlet pipeline. The main water inlet pipeline contained the cooled water from the cooled water reservoir. The main pipelines of the inlet and outlet water are shown in Figure 2.18.



**Figure 2.18 Main pipelines of the inlet and outlet water of the resin plant**

The water inlet valve of the packed partial condenser was closed if the vapour temperature at the top of the packed partial condenser fell below 103°C. This was done to ease the separation of the vapour of the water generated by the reaction from the reacting mixture.

#### **4- Increasing the temperature of the reactor to 230-250°C:**

When the vapour temperature at the top of the partial condenser began to decrease, the reactor was heated further. As mentioned Sections 2.3.2 and 2.3.3, the decrease of the temperature at the top of the partial condenser indicated that the generation of the water of reaction had begun to diminish. At this point, the reactor's temperature was increased by 5°C. This was done by defining the new temperature to the electronic controller of the reactor's pneumatic 3-way hot oil valve i.e. If the reactor's temperature was preferred to be increased from 200°C to 205°C, the electronic controller of the 3-way hot oil valve was programmed to automatically shut the valve when the reactor temperature had reached 205°C. Via this system, the

temperature of the reacting mixture was gradually increased to 230-250°C while the temperature at the top of the partial condenser was maintained between 95-103°C.

#### 5- Esterifying to the lowest possible acid value and ending the polymerisation:

When the generation of the water of reaction diminished after the reactor's temperature reached 230-250°C, samples were taken from the reactor for the determination of the acid value and the viscosity. Similar to the lab and pilot scale processes, as soon as the acid value of the resin did not decrease any further, the polymerisation was halted by cooling the resin inside the reactor. First, the hot oil boiler was turned off. Then the electronic hot oil valve controller was programmed to shut the 3-way valve. The secondary hot oil pump of the reactor was turned off. The inlet valve of the water of the partial condenser was opened. The inlet valve of the reactor's cooling coil on the main pipeline containing the cooled water was opened. When the temperature of the resin inside the reactor fell to 140°C, the lower nitrogen blanket was removed and the diluting solvent was added to the resin. Depending on the size of the reactor, the cooling of the resin took between two to four hours. The solvents of the resins were stored in solvent tanks that were adjacent to the plant. The solvent storage tanks of the resin plant are shown in Figure 2.19.



**Figure 2.19 Solvent storage tanks of the resin plant**

The solvent storage tanks were connected to the reactors via separate pipelines. The solvent was added to the resin inside the reactor by means of pneumatic pump

and solvent meter. The pneumatic pumps of the solvent storage tanks are shown in Figure 2.20



**Figure 2.20** Pneumatic pumps of the solvent storage tanks of the resin plant

Solvent collector and solvent meter of the plant's twelve metric ton reactor are shown in Figure 2.21.



**Figure 2.21** Solvent collector and solvent meter of the resin plant's twelve metric ton reactor

It can be seen, from Figure 2.21, that eight pipelines were connected to the solvent collector of the reactor. Each of these eight pipelines were connected to a separate solvent storage tank. After the addition of the solvent, the speed of the reactor's

mixer was increased to homogenise the diluted resin. The solid content of the resin was then adjusted to the preferred range by sampling and if required, further addition of solvent. The resin was then discharged from the reactor into appropriate barrels by means of pump.

Depending on the size of the reactor and the amount of charged raw material, it often took twelve to twenty hours to synthesise saturated polyesters at the industrial scale according to the procedure described.

### **2.3.5 Examples of lab, pilot, and industrial scale polymerisation details for a single saturated polyester**

Polymerisation records of an example saturated polyester resin are provided in this section. This saturated polyester, namely sample T, was designed and developed throughout the course of this study for coil coatings. Circumstances regarding the development of the formulation of sample T are discussed in detail in Chapter 3. After the formulation of this polyester was designed, it was synthesised at the lab scale. Then it was reproduced at the pilot and industrial scales. In Section 2.3.5.1, the formulation and the general procedure for polymerisation of sample T are described. In Sections 2.3.5.2, 2.3.5.3 and 2.3.5.4, polymerisation records pertaining to the synthesis of sample T at the lab, pilot, and industrial scales are provided. The theoretical evaluations of the lab, pilot, and industrial scale formulations of sample T are also provided in the Sections mentioned. In Section 2.3.5.5, the composition of the diluent solvent of sample T is described. Finally, the characteristics of the diluted resins of various scale reproductions of sample T are provided in Section 2.3.5.6.

#### **2.3.5.1 Procedure of polymerisation**

The procedure of polymerisation is described as follows. The polymerisation procedure concerned consisted of eight steps. The formulation of sample T is shown in Table 2.12.



**Table 2.12 Formulation of the saturated polyester resin synthesised as sample T throughout the course of the study**

	<b>Component</b>	<b>Moles</b>
1	Adipic acid	1.97
2	Isophthalic acid	2.64
3	Terephthalic acid	1.75
4	Neopentyl glycol	4.47
5	1,4 Cyclohexane-dimethanol	1.25
6	1,6 Hexanediol	1.13
	<b>Total</b>	<b>13.22</b>

**1- Neopentyl glycol, 1,4 cyclohexanedimethanol, and 1,6 hexanediol were charged to the reactor and heated until complete meltdown.**

The temperature at which these glycols had completely melted was 95°C.

**2- Adipic acid, terephthalic acid, and 1.58g of mono butyl oxide were added to the reactor.**

The main reason of not adding isophthalic acid at this stage was to facilitate the reaction of terephthalic acid in an environment with an excessive amount of glycol. The exclusion of isophthalic acid at this stage of the cook was also based on the previous cooking experiences. When terephthalic and isophthalic acids were added together, the colour of the resin did not become clear. About half of the esterification catalyst, monobutyltin oxide, was added at this stage. This was due to the presence of an excessive amount of glycol in the mixture. The remainder of monobutyltin oxide was added after isophthalic acid was charged.

**3- The mixture was heated up to 235°C under nitrogen blanket while keeping the temperature at the top of the partial condenser below 103°C.**

The partial condenser's head temperature was controlled below 103°C in order to avoid the loss of glycol.

**4- At 235°C, the resin was esterified to the lowest possible acid value which was 0.5 mgKOH/g. At this acid value, the polyester resin was completely clear.**

Esterifying to the lowest possible acid value was done in order to complete the reaction of adipic acid and terephthalic acid to the highest possible degree.

**5- The polyester resin was cooled to 180°C.**

This was done prior to charging isophthalic acid and in order to avoid the initiation of any esterification reaction during the addition of isophthalic acid to the reaction kettle. If isophthalic acid was added at temperature higher than 180°C, it could result in the initiation of an intense esterification reaction which was not favoured.

**6- Isophthalic acid and the remaining 2.11g of mono butyl oxide were charged into the reactor.**

**7- The mixture was then heated to 235°C under nitrogen blanket and esterified until cleared and to a final acid value range of 7-9 mgKOH/g.**

**8- After completion of the cook, the polyester resin was cooled to 170°C and diluted to 65% solids content with a mixture of solvesso-150 and methoxy propyl acetate.**

Seven parts of solvesso-150 were mixed with three parts of methoxy propyl acetate to prepare the resin's solvent mixture.

### **2.3.5.2 Theoretical evaluation of the lab scale formulation and the relevant polymerisation details**

The theoretical evaluation of the lab scale formulation of sample T is provided in Table 2.13. The designed formulation was theoretically evaluated according to the procedures mentioned in Section 2.2.

Table 2.13 Theoretical evaluation of the lab scale formulation of sample T

Sample T	Molecular weight	Equivalent weight	Charged weight (g)	Moles	Equivalents hydroxyl ( $e_{OH}$ )	Equivalents acid ( $e_{COOH}$ )	Theoretical weight of liberated water (g)
Component							
Adipic Acid	146	73	288.31	1.97	-----	3.95	71.09
Isophthalic acid	166	83	438.24	2.64	-----	5.28	95.04
Terephthalic acid	166	83	290.99	1.75	-----	3.51	63.11
1,4 cyclohexane-dimethanol	144	72	179.52	1.25	2.49	-----	-----
Neopentyl glycol	104	52	464.78	4.47	8.94	-----	-----
1,6 Hexandiol	118	59	133.92	1.13	2.27	-----	-----
Sum total			1795.76	13.22	13.70	12.74	229.2

$$e_{OH} / e_{COOH} = 1.076, H = 34.88 \text{ mgKOH/g}, Y_0 = 1567 \text{ g}, Y_{10} = 1571.6 \text{ g}, M_{10} = 2049 \text{ g/mol}$$

$$F = 1.9263, P_{gel} = 1.0382$$

The polymerisation details of sample T are provided in Tables 2.14A and 2.14B.

Table 2.14A Lab scale polymerisation details of sample T

Date started: 18/03/2008					Date finished: 18/03/2008					
Time	Total Time	Reactor Temperature (°C)	Head Temperature (°C)	Water Off (g)	Acid Value (mg KHO/g)	Viscosity (Poise @ 25°C)	Solid Content (%)	Reactor Solid Content (%)	Clarity	Sample:
										T
										Weight of Charged Material : 1799.36 g (Solid resin)
Comments										
04:15	-----	25	30	-----	-----	-----	-----	-----	-----	NPG, CHDM, and 1,6HD were charged, heating started
04:50	00:35	102	30	-----	-----	-----	-----	-----	Clear	Complete melt-down of the charged material

Table 2.14B Lab scale polymerisation details of sample T

Date started: 18/03/2008										Date finished: 18/03/2008
Time	Total Time	Reactor Temperature (°C)	Head Temperature (°C)	Water Off (g)	Acid Value (mg KHO/g)	Viscosity (Poise @ 25° C)	Solid Content (%)	Reactor Solid Content (%)	Clarity	Sample: T
										Weight of Charged Material : 1799.36 g (Solid resin)
										Comments
04:55	00:40	102	30	-----	-----	-----	-----	-----	Not clear	ADA, TPA, and 1.58g of MBTO were charged, heat up started, nitrogen blanketed
05:35	01:20	155	92	-----	-----	-----	-----	-----	Not clear	Reflux started
06:30	02:15	179	94	-----	-----	-----	-----	-----	Not clear	-----
07:30	03:15	208	99	50.3	-----	-----	-----	-----	Not clear	-----
08:30	04:15	233	65	109	-----	-----	-----	-----	Not clear	-----
08:45	04:30	235	57	112	0.7	-----	65	-----	Clear	Cooling to 180
08:55	04:40	180	48	-----	-----	-----	-----	100	Not clear	IPA and the remaining 2.11g of MBTO were charged, heat up started, nitrogen blanket maintained
09:22	05:27	201	91	-----	-----	-----	-----	100	Not clear	Reflux started
10:30	06:15	215	91	167	-----	-----	-----	100	Not clear	-----
11:30	07:15	228	74	193	-----	-----	-----	100	Not clear	-----
12:30	08:15	232	58	200	12	28	65	100	Clear	Diluted with solvesso-150/MPA : 7/3
14:00	09:45	236	50	203	8.3	44	65	100	Clear	-----
14:30	10:15	236	49	-----	7.3	53	65	100	Clear	The resin was cooled

It took 10:30 hours to synthesise sample T at the laboratory.

### 2.3.5.3 Theoretical evaluation of the pilot scale formulation and the relevant polymerisation details

The theoretical evaluation of the scaled up formulation of sample T for pilot synthesis is provided in Table 2.15.

**Table 2.15 Theoretical evaluation of the scaled up formation of sample T for pilot synthesis**

Sample T pilot scale reproduction	Molecular weight	Equivalent weight	Charged weight (kg)	Kilogram Moles	Equivalents hydroxyl ( $e_{OH}$ )	Equivalents acid ( $e_{COOH}$ )	Theoretical weight of liberated water (kg)
Component							
Adipic Acid	146	73	3.686	0.03	-----	0.05	0.909
Isophthalic acid	166	83	5.613	0.03	-----	0.068	1.2173
Terephthalic acid	166	83	3.730	0.02	-----	0.0449	0.80888
1,4 cyclohexane-dimethanol	144	72	2.300	0.02	0.032	-----	-----
Neopentyl glycol	104	52	5.955	0.06	0.115	-----	-----
1,6 Hexandiol	118	59	1.716	0.01	0.029	-----	-----
Sum total			23	0.17	0.18	0.163	2.935

$$e_{OH} / e_{COOH} = 1.076, H = 34.88 \text{ mgKOH/g}, Y_0 = 20.1 \text{ kg}, Y_{10} = 20.13 \text{ kg}, M_{10} = 2049 \text{ g/mol}$$

$$F = 1.9263, P_{gel} = 1.0382, \text{ Total mono butyl oxide used} = 0.034 \text{ kg}$$

Facilities and equipment explained in Section 2.3.3 were used for the synthesis of the formulation specified in Table 2.15. The method of synthesis described in Section 2.3.3 was followed. The relevant polymerisation details are provided in Table 2.16.

Table 2.16 Pilot scale polymerisation details of Sample T

Date started: 01/05/2008										Date finished: 01/05/2008
Time	Total Time	Reactor Temperature (°C)	Head Temperature (°C)	Water Off (g)	Acid Value (mg KHO/g)	Viscosity (Poise @ 25°C)	Solid Content (%)	Reactor Solid Content (%)	Clarity	Sample: T
										Weight of Charged Material : 23.034 kg (Solid resin)
										Comments
04:15	-----	30	-----	-----	-----	-----	-----	-----	-----	NPG, CHDM, and 1,6HD were charged, heating started
04:50	00:35	102	30	-----	-----	-----	-----	-----	Clear	Complete melt-down of the charged material
04:55	00:40	102	30	-----	-----	-----	-----	-----	Not clear	ADA, TPA, and 13.53g of MBTO were charged heat up started, nitrogen blanketed
05:25	01:10	158	92	-----	-----	-----	-----	-----	Not clear	Reflux started
06:15	02:00	179	97	-----	-----	-----	-----	-----	Not clear	-----
07:30	03:15	213	98	1.24	-----	-----	-----	-----	Not clear	-----
08:24	04:09	231	56	1.47	0.5	-----	65	-----	Clear	Cooling to 180
08:30	04:15	180	47	1.49	-----	-----	-----	100	Not clear	IPA and the remaining 20.3g of MBTO were charged, heat up started, nitrogen blanket maintained
08:55	04:50	200	90	-----	-----	-----	-----	100	Not clear	Reflux started
10:30	06:15	215	86	2.36	-----	-----	-----	100	Not clear	-----
11:30	07:15	230	57	2.66	16.3	19.3	65	100	Not clear	-----
13:00	08:45	236	54	2.71	9.8	35.8	65	100	Not clear	-----
13:45	09:30	235	50	2.73	8.7	41.2	65	100	Clear	-----
14:45	10:30	235	47	2.75	7.2	47.5	65	100	Clear	The resin was cooled

Similar to the laboratory process, it took 10:30 hours to synthesise sample T at the pilot scale.

### 2.3.5.4 Theoretical evaluation of the industrial scale reproduction formulation and the relevant polymerisation details

The theoretical evaluation of the scaled up formulation of sample T for industrial scale synthesis is provided in Table 2.17. This formulation was scaled up for synthesis in a 7000 litre reactor.

**Table 2.17 Theoretical evaluation of the scaled up formulation of sample T for synthesis in the 7000 litre reactor**

Sample T large scale reproduction	Molecular weight	Equivalent weight	Charged weight (kg)	Kilogram Moles	Equivalents hydroxyl ( $e_{OH}$ )	Equivalents acid ( $e_{COOH}$ )	Theoretical weight of liberated water (kg)
Component							
Adipic Acid	146	73	721.245	0	-----	0	0
Isophthalic acid	166	83	1098.25	4.94	-----	9.88	177.84
Terephthalic acid	166	83	729.747	6.62	-----	13.23	238.18
1,4 cyclohexane-dimethanol	144	72	450.001	4.4		8.7921	158.258
Neopentyl glycol	104	52	1165.05	3.13	6.25	-----	-----
1,6 Hexandiol	118	59	335.702	11.2	22.4	-----	-----
		Sum total	4500	2.84	5.69	-----	-----

$$e_{OH} / e_{COOH} = 1.076, H = 34.88 \text{ mgKOH/g}, Y_0 = 3926 \text{ kg}, Y_{10} = 3938 \text{ Kg}, M_{10} = 2049 \text{ g/mol}$$

$$F = 1.9263, P_{gel} = 1.0382, \text{ Total mono butyl oxide used} = 6.62 \text{ kg}$$

For synthesis, the method described in Section 2.3.4 was followed. As mentioned, a 7000 litre reactor was employed for the synthesis of sample T at the industrial scale. This reactor is shown in Figure 2.22.



Figure 2.22 7000 litre reactor used for the industrial scale reproduction of sample T

The polymerisation details of the industrial scale reproduction of sample T are provided in Tables 2.18A and 2.18B.

Table 2.18A Industrial scale polymerisation details of sample T

Date started: 23/09/2008										Date finished: 23/09/2008
Time	Total Time	Reactor Temperature (°C)	Head Temperature (°C)	Water Off (g)	Acid Value (mg KHO/g)	Viscosity (Poise @ 25°C)	Solid Content (%)	Reactor Solid Content (%)	Clarity	Sample:
										T
										Weight of Charged Material : 4506.62 kg (Solid resin)
Comments										
09:00	-----	34	29	-----	-----	-----	-----	-----	-----	NPG, CHDM, and 1,6HD were charged, heating started
09:43	00:43	92	-----	-----	-----	-----	-----	-----	Clear	Complete melt-down of the charged material
09:45	00:45	92	-----	-----	-----	-----	-----	-----	Not clear	ADA, TPA, and 2.65 kg of MBTO were charged heat up started, nitrogen blanketed
10:38	01:38	161	100	-----	-----	-----	-----	-----	Not clear	Reflux started



Table 2.18B Industrial scale polymerisation details of sample T

Date started: 23/09/2008					Date finished: 23/09/2008					
Time	Total Time	Reactor Temperature (°C)	Head Temperature (°C)	Water Off (g)	Acid Value (mg KHO/g)	Viscosity (Poise @ 25°C)	Solid Content (%)	Reactor Solid Content (%)	Clarity	Sample: T
										Weight of Charged Material : 4506.62 kg (Solid resin)
										Comments
11:30	02:30	180	103	150	-----	-----	-----	-----	Not clear	-----
12:38	03:38	205	102	237	-----	-----	-----	-----	Not clear	-----
13:37	04:37	210	102	305	-----	-----	-----	-----	Not clear	-----
14:40	05:40	230	85.5	345	-----	-----	-----	-----	Not clear	-----
15:10	06:10	235	80	-----	0.9	-----	65	-----	Clear	Cooling to 180
15:30	06:30	180	60.5	-----	-----	-----	-----	100	Not clear	IPA and the remaining 3.97 kg of MBTO were charged, heat up started, nitrogen blanket maintained
16:15	07:15	196	95	-----	-----	-----	-----	100	Not clear	Reflux started
17:30	08:30	205	100	-----	-----	-----	-----	100	Not clear	-----
19:00	10:00	230	97	553	19.6	16.9	65	100	Not clear	-----
20:15	11:15	235	79	-----	12.4	27.8	65	100	Not clear	-----
21:00	12:00	236	71	580	10.9	31.1	65	100	Clear	-----
22:00	13:00	235	68	-----	9.5	35	65	100	Clear	-----
23:00	14:00	240	65	-----	7.7	40.6	65	100	Clear	-----
23:30	14:30	240	60.5	-----	7.3	39.3	65	100	Clear	The resin was cooled.

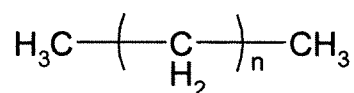
It took 14:30 hours to synthesise sample T in the 7000 litre reactor.

### 2.3.5.5 Diluent solvent composition

As mentioned in Section 2.3.5.1, the solvent used for dilution of sample T and its pilot and industrial scale reproductions was a mixture of seven parts of solvesso-150 and three parts of methoxy propyl acetate. The reason for choosing solvesso-150 and methoxy propyl acetate as solvents for sample T was due to the fact that this saturated polyester resin had been developed as a sole binder for particular coil coating systems. The main reducers of

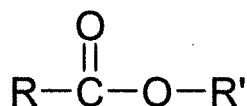
the coil coatings concerned were solvesso-150 and methoxy propyl acetate. Therefore, in order to achieve maximum compatibility with the coil coatings, the saturated polyester resin developed was supplied as a solution in the same solvents as the coil coatings.

Solvesso-150 is an aliphatic hydrocarbon. Aliphatic hydrocarbons that are also referred to as gasolines, benzines, or paraffin hydrocarbons, provide good stability and solvent power for nonpolar to poor polar film forming agents.<sup>115</sup> The general molecular structure of aliphatic hydrocarbon organic solvents is shown in Scheme 2.1



**Scheme 2.1 General molecular structure of aliphatic hydrocarbon organic solvents<sup>115</sup>**

Methoxy propyl acetate is among the ester group of organic solvents. Esters have a high dipole moment, a tendency to form hydrogen bridges, and excellent solvent power for most film forming agents.<sup>115</sup>



**Scheme 2.2 General molecular structure of ester organic solvents<sup>115</sup>**

#### **2.3.5.6 Characteristics of the same polyester after synthesis in the lab, pilot and industrial scales in terms of the acid value, viscosity and hydroxyl value**

As shown in Sections 2.3.5.2 to 2.3.5.4, sample T was synthesised in the lab, pilot and industrial scales. Characteristics of the polyesters obtained after synthesis in each of the scales mentioned are provided in Table 2.19. The more important of the characteristics concerned include the acid value, the viscosity and the hydroxyl value.

**Table 2.19 Characteristics of sample T after synthesis in the lab, pilot, and industrial scales in terms of acid value, viscosity and hydroxyl value**

	Lab scale	Pilot scale	Industrial scale	Test method/ Instrument used
<b>Non-volatile content (%)</b>	65.5	65.5	65.5	ISO 3251
<b>Solvent</b>	Solvesso-150/ MPA : 7/3	Solvesso-150/ MPA : 7/3	Solvesso-150/ MPA : 7/3	-----
<b>Acid value mg KOH/g</b>	6.9	6.9	7.3	ISO 3682
<b>Viscosity (Poise at 25°C)</b>	40.0	41.0	38.3	Brookfield CAP2000
<b>Density (g/cm<sup>3</sup>)</b>	1.07	1.07	1.07	ISO 2811
<b>Theoretical hydroxyl value (mgKOH/g)</b>	34.88	34.88	34.88	According to the method described in Section 2.2
<b>Hydroxyl value mg KOH/g (actual on 65% resin)</b>	18.42	17.72	19.70	ISO 4629
<b>Hydroxyl value mg KOH/g (actual on 100% resin)</b>	28.34	27.27	29.49	ISO 4629

Although minor differences existed in terms of the characteristics shown in Table 2.19 for sample T after its synthesis in the lab, pilot and industrial scales, on the whole it was considered completely reproduced. It could be seen, from Table 2.19, that the determined actual hydroxyl values indicated that although theoretical hydroxyl value is not as accurate as the actual hydroxyl value, its calculation beyond doubt provides a relatively clear picture of the –OH content of any designed formulation.

## **2.4 Equipment used for DSC, NMR, IR and SEC analysis of the saturated polyester resins synthesised and the relevant test parameters**

In Sections 2.4.1 to 2.4.4, the instruments used for the analysis of DSC, NMR, IR and SEC are introduced and the relevant test parameters are mentioned.

### 2.4.1 DSC instrument

For determination of the glass transition temperature of the saturated polyester resins synthesised, the technique of differential scanning calorimetry (DSC) was employed. The instrument used was Perkin Elmer Jade differential scanning calorimeter. This instrument was a heat flux scanning calorimeter and was equipped with Pyris 6 software.

The synthesised saturated polyester resins were introduced to the differential scanning calorimeter in 100% solid form. In other words, the diluted resin could not be used for differential scanning calorimetry. Therefore, the saturated polyester resins that were to be analysed by the differential scanning calorimeter had to be discharged from the reaction kettle without dilution. To discharge saturated polyester resins from the kettle in 100% solid form, they were polymerised according to the usual procedure mentioned in Section 2.3.1. However, after the lowest possible acid value was achieved, the resin was cooled to 150°C and quickly discharged from the kettle at this temperature. The reason for using this practice was because undiluted saturated polyester resins, particularly those with low hydroxyl content, were of extremely high viscosity at temperatures below 100°C. Undiluted saturated polyester resins, particularly those with glass transition temperatures of above 10°C, are rock solid materials at room temperature. After the 100% solid saturated polyester resin was introduced to the differential scanning calorimeter, initially it was maintained at -50°C for one minute by the aid of liquid nitrogen. Then, it was heated from -50°C to 300°C with a heat flow of 10°C/min. The relevant data was then processed and produced as thermograms in which the glass transition temperature of the saturated polyester resin was calculated and specified by the instrument's software.

### 2.4.2 NMR instrument

In order to study the effects of the replacement of polyols on the molecular structure of the saturated polyester resins synthesised, nuclear magnetic resonance spectroscopy was employed. The NMR spectrometer used was a Bruker Avance 400.

Proton NMR and carbon-13 NMR were carried out for the saturated polyester resins synthesised. In order to obtain signals from the saturated polyester resins and the NMR solvent in the spectra only, 100% solid resins were used for sample preparation. If diluted saturated polyester resins were used, signals from the resin's solvent would emerge in the

spectra. The additional signals from the solvent would then overlap the signals from saturated polyester resin in the spectra and complicate the interpretation. For preparation of the samples, 100% percent solid resins were dissolved in deuterated chloroform ( $\text{CDCl}_3$ ). As mentioned in Section 1.7.4, samples to be investigated by the NMR spectrometer are dissolved in a proton free solvent.  $\text{CDCl}_3$  is the most commonly used solvent for this purpose. The conditions of proton and carbon-13 NMR analysis carried out for the saturated polyester resins synthesised are shown in Table 2.20.

**Table 2.20 Details of the  $^{13}\text{C}$  NMR and  $^1\text{H}$  NMR analysis carried out on the saturated polyester resins synthesised**

Type of NMR analysis	Frequency (MHz)	Temperature ( $^{\circ}\text{C}$ )	Solvent	Detection technique
$^{13}\text{C}$ NMR	100.62	25	$\text{CDCl}_3$	Z...G...P...G
$^1\text{H}$ NMR	400.13	25	$\text{CDCl}_3$	Z...G...30 $^{\circ}\text{C}$

### 2.4.3 FTIR instrument

As a complimentary analysis to the nuclear magnetic resonance spectroscopy, the saturated polyester resins synthesised were characterised by Fourier transformed infrared spectroscopy as well. For this analysis, Perkin-Elmer Spectrum One FTIR spectrometer was employed.

Fourier transformed infrared spectroscopy was employed to identify the functional groups present on the polymeric backbone of the saturated polyester resins synthesised. The saturated polyester resin samples were introduced to the FTIR spectrometer in 100% solid form. Similar to the NMR analysis, this practice was carried out as such in order to avoid the emergence of interrupting signals from the solvent of the resin in the FTIR spectrum. The FTIR analysis was carried out at 25 $^{\circ}\text{C}$ .

### 2.4.4 SEC instrument

In order to characterise the molecular weight attributes of various scale reproductions of the standalone coil coating saturated polyester resin to be developed, the technique of size

exclusion chromatography was employed. The instrument used in this regard was an Agilent HP 1100 gel permeation chromatograph.

The Agilent HP 1100 was equipped with an efficient pump, vacuum degasser, large column compartment accommodating multiple columns, and coupled RI and UV detector systems. This instrument provided a variety of information with regard to molecular weight characteristics that included the number average molecular weight ( $M_n$ ), weight average molecular weight ( $M_w$ ), and polydispersity index. For introduction of the saturated polyester resin samples into the gel permeation chromatograph, they were eluted in tetrahydrofuran (THF) with a concentration of 1g/l. The eluted samples were then injected into the gel permeation chromatograph with a flow rate of 1ml/min. After the injected sample had completely eluted from the column's gel, the instrument processed the data acquired from its detectors. The instrument's software provided the processed data in the form of a chromatogram and calculated values of the number average molecular weight, the weight average molecular weight, and the polydispersity index.

## **2.5 Tests of coil coating films and procedures for preparation of coil coatings from the saturated polyester resins synthesised**

In Section 2.5.1, the mechanical tests and the chemical resistance tests carried out on the coil coating films derived from the saturated polyester resins synthesised are introduced and described. Specifications of the competitor products to be replaced by the universal and standalone polyester resin to be developed are provided in Section 2.5.2. Procedures for preparation of the coil top coats and coil primer coats from the saturated polyester resins synthesised will be provided in Section 2.5.3. Finally, the basis of choice with respect to the properties desired is discussed in Section 2.6.

### **2.5.1 Crucial mechanical tests and chemical resistance tests for coil top coatings**

As mentioned in Section 1.2, high flexibility and outstanding adhesion are the major requirements of coil coatings.<sup>7,8,18,19,116</sup> Visual observation of the results of simple mechanical tests and chemical resistance tests constitute the basis for the evaluation of

the coil coating integrity.<sup>20</sup> Five critical tests were employed for evaluation of the coil top coatings derived from the saturated polyester resins synthesised. In this regard, the top coat was required to meet the desired properties according to the test methods of ECCA-T7 (Resistance to cracking on bending), ECCA-T11 (MEK solvent rubbing test), ECCA-T5 (Resistance to rapid deformation) and ECCA-T8 (Resistance to salt spray). As mentioned in Section 1.2, the ECCA test methods are established by the European Coil Coating Association. In addition to these, König Pendulum film hardness of the top coats according to ISO 1522 test method was determined. The following is a description to the test methods concerned.

### 2.5.1.1 Resistance to cracking on bending or the T-bend test

The most important quality of coil coatings is considered to be flexibility as defined by the T-bend test.<sup>117</sup>

In principle, the purpose of the T-bend test is to evaluate the resistance to cracking of a coating when bent through 135-180°. This test method involves bending the coil coated panel parallel to rolling direction of the coil with the coating on the outside. The bending is carried out through radii between 135-180° over a period of 1-2 seconds. Close contact has to be maintained between the sample and the wedge to ensure a uniform bend. Any bending device allowing a uniform and smooth bend as such may be used. The minimum bending radius at which the sample panel can be bent without cracking is expressed as the crack resistant radius. The smallest bending radius is stated as 0T as shown in Figure 2.23 and Figure 2.24. The next radii are stated as ½T, 1T, 1½T, 2T, etc.... as shown in Figure 2.24.<sup>118</sup>

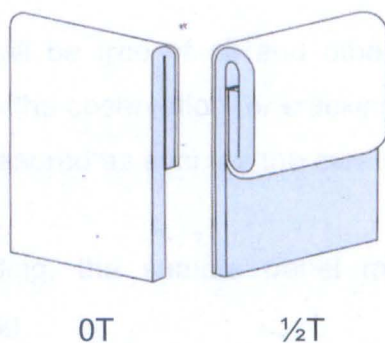


**Figure 2.23 Schematic illustration of ECCA T-bends-1**

As the level of adhesion between the top coating, the primer coating and the substrate

must remain intact, the adhesion of the coating on each bending radius may also be evaluated. This is done by peeling off the coating on the bent area by means of adhesive tape. In this regard, the minimum radius at which the coating is not at all peeled off is stated as the adhesion radius. The smallest radius in this regard is expressed as  $0T$ .

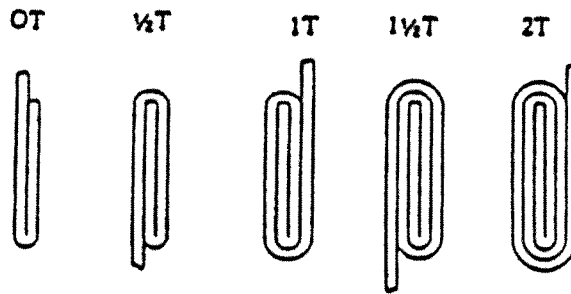


**Figure 2.24 Schematic illustration of ECCA T-bends-2<sup>118</sup>**

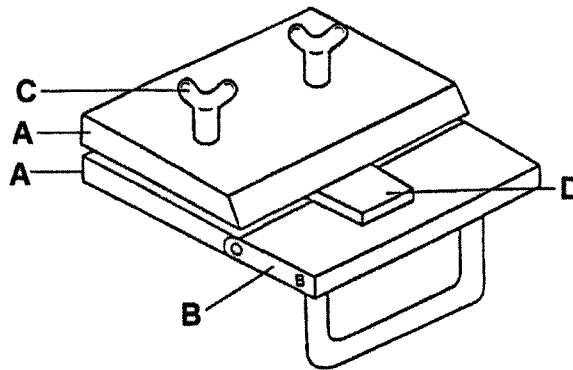
Adhesion has been described by different theories such as mechanical interlocking, chemical bonding, diffusion, physical adsorption and electrostatic force.<sup>19</sup> Although these theories must be considered for understanding the process of adhesion, tests such as the peeling test are always required for the evaluation of the adhesion of coatings at a macroscopic level.

After the application and curing of the coating, the sample has to be prepared as following;<sup>118</sup>

- 1) The coating under the test should always be at the outside of the bend.
- 2) Only flat strip should be used, in such a size that the required bending procedure can be executed.
- 3) The coating surface shall be free of oil and other matter that can influence the flexibility or interfere with the observation for cracking or adhesion.
- 4) The samples can be measured as soon as the cured coating is cooled down to room temperature.
- 5) Immediately after bending, the sample panel must be examined with a  $\times 10$  magnifier for any cracking.
- 6) Because of possible burrs, one should ignore up to 5mm on extreme edges of the sample panel.



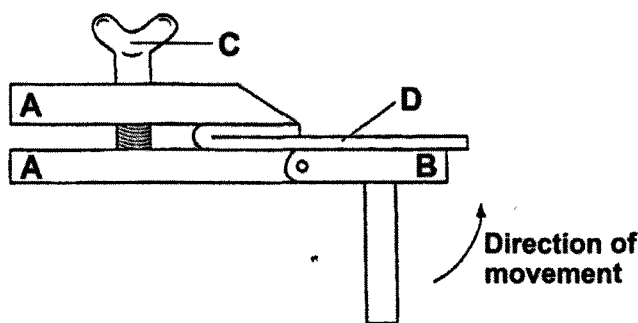
For bending, either folding or mandrel methods can be used.<sup>118</sup> Deflorian et al<sup>20</sup> used cylindrical mandrels with different diameters to bend coil coated panels (p.1285). The bending method is selected according to the size of the sample panel.<sup>118</sup> In the folding method, "the bending apparatus is firmly secured near the edge of a bench, so that the handle can be operated freely. The sample is firmly clamped between the jaws of the device or vice (Figure 2.25), with the painted surface to be evaluated downward, or, in the case of the vice, facing the operator. The handle operating the bending plate is smoothly lifted over a period of 1-2 seconds."<sup>118</sup>



A. Apparatus jaws B. Bending plate C. Clamping screws D. Sample

**Figure 2.25 Schematic illustration of apparatus forming bends through folding-1<sup>118</sup>**

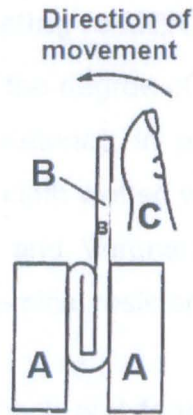
The direction of movement of the handle for bending the sample is shown in Figure 2.26.



A. Apparatus jaws B. Bending plate C. Clamping screws D. Sample

**Figure 2.26 Schematic illustration of apparatus forming bends through folding-2<sup>83</sup>**

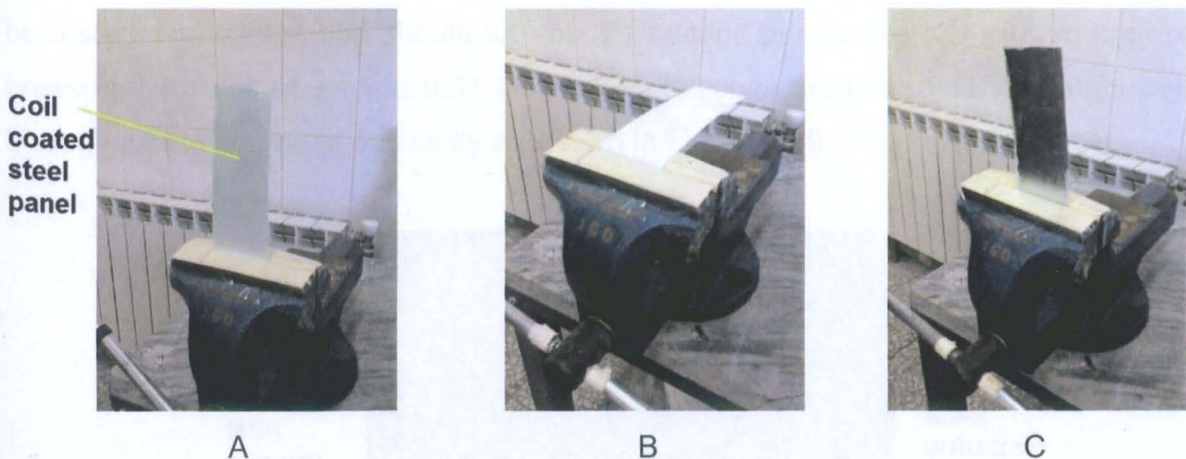
"This operation is continued with the sample being examined immediately after each bend,"<sup>118</sup> with a  $\times 10$  magnifier for cracking, and by peeling off the coating on the bent area by adhesive tape for evaluation of the adhesion. "In the instance of a vice being used where no bending plate is available, even pressure should be applied with both thumbs as shown in Figure 2.27 to ensure a smooth bending operation"<sup>118</sup>



A. Apparatus jaws B. Sample C. Thumb

**Figure 2.27 Schematic illustration of forming bends with vice and thumbs<sup>118</sup>**

The cracking and adhesion radii are stated in correct T-expressions. Throughout this study, the folding method was used for bending the coil coated panels. A bench vice was used as the bending apparatus as shown in Figure 2.28.



- A) Secured sample panel (coated side facing the operator)  
 B) Sample bent by thumbs  
 C) Sample folded (back side facing the operator)

**Figure 2.28 T-bend test apparatus and procedure**

For the evaluation of the flexibility of coil coatings, other test methods may also be used. Deflorian et al<sup>20</sup> used the test method defined by ISO 1519 standard for bending coil coated substrates.

### 2.5.1.2 Resistance of the coil top coating to MEK solvent Impact

The purpose of this test is to evaluate the degree of curing of the coil coating film through its resistance to MEK (Methyl Ethyl Ketone). In principle, this test method consists of rubbing the coating surface with a test cloth wetted with MEK until the coating begins to be removed.<sup>119</sup> Rossi et al<sup>12</sup> and Perou and Vergnaud<sup>71</sup> also used the same method for evaluating the degree of curing and chemical resistance of coil coating systems.

The rubbing is made by longitudinal back and forth rubs (double rubs) with the rubbing length being 5 times the length of the contact area. The contact area must be 100 mm<sup>2</sup> minimum. A variety of test cloths can be used. Different cloths yield different results and thus have to be mentioned in the expressions of test results. For preparation, the sample panel has to be cooled down to room temperature after curing and must be of the appropriate size.<sup>119</sup>

Procedure wise, the cloth is wetted with MEK and the finger tip is placed on the sample to be tested. Rubbing speed should be about 1 second per double rub with an approximate pressure load not exceeding 0.04 MPa.<sup>119</sup> MEK solvent rubbing test was manually done throughout the course of this study as shown in Figure 2.29.

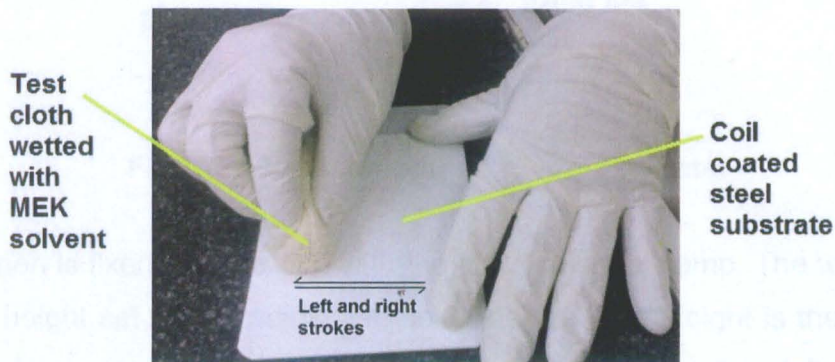


**Figure 2.29 MEK solvent rubbing test on a coil coated steel substrate**

The test cloth must remain wet throughout the whole rubbing procedure. At the point where the coating begins to be removed and the material underneath can be seen, the rubbing must stop. The result of the test is expressed as the number of double rubs by which the coating was removed.<sup>119</sup>

### 2.5.1.3 Resistance to cracking after rapid deformation by impact

The purpose of this test is to evaluate the elongation tolerance, resistance to cracking and adhesion of an organic coating upon impact with a predefined weight. In principle, a weight with hemispherical ends falls on the coated side or reverse of a sheet metal specimen fixed onto a corresponding die.<sup>120</sup>

Other methods may also be used for the evaluation of the deformation resistance of coil coatings. Deflorian et al<sup>20</sup> used the cupping test according to the test method defined by ISO 1519 to deform coil coated substrates. Throughout the course of this study, an impact tester was used for deformation of coil coated galvanised steel substrates. The impact tester used is shown in Figure 2.30

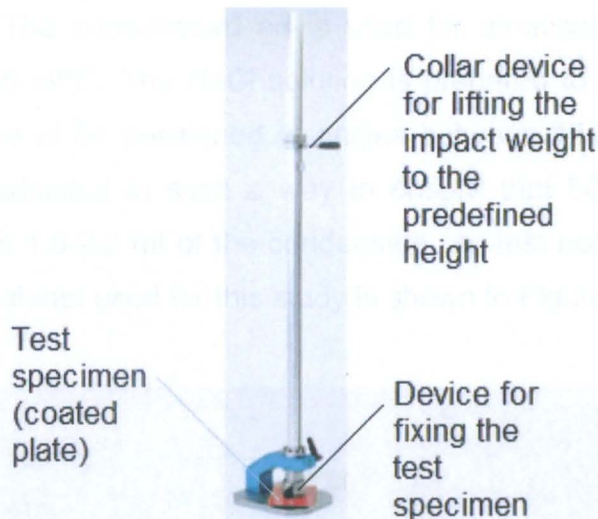


**Figure 2.30 Elcometer 1615 impact tester**

The test specimen is fixed into position with the quick release clamp. The weight is lifted to the predefined height set by the adjustable collar device. The weight is then released and the resulting deformation is observed. The coating adhesion on the deformed area may also be evaluated if required by the peeling test. The coated and back sides of the sample panel must be subjected to the impact. The peel test must be carried out on the coating area deformed as the result of the impact on the backside of the sample panel by means of adhesive tape. The impact force employed for the coil coatings concerned is usually 15 Joules. To create this force, a 2lb weight is lifted to a 40inch height and released. Any cracking and chipping of the coating film after the impact and the peel tests are visually observed and reported as the result of the test.

#### 2.5.1.4 Resistance to salt spray

Coil coated steel sheets that are intended for outdoor structures must have an outstanding resistance against corrosion.<sup>12</sup> The test methods described in Sections 2.5.1.1 to 2.5.1.3 do not evaluate the corrosion resistance and durability of coil coatings.<sup>19</sup>

One of the more important tests for evaluation of the corrosion resistance of coil coatings is resistance to salt spray. The purpose of this test is to evaluate the degree of corrosion of a coil primer coated and coil top coated steel panel after its exposure to neutral salt solution for a specific period of time. The apparatus of this test consists of a cabinet with a salt solution container and compressed air facilities. This cabinet generates fog of the salt solution by means of one or several spray nozzles. The temperature of the cabinet is maintained at  $35\pm 2^\circ\text{C}$ . The compressed air is used for atomisation of the salt solution which is preheated to  $46\text{--}49^\circ\text{C}$ . The NaCl solution is prepared to give a concentration of 5%. Sample panels have to be positioned at angles between  $15\text{--}25^\circ$  to the vertical. The flow of the salt fog is adjusted in such a way to ensure that  $80\text{cm}^2$  of the specimen's horizontal surface collect  $1.0\text{--}2.0\text{ ml}$  of the condensate per test hour.<sup>121</sup> A picture from the inside of the salt spray cabinet used for this study is shown in Figure 2.31.

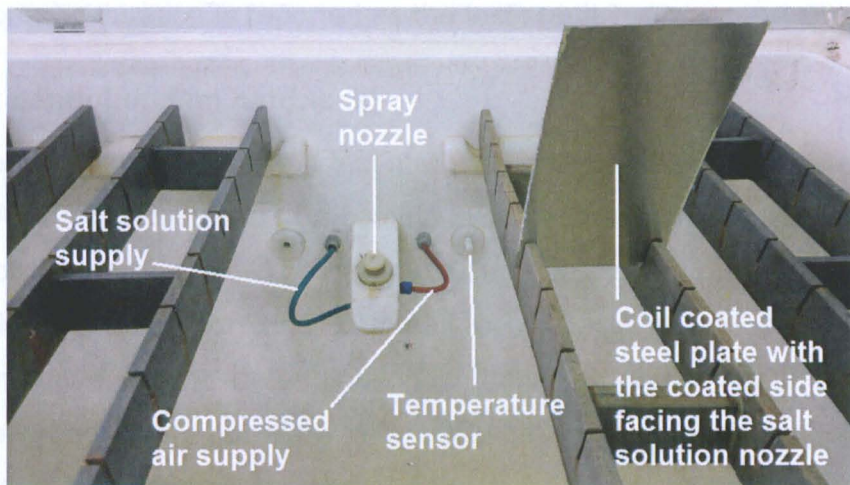


**Figure 2.31** Inside of the salt spray cabinet

The backside and edges of the sample panels are protected during the exposure to prevent any corrosive influence from the reverse side on the front side. The front coated side of the test panel is scored by an appropriate cutting tool. This cut extends only through the top and primer coats and should expose  $0.2\text{ mm}$  of the steel substrate. The cut must be

of a X-shaped sketch.<sup>121</sup> A schematic illustration of the cut profile and dimensions of the specimen is provided in Figure 2.32.

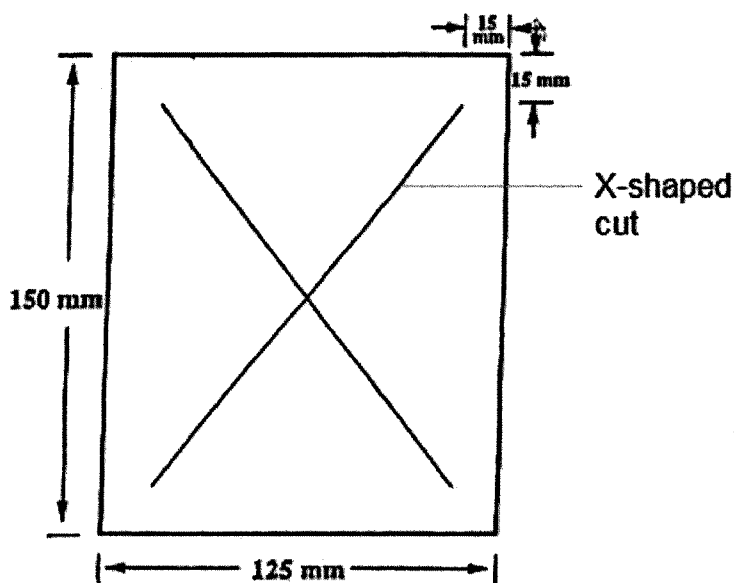


**Figure 2.32 Schematic illustration of the cut profile and dimensions of the primer and top coated specimen to be exposed to salt spray<sup>121</sup>**

The extent of creep and blistering in millimeters from the X-shaped cuts after the predefined exposure duration is reported as the test result.

#### 2.5.1.5 Konig pendulum film hardness

There are a number of definitions and test methods associated with the abrasive resistance of a coating. Abrasive resistance of a coating is sometimes considered to be a function of the hardness of the coating film. The hardness of a coating film relates to various material properties including elongation ability, modulus of elasticity and cohesion. There are various test methods for the determination of these properties for a coating film. The properties concerned rarely correlate with each other, i.e. a high modulus of elasticity cannot be equated with a high hardness.<sup>122</sup>

For the determination of the film hardness of coatings, there are various instruments by which indentation resistance, influence of coatings on damping of vibrations and resistance to damaging effects of scratching tools can be measured.<sup>122</sup> With respect to this study, the vibration damping influence of the coil coatings derived from the polyesters synthesised was determined as a measure of film hardness. A pendulum hardness tester

corresponding to the instrument introduced in ISO 1522<sup>123</sup> test method was used. A schematic illustration of the said pendulum hardness tester is shown in Figure 2.33.

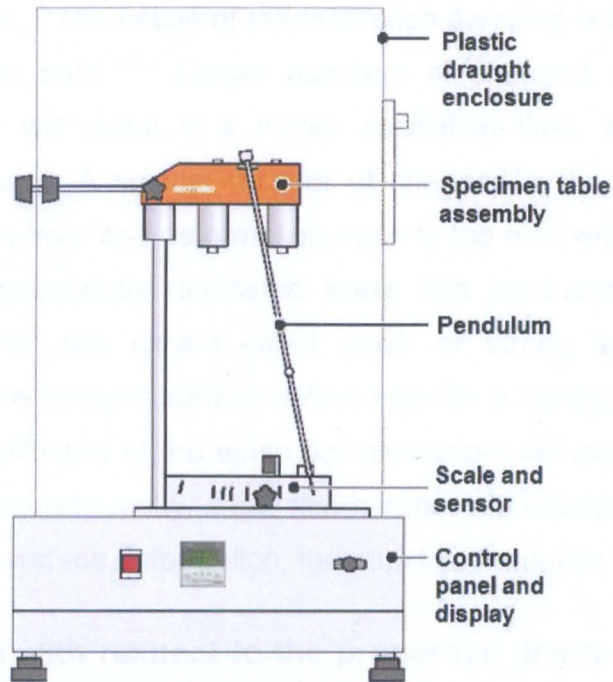


**Figure 2.33 Schematic illustration of Elcometer 3034 pendulum hardness tester**

It can be seen, from Figure 2.33, that one of the major components of a pendulum hardness tester is a pendulum. To the support of this pendulum, two agate balls are attached. The diameters of the balls are 5mm. A variety of pendulums with different weights are used. One the more important pendulums is the Konig pendulum. The Konig pendulum weighs 200g. The pendulum is placed on the coating by the agate balls 6° away from the rest position. A schematic illustration of the position of the pendulum's agate balls on the surface of the coating is shown in Figure 2.34.

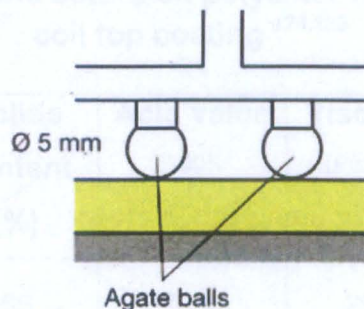


**Figure 2.34 Schematic illustration of the position of the pendulum's agate balls on the coating film**<sup>122</sup>

The pendulum is then released and the number of oscillations occurred are recorded by a counter. The time elapsed in seconds until the amplitude of the pendulum drops from 6° to 3° is the measure of damping. For comparison purposes, measurements were made at constant room temperatures. "The cause of the oscillation damping is the cyclic change in deformation caused by the balls."<sup>122</sup> Larger numbers of changed cyclic deformations allowed by a coating film will result in a longer oscillation time, which consequently indicates higher film hardness. A smaller number of changed cyclic deformations, or in other words, greater change from one deformation cycle to the next will result in a reduced oscillation time which consequently, indicates lower film hardness. The viscoelastic properties of a coating film will exhibit either weak or strong surface deformation resistance. Strong resistance towards surface deformation by a coating film will hinder the agate ball movement. The difficulty of the agate ball movement will result in the oscillation being damped rapidly and consequently, a low film hardness is recorded. If a coating film exhibits weak resistance to surface deformation, then the film hardness will be high.

### 2.5.2 Basis of selection with respect to the properties desired to be achieved by the standalone and universal resin system to be developed

As mentioned in Section 1.9, the objective of this project was to develop a novel and standalone coil coating saturated polyester resin that would provide multiple properties all together. As such, the resin system to be developed was desired to replace four competitor polyesters in a particular coil top coating and a particular coil primer coating. The properties of the competitor polyesters were set as control throughout the course of this study. In Table 2.21, specifications of two saturated polyester resins that were employed in the control coil top coating are shown.

**Table 2.21 Specifications of the saturated polyester resins employed in the control coil top coating**<sup>124,125</sup>

Saturated polyester resin	Structure	Solids content (%)	Acid value (100% (mgKOH/g))	Viscosity (Poise @ 25°C)	Hydroxyl value (mgKOH/g)	Solvent composition
FINNRESIN PE-2/65GS	Semi-branched	65	7-10	25.7	20-30	Solvesso-150/PMA: 8/2
Uralac SN 865	Linear	75	3-7	26.4	15-30	Solvesso-150



In the control coil top coating, FINNRESIN was flexibilised with the linear Uralac SN865 at a solid resin mixing ratio of 79.56 (FINNRESIN) /20.44 (Uralac SN865). The curing agent employed for the control polyesters was a hexamethoxymethyl melamine known as CYMEL 303. Specifications of CYMEL 303 are shown in Table 2.22.

**Table 2.22 Specifications of Cymel 303<sup>126</sup>**

Solids content (%)	Degree of alkylation	Alkylation alcohol	Viscosity (Poise @ 25°C)	Free formaldehyde content
≥98	High	Methanol	45	<0.25

The polyester to HMMM ratio of the control coil top coating was 81.2/18.8. FINNRESIN PE-2/65GS was specifically developed by Teknos for coil top coatings with excellent hardness and adhesion to aluminum and steel substrates and some flexibility.<sup>124</sup> Uralac SN 865S2-75, supplied by DSM, was a flexibiliser for can and coil coatings.<sup>125</sup> The HMMM curing agent of Cymel 303 was a product supplied by Cytec. The control coil top coating contained titanium dioxide and was highly pigmented. The pigment to binder ratio of the control coil top coating was 48:52 (m:m).

Prior to application of the control coil top coating, the galvanised steel substrate was primer coated. In the control primer coating, two saturated polyesters with the specifications shown in Table 2.23 were employed.

**Table 2.23 Specifications of the saturated polyesters employed in the control coil primer coating<sup>125</sup>**

Saturated polyester resin	Structure	Solids content (%)	Acid value (100% (mgKOH/g))	Viscosity (Poise)	Hydroxyl value (mgKOH/g)	Solvent composition
Uralac SN 905	Linear	60	13-17	68-70 @ 30°C	20	Solvesso-100/DBE
Uralac SH 974	Linear	35	0-2	26-27 @ 25°C	5	Solvesso-150/DBE

Similar to FINNRESIN in the control coil top coating, both of the resins in the control coil primer coating were flexibilised with the linear Uralac SN865 at a solid resin mixing ratio of 56.22 (Uralac SN905) /34.22 (Uralac SH974)/ 34.22 (Uralac SN865). The polyester to HMMM ratio of the control primer coating was 89 /11 and the same HMMM curing agent as used in the top coating (Cymel 303) was employed. The pigment to binder ratio of the control coil primer coating was 19:81 (m:m).

The control coil primer coating was applied on the galvanised steel substrate and cured for 30 seconds at 320°C with the peak metal temperature reaching 235-240°C. The wet film thickness of the primer coating was appropriately adjusted so that a final dried film thickness of 5-7µm could be achieved. After the steel substrate was primer coated, the control coil top coating was applied and cured for 30 seconds at 320°C with the peak metal temperature reaching 230-235°C. The wet film thickness of the coil top coating was appropriately adjusted so that a final dried film thickness of 22-25µm could be achieved. The properties of the control coil primer coating and the control coil top coating in terms of the tests of T-bend, MEK solvent resistance, impact resistance, resistance to salt spray and pendulum film hardness are shown in Table 2.24.

**Table 2.24 Mechanical and chemical resistance properties of the control coil primer coating and control coil top coating**

Coating property Curing schedule : 30 seconds/ PMT=230-235°C, dried film thickness: 27-32 µm		Test method
T-bend test	cracking radius : 0T	ECCA-T7
	adhesion radius : 0T	
MEK solvent rubbing test ( double rubs)	100	ECCA-T11
Impact test	No cracks after indentation with 15 Joules	ECCA-T5
	No paint chipping after the peel test of the deformed area	
Resistance to salt spray	Less than 2mm of creep and blistering	ECCA-T8
Konig pendulum film hardness (seconds @ 23°C)	77	ISO 1522

It can be seen, from Table 2.24, that the control coil primer coating and the control coil top coating provided an efficient compromise among hardness and flexibility. However, the balance between hardness and flexibility was achieved through a combination of four saturated polyester resins. As such, the same exceptional properties were desired to be achieved with a single and novel resin system to be developed, synthesised and characterised throughout the course of this study.

### 2.5.3 Preparation procedures for the coil coatings and coil coated substrates

#### 2.5.3.1 Equipment used for preparation, application, and curing of the coil coatings

A list of the major lab equipment employed for the preparation of the coil coatings that were derived from the saturated polyester resins synthesised is provided in Table 2.25.

**Table 2.25 Lab equipment used for the preparation, application and curing of the coil coatings**

EQUIPMENT	QUANTITY	FUNCTION
0.001 g accuracy balance	1	Weighing raw materials
250 cm <sup>3</sup> glass beaker	1	Weighed material container
500 cm <sup>3</sup> glass beaker	1	Weighed material container
Mechanical agitator	1	Mixing
Stirrer bead mill (FrymaKoruma MS 12)	1	Disperser of the millbase of the coil coating
DIN 4 flow cup (Elcometer 2350)	1	Adjusting the viscosity of the let down added coil coating
20cm × 10cm galvanised steel panels with a thickness of 0.55 millimeters	As required	Substrate
16µm spiral bar coater (Elcometer 4361/6)	1	Applying the coil primer coating
60µm spiral bar coater (Elcometer 4361/16)	1	Applying the coil top coating
Chamber furnace with air circulation (Nabertherm N30 65HA)	1	Curing the coil coated substrates
Temperature-tape indicator	As required	For determination of the peak metal temperature

For curing of the coil coated galvanised steel substrates, a peak metal temperature of 230-235°C was required. To achieve the peak metal temperature of 230-235°C, the temperature of the chamber of the furnace specified in Table 2.21 was set on 320°C during the experiments.

### **2.5.3.2 Method of preparation for coil top coatings derived from the saturated polyester resins synthesised**

For preparation of the coil top coatings from the polyester resins synthesised, each polyester resin sample was incorporated as the sole binder in the coil top coating and as a replacement for the control polyesters. As such, titanium dioxide containing coil top coatings were prepared. Details of the control polyesters and the control coil top coating were provided in Section 2.5.2. The same amount of pigmentation as used for the control coil top coating was used for the coil top coatings that were prepared from the polyesters synthesised. Also, the same polyester to HMMM ratio of the control coil top coating was maintained for the coil top coatings that were derived from the saturated polyester resins synthesised.

### **2.5.3.3 Method of preparation for the coil primer coating to be derived from the standalone universal saturated polyester resin to be developed**

According to the outline mentioned in Section 1.9, if a standalone saturated polyester resin with balanced hardness and flexibility was developed for the coil top coating, then a primer coating would be derived from this standalone resin. The primer coating would be prepared by replacing the control polyester resins of the coil primer coating with the standalone resin. The same pigmentation and polyester to HMMM ratio of the control coil primer coating would be maintained for the coil primer coating to be derived from the standalone saturated polyester resin to be developed. Details of the control coil primer coating and its control polyesters were provided in Section 2.5.2.

### **2.5.3.4 Substrates used, pre-treatment of the substrates and method of application and curing schedule of the coil primer coatings**

The substrates used were 20cm×10cm galvanised steel panels with a thickness of 0.55 millimeters. These panels were initially chromium treated. The same treatment had also been used by Souto et al<sup>13,127</sup>. Phosphate pretreatment may also be used for this purpose as practiced by Rossi et al<sup>12</sup>. After the chromium pre-treatment, the control coil primer coating was applied on the substrate with the 16µm spiral bar coater. The same application

method was practiced by Boyes et al<sup>107</sup>. The wet primer coated panels were then cured at 320°C for 30 seconds during which time the peak metal temperature reached 230-235°C. The peak metal temperatures were determined with temperature-tape indicators attached to the substrates. Boyes et al<sup>107</sup> cured coil primer coatings at the same peak metal temperature. After curing, the final dried film thicknesses of the primer coatings were within 5-7 µm. Souto et al<sup>13,127</sup> also applied coil primer coatings with the same dried film thickness. Throughout the entire experiments of this study, the galvanised steel sheets were pre-treated and primer coated according to the procedure described.

#### **2.5.3.5 Method of application and curing schedule for the coil top coatings derived from the saturated polyester resins synthesised**

After the galvanised steel sheets were pretreated and primer coated, coil top coatings that were prepared from the polyester resins synthesised were applied on them. The top coatings were applied on the primer coated panels with the 60µm spiral bar coater. Johansson and Johansson<sup>8,18</sup> also used spiral applicators to apply coil top coatings. The coil top coated substrates were cured for 30 seconds at 320°C. The peak metal temperature of the substrates reached 230-235°C as determined by temperature-tape indicators. Johansson and Johansson<sup>18</sup> and Boyes et al<sup>107</sup> cured coil top coatings at the same peak metal temperature. The final dried film thicknesses of the top coatings were within 22-25 µm. The final dried film thicknesses of the coil top coatings applied by Johansson and Johansson<sup>18</sup>, Santos et al<sup>116</sup> and Souto et al<sup>13,127</sup> were within the same range as well. As flexibility changes inversely with the film thickness<sup>59</sup>, close control of the film thickness was maintained throughout the experiments. During the entire experiments of this study, the pre-treated and primer coated galvanised steel sheets were top coated according to the procedure described. After preparation, the coil coated steel panels were subjected to the tests described in Section 2.5.1.

#### **2.5.3.6 Method of application and curing schedule for the coil primer coating and the coil top coating to be derived from the standalone saturated polyester resin to be developed**

The coil primer coating to be derived from the standalone saturated polyester resin to be developed would be applied and cured exactly according to the methods described in Section 2.5.3.4. Then the coil top coating, also to be derived from the same standalone resin, would be applied and cured on the primer coated panel mentioned. The preparation,

application and curing of this particular coil top coating would be carried out according to the procedures described in Sections 2.5.3.2 and 2.5.3.5. As such, the steel substrate would be coated with a coil primer coating and a coil top coating that are both derived from a single polyester resin. This specimen panel would then be subjected to the tests described in Section 2.5.1.1.

## **CHAPTER 3 - RESULTS AND DISCUSSION**

### **3.1 Saturated polyester resins synthesised during the early stages of the study and their defect**

The aim of the synthesis carried out during the early stages of the study was to develop a saturated polyester resin that could only provide an efficient balance between flexibility and adhesion. In other words, a saturated polyester resin was to be developed that could initially provide the coil top coating with enough flexibility and adhesion so that it could meet the requirements of the tests of T-bend, impact resistance and MEK solvent resistance. Properties desired to be achieved through the tests mentioned were specified in Section 2.5.2. The methods for the said tests were described in detail in Sections 2.5.1.1, 2.5.1.2, and 2.5.1.3. By developing a saturated polyester resin as such, a valuable understanding with regard to designing polyester systems for achievement of balanced flexibility and adhesion would be obtained. The product developed could then be modified to meet the total requirements as specified in Section 2.5.2 according to its thermal properties to be determined by DSC. Two products were developed through the synthesis carried out during the early stages of the study. These polyesters that were selected as samples M and N, did provide the coil top coat film with balanced flexibility and adhesion. Both of the coil top coatings, one solely derived from sample M and one solely derived from sample N, met the requirements of the tests of T-bend, impact resistance, and MEK solvent resistance. In the coil top coatings concerned, each polyester sample had completely replaced two control polyesters. Although efficient flexibility and adhesion had been achieved, the resulting coil top coating films of samples M and N were of low pendulum film hardness. Eventually, samples M and N were considered as flexibilising polyesters for branched or highly polydispersed coil coating saturated polyester resins as will be discussed in Section 3.1.5. In the following Sections, the composition-property links of the polyesters developed during the early stages of the study are discussed.

#### **3.1.1 Composition of the saturated polyesters synthesised during the early stages of the study and properties of the resulting coil top coatings**

The composition of the coil coating polyesters synthesised during the early stages of the study are provided in Table 3.1. Properties of the resulting coil top coating films of the polyesters concerned are provided in Table 3.2.

**Table 3.1 Composition and hydroxyl values of the coil coating saturated polyester resins synthesised during the early stages of the study**

Sample	A*	B	C	D	E	F	G	H	I	J	K	L	M	N
Monomer														
Pripol 1022	1.18	0.83	0.75	0.77	0.86	0.99	1.12	1.26	1.12	0.00	1.10	1.12	1.13	0.00
Pripol 1013	----	----	----	----	----	----	----	----	----	1.12	----	----	----	----
Adipic acid	----	0.52	1.73	3.94	4.23	3.59	4.08	4.16	3.85	4.08	2.11	2.15	2.16	2.67
Isophthalic acid	----	2.66	3.87	3.99	4.27	2.41	4.43	4.24	2.92	4.43	1.78	2.09	2.26	2.40
Terephthalic acid	----	----	----	----	----	2.41	----	----	1.51	----	3.60	3.94	4.12	4.39
Phthalic anhydride	5.82	----	----	----	----	----	----	----	----	----	----	----	----	----
Maleic anhydride	1.65	4.67	2.34	----	----	----	----	----	----	----	----	----	----	----
Trimethylol propane	2.47	3.27	2.56	2.61	1.80	1.84	1.64	1.91	1.63	1.64	----	----	----	----
M-propylene glycol	2.42	----	----	----	----	----	----	----	----	----	----	----	----	----
Neopentyl glycol	6.46	5.98	5.27	5.42	5.51	5.63	5.42	4.92	5.41	5.42	5.92	5.12	4.71	5.01
1,6 Hexanediol	----	2.08	3.49	3.27	3.32	3.13	3.32	3.52	3.57	3.32	5.48	5.58	5.62	5.53
Total moles	20	20	20	20	20	20	20	20	20	20	20	20	20	20
Hydroxyl value (mgKOH/g)	130	191	170	165	90.7	86.5	62.9	64.9	82	63	114	55.8	26.5	51.6

\*: The formulation of sample A was a starting point formulation from Uniqema Int'l. <sup>128,129</sup>

**Table 3.2 Properties of the resulting coil top coating films of the saturated polyester resins synthesised during the early stages of the study**

Sample	A	B	C	D	E	F	G	H	I	J	K	L	M	N	Mixture of two control polyesters**	
T-bend cracking radius	2.5T	2T	1.5T	1.5T	1T	0.5T	0.5T	0.5T	0T	1T	0.5T	0T	0T	0T	0T	
T-bend adhesion radius	2.5T	1.5T	1.5T	1T	1T	0.5T	0.5T	1T	1T	1T	0.5T	0.5T	0T	0T	0T	
MEK solvent resistance	85	100	100	100	100	100	100	30	130	100	150	170	200	200	100	
15 Joules impact resistance (% pass)	100 ^	100 ^	100 ^	100 ^	100 ^	100 ^	100 ^	100 ^	100 ^	100 ^	100 ^	100	100	100	100	
Konig pendulum hardness (seconds @23°C)	N/A	N/A	N/A	N/A	N/A	N/A	N/A	N/A	N/A	N/A	N/A	N/A	N/A	21	20	77

\*\* : Specifications of the control polyesters and their mixing ratio in the coil top coating were provided in Section 2.5.2.



Table 3.1 and Table 3.2 demonstrate the progress of the polyester resins synthesised during the early stages of the study in providing the capability for the coil top coating to meet the requirements of tests of T-bend, impact resistance and MEK solvent resistance. That is to say 0T cracking and adhesion radii, over 100 MEK solvent double rub resistance and appropriate resistance to 15 Joules impact. Separate discussions with regard to the result of each of these tests are provided in Sections 3.1.2, 3.1.3 and 3.1.4. In addition, it is mentioned that sample N was a saturated polyester resin with similar characteristics as Sample M. However, Pripol 1022 dimer acid was excluded from its formulation in order to remove any possible unsaturation of the backbone.

### **3.1.2 Cracking resistance of the coil top coating after the T-bend test**

The coil top coatings derived from the saturated polyester resins synthesised after sample A showed improved flexibility and adhesion. However, the real breakthrough in terms of achieving 0T cracking and adhesion radii was made after sample K was synthesised.

The formulation of sample K was designed by modification of the formulation of sample I. The top coating based on sample I had achieved 0T cracking radius and 1T adhesion radius. Although sample I had provided the coil top coating with the flexibility required, it had weak adhesion. Therefore, the formulation of sample K was designed by modification of the formulation of sample I for better adhesion properties. The content of isophthalic acid was reduced by 1.14 moles and trimethylol propane was excluded from the formulation. These reductions were compensated by the inclusion of terephthalic acid to provide the required adhesion for the resin. The content of adipic acid was reduced by 1.74 moles which was compensated through the inclusion of 1,6 hexanediol. The theoretical OH value of sample K after these modifications was 114 mgKOH/g. The coil top coating based on sample K achieved 0.5T cracking and adhesion radii.

Based on the performance of sample K in the coil top coating, it was concluded that the resin needed to be more linear as well as more adhesive. The formulation of the next sample, that is to say sample L, was designed by modification of the formulation of sample K. The content of neopentyl glycol was reduced by 0.8 mole. This reduction was compensated by the inclusion of 0.34 mole of terephthalic acid and 0.31 mole of isophthalic acid. The theoretical OH value of sample L after these modifications was 55.8 mgKOH/g. The theoretical hydroxyl value of sample K was 114 mgKOH/g. This indicated that slight

reductions in the contents of glycols would dramatically reduce the hydroxyl content of a polyester resin. The coil top coating based on sample L achieved 0T cracking radius and 0.5T adhesion radius.

Sample L provided the required flexibility for the coil top coating. However, it was still weak in terms of adhesion. The formulation of the next sample, that is to say sample M, was designed by modification of the formulation of sample L. The same modification approach as carried out from sample K to sample L was employed. The content of neopentyl glycol was reduced by 0.39 mole. This reduction was compensated through the inclusion of 0.18 mole of terephthalic acid and 0.17 mole of isophthalic acid. The theoretical OH value of Sample M after these modifications was 26.5 mgKOH/g. In comparison to sample L, the theoretical hydroxyl value was reduced by 29.34 mgKOH/g. Sample M was a saturated polyester resin with relatively a low hydroxyl functionality. The coil top coating derived from sample M achieved the satisfactory 0T cracking and adhesion radii.

With regard to the T-bend test, the following were concluded as performances of the coil top coatings derived from the saturated polyesters synthesised during the early stages of the study with the compositions shown in Table 3.1 were compared.

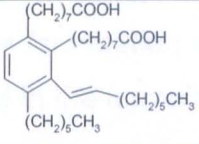
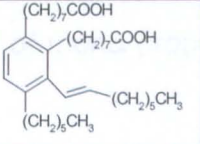
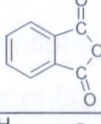
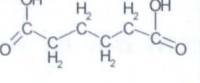
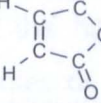
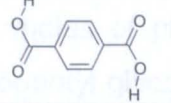
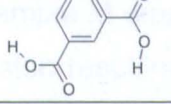
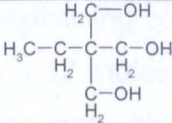
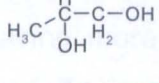
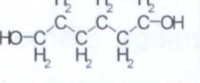
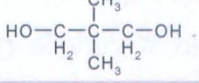
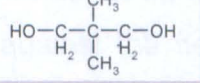
- 1- When trimethylol propane was employed in the compositions, the required linearity for the saturated polyester resin to meet the 0T cracking radius of the T-bend test could not be achieved. Trimethylol propane was a triol and its chemical structure was shown in Scheme 1.11. Saturated polyester resins that were prepared from this triol acquired a branched structure rather than a linear one. As trimethylol propane was not employed in designing the formulations of samples K, L and M, the required linearity was achieved. Observations pointed out that for the design of such saturated polyester resin systems, only diols must be employed.
- 2- Reduction of the theoretical hydroxyl value of the saturated polyester from as high as 190.6 mgKOH/g in sample B to as low as 26.5 mgKOH/g in sample M had a positive effect on making the resins' film efficiently flexible after its crosslinking with the HMMM curing agent. The content of trimethylol propane in sample B was 3.27 moles while trimethylol propane was not employed in designing the formulation of sample M. The reduction of the hydroxyl content of sample M in comparison to

sample K was done through the reduction of the content of neopentyl glycol from 5.92 moles to 4.71 moles. This was carried out while the molar content of 1,6 hexanediol was kept constant and within 5.48-5.62. The chemical structures of neopentyl glycol and 1,6 hexanediol were provided in Schemes 1.10 and 1.12. Reduction of the molar content of the branched neopentyl glycol, increasing the molar contents of the aromatic terephthalic and isophthalic acids and maintaining the molar contents of the linear monomers lowered the theoretical hydroxyl value from 114 mgKOH/g in sample K to 26.5 mgKOH/g in sample M. These modifications also improved the flexibility of sample M. The linear monomers of sample M included tripol 1022 dimer acid, adipic acid and 1,6 hexanediol. The chemical structures of adipic acid and a general structure for dimer acids were shown in Schemes 1.18 and 1.19 respectively. Overall, the modifications mentioned resulted in the achievement of 0T cracking radius by the coil top coating based on sample M. On the other hand, the cracking radius of the coil top coating derived from sample K was 0.5T.

- 3- Terephthalic acid and isophthalic acid provided better adhesion properties in comparison to neopentyl glycol. This was concluded according to the performance of the coil top coatings based on sample L and sample M. The content of neopentyl glycol in sample M had been reduced by 0.39 mole in comparison to sample L. This was compensated by the addition of 0.18 mole to terephthalic acid and 0.17 mole to isophthalic acid. This modification provided the coil top coating with 0T adhesion radius. Terephthalic acid and isophthalic acid are rigid. This is due to the presence of the moiety of benzene ring in their molecular structure. The molecular structures of isophthalic acid and terephthalic acid were shown in Schemes 1.15 and 1.16. Based on the performance of sample L and sample M, it was concluded that aromatic structures provided better adhesion properties in comparison to branched structures such as that of neopentyl glycol. This was particularly true when the extremely demanding 0T T-bend adhesion radius could be achieved by sample M. It is known that good adhesion of the cured film can be achieved if the coating makes close contact with the surface.<sup>59</sup> Based on the suitable adhesion of sample M, it can be concluded that presence of aromatic moieties in a polyester's backbone would result in an effective contact between the coating and the substrate.

4- A comparison was made between the composition of sample A and sample M in terms of the polyols, polyacids, their chemical structure and molar contents as shown in Table 3.3.

**Table 3.3 Chemical structures and molar contents of the polyols and polyacids used in the preparation of samples A and M**

Sample A (Hydroxyl value: 130 mgKOH/g)				Sample B (Hydroxyl value: 26.5 mgKOH/g)			
T-bend test cracking radius of the resulting coil top coating: <b>2.5T</b>				T-bend test cracking radius of the resulting coil top coating: <b>0T</b>			
T-bend test adhesion radius of the resulting coil top coating: <b>2.5T</b>				T-bend test adhesion radius of the resulting coil top coating: <b>0T</b>			
Monomer				Monomer			
Polyacid	Polyol	Structure	Moles	Polyacid	Polyol	Structure	Moles
Pripol 1022	-----		1.18	Pripol 1022	-----		1.13
Phthalic anhydride	-----		5.82	Adipic acid	-----		2.16
Maleic anhydride	-----		1.65	Terephthalic acid	-----		4.12
-----	-----	-----	-----	Isophthalic acid	-----		2.26
-----	Trimethylol propane		2.47	-----	-----	-----	-----
-----	Mono propylene glycol		2.42	-----	1,6 Hexane-diol		4.71
-----	Neopentyl glycol		6.46	-----	Neopentyl glycol		5.62
Sum total			20	Sum total			20

It can be seen, from Table 3.3, that a great deal of modification was made on the composition of sample A in terms of excluding monomers, incorporating new monomers, as well as molar content adjustments. Regardless of the molar contents

of the monomers, a comparison between the chemical structures of the monomers of sample A and sample M indicated that the polyester formed through the components of sample M would be more linear as it was.

Sample A contained 3.6 moles of flexibilising components (1.18 moles of pripol 1022 and 2.42 moles of mono propylene glycol). Sample M contained 8.91 moles of flexibilising components (1.13 moles of pripol 1022, 2.16 moles of adipic acid and 5.62 moles of 1,6 hexanediol). The coil top coating based on sample A achieved a cracking radius of 2.5T. The coil top coating based on sample M achieved 0T cracking radius. This was due to the higher content of flexibilising components in sample M as well as their greater flexibilising efficiency. Having almost the same amount of the dimer acid, sample M provided excellent flexibility through adipic acid and 1,6 hexanediol. The flexibilising efficiency of adipic acid and 1,6 hexanediol employed in the formulation of sample M was greater than that of mono propylene glycol employed in the formulation of sample A.

In order to compensate for the loss of adhesion resulting from its 3.6 moles of flexibilising components, sample A employed 13.93 moles of hard monomers. The molar contents of the hard monomers of sample A were 5.82 moles of phthalic anhydride, 1.65 moles of maleic anhydride and 6.46 moles of neopentyl glycol. The hard:soft molar ratio of the monomers in sample A was 3.87:1. Sample M employed 12 moles of hard monomers to compensate for the loss of adhesion resulting from its 8 moles of flexibilising components. The molar contents of the hard monomers of sample M were 4.12 moles of terephthalic acid, 2.26 moles of isophthalic acid and 5.62 moles of neopentyl glycol. The hard:soft molar ratio of the monomers of sample M was 1.5:1. Having more than twice the amount of hard monomers against the flexible ones, the coil top coating based on sample A achieved an adhesion radius of 2.5T. Having slightly a higher amount of hard monomers against the flexible monomers, the coil top coating based on sample M achieved the 0T adhesion radius. This was indicative of the absolute superiority of terephthalic acid and isophthalic acid in compensating for the loss of adhesion in comparison to phthalic anhydride and maleic anhydride.

### 3.1.3 Resistance of the coil top coating to MEK solvent

As described in Section 2.5.1.2, this test was carried out for the coil top coatings derived from the polyester resins synthesised for evaluation of the degree of curing. All of the coil coatings prepared from the synthesised polyesters were cured in similar conditions as described in Section 2.5.3.5. The curing agent used for the samples was the same curing agent that had been used for the control polyesters. The amount of the curing agent used for the samples was similar to the amount used for the control polyesters. Details of the curing agent used and its incorporation amount in the coil top coating were provided in Section 1.7.1 and Section 2.5.2. Table 3.1 and Table 3.2 can be used for links between the composition of the polyesters and their resistance to MEK solvent in the coil top coating.

Theoretically, it was expected that a higher degree of crosslinking or curing would be achieved by a polyester resin with higher hydroxyl functionality. In other words, it was assumed that a polyester resin with higher hydroxyl content would result in a higher resistance to MEK solvent. This assumption was based on having prior knowledge of the low self-condensation tendency of the curing agent used in the presence of the hydroxyl groups of the polyester resin.<sup>69,70</sup> Interestingly, the results showed that there were exceptions. Regardless of the hydroxyl content, the nature of the hard monomers employed in the polyesters synthesised had a significant influence on the MEK resistance of the resulting coil top coating film. Earlier studies have shown that the solvent resistance of a resin can be associated with its state of cure.<sup>71</sup> However, as the curing agent, the content of the curing agent and the curing conditions were kept constant for the samples of this study, it was concluded that resistance towards a solvent was mostly dependent on the composition of the polyester. In this regard, the following were concluded as performances of the coil top coatings derived from the saturated polyester resins shown in Table 3.1 were compared.

- 1- Only the coil top coatings that were derived from samples A and H gave 85 and 30 MEK double rubs. The coil top coatings derived from rest of the polyester samples gave 100 or over 100 MEK double rubs.
- 2- Regarding the probable increase in the number of MEK double rubs by higher hydroxyl content and consequently higher degree of crosslinking, samples B, C and D were considered. The hydroxyl contents of the said polyesters were above 160

mgKOH/g. The coil top coatings based on samples B, C and D gave 100 MEK double rubs.

- 3- Regarding the probable decrease in the number of MEK double rubs by lower hydroxyl content and consequently lower degree of crosslinking, sample H could be pointed out. The hydroxyl content of sample H was 64.9 mgKOH/g. In addition, the hard to flexible molar ratio of the monomers in sample H was 1.02:1. In other words, sample H contained the lowest amount of hard monomers among the other samples shown in Table 3.1. The coil top coating derived from sample H gave 30 MEK double rubs.
- 4- The nature of the hard diacid used in formulating the saturated polyester resins synthesised greatly affected the solvent resistance of the resulting coil top coating film. Regardless of the hydroxyl content of the saturated polyester, exclusion of phthalic anhydride and maleic anhydride and inclusion of isophthalic acid and terephthalic acid definitely increased the solvent resistance. This phenomenon was observed after samples K, L, and M were synthesised. The hydroxyl contents of samples K, L, and M were lower than the hydroxyl content of sample A. The hydroxyl value of sample A was 130 mgKOH/g. However, the solvent resistance of the coil top coatings based on samples K, L, and M were higher than the coil top coating based on sample A. Interestingly, the coil top coating based on sample M was of the highest solvent resistance among the resins shown in Table 3.1. In addition, sample M was of the lowest hydroxyl content. The hydroxyl value of sample M was 26.5 mgKOH/g. In comparison to sample K with a hydroxyl value of 117 mgKOH/g, sample M contained 0.52 mole extra terephthalic acid, 0.48 mole extra isophthalic acid, and 1.21 moles less neopentyl glycol. By lowering the hydroxyl content of sample M and increasing the content of the aromatic moieties in its backbone, higher solvent resistance had been achieved.

The effect of the nature of the hard diacid in increasing the solvent resistance of the coil top coating was also observed in the coatings based on samples E, F, and G. The hydroxyl contents of samples E, F, and G were lower than sample A. But samples E, F, and G were of higher solvent resistance in comparison to sample A. samples E, F, and G were based on isophthalic acid while sample M was based on phthalic anhydride and maleic anhydride.

### **3.1.4 Resistance of the coil top coating to cracking after deformation by 15 Joules impact**

Resistance of the coil top coating to cracking after deformation by impact highly depends on efficient flexibility and good adhesion.<sup>59</sup> Similar to the T-bend test, the real breakthrough in terms of satisfactory impact resistance was made after sample K was synthesised. In this regard, the following were concluded as performances of the coil top coatings derived from the synthesised polyester resins shown in Table 3.1 were compared.

- 1- As discussed in Section 3.1.2, the exclusion of trimethylol propane from the formulation of the polyesters that were synthesised after sample J resulted in the achievement of better linearity. In other words, the flexibility of the polyesters that were synthesised after sample J had been improved through the exclusion of the triol. Therefore, a great deal of improvement with regard to the elimination of cracking after deformation of the coil top coating film was achieved.
- 2- Sample L improved better flexibility and adhesion properties. This was due to modification of the formulation of sample K. The content of neopentyl glycol was reduced by 0.8 mole which was compensated by further inclusion of terephthalic acid and isophthalic acid. There was no cracking for the coil top coating film based on sample L after deformation by impact. Moreover, the paint film did not chip after the peeling test of the deformed area by the adhesive tape. The same result was also achieved for the coil top coating derived from sample M. The formulation of sample M was designed by modification of the formulation of sample L. The content of neopentyl glycol was reduced by 0.41 mole which was compensated by further inclusion of 0.18 mole of terephthalic acid and 0.17 mole isophthalic acid.
- 3- As the coil top coating derived from sample M passed the T-bend test, it also resisted to cracking after being deformed by the 15 Joules impact. In other words, as sample M compromised between adhesion and flexibility effectively, the requirement of the impact test was also met.

### **3.1.5 Suitability of the early polyesters as flexibilisers for coil coatings**

Although in terms of the tests of T-bend, MEK solvent resistance and deformation by impact the coil top coatings derived from samples M and N had achieved the desired



results, they were unsuitable for application as standalone binders for the coil top coating system concerned. A discussion with respect to this matter is provided in Sections 3.1.5.1, 3.1.5.2 and 3.1.5.3 as follows.

### 3.1.5.1 Pendulum film hardness of the coil top coating derived from the control polyesters and the coil top coatings derived from samples M and N

The pendulum film hardness of the coil top coating derived from two control saturated polyester resins and the coil top coatings derived from samples M and N are shown in Table 3.4.

**Table 3.4 Pendulum film hardness of the control coil top coating and the coil top coatings derived from samples M and N**

	Coil top coating derived from two control saturated polyesters	Coil top coating derived from sample M	Coil top coating derived from sample N
Konig pendulum film hardness according to ISO 1522	77 seconds at 23°C	21 seconds at 23°C	20 seconds at 23°C

Specifications of the control polyester resins were provided in Section 2.5.2. In comparison to the control coil top coating, the coil top coatings derived from samples M and N had resulted in the reduction of the oscillation time of the pendulum of the hardness tester. Due to the fact that the only difference between the control coil top coating and the coil top coatings prepared from samples M and N was in the saturated polyester resin, this particular loss of film hardness was definitely caused by the polyester coating films formed by samples M and N. Therefore, samples M and N were unsuitable for sole application in the coil top coating as their cured films were of low pendulum film hardness. A coil top coating film with low pendulum hardness would be of high abrasive resistance properties.

### 3.1.5.2 Similarity of the mechanical and pendulum film hardness properties of the control flexibiliser polyester resin with samples M and N

After the results described in the previous section were achieved, a coil top coating was prepared that was derived solely from the control flexibiliser polyester resin. Specifications of the control flexibiliser polyester resin (Uralac SN 865) were provided in Section 2.5.2.

The coil top coating concerned was prepared and applied according to the procedures described in Sections 2.5.3.2, 2.5.3.4 and 2.5.3.5. The tests of T-bend, MEK solvent resistance, 15 Joules impact and Konig pendulum film hardness was then carried out on the coil top coating concerned. The results of the said tests are shown in Table 3.5. For comparison, the results of the same tests for the coil top coatings solely derived from samples M and N are also shown in Table 3.5.

**Table 3.5 Properties of the coil top coating derived from the control flexibiliser polyester resin and the coil top coatings derived from samples M and N**

<b>Resin</b> <b>Property</b>	<b>Control</b> <b>flexibiliser</b> <b>polyester resin</b>	<b>Sample M</b>	<b>Sample N</b>	<b>Test method</b>
<b>T-bend test</b>	cracking radius: 0T	cracking radius : 0T	cracking radius : 0T	ECCA-T7
	adhesion radius: 0T	adhesion radius: 0T	adhesion radius: 0T	
<b>MEK solvent</b> <b>resistance</b> ( double rubs)	>100	>100	>100	ECCA-T11
<b>Impact test</b> (% pass)	100	100	100	ECCA-T5
<b>Konig film</b> <b>hardness</b> (seconds @ 23°C)	19	21	20	ISO 1522

It can be seen, from Table 3.5, that the properties of the coil top coating derived from the control flexibiliser polyester resin was similar to the properties of the coil top coatings derived from samples M and N.

### **3.1.5.3 Employment of samples M and N as flexibiliser polyester resins in the control coil top coating**

After the results mentioned in Sections 3.1.5.1 and 3.1.5.2 were obtained, three coil top coatings were prepared. The first one was derived solely from the semi-branched control polyester resin. Specifications of the semi-branched control polyester resin (FINNRESIN PE-2/65GS) were provided in Section 2.5.2. The second coil top coating was derived from both the semi-branched control polyester resin and Sample M. The third coil top coating

was derived from both the semi-branched control polyester resin and Sample N. In the second and the third coil top coatings, samples M and N had been employed as replacements for the control flexibiliser polyester resin. The reason for employment of samples M and N as flexibiliser resins was due to the similarity of their coating film properties with the control flexibiliser resin as discussed in the previous section. The semi-branched competitor resin was mixed with samples M and N according to the solid resin mixing ratio mentioned in Section 2.5.2. The three coil top coatings were prepared and applied according to the procedures mentioned in Sections 2.5.3.2 and 2.5.3.5. The properties of the coil top coatings concerned are shown in Table 3.6.

**Table 3.6 Properties of the coil top coating solely derived from the semi-branched control polyester resin and the coil top coatings derived from the mixture of the same control resin with samples M and N**

<b>Resin Property</b>	<b>Semi-branched control polyester</b>	<b>Control + sample M</b>	<b>Control + sample N</b>	<b>Test method</b>
<b>T-bend test</b>	cracking radius: 1T	cracking radius : 0T	cracking radius : 0T	ECCA-T7
	adhesion radius: 0T	adhesion radius: 0T	adhesion radius: 0T	
<b>MEK solvent resistance</b> ( double rubs)	>100	>100	>100	ECCA-T11
<b>Impact test</b> (% pass)	100	100	100	ECCA-T5
<b>Konig film hardness</b> (seconds @ 23°C)	98	76	78	ISO 1522

Based on the results shown in Table 3.6, sample M and sample N were considered as flexibiliser polyester resins for branched or highly polydispersed coil coating binder systems.

### **3.2 Development of a novel and standalone saturated polyester resin system for coil primer coating and coil top coating and the relevant characterisation**

Through synthesis of the polyesters described in Section 3.1 and evaluation of their resulting coil top coating films, adequate understanding for designing coil coating saturated polyester resins with balanced flexibility and adhesion was achieved. The fundamental rule that had to be considered in designing the formulation of such polyester systems was that only diols and diacids had to be employed. This basic rule along with differential scanning calorimetry were employed for the development of a standalone coil top coating and coil primer coating saturated polyester resin. As such, a novel polyester resin system was developed which provided the desired properties. Basis of selection with respect to the properties desired to be achieved were mentioned in Section 2.5.2. The coil top coating and the coil primer coating derived from this novel polyester system was of balanced flexibility, adhesion, chemical resistance and high pendulum film hardness. The novel polyester system developed was designated as sample T. In the coil primer coating and the coil top coating concerned, sample T had completely replaced four control saturated polyester resins and had performed as a novel and standalone polyester binder system.

In the following Sections, the development of the novel coil coating polyester resin system with multiple properties will be discussed in detail. The results of the techniques of DSC,  $^1\text{H}$ NMR,  $^{13}\text{C}$ NMR and FT-IR that were employed for the development of the polyester system concerned are provided, interpreted and discussed. The coating film performance of the coil coatings derived from the saturated polyester resins synthesised are provided and discussed. The molecular weight characteristics of the pilot and industrial scale reproductions of the standalone polyester resin system developed are provided and discussed. The said molecular weight characteristics were determined by SEC analysis.

#### **3.2.1 Incorporation of high level of flexibility, adequate adhesion and suitable glass transition temperature into a saturated polyester resin**

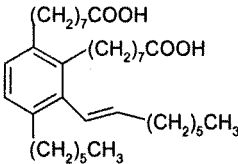
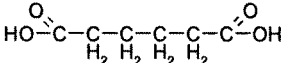
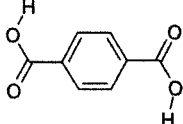
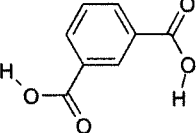
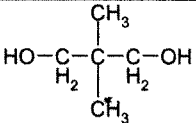
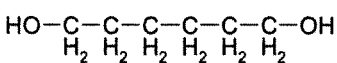
As will be discussed in Sections 3.2.1.1 to 3.2.1.3, a saturated polyester resin with a glass transition temperature between 8-10°C and balanced flexibility and adhesion properties

can be used as a universal and standalone binder system for coil primer coating and coil top coating.

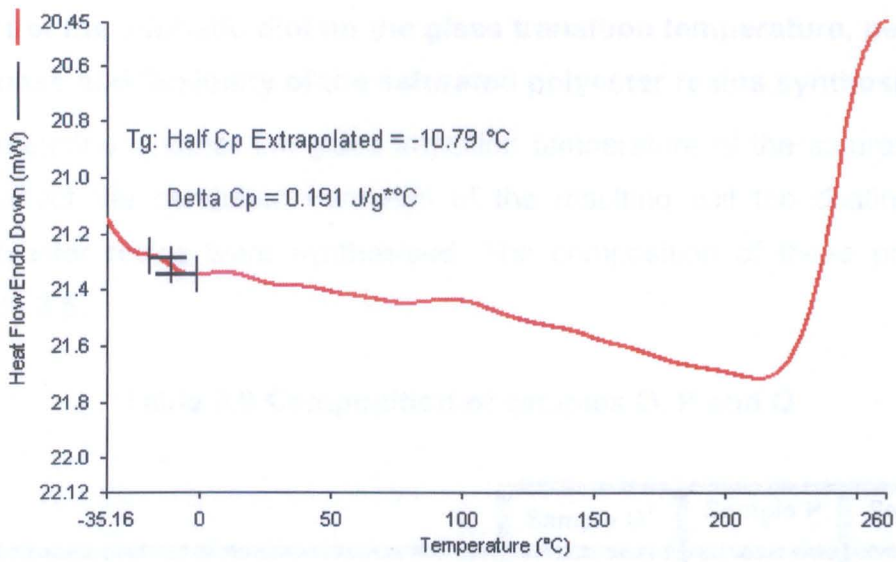
### 3.2.1.1 Glass transition temperature of the saturated polyester resins synthesised during the early stages of the study

Composition of the saturated polyester resins synthesised as samples M and N during the early stages of the study are shown in Table 3.7.

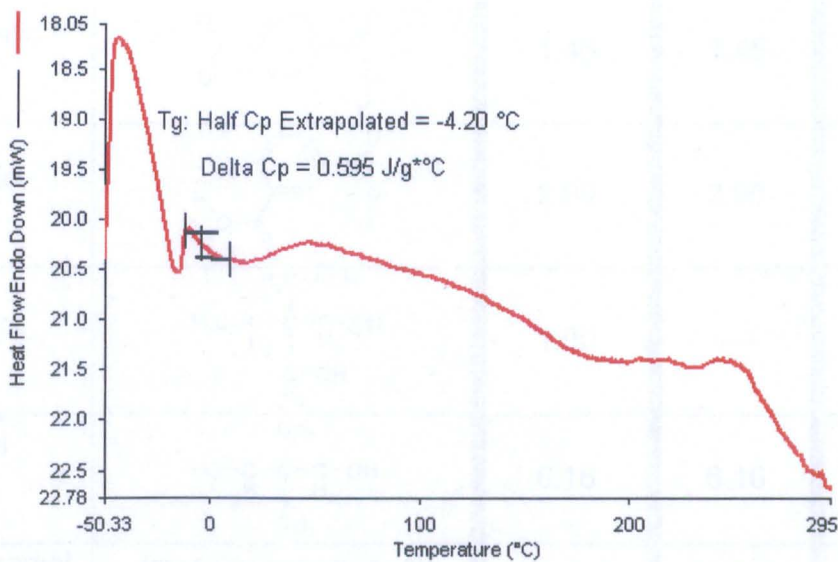
**Table 3.7 Composition of sample M and sample N**

Monomer	Structure	Sample M	Sample N
		Moles	Moles
Pripol 1022 dimer acid		0.76	----
Adipic acid		1.46	1.78
Terephthalic acid		2.78	2.93
Isophthalic acid		1.56	1.60
Neopentyl glycol		3.18	3.34
1,6 hexanediol		3.79	3.69
Total moles		13.49	13.35

The properties of the resulting coil top coatings of samples M and N were provided in Table 3.2. The DSC thermograms of samples M and N are shown in Figure 3.1.



Sample M



Sample N

**Figure 3.1 DSC thermograms of sample M and sample N**

The glass transition temperature of sample M was  $-10.79\text{ }^{\circ}\text{C}$  and the glass transition temperature of sample N was  $-4.20\text{ }^{\circ}\text{C}$ . As discussed in Section 3.1.5.1, the pendulum film hardness of the coil top coatings derived from samples M and N were low and unsatisfactory. The pendulum film hardness of the coil top coatings concerned were provided in Table 3.4. In the following Section, the cause of the low pendulum film hardness and its relevance to the glass transition temperature are discussed.

### 3.2.1.2 Effect of the aliphatic diol on the glass transition temperature, pendulum film hardness and flexibility of the saturated polyester resins synthesised

In order to determine whether the glass transition temperature of the saturated polyester resin would affect the pendulum hardness of the resulting coil top coating film, three saturated polyester resins were synthesised. The composition of these polyesters are shown in Table 3.8.

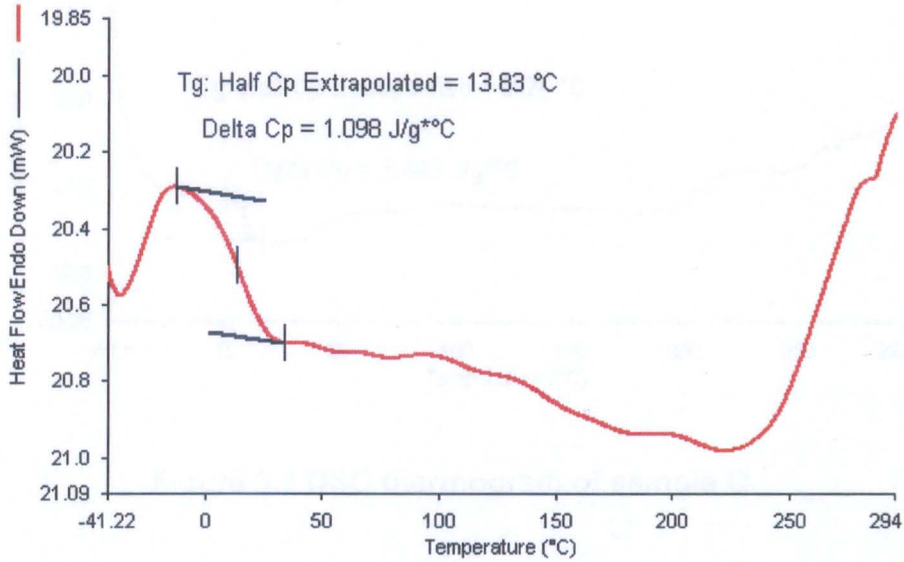
Table 3.8 Composition of samples O, P and Q

Monomer	Structure	Sample O*	Sample P	Sample Q
		Moles	Moles	Moles
Adipic acid		2.01	2.01	2.01
Terephthalic acid		1.45	1.45	1.45
Isophthalic acid		2.90	2.90	2.90
Trimethylol propane		1.00	----	----
Neopentyl glycol		6.16	6.16	7.44
1,6 hexanediol		----	1.13	----
Total moles		13.52	13.65	13.80

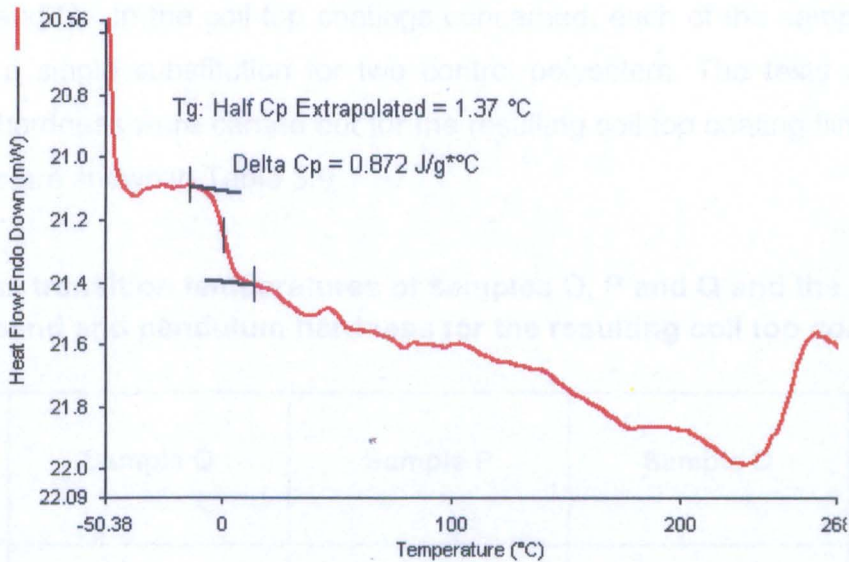
\*: The formulation of sample O was obtained from reference 130.<sup>130</sup>

Sample O contained 1.00 mole of trimethylol propane. As discussed in Section 3.1.2, the required flexibility would not be achieved when a triol is employed. Therefore, samples P and Q were also synthesised. Formulations of samples P and Q were designed by modification of the formulation of sample O. In the formulation of sample P, trimethylol propane was excluded and was compensated by the inclusion of 1.13 moles of 1,6 hexanediol. In the formulation of sample Q, trimethylol propane was excluded and was

compensated through further inclusion of neopentyl glycol by 1.28 moles. The glass transition temperature of samples O, P and Q were determined by differential scanning calorimetry. The thermograms of samples O and P are shown in Figure 3.2.



Sample O



Sample P

Figure 3.2 DSC thermograms of samples O and P

The DSC thermogram of sample Q is shown in Figure 3.3.



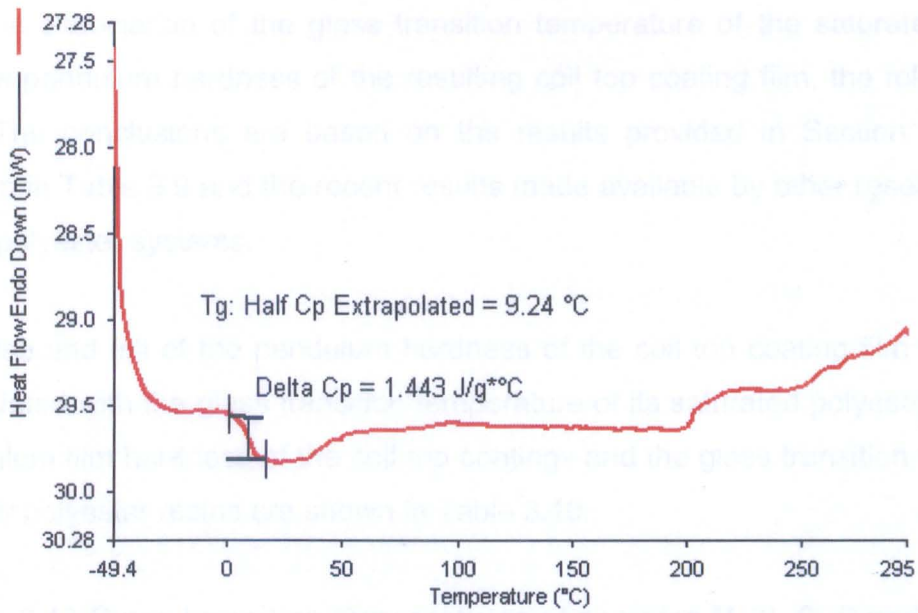


**Figure 3.3 DSC thermogram of sample Q**

It could be seen, from the thermograms shown in Figure 3.2 and Figure 3.3, that sample P was of the lowest glass transition temperature. Coil top coatings were derived from samples O, P and Q. In the coil top coatings concerned, each of the samples mentioned were used as a single substitution for two control polyesters. The tests of T-bend and pendulum film hardness were carried out for the resulting coil top coating films. The results of the said tests are shown in Table 3.9.

**Table 3.9 Glass transition temperatures of samples O, P and Q and the results of the tests of T-bend and pendulum hardness for the resulting coil top coating films**

Resin	Sample O	Sample P	Sample Q	Test method
Property				
Glass transition temperature	13.83°C	1.37°C	9.24°C	DSC
Konig pendulum film hardness	151 (seconds @ 23°C)	43 (seconds @ 23°C)	126 (seconds @ 23°C)	ISO 1522
T-bend test	cracking radius: <b>2T</b>	cracking radius : <b>0T</b>	cracking radius : <b>1T</b>	ECCA-T7
	adhesion radius: <b>0T</b>	adhesion radius: <b>0T</b>	adhesion radius: <b>0T</b>	

Regarding the association of the glass transition temperature of the saturated polyester resin and the pendulum hardness of the resulting coil top coating film, the following were concluded. The conclusions are based on the results provided in Section 3.2.1.1, the results shown in Table 3.9 and the recent results made available by other researchers who had studied polyester systems.

- 1- The rise and fall of the pendulum hardness of the coil top coating film was directly associated with the glass transition temperature of its saturated polyester resin. The pendulum film hardness of the coil top coatings and the glass transition temperature of their polyester resins are shown in Table 3.10.

**Table 3.10 Glass transition temperatures of samples M, N, O, P and Q and the pendulum hardness of their resulting coil top coating films**

<b>Property</b> \ <b>Resin</b>	<b>Sample M</b>	<b>Sample N</b>	<b>Sample O</b>	<b>Sample P</b>	<b>Sample Q</b>	<b>Test method</b>
<b>Konig pendulum film hardness of the coil top coating (seconds @ 23°C)</b>	21	20	151	43	126	ISO 1522
<b>Glass transition temperature</b>	-10.79°C	-4.20°C	13.83°C	1.37°C	9.24°C	DSC

The pendulum film hardness of the coil top coatings that were derived from polyesters with low glass transition temperatures was low and unsatisfactory. On the other hand, polyesters with glass transition temperatures above 9°C resulted in coil top coating films with high and satisfactory pendulum hardness. This observation specifically applied to samples O and Q.

- 2- The aliphatic 1,6 hexanediol reduced the glass transition temperature of the saturated polyester resin and as a result, the pendulum film hardness of the coil top coating was reduced. On the other hand, neopentyl glycol augmented the glass transition temperature of the saturated polyester resin and as a result, the pendulum film hardness of the coil top coating was increased. This was concluded according to

the glass transition temperatures of samples P and Q, their composition and the pendulum film hardness of the resulting coil top coating films. The pendulum film hardness of the coil top coating based on sample P was 43 seconds at 23°C. Sample P contained 1.13 moles of 1,6 hexanediol and its glass transition temperature was 1.37°C. The pendulum film hardness of the coil top coating based on sample Q was 126 seconds at 23°C. The glass transition temperature of sample Q was 9.24°C. Sample Q did not contain 1,6 hexanediol. Reduction of the glass transition temperature of polyesters through inclusion of aliphatic moieties such as 1,6 hexanediol had also been reported in the works of other researchers. Pang et al<sup>39</sup> reported that the inclusion of 1,3 propanediol and 1,4-butanediol in the preparation of poly (ethylene terephthalate) resulted in the reduction of the glass transition temperature (p.1015). Wang et al<sup>23</sup> reported that the glass transition temperature of aromatic polyesters could be decreased through attachment of alkyl side chains (p.3020). Tsai et al<sup>36</sup> derived polyesters from succinic acid, ethylene glycol and 1,3 propanediol and showed that the glass transition temperature of these polyesters decreased as the content of 1,3 propanediol increased (p.2344). Lozano et al<sup>60</sup> synthesised poly(ester amide)s from 1,4-butanediol, adipic acid (hexanedioic acid), terephthalic acid and 6-aminohexanoic acid and showed that the glass transition temperature was low when the content of hexanedioic acid was high (p.600). Bao et al<sup>131</sup> modified a hydroxyl functional polyester with succinic anhydride and showed that the glass transition temperature of the modified product had been reduced (p.178). McKee et al<sup>41</sup> associated such reductions in the glass transition temperatures to the increase of the fractional volume of the polyesters by aliphatic moieties. Johansson and Johansson<sup>8,18</sup> related the reduction of the glass transition temperature to the lower crosslink-density achieved as a result of the inclusion of aliphatic moieties to the polyester backbone.

- 3- Inclusion of a large proportion of linear polyols and polyacids, such as dimer acids, adipic acid and 1,6 hexanediol would result in the achievement of glass transition temperatures below 0°C. This would lead to a massive decline in the pendulum hardness of the resulting coil coating film. This was concluded according to the evaluation made with respect to the hard to soft molar ratio of the monomers of samples M, N and Q. The hard to soft molar ratio of the monomers of samples M and N were 1.5:1 and 1.44:1 and their glass transition temperatures were -10.79°C

and  $-4.20^{\circ}\text{C}$  respectively. The hard to soft molar ratio of the monomers of sample Q was 5.86:1 and its glass transition temperature was  $9.24^{\circ}\text{C}$ . The hard to soft molar ratio of the monomers of samples M, N and Q and its relevance to the rise and fall of the glass transition temperature, indicated that if a saturated polyester resin is to be designed to provide high pendulum film hardness to a coil coating, it definitely should not contain large proportions of aliphatic polyols or polyacids.

With respect to the flexibility of the resulting coil top coating films of samples O, P and Q, the following were concluded. The conclusions are based on the composition of the said samples as shown in Table 3.8 and the results of the T-bend test as shown in Table 3.9.

- 1- The cracking radius of the coil top coating derived from sample O was 2T. The weak flexibility of the resulting coil top coating film derived from sample O was due to the inclusion of 1 mole of trimethylol propane. As discussed in Section 3.1.2, when trimethylol propane was used in the preparation of the polyesters synthesised during the early stages of the study, the flexibility of the resulting coil top coating films were also weak. The performance of the coil top coating based on sample O showed that coil coating saturated polyester resins should not contain triols. In terms of adhesion however, the performance of the coil top coating based on sample O was satisfactory. The adhesion radius of the resulting coil top coating film of sample O was 0T. The satisfactory adhesion of sample O could be associated to the inclusion of isophthalic acid, terephthalic acid and neopentyl glycol in its formulation. Promotion of the adhesion of such saturated polyester resin systems through inclusion of aromatic and branched moieties to their backbones were previously discussed in Section 3.1.2.
- 2- The result of the T-bend test of the coil top coating derived from sample P signified the flexibilising efficiency of 1,6 hexanediol. The T-bend cracking radius of the resulting coil top coating film of sample P was 0T. Trimethylol propane was not included in the formulation of sample P. It was replaced by 1,6 hexanediol. In terms of adhesion, the performance of the coil top coating based on sample P was acceptable. The adhesion radius of the resulting coil top coating film of sample P was 0T. The contents of isophthalic acid, terephthalic acid and neopentyl glycol in

samples O and P were similar. Therefore, the satisfactory adhesion of sample O had also been reproduced by sample P.

- 3- The flexibility of sample Q was better than sample O. The cracking radius of the resulting coil top coating film of sample Q was 1T. Trimethylol propane was not included in the formulation of sample Q. It was replaced by neopentyl glycol. Neopentyl glycol is not an aliphatic monomer. However, it is a diol. Due to this, sample Q that contained neopentyl glycol only was more flexible than sample O. The only flexibilising monomer used in sample Q was adipic acid with a content of 2.01 moles. Obviously, the flexibilising efficiency of adipic acid with the said content was not enough for the resulting coil top coating film to achieve the 0T cracking radius. The adhesion strength of sample Q was satisfactory and remained unchanged in comparison to samples O and P. This was due to the similarity of the contents of the aromatic moieties of isophthalic acid and terephthalic acid in the backbones of samples O, P, and Q.

### **3.2.1.3 Stages of development for a saturated polyester resin with suitable glass transition temperature, excellent flexibility and adequate adhesion**

Based on the results achieved so far, a novel and standalone saturated polyester resin with a glass transition temperature between 8-10°C, excellent flexibility and adequate adhesion was developed in four stages. The results concerned were discussed in Sections 3.1, 3.2.1.1 and 3.2.1.2. In the following, a description of each developmental stage is provided.

#### **a) Stage one:**

As discussed in Section 3.1.5, sample N was considered as a flexibiliser polyester resin for coil coating systems. In addition, it was shown in Section 3.2.1.2 that the flexibility of sample Q was weak. Therefore, a coil top coating was derived from the mixture of samples N and Q. The mixing ratio was 79.56<sub>(sample Q)</sub>: 20.44<sub>(sample N)</sub> (m:m). The tests of T-bend and pendulum film hardness were then carried out for the resulting coil top coating film. The results of the said tests are shown in Table 3.11. The glass transition temperature of samples N and Q and the results of the tests of T-bend and pendulum hardness for the coil top coatings that were derived separately from each of these polyester samples are also shown in Table 3.11.

**Table 3.11 Glass transition temperatures of samples N and Q and the results of the tests of T-bend and pendulum hardness for the resulting coil top coating films**

Property \ Resin	Sample N	Sample Q	Mixture of samples N and Q*	Test method
Glass transition temperature	-4.20°C	9.24°C	N/A	DSC
Konig pendulum film hardness	20 seconds @ 23°C	126 seconds @ 23°C	88 seconds @ 23°C	ISO 1522
T-bend test	cracking radius: 0T	cracking radius: 1T	cracking radius : 0T	ECCA-T7
	adhesion radius: 0T	adhesion radius: 0T	adhesion radius: 0T	

\*: Mixing ratio;  $79.56_{(\text{Sample Q})} / 20.44_{(\text{Sample N})}$

**b) Stage two:**

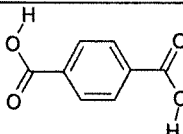
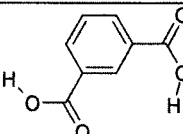
As shown in Table 3.11, the results of the tests of T-bend and pendulum film hardness for the coil top coating derived from the mixture of samples N and Q were satisfactory. Based on this result, a polyester formulation was designed through the combination of the formulations of samples N and Q according to their mixing ratio in the coil top coating. The relevant calculations are shown in Table 3.12.

**Table 3.12 Combination of the formulations of samples N and Q into a single formulation according to their mixing ratio in the coil top coating**

	Sample N (Moles)	Sample Q* (Moles)	Sample N multiplied by 20.44%	Sample Q multiplied by 79.56%	Columns 4 and 5 summed to form sample R
Adipic Acid	1.78	2.01	0.36	1.60	1.96
Isophthalic acid	1.60	2.90	0.33	2.31	2.63
Terephthalic acid	2.93	1.45	0.60	1.15	1.75
Neopentyl glycol	3.34	7.44	0.68	5.92	6.60
1,6 Hexandiol	3.69	2.01	0.75	0.00	0.75
Sum total	13.34	13.8	2.73	10.98	13.71

The new polyester formulation designed through the combination of the formulations of samples M and N was labeled as sample R. Composition of sample R is shown in Table 3.13.

**Table 3.13 Composition of sample R**

		Sample R
Monomer	Structure	Moles
Adipic acid	$\begin{array}{c} \text{O} & & \text{O} \\ \parallel & & \parallel \\ \text{HO}-\text{C}-\text{C}-\text{C}-\text{C}-\text{C}-\text{C}-\text{OH} \\   &   &   &   \\ \text{H}_2 & \text{H}_2 & \text{H}_2 & \text{H}_2 \end{array}$	1.96
Terephthalic acid		1.75
Isophthalic acid		2.63
Trimethylol propane	$\begin{array}{c} \text{H}_2\text{C}-\text{OH} \\   \\ \text{H}_3\text{C}-\text{C}-\text{C}-\text{C}-\text{OH} \\   &   &   \\ \text{H}_2 & & \text{H}_2 \\ &   & \\ & \text{C}-\text{OH} & \\ &   & \\ & \text{H}_2 & \end{array}$	-----
Neopentyl glycol	$\begin{array}{c} \text{CH}_3 \\   \\ \text{HO}-\text{C}-\text{C}-\text{C}-\text{OH} \\   &   &   \\ \text{H}_2 & & \text{H}_2 \\ &   & \\ & \text{CH}_3 & \end{array}$	6.60
1,6 hexanediol	$\begin{array}{c} \text{HO}-\text{C}-\text{C}-\text{C}-\text{C}-\text{C}-\text{C}-\text{OH} \\   &   &   &   &   &   \\ \text{H}_2 & \text{H}_2 & \text{H}_2 & \text{H}_2 & \text{H}_2 & \text{H}_2 \end{array}$	0.75
Total moles		13.71

Theoretical evaluation of the formulation of sample R according to the method described in Section 2.2 showed that it would be safe for polymerisation. Therefore, sample R was synthesised and its glass transition temperature was determined by differential scanning calorimetry. The relevant thermogram is shown in Figure 3.4.

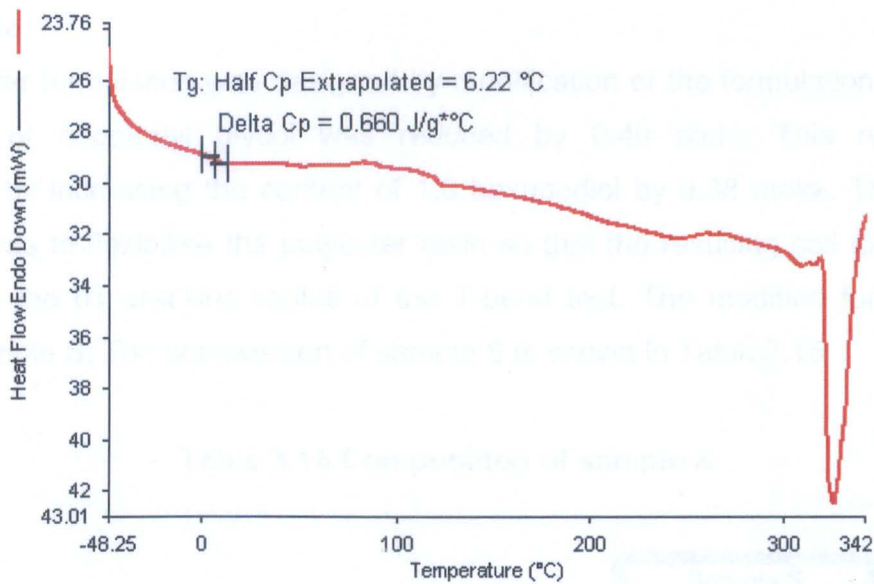


**Figure 3.4 DSC thermogram of sample R**

A coil top coating was derived from sample R. In the said coil top coating, sample R had replaced two control polyesters. The tests of T-bend and pendulum film hardness were carried out for the coil top coating derived from sample R. The results of the said tests are shown in Table 3.14.

**Table 3.14 Glass transition temperature of sample R and the results of the tests of T-bend and pendulum hardness for the resulting coil top coating film**

Property \ Resin	Sample R	Test method
Glass transition temperature	6.22°C	DSC
Konig pendulum film hardness	93 seconds @ 23°C	ISO 1522
T-bend test	cracking radius: 0.5T	ECCA-T7
	adhesion radius: 0T	

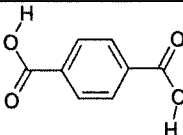
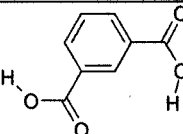
The resulting coil top coating film of sample R was not flexible enough to achieve the 0T cracking radius of the T-bend test.



**c) Stage three:**

A new polyester formulation was designed by modification of the formulation of sample R. The content of neopentyl glycol was reduced by 0.40 mole. This reduction was compensated by increasing the content of 1,6 hexanediol by 0.38 mole.. The aim of this modification was to flexibilise the polyester resin so that the resulting coil top coating film could achieve the 0T cracking radius of the T-bend test. The modified formulation was labeled as sample S. The composition of sample S is shown in Table 3.15.

**Table 3.15 Composition of sample S**

		Sample S
Monomer	Structure	Moles
Adipic acid	$\begin{array}{c} \text{O} & & \text{O} \\ \parallel & & \parallel \\ \text{HO}-\text{C} & -\text{C}- & \text{C}-\text{C}-\text{C}-\text{C}-\text{C}-\text{OH} \\ & \text{H}_2 & \text{H}_2 & \text{H}_2 & \text{H}_2 \end{array}$	1.96
Terephthalic acid		1.75
Isophthalic acid		2.63
Trimethylol propane	$\begin{array}{c} \text{H}_2\text{C}-\text{OH} \\   \\ \text{H}_3\text{C}-\text{C}-\text{C}-\text{C}-\text{OH} \\   &   \\ \text{H}_2 & \text{H}_2 \\   \\ \text{C}-\text{OH} \\   \\ \text{H}_2 \end{array}$	-----
Neopentyl glycol	$\begin{array}{c} \text{CH}_3 \\   \\ \text{HO}-\text{C}-\text{C}-\text{C}-\text{OH} \\   &   \\ \text{H}_2 & \text{H}_2 \\   \\ \text{CH}_3 \end{array}$	6.20
1,6 hexanediol	$\text{HO}-\text{C}-\text{C}-\text{C}-\text{C}-\text{C}-\text{C}-\text{OH} \\ \text{H}_2 \quad \text{H}_2 \quad \text{H}_2 \quad \text{H}_2 \quad \text{H}_2 \quad \text{H}_2$	1.13
Total moles		13.69

The formulation of sample S was theoretically evaluated according to the method mentioned in Section 2.2. The theoretical evaluation showed that the formulation of sample S would be safe for polymerisation. Therefore, it was synthesised and its glass transition temperature was determined by differential scanning calorimetry. The relevant thermogram is shown in Figure 3.5.

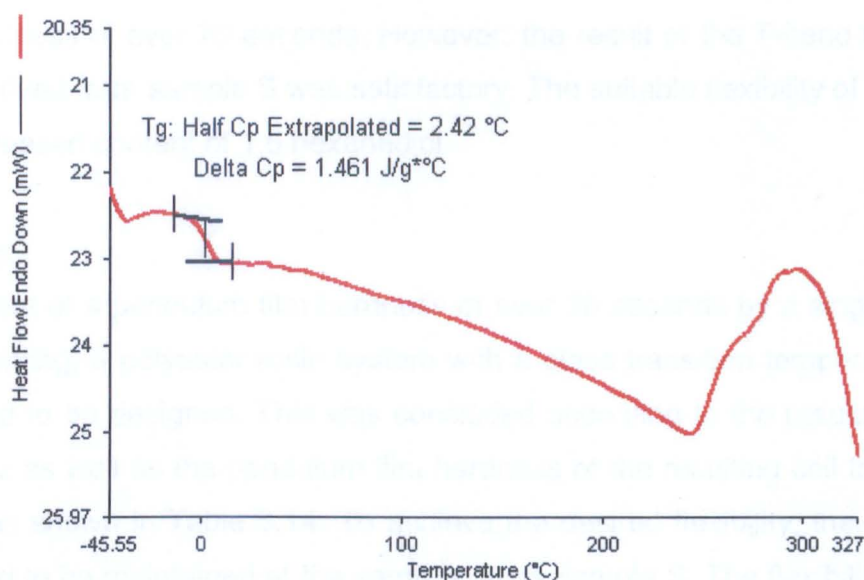


**Figure 3.5 DSC thermogram of sample S**

Increase in the content of 1,6 hexanediol, resulted in the reduction of the glass transition temperature of sample S. Based on the results discussed in Section 3.2.1.2, it was presumed that the resulting coil top coating film of sample S would not achieve the desired pendulum hardness. The results of the tests of the tests of T-bend and pendulum hardness of the coil top coating solely derived from sample S are shown in Table 3.16.

**Table 3.16 Glass transition temperature of sample S and the results of the tests of T-bend and pendulum hardness for the resulting coil top coating film**

Property \ Resin	Sample S	Test method
Glass transition temperature	2.42°C	DSC
Konig pendulum film hardness	55 seconds @ 23°C	ISO 1522
T-bend test	cracking radius: 0T	ECCA-T7
	adhesion radius: 0T	

As expected, the resulting coil top coating film of sample S did not achieve the desired

pendulum hardness of over 70 seconds. However, the result of the T-bend test of the coil top coating derived from sample S was satisfactory. The suitable flexibility of sample S was due to the increased content of 1,6 hexanediol.

**d) Stage four:**

For achievement of a pendulum film hardness of over 70 seconds by a single polyester in the coil top coating, a polyester resin system with a glass transition temperature between 8-10°C needed to be designed. This was concluded according to the results discussed in Section 3.2.1.2 as well as the pendulum film hardness of the resulting coil top coating film of sample R as shown in Table 3.14. To achieve the desired flexibility, the content of 1,6 hexanediol had to be maintained at the same level as sample S. The flexibility of sample S was satisfactory. However, such content of 1,6 hexanediol would not allow the glass transition temperature of the polyester to exceed 3°C. This was concluded according to the performance of the resulting coil top coating films of samples P and S as shown in Tables 3.9 and 3.16 respectively.

To overcome this problem, it was decided to incorporate a cycloaliphatic structure to the polyester backbone to some extent. This decision was based on the works published by Tsai et al<sup>52</sup>, Ni et al<sup>54</sup> and Awasthi and Agrawal<sup>56</sup>. In the works mentioned, it had been claimed that cycloaliphatic moieties would impart transitional thermal and mechanical properties to the polyester. The transitional properties concerned were with respect to pure aliphatic polyesters and pure aromatic polyesters. In addition, Tsai et al<sup>52</sup> and Awasthi and Agrawal<sup>56</sup> showed that incorporation of cycloaliphatic moieties to polyesters would result in increased glass transition temperatures.

As such, the formulation of sample S was modified. The content of neopentyl glycol was reduced by 1.73 moles. This reduction was compensated through the inclusion of 1.25 moles of 1,4 cyclohexanedimethanol. The new polyester formulation was labeled as sample T. Theoretical evaluation of the formulation of sample T according to the method described in Section 2.2 showed that it would be safe for polymerisation. The composition of sample T is shown in Table 3.17.

Table 3.17 Composition of sample T

		Sample T
Monomer	Structure	Moles
Adipic acid		1.96
Terephthalic acid		1.75
Isophthalic acid		2.63
Neopentyl glycol		4.47
1,6 hexanediol		1.13
1,4 cyclohexane-dimethanol		1.25
Total moles		13.22

The DSC thermogram of sample T is shown in Figure 3.6.

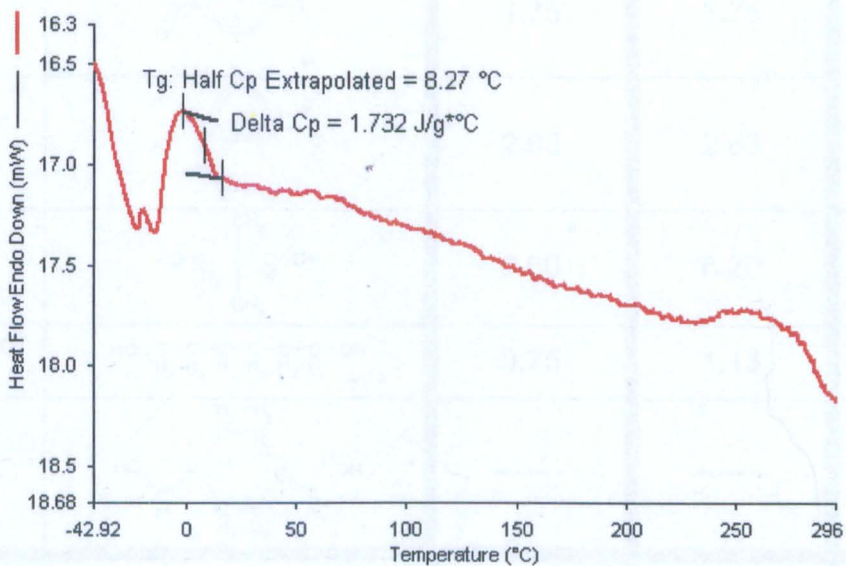


Figure 3.6 DSC thermogram of sample T

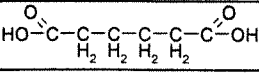
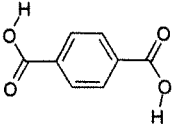
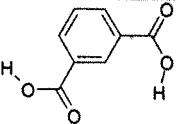
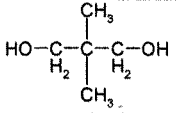
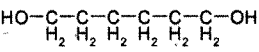
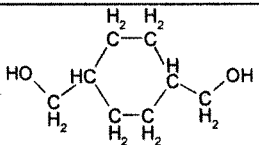
The glass transition temperature of sample T and the results of the tests of T-bend and pendulum hardness of its resulting coil top coating film are shown in Table 3.18.

**Table 3.18 Glass transition temperature of sample T and the results of the tests of T-bend and pendulum hardness for the resulting coil top coating film**

Property \ Resin	Sample T	Test method
Glass transition temperature	8.27°C	DSC
Konig pendulum film hardness	100 seconds @ 23°C	ISO 1522
T-bend test	cracking radius: 0T	ECCA-T7
	adhesion radius: 0T	

Composition of samples R, S and T are reviewed in Table 3.19.

**Table 3.19 Composition of samples R, S and T**

Monomer	Structure	Sample R	Sample S	Sample T
		Moles	Moles	Moles
Adipic acid		1.96	1.96	1.96
Terephthalic acid		1.75	1.75	1.75
Isophthalic acid		2.63	2.63	2.63
Neopentyl glycol		6.60	6.20	4.47
1,6 hexanediol		0.75	1.13	1.13
1,4 cyclohexane-dimethanol		-----	-----	1.25
Total moles		13.71	13.69	13.22

The glass transition temperatures of samples R, S and T and the performance of the resulting top coating films in terms of the tests of T-bend and pendulum hardness are reviewed in Table 3.20.

**Table 3.20 Glass transition temperatures of samples R, S and T and the results of the tests of T-bend and pendulum hardness for the resulting coil top coating films**

Resin Property	Sample R	Sample S	Sample T	Test method
Glass transition temperature	6.22°C	2.42°C	8.27°C	DSC
Konig pendulum film hardness	93 seconds @ 23°C	55 seconds @ 23°C	100 seconds @ 23°C	ISO 1522
T-bend test	cracking radius: 0.5T	cracking radius: 0T	cracking radius : 0T	ECCA-T7
	adhesion radius: 0T	adhesion radius: 0T	adhesion radius: 0T	

The results shown in Table 3.20 indicated that sample T had performed as a novel and standalone polyester resin system in the coil top coating. Sample T had been used as a replacement for two control polyesters in the coil top coating and it had provided the same level of hardness and flexibility.

With respect to the glass transition temperature of samples R, S and T and the pendulum hardness of their resulting coil top coating films, the following were concluded. The conclusions are based on the results discussed in Section 3.2.1.2, the results shown in Table 3.20 and the recent results made available by other researchers.

- 1- As shown and concluded in Section 3.2.1.2, the rise and fall of the pendulum hardness of the coil top coating film was directly related to the glass transition temperature of its base saturated polyester resin. This conclusion was reproduced according to the glass transition temperature and pendulum film hardness of the resulting coil top coatings of samples R, S and T.
- 2- As shown and concluded in Section 3.2.1.2, increase in the content of the aliphatic moiety of 1,6 hexanediol in the polyester backbone resulted in the reduction of the

glass transition temperature. This conclusion was reproduced according to the comparison made between the glass transition temperature of samples R and S. Sample R contained 0.75 mole of 1,6 hexanediol and its glass transition temperature was 6.22°C. Sample S contained 1.13 moles of 1,6 hexanediol and its glass transition temperature was 2.42°C.

- 3- Introduction of the cycloaliphatic moiety to the polyester backbone resulted in the augmentation of the glass transition temperature. While the content of the aliphatic moiety of 1,6 hexanediol was maintained, the glass transition temperature of the polyester was increased. This was concluded according to the comparison made between the glass transition temperatures of samples S and T. As shown in Table 3.19, the molar content of 1,6 hexanediol in samples S and T were similar. However, sample T contained 1.25 moles of 1,4 cyclohexanedimethanol. Sample S did not contain 1,4 cyclohexanedimethanol. The glass transition temperature of sample S was 2.42°C while the glass transition temperature of sample S was 8.27°C. Inclusion of 1,4 cyclohexanedimethanol in sample T increased the glass transition temperature by 5.85°C. As a consequence, the pendulum hardness of the resulting coil top coating film of sample T was significantly increased. The pendulum film hardness of the coil top coating derived from sample T was 100 seconds. On the other hand, the pendulum hardness of the resulting coil top coating film of sample S was 55 seconds.
- 4- Such augmentation of the glass transition temperature of polyester systems through introduction of cycloaliphatic moieties had also been reported in some of the recent literature. Tsai et al<sup>52</sup> showed that the glass transition temperature of polyesters prepared from butanedioic acid, 1,4 butanediol and 1,3/1,4 cyclohexanedimethanol increased as the contents of 1,3/1,4 cyclohexanedimethanol increased (p.75). Awasthi and Agrawal<sup>56</sup> showed that the glass transition temperature of a pure cycloaliphatic polyester derived from 1,4 cyclohexanedimethanol and 1,4 cyclohexanedicarboxylic acid was higher than an aliphatic-cycloaliphatic polyester derived from 1,4 cyclohexanedimethanol, hexanedioic acid and nonanedioic acid (p.47).

Regarding the flexibility of the coil top coating derived from the mixture of samples N and Q and the coil top coatings derived solely and separately from samples R, S and T, the

following were concluded. These conclusions are based on the results of the T-bend test shown in Tables 3.11 and 3.20 as well as the composition of the said samples as shown in Tables 3.7, 3.8 and 3.19.

- 1- Saturated polyester resins that are prepared from different dicarboxylic acids and neopentyl glycol are of linear characteristics and can be used as coil coating binder systems. However, they have to be properly flexibilised with a saturated polyester resin of high linearity. This was concluded after it was observed that the coil top coating derived from the mixture of samples N and Q was of sufficient flexibility. Sample Q contained neopentyl glycol only. As concluded and discussed in Section 3.1.5, sample N was a flexibiliser resin. Composition of samples N and Q were shown in Tables 3.7 and 3.8 respectively. The coil top coating film derived from the mixture of samples N and Q achieved the 0T cracking radius of the T-bend test. The adhesion radius of the coil top coating film derived from the mixture of samples N and Q was satisfactory as well. This was due to incorporation of aromatic moieties in the backbones of samples N and Q through inclusion of terephthalic acid and isophthalic acid.
- 2- Combination of two polyester formulations into a single formulation according to their mixing ratio in a coating and polymerising it with the aim of obtaining the same coating film properties with a singular binder system, proved to be inapplicable. This was concluded according to the result of the T-bend test of the resulting coil top coating film of sample R. The formulation of sample R was designed by combining the formulations of samples N and Q according to their mixing ratio of  $79.56_{(\text{sample Q})} / 20.44_{(\text{sample N})}$  in the coil top coating. The relevant calculations were shown in Table 3.12. The coil top coating that was derived from the mixture of samples N and Q had achieved the 0T cracking radius. However, the cracking radius of the resulting coating film of sample R was 0.5T. In other words, the flexibility of sample R as the combined formulation of samples N and Q was weaker than the actual mixture of samples N and Q. The adhesion radius of the resulting coil top coating film of sample R remained unchanged in comparison to the coil top coating film resulted from the mixture of samples N and Q. Similar to samples N and Q, the aromatic diacids of terephthalic acid and isophthalic acid were also employed in sample R. Therefore, the adhesion strength of the resulting coating film of sample R was



comparable to the adhesion strength of the coating film derived from the mixture of samples N and Q.

- 5- As concluded according to the results provided in Section 3.2.1.2, 1,6 hexanediol was of high flexibilising efficiency. This conclusion was reproduced based on the comparison made between the T-bend test results of the resulting coil top coating films of samples R and S. The molar content of 1,6 hexanediol in samples S was higher than sample R. As a consequence, the resulting coil top coating film of sample S achieved the 0T cracking radius of the T-bend test. On the other hand, the cracking radius of the coil top coating film derived from sample R was 0.5T.
  
- 6- The balance among adhesion and flexibility remained intact as 1,4 cyclohexanedimethanol was incorporated in the formulation of sample T. 1,4 cyclohexanedimethanol had been used as a partial replacement for neopentyl glycol. Thus, it is presumed that the conformational interchange of the cyclohexyl ring could have resulted in even a better balance between flexibility and adhesion. The formulation of sample T was designed by modification of the formulation of sample S. The formulations of samples S and T were reviewed in Table 3.19. According to the results shown in Table 3.20, inclusion of 1,4 cyclohexanedimethanol in sample T promoted the glass transition temperature without disturbing the flexibility. Such phenomenon had also been reported by other researchers. In the works of Awasthi and Agrawal<sup>56</sup> and Heidt and Elliot<sup>64</sup>, it was shown that incorporation of cycloaliphatic moieties to polyester backbones resulted in the same flexibility as aliphatic moieties with the advantage of preservation or augmentation of adhesion, hardness and glass transition temperature. Excellent flexibility, adequate adhesion, and suitable glass transition temperature were simultaneously achieved as sample T was designed and synthesised. These multiple properties could not be incorporated into sample T and a standalone and novel polyester system for coil coatings could not be developed without 1,4 cyclohexanedimethanol. Therefore, it was concluded that for designing a novel and standalone coil coating saturated polyester resin system with all the properties mentioned, an appropriate content of 1,4 cyclohexanedimethanol should be employed.

### 3.2.2 Moieties present in the molecular structure of the copolyesters synthesised

Moieties present in the molecular structure of the saturated polyester resins synthesised were confirmed by the spectroscopic techniques of  $^{13}\text{C}$  NMR,  $^1\text{H}$  NMR and FTIR. In this regard, the said techniques were carried out for samples O, P, Q, R, S and T. The dicarboxylic acids employed for preparation of the saturated polyester resins mentioned were similar. However, as discussed in detail in Sections 3.2.1.2 and 3.2.1.3, these polyesters were chemically modified by exclusion or inclusion of polyols. The said modifications were carried out in order to develop a novel and standalone polyester system for coil coatings with a glass transition temperature between 8-10°C, excellent flexibility and sufficient adhesion. As such, the variety of the polyols employed for the chemical modifications would have resulted in the presence of a variety of moieties in the molecular structure of the copolyesters concerned. As mentioned in Section 1.7.4, NMR spectroscopy was a powerful technique for studying the effect of the replacement of polyols on the molecular structure of the resulting polyester resin.

#### 3.2.2.1 $^{13}\text{C}$ NMR spectra

In this section, the  $^{13}\text{C}$  NMR spectra of the copolyesters synthesised are provided, interpreted and discussed. The  $^{13}\text{C}$  NMR spectra are proton decoupled and are provided in specific frequency ranges in which signals had appeared. These frequency ranges included 21-22 ppm, 24-29 ppm, 33-37 ppm, 62-66 ppm, 67-72 ppm, 77-78 ppm, 124-130 ppm, 130-132 ppm, 164-167 ppm and 171-175 ppm. As mentioned in Section 3.2.1.2, sample Q contained neopentyl glycol only. The rest of the samples that were analysed by  $^{13}\text{C}$  NMR contained additional polyols beside neopentyl glycol. Therefore, interpretation of the  $^{13}\text{C}$  NMR spectra of the other samples was made by comparing them with the  $^{13}\text{C}$  NMR spectrum of sample Q. By doing as such, peaks that appeared from the additional moieties that were incorporated to the molecular structure of these samples through inclusion of other polyols could be distinguished. The interpretations were made according to spectral shift and correlation charts. In addition, the results published by other researchers for copolyesters with some resemblance to the copolyesters prepared throughout the course of this study were also considered. Feed composition and the hydroxyl value of the copolyester samples analysed by  $^{13}\text{C}$  NMR are reviewed in Table 3.21.

**Table 3.21 Feed composition and free hydroxyl content of the synthesised copolyester samples that were examined by NMR spectroscopy**

		Sample O	Sample P	Sample Q	Sample R	Sample S	Sample T
Monomer	Chemical structure	Moles	Moles	Moles	Moles	Moles	Moles
Adipic acid		2.01	2.01	2.01	1.97	1.97	1.97
Terephthalic acid		1.45	1.45	1.45	1.75	1.75	1.75
Isophthalic acid		2.90	2.90	2.90	2.64	2.64	2.64
Trimethylol propane		1.00	----	----	----	----	----
Neopentyl glycol		6.16	6.16	7.44	6.63	6.20	4.47
1,6 hexanediol	$\text{HO}-(\text{C}_2\text{H}_4)_6-\text{OH}$	----	1.13	----	0.75	1.13	1.13
1,4 cyclohexane dimethanol		----	----	----	----	----	1.25
Total moles		13.52	13.65	13.80	13.74	13.69	13.22
Hydroxyl value (mgKOH/g)		93.44	67.42	78.37	72.91	69.23	34.88

Parameters of the  $^{13}\text{C}$  NMR analysis were provided in Table 2.20. The  $^{13}\text{C}$  NMR spectra of the synthesised copolyesters, in the range of 21-22 ppm, are shown in Figure 3.7.

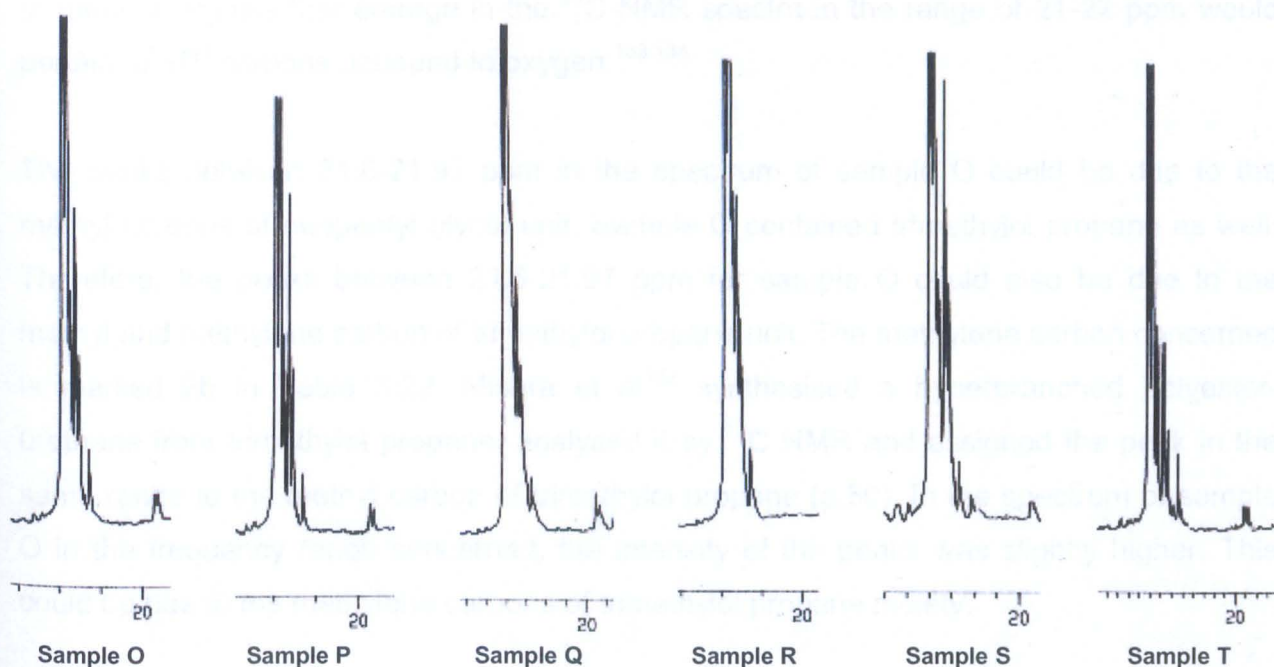


Figure 3.7  $^{13}\text{C}$  NMR spectra in the range of 21-22 ppm

Assignments that could be made for the spectra shown in Figure 3.7 are provided in Table 3.22.

Table 3.22 Assignments for the  $^{13}\text{C}$  NMR spectra in the range of 21-22 ppm <sup>106,132-134</sup>

$\text{---O---CH}_2\text{---}\overset{\text{1a}}{\underset{\text{1a}}{\text{C}}}\begin{matrix} \text{CH}_3 \\ \text{---} \\ \text{CH}_3 \end{matrix}\text{---CH}_2\text{---O---}$	1a	$\text{---O---}\overset{\text{1c}}{\text{C}}\text{---}\overset{\text{1c}}{\text{C}}\text{---}\overset{\text{1c}}{\text{C}}\text{---}\overset{\text{1c}}{\text{C}}\text{---}\overset{\text{1c}}{\text{C}}\text{---O---}$	1c
$\begin{matrix} \text{H}_2\text{---O---} \\ \text{---} \\ \text{1b} \text{---}\text{C} \text{---}\text{2b} \text{---} \\ \text{H}_3\text{C---}\text{C} \text{---} \text{C} \text{---}\text{O---} \\ \text{---} \\ \text{H}_2\text{---O---} \\ \text{---} \\ \text{H}_2\text{---O---} \end{matrix}$	1b-2b	$\begin{matrix} \text{H}_2 & \text{H}_2 \\ \text{---} & \text{---} \\ \text{1d} & \text{C} & \text{C} & \text{1d} \\ \text{---} & \text{---} & \text{---} & \text{---} \\ \text{---O---}\text{C} & \text{---}\text{CH} & \text{---}\text{HC} & \text{---}\text{C} \text{---}\text{O---} \\ & \text{H}_2 & & \text{H}_2 \\ & \text{---} & \text{---} & \text{---} \\ & \text{1d} & \text{C} & \text{C} & \text{1d} \\ & \text{---} & \text{---} & \text{---} & \text{---} \\ & \text{H}_2 & \text{H}_2 & & \end{matrix}$	1d
<b>Sample</b>	<b><math>\delta</math> (PPM)</b>		<b>Assignment</b>
O	21.6-21.97		1a-1b-2b
P	21.27-21.89		1a-1c
Q	21.08-21.99		1a
R	21.31-21.97		1a-1c
S	21.29-21.93		1a-1c
T	21.5-22.01		1a-1c-1d

In general, signals that emerge in the  $^{13}\text{C}$  NMR spectra in the range of 21-22 ppm would pertain to  $\text{SP}^3$  carbons unbound to oxygen.<sup>133,134</sup>

The peaks between 21.6-21.97 ppm in the spectrum of sample O could be due to the methyl carbons of neopentyl glycol unit. Sample O contained trimethylol propane as well. Therefore, the peaks between 21.6-21.97 ppm for sample O could also be due to the methyl and methylene carbon of trimethylol propane unit. The methylene carbon concerned is marked 2b in Table 3.22. Mishra et al<sup>132</sup> synthesised a hyperbranched polyester-urethane from trimethylol propane, analysed it by  $^{13}\text{C}$  NMR and assigned the peak in the same range to the methyl carbon of trimethylol propane (p.50). In the spectrum of sample O in the frequency range concerned, the intensity of the peaks was slightly higher. This could be due to the methylene carbons of trimethylol propane moiety.

The sharp peaks between 21.27-21.89 ppm in the spectrum of sample P could be due to the methyl carbons of neopentyl glycol unit. The medium height and short height peaks could be due to the central methylene carbons of 1,6 hexanediol moiety. Due to the similarity of the compositions of samples P, R and S, the assignments made for sample P could also be made for the peaks of samples R and S in the same range of the  $^{13}\text{C}$  NMR spectra.

The sharp peaks in the range of 21.08-21.99 ppm in the spectrum for sample Q could be due to the methyl carbons of neopentyl glycol moiety. It could be seen, from the spectrum of sample Q, that fewer peaks had emerged in the range of 21-22ppm. Sample Q contained neopentyl glycol only and this could be the reason for availability of fewer peaks in the range concerned.

The sharp peaks between 21.27-21.89 ppm in the spectrum of sample T could be due to the methyl carbons of neopentyl glycol unit. The medium height and short height peaks could be due to the central methylene carbons of 1,6 hexanediol residue and methylene carbons of 1,4 cyclohexanedimethanol moiety. The said carbons are marked 1c and 1d in Table 3.22. In the spectrum of sample T in the frequency range concerned, a greater multiplicity could be seen. This could be due to the availability of the moieties of three diols in the molecular structure of sample T.

Overall, the peaks in the  $^{13}\text{C}$  NMR spectra of the copolyester samples in the range of 21-22 ppm were similar to a great extent. Slight differences that existed could be due to the availability of different numbers of methyl or methylene carbons in the samples as the result of the inclusion or exclusion of polyols.

The  $^{13}\text{C}$  NMR spectra of the synthesised copolyesters, in the range of 24-29 ppm, are shown in Figure 3.8.

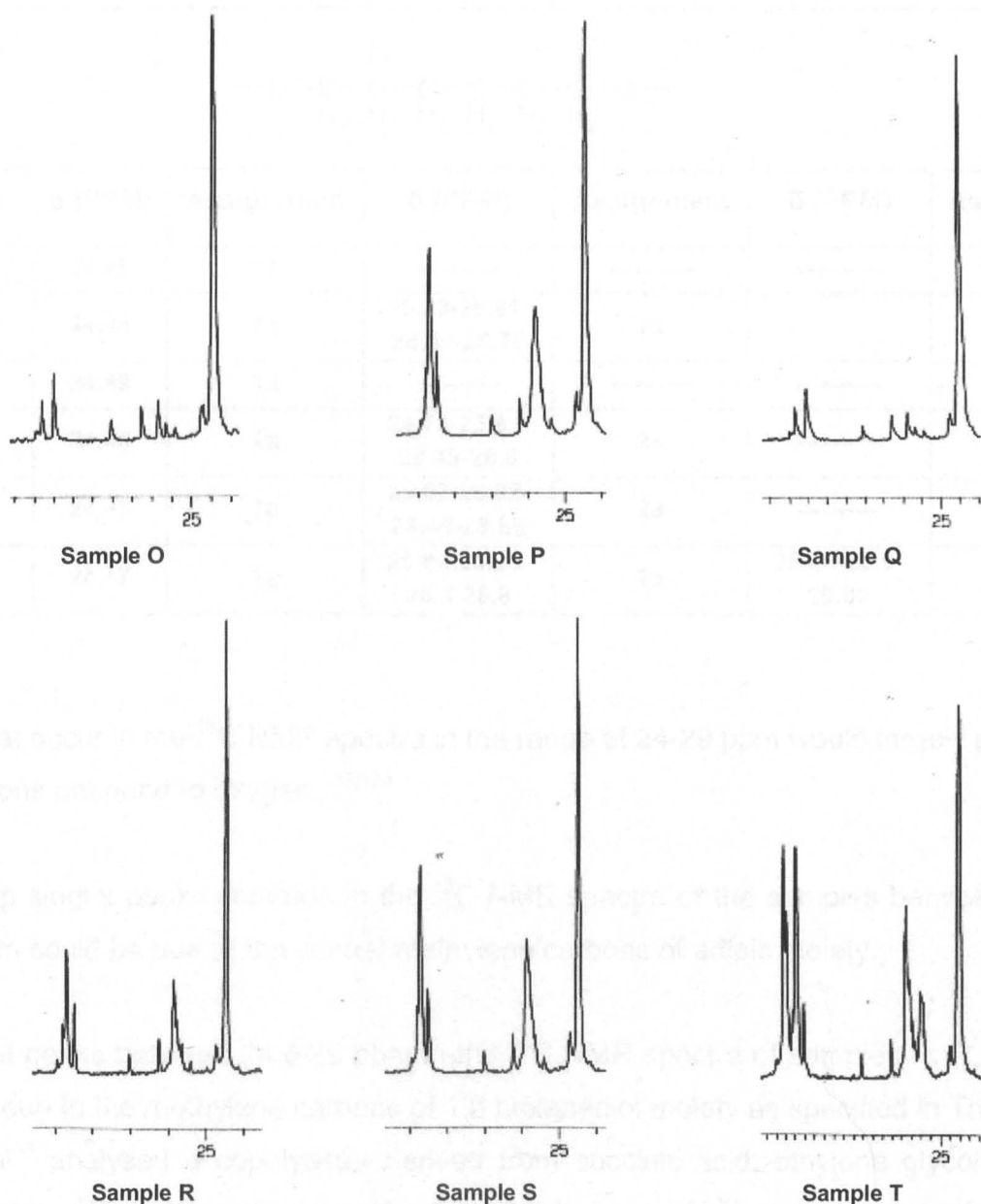


Figure 3.8  $^{13}\text{C}$  NMR spectra in the range of 24-29 ppm

Assignments that could be made for the spectra shown in Figure 3.8 are provided in Table 3.23.

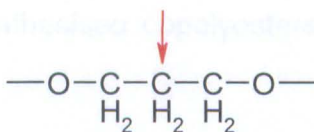
**Table 3.23 Assignments for the  $^{13}\text{C}$  NMR spectra in the range of 24-29 ppm**<sup>36,133,134</sup>

Sample	$\delta$ (PPM)	Assignment	$\delta$ (PPM)	Assignment	$\delta$ (PPM)	Assignment
O	24.45	1a	-----	-----	-----	-----
P	24.44	1a	25.38-25.81- 28.49-28.79	2a	-----	-----
Q	24.49	1a	-----	-----	-----	-----
R	24.45	1a	24.73-25.83- 28.49-28.8	2a	-----	-----
S	24.45	1a	25.62-26.32- 28.49-28.69	2a	-----	-----
T	24.47	1a	25.64-25.86- 28.4-28.8	2a	25.48-28.9- 29.02	2b

Peaks that occur in the  $^{13}\text{C}$  NMR spectra in the range of 24-29 ppm would largely pertain to  $\text{SP}^3$  carbons unbound to oxygen.<sup>133,134</sup>

The sharp singlet peaks common in the  $^{13}\text{C}$  NMR spectra of the samples between 24.44-24.50 ppm could be due to the central methylene carbons of adipic moiety.

The triplet peaks between 24.6-29 ppm in the  $^{13}\text{C}$  NMR spectra of samples P, R, S and T could be due to the methylene carbons of 1,6 hexanediol moiety as specified in Table 3.23. Tsai et al<sup>36</sup> analysed a copolyester derived from succinic acid, ethylene glycol and 1,3 propanediol by  $^{13}\text{C}$  NMR and assigned a peak in the same frequency range to the central methylene carbon of 1,3 propanediol moiety (p.2342). This carbon is shown in Scheme 3.1



### Scheme 3.1 Central methylene carbon in the moiety of 1,3 propanediol

It can be assumed that some resemblance could exist for the chemical environment of the methylene carbons of 1,6 hexanediol residue shown in Table 3.23 and the central methylene carbon of 1,3 propanediol unit. The intensity of the peaks between 24.6-29 ppm could be due to the incorporated moles of 1,6 hexanediol. The same content of 1,6 hexanediol had been used for preparation of samples P, S and T. However, the molar content of 1,6 hexanediol in sample R was lower than samples P, S and T. The peaks for samples P, S and T in the range of 24.6-29ppm were of similar intensities. On the other hand, in the spectrum of sample R the corresponding peak was of reduced intensity. Therefore, it could be assumed that the increased content of 1,6 hexanediol in samples P, S and T had increased the intensity of the peaks in the range of 24.6-29 ppm.

In the spectrum of sample T, additional peaks could be seen at 25.48 ppm, 28.9 ppm and 29.02 ppm. There were no peaks in the same frequencies in the spectra of the other samples. Sample T was the only sample in which 1,4 cyclohexanedimethanol had been incorporated. Therefore, the additional peaks seen in the spectrum of sample T in the frequency range concerned could be due to the carbons of 1,4 cyclohexanedimethanol moiety as shown in Table 3.23

In the spectra of samples O and Q which did not contain 1,6 hexandiol and 1,4 cyclohexanedimethanol, no peaks could be seen in the range of 24.6-29 ppm.

Modifications made to the molecular structure of the synthesised copolyesters were visible in the  $^{13}\text{C}$  NMR spectra in the range of 24-29 ppm. It could be seen, from the  $^{13}\text{C}$  NMR spectra of samples P, R and S, that unique peaks appeared in the range of 25.38-28.69 ppm. As shown in Table 3.23, the peaks concerned could pertain to the methylene carbons of 1,6 hexanediol moiety. Inclusion of 1,4 cyclohexanedimethanol in sample T also resulted in the rise of exclusive peaks in the frequency range concerned. On the other hand, in the  $^{13}\text{C}$  NMR spectra samples O and Q in the range of 24-29 ppm, no peaks had emerged.



The  $^{13}\text{C}$  NMR spectra of the synthesised copolyesters, in the range of 33-37 ppm, are shown in Figure 3.9.

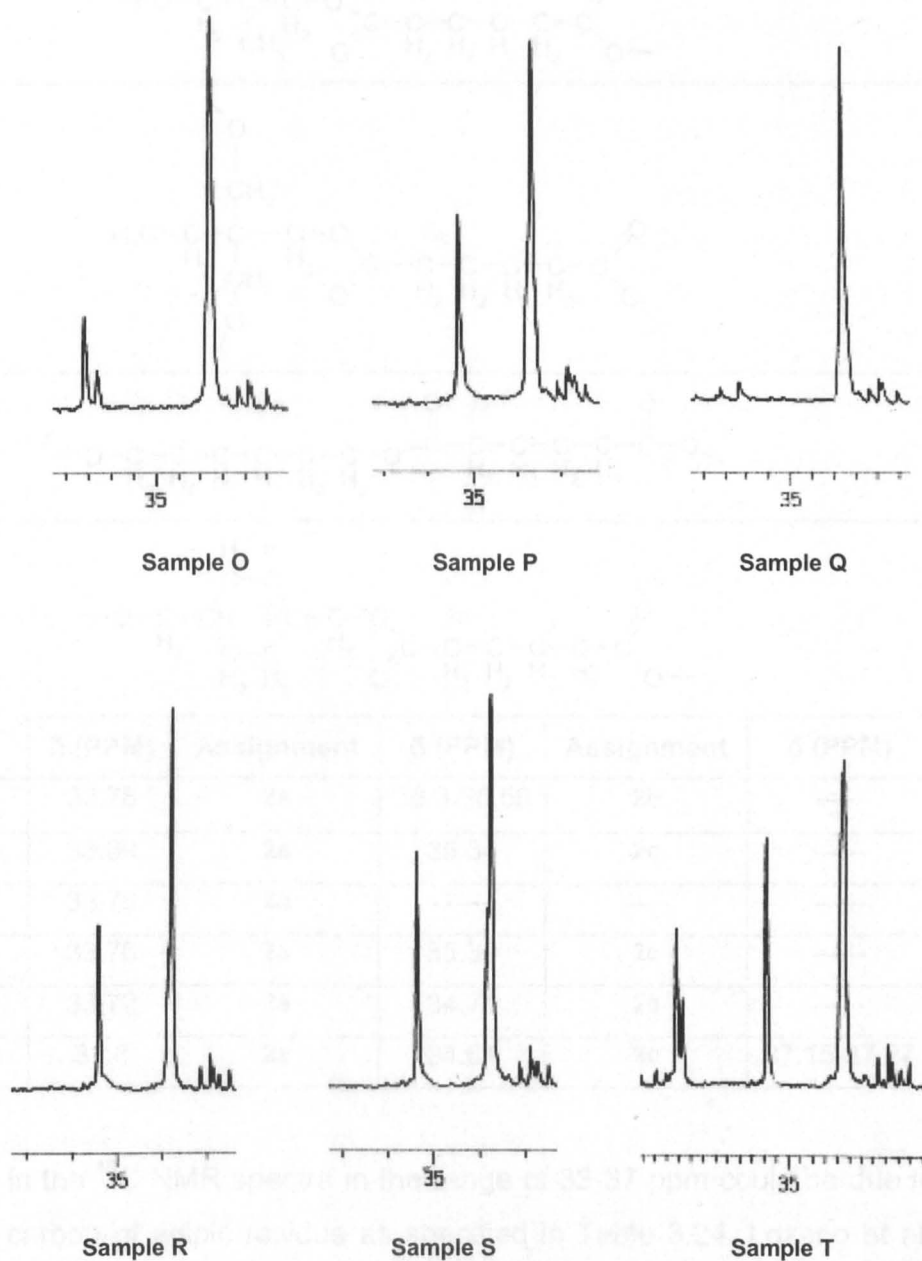


**Figure 3.9**  $^{13}\text{C}$  NMR spectra in the range of 33-37 ppm

Assignments that could be made for the spectra shown in Figure 3.9 are provided in Table 3.24.

**Table 3.24 Assignments for the  $^{13}\text{C}$  NMR spectra in the range of 33-37 ppm** <sup>60,133,134</sup>

			<b>2a</b>			
			<b>2b</b>			
			<b>2c</b>			
			<b>2d</b>			
Sample	$\delta$ (PPM)	Assignment	$\delta$ (PPM)	Assignment	$\delta$ (PPM)	Assignment
O	33.78	2a	36.3-36.58	2b	-----	-----
P	33.69	2a	35.34	2c	-----	-----
Q	33.79	2a	-----	-----	-----	-----
R	33.76	2a	35.39	2c	-----	-----
S	33.72	2a	34.71	2c	-----	-----
T	33.8	2a	34.61	2c	37.15-37.27	2d

The peaks in the  $^{13}\text{C}$  NMR spectra in the range of 33-37 ppm could be due to the terminal methylene carbon of adipic residue as specified in Table 3.24. Lozano et al.<sup>60</sup> analysed a poly(ester amide) that contained adipic acid by  $^{13}\text{C}$  NMR and assigned the signal in the same frequency range to the same carbon (p.599).

Adipic acid had reacted with different polyols included in the formulation of the synthesised copolyesters. This could have resulted in the creation of different chemical environments for the considered carbon of adipic moiety. Therefore, the signals seen in the range of 33-37 ppm could pertain to the same carbon of adipic moiety, but in different chemical

environments. The number of the peaks in the range of 33-37 ppm could match with the number of the polyols included in the formulation of the copolyester samples. There was one peak in the  $^{13}\text{C}$  NMR spectrum of sample Q in the range of 33-37 ppm. Sample Q contained neopentyl glycol only. In addition to neopentyl glycol, other polyester samples contained either 1,6 hexanediol, 1,4 cyclohexanedimethanol or trimethylol propane. Therefore, the number of their signals and the relevant assignments in the range of 33-37 ppm are discussed in comparison with the signal of sample Q in the same range.

The  $^{13}\text{C}$  NMR spectrum of sample Q in the range of 33-37 ppm showed a sharp singlet peak at 33.79 ppm. This peak could be assigned to the terminal methylene carbon of adipic residue marked 2a in Table 3.24. As shown in Table 3.24, carbon 2a would be adjacent to the ester group formed as the result of the reaction of adipic acid with neopentyl glycol. This assignment could be made since sample Q contained neopentyl glycol only.

The  $^{13}\text{C}$  NMR spectrum of sample O in the range of 33-37 ppm showed a sharp peak at 33.78 ppm and a short height peak between 36.3-36.58 ppm. The peak at 33.78 ppm could be assigned to the terminal methylene carbon of adipic moiety (carbon 2a in Table 3.24). The short height peak between 36.3-36.58 ppm could be assigned to carbon 2b in Table 3.24. As shown in Table 3.24, carbon 2b would be adjacent to the ester group formed as the result of the reaction of adipic acid with trimethylol propane. In terms of polyols, sample O contained neopentyl glycol and trimethylol propane. The peak between 36.3-36.58 ppm in the spectrum of sample O could be assigned to carbon 2b since no signals could be seen in the corresponding frequency range in the spectrum of sample Q. Trimethylol propane had not been included in sample Q.

The  $^{13}\text{C}$  NMR spectra of samples P, R and S in the range of 33-37 ppm showed two peaks. The first peak was stretched and was between 33.69-33.76 ppm. The second peak was medium height and was between 34.71-35.34 ppm. The sharp peaks between 33.69-33.76 ppm could be assigned to the terminal methylene carbon of adipic residue (carbon 2a in Table 3.24). The medium height peaks between 34.71-35.34 ppm could be assigned to methylene carbon 2c in the adipic moiety. As shown in Table 3.24, carbon 2c would be adjacent to the ester group formed as the result of the reaction of adipic acid with 1,6 hexanediol. In terms of polyols, samples P, R and S contained neopentyl glycol and 1,6 hexanediol. The medium height peaks between 34.71-35.34 ppm in the spectra for

samples P, R and S could be assigned to carbon 2c since there was no signal in the corresponding frequency range in the spectrum for sample Q. 1,6 hexanediol had not been included in sample Q.

The  $^{13}\text{C}$  NMR spectrum of sample T in the range of 33-37 ppm showed three peaks. The first peak was stretched and was at 33.8 ppm. The second peak was medium height and was at 34.61 ppm. The third peak was between 37.15-37.27 ppm. The signal at 33.8 ppm could be due to the terminal methylene carbon of adipic residue (carbon 2a in Table 3.24). The second peak at 34.61 ppm could be due to carbon 2c in the adipic residue as shown in Table 3.24. The third doublet peak between 37.15-37.27 ppm could be assigned to the terminal methylene carbon of adipic residue marked 2d in Table 3.24. As shown in Table 3.24, carbon 2d would be adjacent to the ester group formed as the result of the reaction of adipic acid with 1,4 cyclohexanedimethanol. The second and third peaks in the range of 33-37 ppm in the spectrum of sample T could be assigned to carbons 2c and 2d since no signal could be seen in the corresponding frequency range in the spectrum of sample Q. 1,6 hexanediol and 1,4 cyclohexanedimethanol were not included in sample Q. In addition, only sample T had resulted in a signal in the range of 37.15-37.27 ppm. Sample T was the only sample in which 1,4 cyclohexanedimethanol had been included.

Similar to the  $^{13}\text{C}$  NMR spectra in the range of 24-29 ppm, alterations made to the molecular structure of the synthesised copolyesters could also be observed in the  $^{13}\text{C}$  NMR spectra in the range of 33-37 ppm.

The  $^{13}\text{C}$  NMR spectra of samples O, P and Q, in the range of 62-66 ppm, are shown in Figure 3.10.

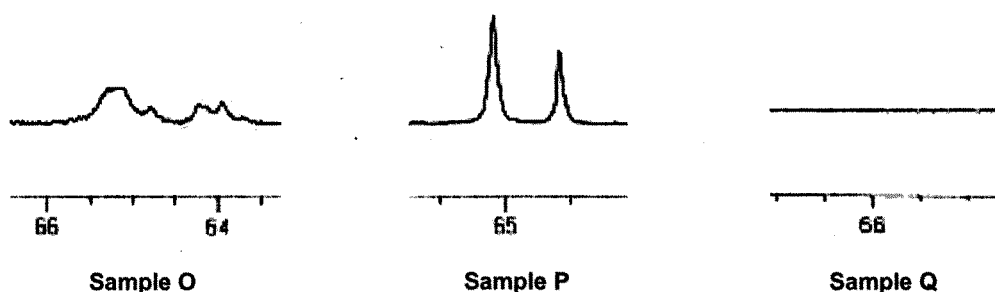


Figure 3.10  $^{13}\text{C}$  NMR spectra of samples O, P and Q in the range of 62-66 ppm

The  $^{13}\text{C}$  NMR spectra of samples R, S and T, in the range of 62-66 ppm, are shown in Figure 3.11.

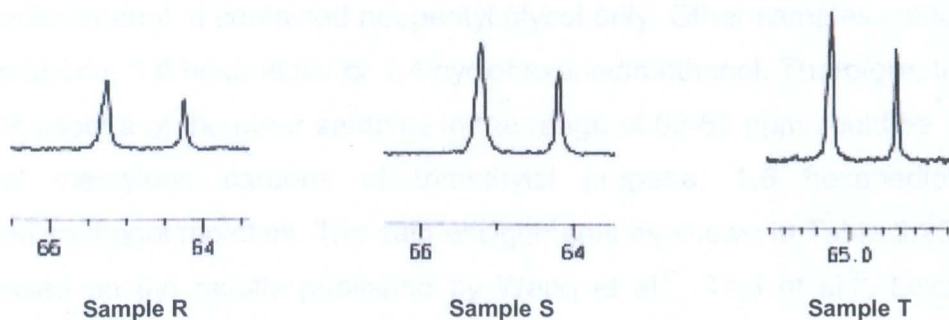


Figure 3.11  $^{13}\text{C}$  NMR spectra of samples O, P and Q in the range of 62-66 ppm

Assignments that could be made for the spectra shown in Figures 3.10 and 3.11 are provided in Table 3.25.

Table 3.25 Assignments for the  $^{13}\text{C}$  NMR spectra in the range of 62-66 ppm<sup>31,36,60,132-135</sup>

	2a -2b		3a-3b	
		3c-3d		
Sample	$\delta$ (PPM)	Assignment	$\delta$ (PPM)	Assignment
O	63.94	2a	65.13	2b
P	64.16	3a	65.18	3b
Q	-----	-----	-----	-----
R	64.24	3a	65.24	3b
S	64.18	3a	65.20	3b
T	64.28	3a-3c	65.27	3b-3d

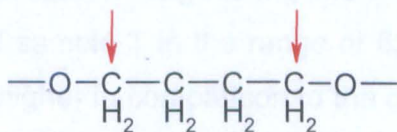
On the whole, peaks that appear in the  $^{13}\text{C}$  NMR spectra in the range of 62-66 ppm would pertain to  $\text{SP}^3$  carbons neighboring oxygen.<sup>133,134</sup>

As shown in Figure 3.10, there were no peaks in the  $^{13}\text{C}$  NMR spectrum of sample Q in the range of 62-66 ppm. Sample Q did not contain trimethylol propane, 1,6 hexanediol and 1,4 cyclohexanedimethanol. It contained neopentyl glycol only. Other samples contained either trimethylol propane, 1,6 hexanediol or 1,4 cyclohexanedimethanol. Therefore, the peaks in the  $^{13}\text{C}$  NMR spectra of the other samples in the range of 62-66 ppm could be assigned to the terminal methylene carbons of trimethylol propane, 1,6 hexanediol and 1,4 cyclohexanedimethanol moieties. The said assignments as shown in Table 3.25 could also be made based on the results published by Wang et al<sup>31</sup>, Tsai et al<sup>36</sup>, Lozano et al<sup>60</sup>, Mishra et al<sup>132</sup> and Zagar et al<sup>135</sup>. Tsai et al<sup>36</sup> characterised a copolyester derived from succinic acid, ethylene glycol and 1,3 propanediol by  $^{13}\text{C}$  NMR and assigned the peaks between 60-65 ppm to the terminal methylene carbons of 1,3 propanediol and ethylene glycol units as shown in Scheme 3.2 (p.2342).



**Scheme 3.2 Terminal methylene carbons in the moieties of 1,3 propanediol and ethylene glycol<sup>36</sup>**

In the  $^{13}\text{C}$  NMR spectrum of a copolyester containing butylene terephthalate, Wang et al<sup>31</sup> allocated the peaks between 64-66 ppm to the terminal methylene carbons in the moiety of 1,4 butanediol (p.2224). Lozano et al<sup>60</sup> analysed a poly(ester amide) that contained 1,4 butanediol by  $^{13}\text{C}$  NMR and assigned the peaks between 65-67 ppm to the terminal methylene carbons in the 1,4 butanediol residue (p.599). The methylene carbons concerned are shown in Scheme 3.3.



**Scheme 3.3 Methylene carbons neighboring oxygen in the moiety of 1,4 butanediol<sup>60</sup>**

Mishra et al<sup>132</sup> analysed a polyester that contained trimethylol propane by  $^{13}\text{C}$  NMR and assigned the signals between 65-70 ppm to the terminal methylene carbons in the moiety of trimethylol propane (p.50). Zagar et al<sup>135</sup> characterised a commercial polyester by  $^{13}\text{C}$

NMR and assigned the peak at 60.2 ppm to the carbon of the unreacted  $-\text{CH}_2\text{OH}$  groups (p.170).

The  $^{13}\text{C}$  NMR spectrum of sample O in the range of 62-66 ppm showed two peaks. The first peak at 63.94 ppm could be due to the terminal methylene carbon neighboring the free hydroxyl group in the moiety of trimethylol propane. This carbon is marked 2a in Table 3.25. The second peak at 65.13 ppm could be due to the terminal methylene carbon neighboring the ester group in the trimethylol propane moiety (carbon 2b in Table 3.25).

The  $^{13}\text{C}$  NMR spectra of samples P, R and S in the range of 62-66 ppm showed two peaks. The first peaks between 64.16-64.24 ppm could be due to the terminal methylene carbon neighboring the free hydroxyl group in the moiety of 1,6 hexanediol. This carbon is marked 3a in Table 3.25. The second peaks between 65.18-65.24 ppm could be due to the terminal methylene carbon neighboring the oxygen of the ester group in the moiety of 1,6 hexanediol. This carbon is marked 3b in Table 3.25. The intensity of the peaks of samples P, R and S in the range of 62-66 ppm could be related to the molar content of 1,6 hexanediol. An equal molar content of 1,6 hexanediol had been used for samples P and S. The intensity of the peaks of samples P and S in the range of 62-66 ppm was similar to a great extent. The molar content of 1,6 hexanediol in sample R was lower than samples P and S. It could be seen, from  $^{13}\text{C}$  NMR the spectrum of sample R in the same range (Figure 3.11), that the intensity of the peaks had been reduced.

The  $^{13}\text{C}$  NMR spectrum of sample T in the range of 62-66 ppm showed two peaks. The first peak at 64.28 ppm could be due to the terminal methylene carbon neighboring the free hydroxyl group in the moiety of 1,6 hexanediol. The second peak at 65.27 ppm could be due to the terminal methylene carbon neighboring the ester group in the moiety of 1,6 hexanediol. In the spectrum of sample T in the range of 62-66 ppm, it could be seen that the intensity of the peaks was higher in comparison to the corresponding peaks of samples P and S. The same content of 1,6 hexanediol had been used for samples P, S and T. However, sample T contained 1,4 cyclohexanedimethanol. 1,4 cyclohexanedimethanol was not included in samples P and S. Therefore, the higher intensity of the peaks of sample T in the range of 62-66 ppm could be due to the terminal methylene carbons in the moiety of 1,4 cyclohexanedimethanol. These carbons are marked 3c and 3d in Table 3.25.

Similar to the  $^{13}\text{C}$  NMR spectra in the ranges of 24-29 ppm and 33-37 ppm, alterations made to the molecular structure of the saturated polyester resins synthesised could be observed in the  $^{13}\text{C}$  NMR spectra in the range of 62-66 ppm.

The  $^{13}\text{C}$  NMR spectra for samples O, P and Q, in the range of 67-71 ppm, are shown in Figure 3.12.

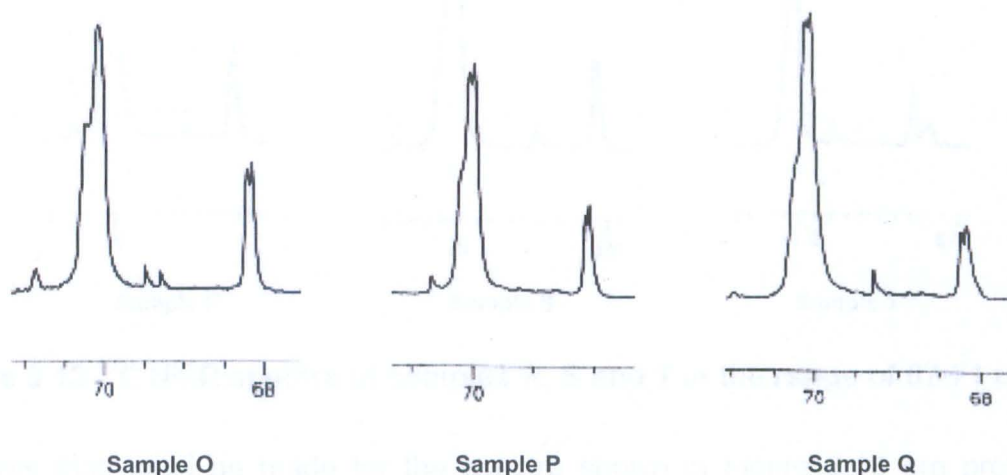


**Figure 3.12**  $^{13}\text{C}$  NMR spectra of samples O, P and Q in the range of 67-71 ppm

Assignments that could be made for the spectra shown in Figure 3.12 are provided in Table 3.26.

**Table 3.26** Assignments for the  $^{13}\text{C}$  NMR spectra of samples O, P and Q in the range of 67-71 ppm <sup>106,133,134</sup>

<b>Sample</b>	<b><math>\delta</math> (PPM)</b>	<b>Assignment</b>	<b><math>\delta</math> (PPM)</b>	<b>Assignment</b>
<b>O</b>	68.15-68.21	<b>2a</b>	70.09	<b>2b</b>
<b>P</b>	68.09-68.15	<b>2a</b>	69.98-70.06	<b>2b</b>
<b>Q</b>	68.17-68.23	<b>2a</b>	70.05-70.11	<b>2b</b>



The  $^{13}\text{C}$  NMR spectra of samples R, S and T, in the range of 67-72 ppm, are shown in Figure 3.13.

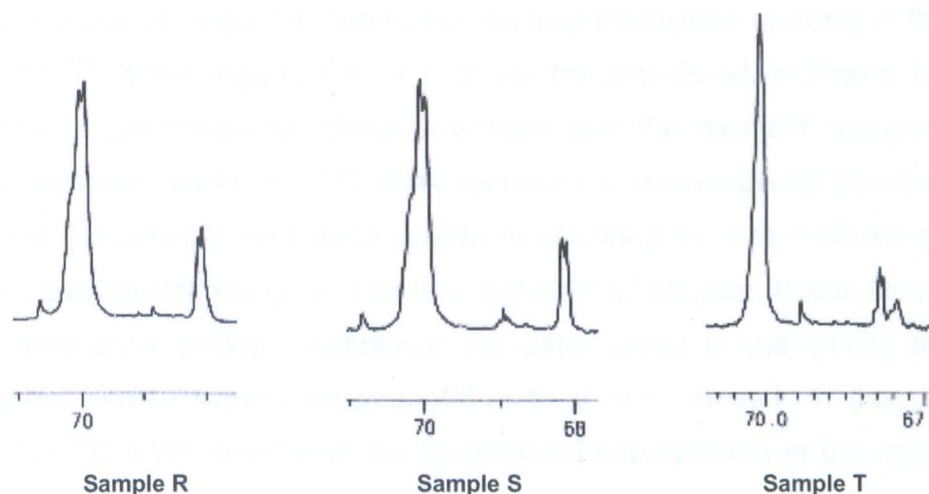


Figure 3.13  $^{13}\text{C}$  NMR spectra of samples R, S and T in the range of 67-71 ppm

Assignments that could be made for the spectra shown in Figure 3.13 are provided in Table 3.27.

Table 3.27 Assignments for the  $^{13}\text{C}$  NMR spectra of samples R, S and T in the range of 67-71 ppm<sup>106,133,134</sup>

		2a			2b
Sample	$\delta$ (PPM)	Assignment	$\delta$ (PPM)	Assignment	
R	68.14-68.2	2a	70.02-70.08	2b	
S	68.14-68.17	2a	70.00-70.07	2b	
T	67.93-68.21	2a	70.09	2b	

In general, peaks that occur in the  $^{13}\text{C}$  NMR spectra in the range of 67-71 ppm would pertain to  $\text{SP}^3$  carbons bound to oxygen.<sup>133,134</sup>

It could be seen, from the  $^{13}\text{C}$  NMR spectra shown in Figures 3.12 and 3.13, that the synthesised copolyesters had resulted in similar signals in the range of 67-71 ppm. Previous  $^{13}\text{C}$  NMR studies on polyesters containing neopentyl glycol had shown that signals in this frequency range are due to the terminal methylene carbons in the moiety of neopentyl glycol.<sup>106</sup> In this regard, Figure 1.22 can be considered. In Figure 1.22, the  $^{13}\text{C}$  NMR spectrum of polyneopentyl glycol succinate and the relevant assignments were shown. In the assignments for the  $^{13}\text{C}$  NMR spectrum of polyneopentyl glycol succinate, it was shown that the terminal methylene carbon neighboring the free hydroxyl group in the moiety of neopentyl glycol had given rise to a signal at 67.35 ppm. It was also shown that the terminal methylene carbon neighboring the ester group in the moiety of neopentyl glycol had given rise to signals between 68.88-69.6 ppm. Based on this, signals that appeared in the  $^{13}\text{C}$  NMR spectra of the synthesised copolyesters in the range of 67-71 ppm could be assigned to the terminal methylene carbons in the moiety of neopentyl glycol.

The  $^{13}\text{C}$  NMR spectra of the copolyester samples in the range of 67-71 ppm showed two peaks. The first peaks were between 67.93-68.23 ppm. These peaks could be due to the terminal methylene carbon neighboring the free hydroxyl group in the moiety of neopentyl glycol. This carbon is marked 2a in Tables 3.26 and 3.27. The second peaks were between 69.98-70.11 ppm. These peaks could be due to the terminal methylene carbons adjacent to the ester group in the moiety of neopentyl glycol. These carbons are marked 2b in Tables 3.26 and 3.27.

In the  $^{13}\text{C}$  NMR spectrum of sample T in the range of 67-71 ppm, it could be seen that the intensity of the first peak between 67.93-68.21 ppm had been reduced. In comparison to the other samples, the molar content of neopentyl glycol in sample T was lower. The free hydroxyl content of sample T was also lower than the other samples. Therefore, the reduced intensity of the first peak in the range of 67-71 ppm in the  $^{13}\text{C}$  NMR spectrum of sample T could be due to the lower hydroxyl content as well as availability of less neopentyl glycol moiety. For comparison between the composition and the hydroxyl content of the synthesised copolyesters, Table 3.21 can be used.

The  $^{13}\text{C}$  NMR spectra of the synthesised copolyester samples, in the range of 77-78 ppm, are shown in Figure 3.14.

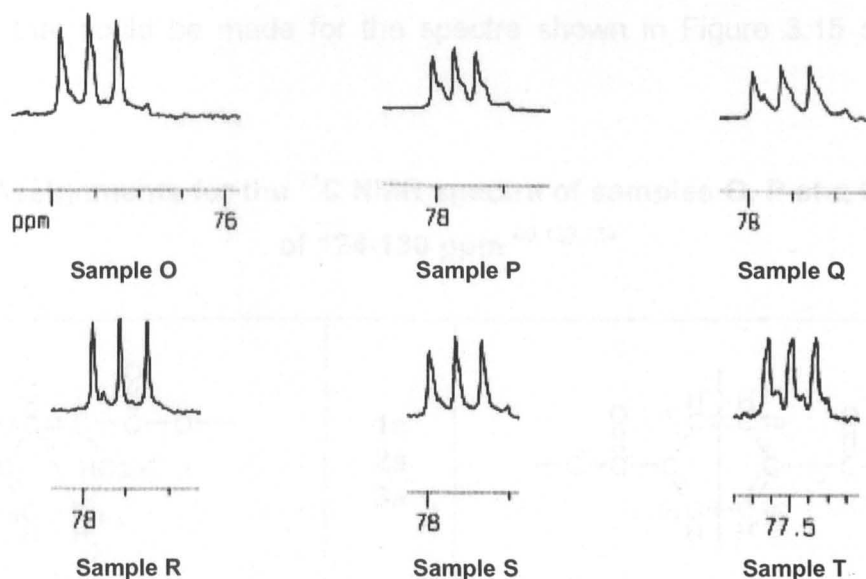
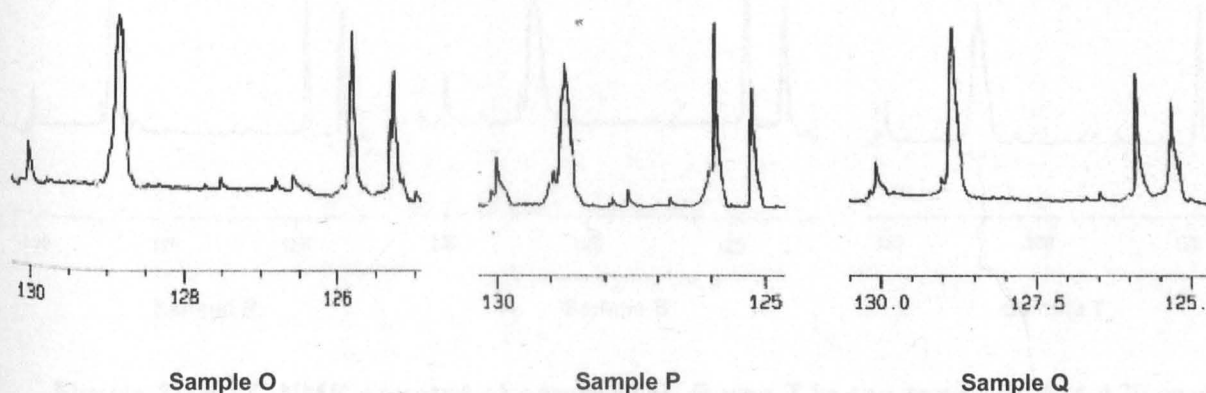


**Figure 3.14**  $^{13}\text{C}$  NMR spectra in the range of 77-78 ppm

Peaks that appeared in the  $^{13}\text{C}$  NMR spectra in the range of 77-78 ppm pertained to deuterated chloroform ( $\text{CDCl}_3$ ).<sup>136</sup> As mentioned in Section 2.4, deuterated chloroform was used as solvent for the copolyester samples.

No peaks appeared in the  $^{13}\text{C}$  NMR spectra of the polyester samples in the range of 79-124 ppm.

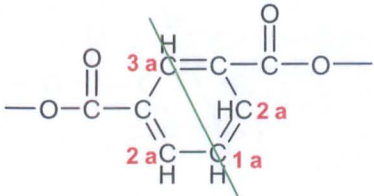
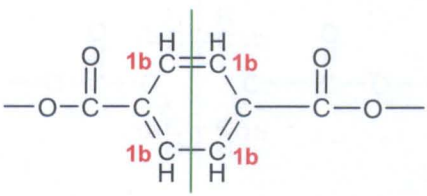
The  $^{13}\text{C}$  NMR spectra of samples O, P and Q, in the range of 124-130 ppm, are shown in Figure 3.15.



**Figure 3.15**  $^{13}\text{C}$  NMR spectra of samples O, P and Q in the range of 124-130 ppm

Assignments that could be made for the spectra shown in Figure 3.15 are provided in Table 3.28.

**Table 3.28 Assignments for the  $^{13}\text{C}$  NMR spectra of samples O, P and Q in the range of 124-130 ppm** <sup>60,133,134</sup>

								
Sample	$\delta$ (PPM)	Assignment	$\delta$ (PPM)	Assignment	$\delta$ (PPM)	Assignment	$\delta$ (PPM)	Assignment
O	125.1-125.29	1a	125.8-126.07	2a	128.79-128.83	1b	130.02	3a
P	125.27-125.52	1a	126.03-126.24	2a	128.73-128.77	1b	130	3a
Q	125.29-125.33	1a	125.85-125.89	2a	128.80-128.83	1b	130.06	3a

The  $^{13}\text{C}$  NMR spectra of samples R, S and T, in the range of 124-130 ppm, are shown in Figure 3.16.

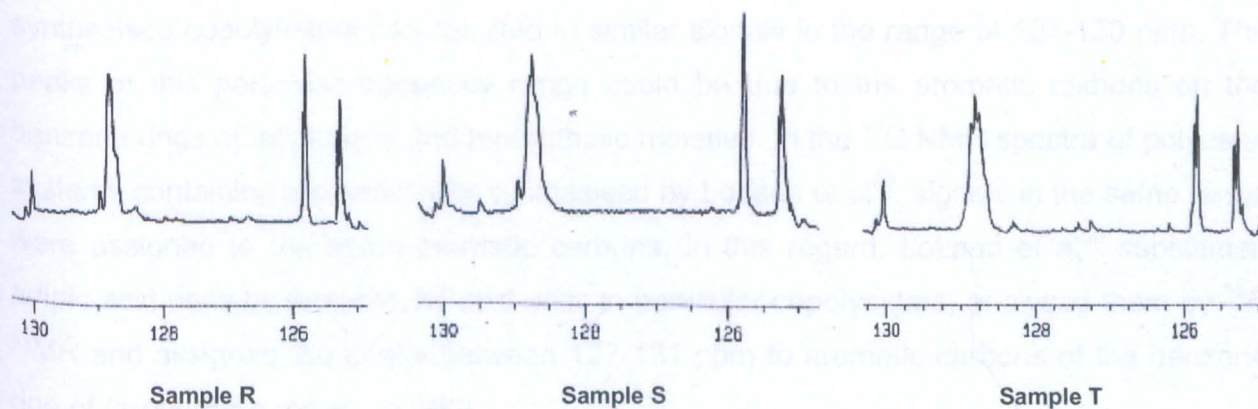


**Figure 3.16  $^{13}\text{C}$  NMR spectra of samples R, S and T in the range of 124-130 ppm**



ring of isophthalic moiety were of unique chemical environments. In other words, these carbons are bound to dissimilar atoms. This could have resulted in the rise of three exclusive peaks in the  $^{13}\text{C}$  NMR spectra. In Tables 3.28 and 3.29, the aromatic carbons on the benzene ring of isophthalic moiety with unique chemical environments are marked 1a, 2a and 3a. It can be seen, from Table 3.29, that the chemical environments of the carbons on the benzene ring of terephthalic residue were similar. This could have resulted in the rise of one exclusive signal in the  $^{13}\text{C}$  NMR spectra.

The first and second peaks between 125.10-125.89 ppm could be due to carbons 1a and 2a on the benzene ring of isophthalic moiety as shown in Tables 3.28 and 3.29. The third signal between 128.73-128.83 ppm could be due to the aromatic carbons on the benzene ring of terephthalic moiety. These carbons are labeled 1b in Tables 3.28 and 3.29. The fourth peak between 130.01-130.06 ppm could be assigned to carbon 3a on the benzene ring of isophthalic moiety as shown in Tables 3.28 and 3.29. The assignments mentioned were made based on the number of hydrogens neighboring the carbons concerned. In other words, the carbons concerned could have given rise to signals in a stronger frequency range if both of their adjacent carbons were bound to hydrogen.

The  $^{13}\text{C}$  NMR spectra of samples O and Q, in the range of 130-132 ppm, are shown in Figure 3.17.

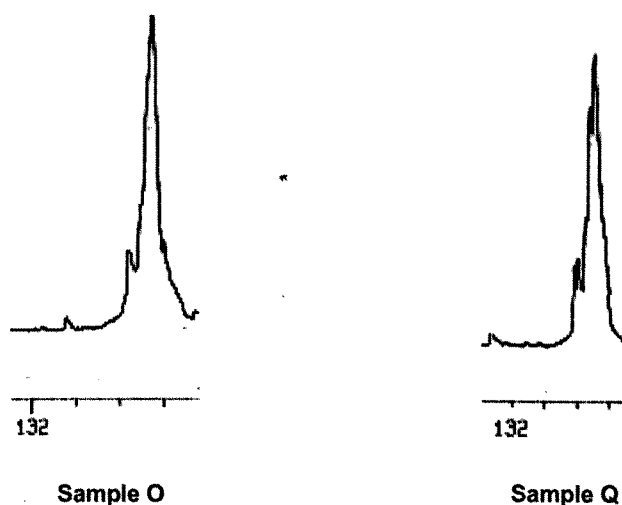
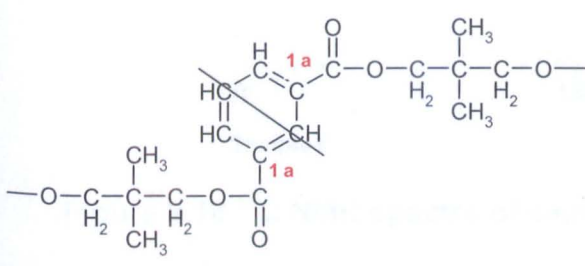
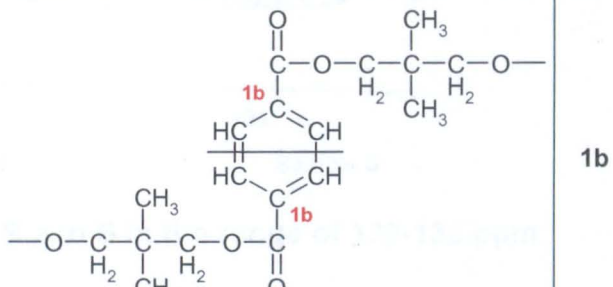
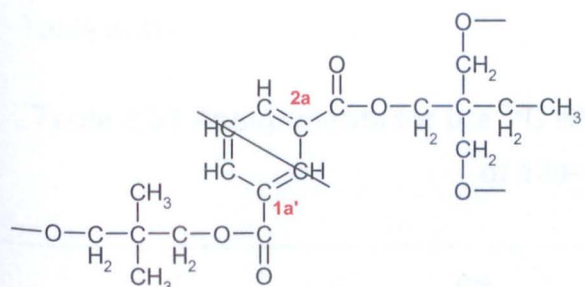
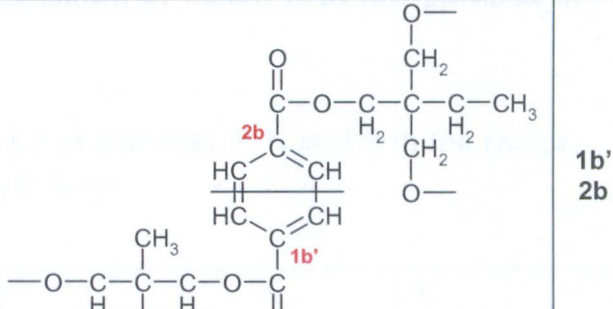
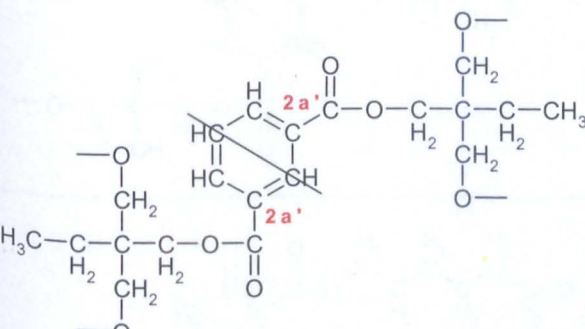
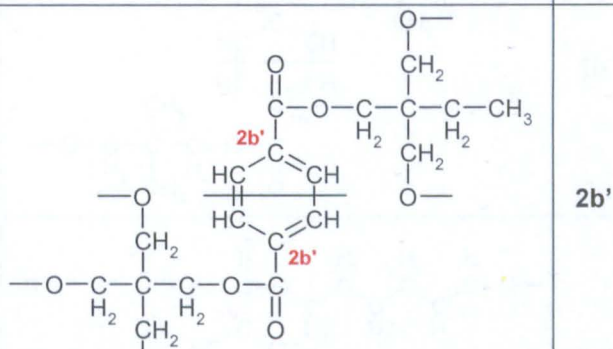


Figure 3.17  $^{13}\text{C}$  NMR spectra of samples O and Q in the range of 130-132 ppm

Assignments that could be made for the spectra shown in Figure 3.17 are provided in Table 3.30.

**Table 3.30 Assignments for the  $^{13}\text{C}$  NMR spectra of samples O and Q in the range of 130-132 ppm** <sup>60,132-134</sup>

	<b>1a</b>		<b>1b</b>
	<b>1a'</b> <b>2a</b>		<b>1b'</b> <b>2b</b>
	<b>2a'</b>		<b>2b'</b>
<b>Sample</b>	<b><math>\delta</math> (PPM)</b>	<b>Assignment</b>	
<b>O</b>	130.48-130.89	<b>1a, 1b, 1a'-2a, 1b'-2b, 2a', 2b'</b>	
<b>Q</b>	130.65-131.14	<b>1a-1b</b>	

The  $^{13}\text{C}$  NMR spectra of samples P, R and S, in the range of 130-132 ppm, are shown in Figure 3.18.

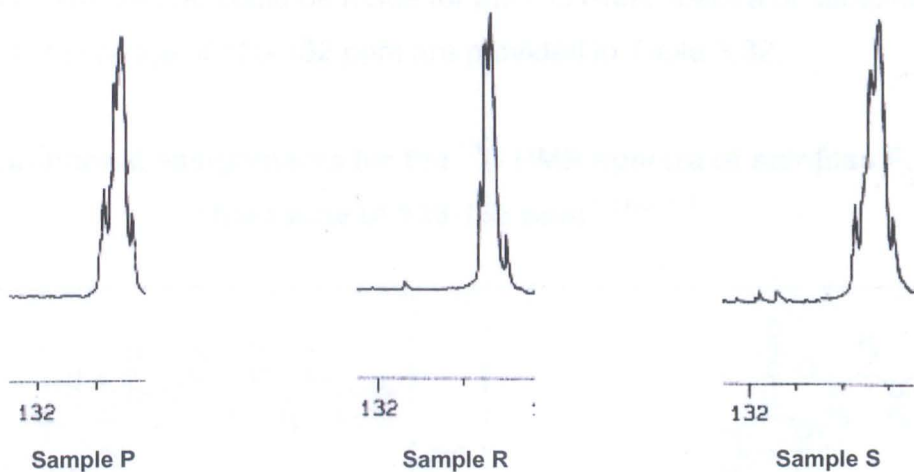


Figure 3.18  $^{13}\text{C}$  NMR spectra of samples P, R and S in the range of 130-132 ppm

Assignments that could be made for the spectra shown in Figure 3.18 are provided in Table 3.31.

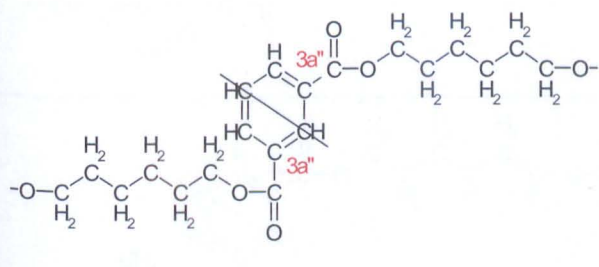
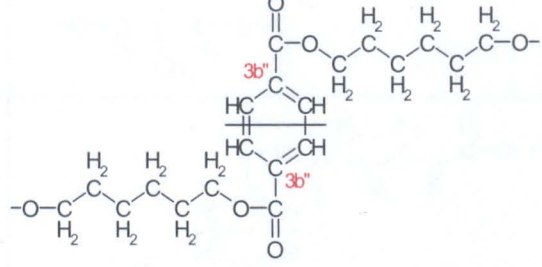
Table 3.31 Assignments for the  $^{13}\text{C}$  NMR spectra of samples P, R and S in the range of 130-132 ppm<sup>60,132-134</sup>

	1a		1b
	1a'' 3a		1b'' 3b
<b>Sample</b>	<b><math>\delta</math> (PPM)</b>	<b>Assignment</b>	
P	130.56-130.95	1a, 1b, 1a''-3a, 1b''-3b	
R	130.47-130.98	1a, 1b, 1a''-3a, 1b''-3b	
S	130.01-130.92	1a, 1b, 1a''-3a, 1b''-3b	



Additional assignments that could be made for the  $^{13}\text{C}$  NMR spectra of samples P, R and S (Figure 3.18) in the range of 130-132 ppm are provided in Table 3.32.

**Table 3.32 Additional assignments for the  $^{13}\text{C}$  NMR spectra of samples P, R and S in the range of 130-132 ppm**<sup>60,132-134</sup>

	<b>3a''</b>		<b>3b''</b>
Sample	$\delta$ (PPM)		Assignment
P	130.56-130.95		3a'', 3b''
R	130.47-130.98		3a'', 3b''
S	130.01-130.92		3a'', 3b''

The  $^{13}\text{C}$  NMR spectrum of sample T, in the range of 130-132 ppm, is shown in Figure 3.19.



**Figure 3.19  $^{13}\text{C}$  NMR spectrum of sample T in the range of 130-132 ppm**

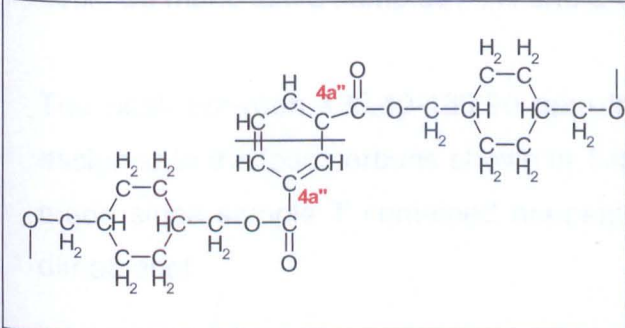
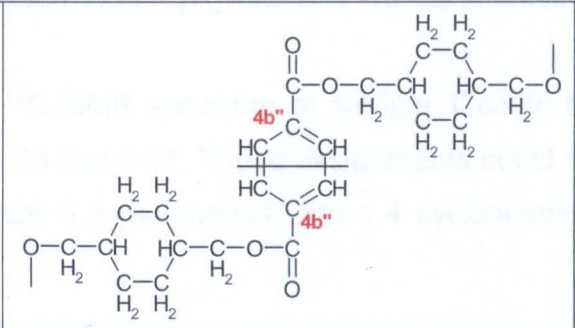
Assignments that could be made for the spectrum shown in Figure 3.19 are provided in Table 3.33.

**Table 3.33 Assignments for the  $^{13}\text{C}$  NMR spectrum of sample T in the range of 130-132 ppm** <sup>60,132-134</sup>

	1a		1b
	1a'' 3a		1b'' 3b
	3a''		3b''
	1a''' 4a		1b''' 4b
	3a' 4a'		3b' 4b'
Sample	$\delta$ (PPM)	Assignment	
T	130.40-130.90	1a, 1b, 1a''-3a, 1b''-3b, 3a'', 3b'', 1a'''-4a, 1b'''-4b, 3a'-4a', 3b'-4b'	

Additional assignments that could be made for the  $^{13}\text{C}$  NMR spectrum of sample T (Figure 3.19) in the range of 130-132 ppm are provided in Table 3.34.

**Table 3.34 Additional assignments for the  $^{13}\text{C}$  NMR spectrum of sample T in the range of 130-132 ppm**<sup>60,132-134</sup>

	<b>4a''</b>		<b>4b''</b>
<b>Sample</b>	<b><math>\delta</math> (PPM)</b>		<b>Assignment</b>
<b>T</b>	130.40-130.90		<b>4a''-4b''</b>

It could be seen, from the  $^{13}\text{C}$  NMR spectra shown Figures 3.17, 3.18 and 3.19, that the synthesised copolyesters had resulted in similar signals in the range of 130-132 ppm. The signals of this particular frequency range could be due to the ipso carbons of the benzene rings of isophthalic and terephthalic moieties. In the benzene ring, the carbon which is not bound to hydrogen is referred to as the ipso carbon.<sup>137</sup> Due to the long relaxation time of the ipso carbon, its signal in the  $^{13}\text{C}$  NMR spectra appears in a weaker frequency range in comparison to the rest of the carbons on the benzene ring.<sup>138</sup> As shown in Figures 3.17, 3.18 and 3.19, there was one peak in the  $^{13}\text{C}$  NMR spectra for each of the samples in the range of 130-132 ppm.

The peak between 130.65-131.14 ppm in the  $^{13}\text{C}$  NMR spectrum of sample Q could be assigned to the ipso carbons that are marked 1a and 1b in Table 3.30. This assignment could be made since sample Q contained neopentyl glycol only. The rest of the samples contained neopentyl glycol as well. Thus, the same assignment could be made for their corresponding signal in the  $^{13}\text{C}$  NMR spectra.

The peak between 130.48-130.89 ppm in the  $^{13}\text{C}$  NMR spectrum of sample O could be

assigned to the ipso carbons shown in Table 3.30. These assignments could be made since sample O contained neopentyl glycol and trimethylol propane.

The peaks between 130.01-130.95 ppm in the  $^{13}\text{C}$  NMR spectra of samples P, R and S could be assigned to the ipso carbons shown in Tables 3.31 and 3.32. These assignments could be made since samples P, R and S contained neopentyl glycol and 1,6 hexanediol.

The peak between 130.40-130.90 ppm in the  $^{13}\text{C}$  NMR spectrum of sample T could be assigned to the ipso carbons shown in Tables 3.33 and 3.34. These assignments could be made since sample T contained neopentyl glycol, 1,6 hexanediol, and 1,4 cyclohexane-dimethanol.

The  $^{13}\text{C}$  NMR spectra of the synthesised copolyesters, in the range of 164-167 ppm, are shown in Figure 3.20.

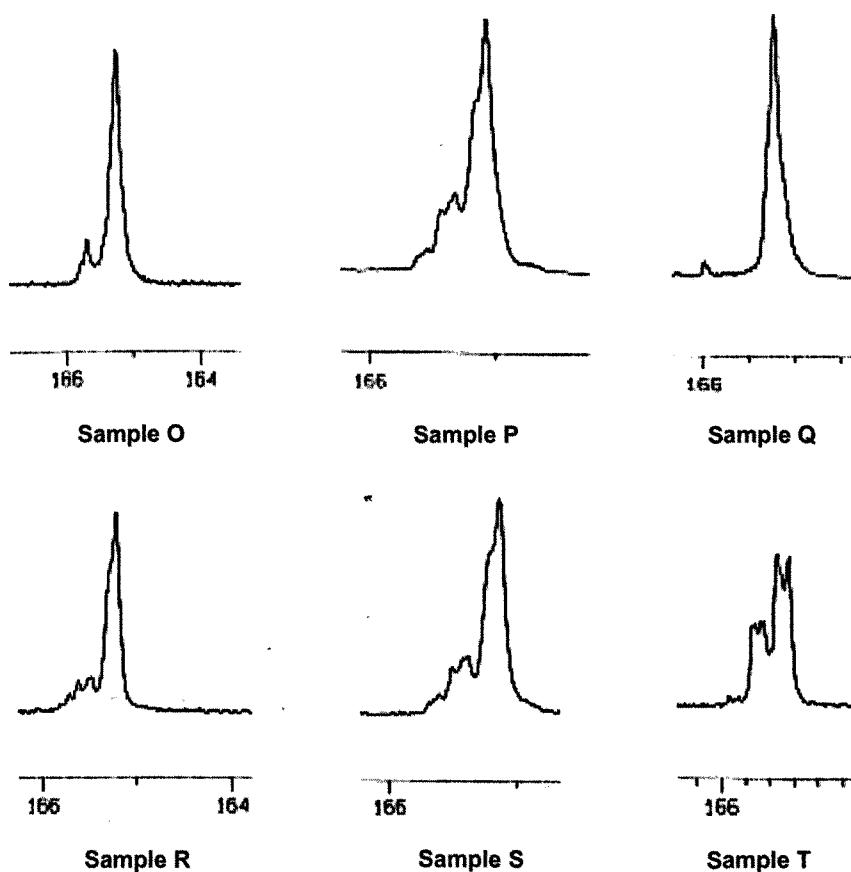
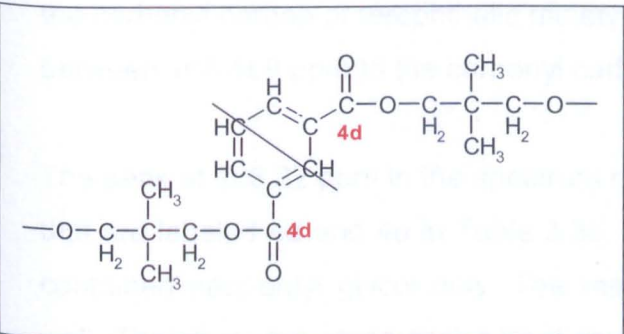
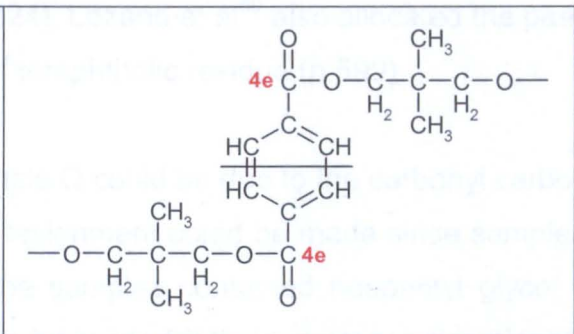
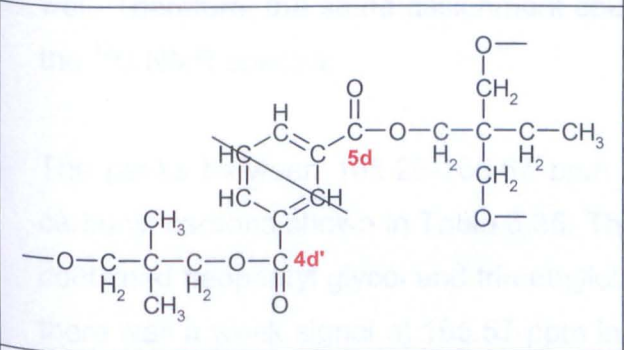
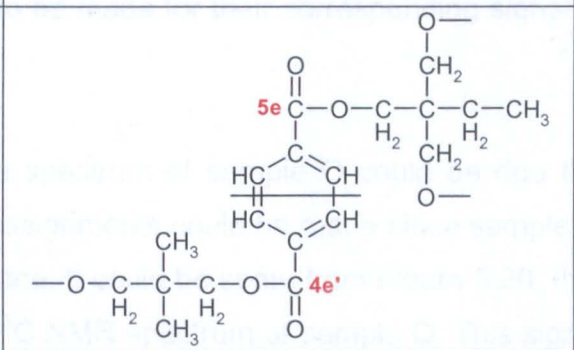
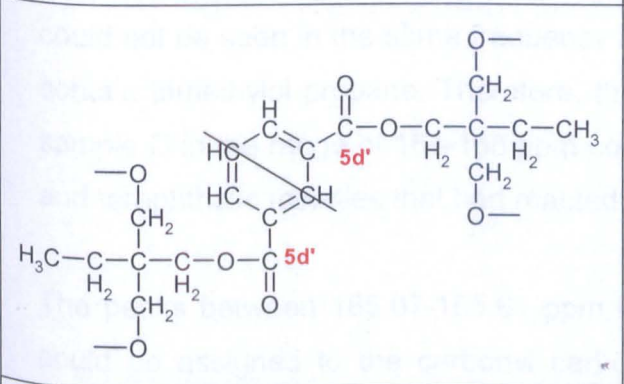
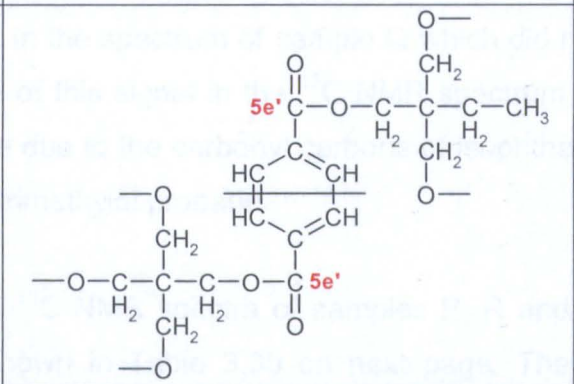


Figure 3.20  $^{13}\text{C}$  NMR spectra in the range of 164-168 ppm

Assignments that could be made for the  $^{13}\text{C}$  NMR spectra of samples O and Q in the range of 164-168 ppm are provided in Table 3.35.

**Table 3.35 Assignments for the  $^{13}\text{C}$  NMR spectra of samples O and Q in the range of 164-168 ppm**<sup>29,31,60,132,138,139</sup>

	<b>4d</b>		<b>4e</b>
	<b>4d'</b> <b>5d</b>		<b>4e'</b> <b>5e</b>
	<b>5d'</b>		<b>5e'</b>
<b>Sample</b>	<b><math>\delta</math> (PPM)</b>	<b>Assignment</b>	
<b>O</b>	165.26-165.67	<b>4d, 4e, 4d'-5d, 4e'-5e, 5d', 5e'</b>	
<b>Q</b>	165.07-165.43	<b>4d-4e</b>	

The  $^{13}\text{C}$  NMR spectra in the range of 164-168 ppm would pertain to  $\text{SP}^2$  carbons neighboring oxygen.<sup>133,134</sup> The signals of this frequency range could be due to the carbonyl carbon of isophthalic and terephthalic moieties.<sup>138,139</sup> In the  $^{13}\text{C}$  NMR spectra of copolyesters containing aromatic residues synthesised by Boyes et al<sup>29</sup>, Wang et al<sup>31</sup> and

Lozano et al<sup>60</sup>, signals in the same range were assigned to the same carbonyl carbons. Boyes et al<sup>29</sup> esterified a hydroxyl functional polyester with *p*-hydroxybenzoic acid, characterised the product by <sup>13</sup>C NMR and assigned the peak at 165.9 ppm to the carbonyl carbon of reacted *p*-hydroxybenzoic acid (p.139). Wang et al<sup>31</sup> analysed a copolyester containing terephthalic acid by <sup>13</sup>C NMR and assigned the peak between 165-167 ppm to the carbonyl carbon of terephthalic moiety (p.2224). Lozano et al<sup>60</sup> also allocated the peaks between 168-169 ppm to the carbonyl carbon of terephthalic residue (p.599).

The peak at 165.22 ppm in the spectrum of sample Q could be due to the carbonyl carbons that are labeled 4d and 4e in Table 3.35. This assignment could be made since sample Q contained neopentyl glycol only. The rest of the samples contained neopentyl glycol as well. Therefore, the same assignment could also be made for their corresponding signal in the <sup>13</sup>C NMR spectra.

The peaks between 165.26-165.67 ppm in the spectrum of sample O could be due the carbonyl carbons shown in Table 3.35. These assignments could be made since sample O contained neopentyl glycol and trimethylol propane. It could be seen, from Figure 3.20, that there was a weak signal at 165.57 ppm in the <sup>13</sup>C NMR spectrum of sample O. This signal could not be seen in the same frequency range in the spectrum of sample Q which did not contain trimethylol propane. Therefore, the rise of this signal in the <sup>13</sup>C NMR spectrum of sample O in the range of 164-168 ppm could be due to the carbonyl carbons of isophthalic and terephthalic moieties that had reacted with trimethylol propane.

The peaks between 165.07-165.61 ppm in the <sup>13</sup>C NMR spectra of samples P, R and S could be assigned to the carbonyl carbons shown in Table 3.36 on next page. These assignments could be made since samples P, R and S contained neopentyl glycol and 1,6 hexanediol. It could be seen, from the <sup>13</sup>C NMR spectra shown Figure 3.20, that samples P, R and S had resulted in similar signals in the range of 164-168 ppm. Weak signals could be seen between 165.32-165.61 ppm in the <sup>13</sup>C NMR spectra of samples P, R and S. No signal appeared in the same frequency range in the <sup>13</sup>C NMR spectrum of sample Q which did not contain 1,6 hexanediol. Therefore, the rise of these weak signals in the <sup>13</sup>C NMR spectra of samples P, R and S could be due to the carbonyl carbons of isophthalic and terephthalic moieties that had reacted with 1,6 hexanediol. In addition, it could be seen that the intensity of the peak between 165.46-165.61 ppm in the <sup>13</sup>C NMR spectrum of sample

R was lower than the corresponding peaks in the spectra of samples P and S. The molar content of 1,6 hexanediol in sample R was lower than samples P and S. Therefore, the reduced intensity of the peak between 165.46-165.61 ppm in the  $^{13}\text{C}$  NMR spectrum of sample R could be due to availability of less 1,6 hexanediol moiety in its molecular structure.

Assignments for the  $^{13}\text{C}$  NMR spectra of samples P, R and S in the range of 164-168 ppm (Figure 3.20) are provided in Table 3.36.

**Table 3.36 Assignments for the  $^{13}\text{C}$  NMR spectra of samples P, R and S in the range of 164-168 ppm**<sup>29,31,60,132,138,139</sup>

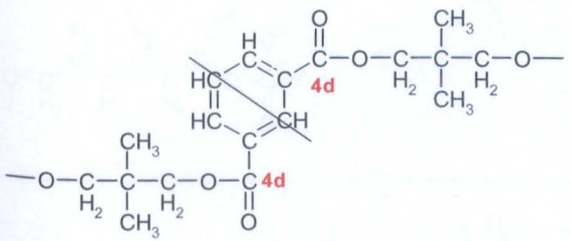
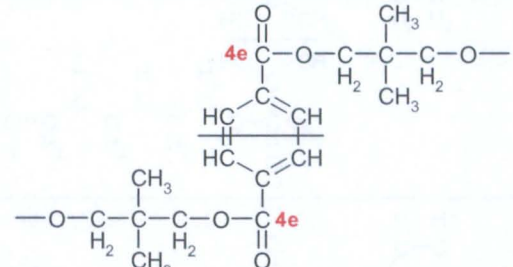
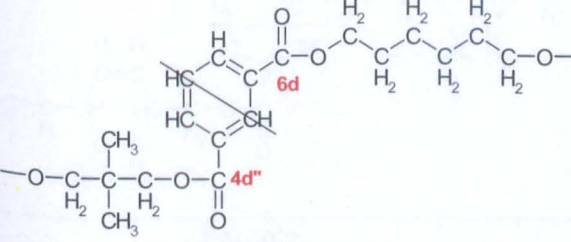
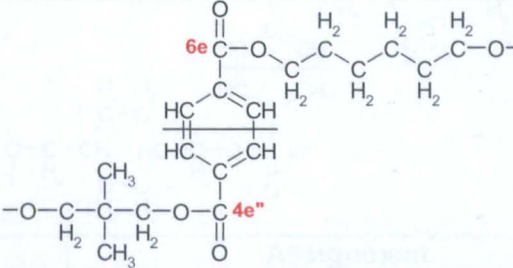
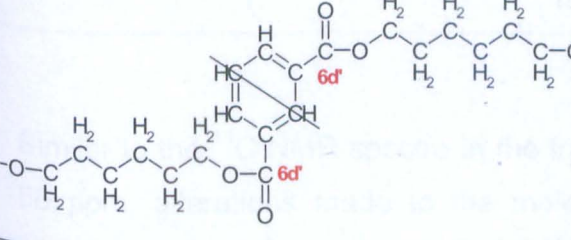
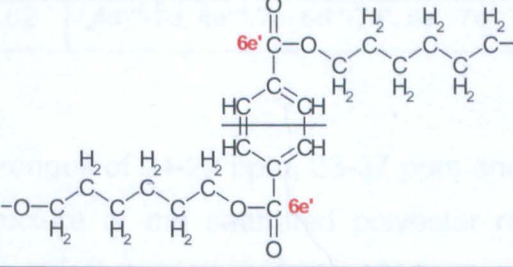
	4d		4e
	4d'' 6d		4e'' 6e
	6d'		6e'
Sample	$\delta$ (PPM)	Assignment	
P	165.07-165.43	4d, 4e, 4d''-6d, 4e''-6e, 6d', 6e'	
R	165.21-165.61	4d, 4e, 4d''-6d, 4e''-6e, 6d', 6e'	
S	165.12-165.5	4d, 4e, 4d''-6d, 4e''-6e, 6d', 6e'	

The signals between 165.28-165.62 ppm in the  $^{13}\text{C}$  NMR spectrum of sample T could be due to the carbonyl carbons shown in Tables 3.37 and 3.38 as follows. These assignments

could be made since sample T contained neopentyl glycol, 1,6 hexanediol and 1,4 cyclohexanedimethanol. It could be seen, from Figure 3.20, that there were additional signals at 165.39 ppm, 165.54 ppm and 165.62 ppm in the  $^{13}\text{C}$  NMR spectrum of sample T. These signals could not be seen in the corresponding frequency range in the  $^{13}\text{C}$  NMR spectrum of sample Q which contained neopentyl glycol only. Therefore, the rise of these signals in the  $^{13}\text{C}$  NMR spectrum of sample T in the range concerned could be due to the carbonyl carbons of isophthalic and terephthalic moieties that had reacted with 1,6 hexanediol and 1,4 cyclohexanedimethanol.

Assignments for the  $^{13}\text{C}$  NMR spectrum of sample T in the range of 164-168 ppm (Figure 3.20) are provided in Table 3.37.

**Table 3.37 Assignments for the  $^{13}\text{C}$  NMR spectrum of sample T in the range of 164-168 ppm** <sup>29,31,60,132,138,139</sup>

	4d		4e
	4d'' 6d		4e'' 6e
	6d'		6e'
Sample	$\delta$ (PPM)	Assignment	
T	165.28-165.62	4d, 4e, 4d''-6d, 4e''-6e, 6d', 6e'	



Additional assignments that could be made for the  $^{13}\text{C}$  NMR spectrum of sample T in the range of 164-168 ppm are provided in Table 3.38.

**Table 3.38 Additional assignments for the  $^{13}\text{C}$  NMR spectrum of sample T in the range of 164-168 ppm**<sup>29,31,60,132,138,139</sup>

	<p><b>4d'''</b> <b>7d</b></p>		<p><b>4e'''</b> <b>7e</b></p>
	<p><b>6d''</b> <b>7d'</b></p>		<p><b>6e''</b> <b>7e'</b></p>
	<p><b>7d''</b></p>		<p><b>7e''</b></p>
<p><b>Sample</b></p>	<p><b><math>\delta</math> (PPM)</b></p>	<p><b>Assignment</b></p>	
<p><b>T</b></p>	<p>165.28-165.62</p>	<p><b>4d'''-7d, 4e'''-7e, 6d''-7d', 6e''-7e', 7d''-7e''</b></p>	

Similar to the  $^{13}\text{C}$  NMR spectra in the frequency ranges of 24-29 ppm, 33-37 ppm and 62-66 ppm, alterations made to the molecular structure of the saturated polyester resins synthesised could be observed in the  $^{13}\text{C}$  NMR spectra in the range of 164-168 ppm.

The  $^{13}\text{C}$  NMR spectra of the synthesised copolyesters, in the range of 171-175 ppm, are shown in Figure 3.21.

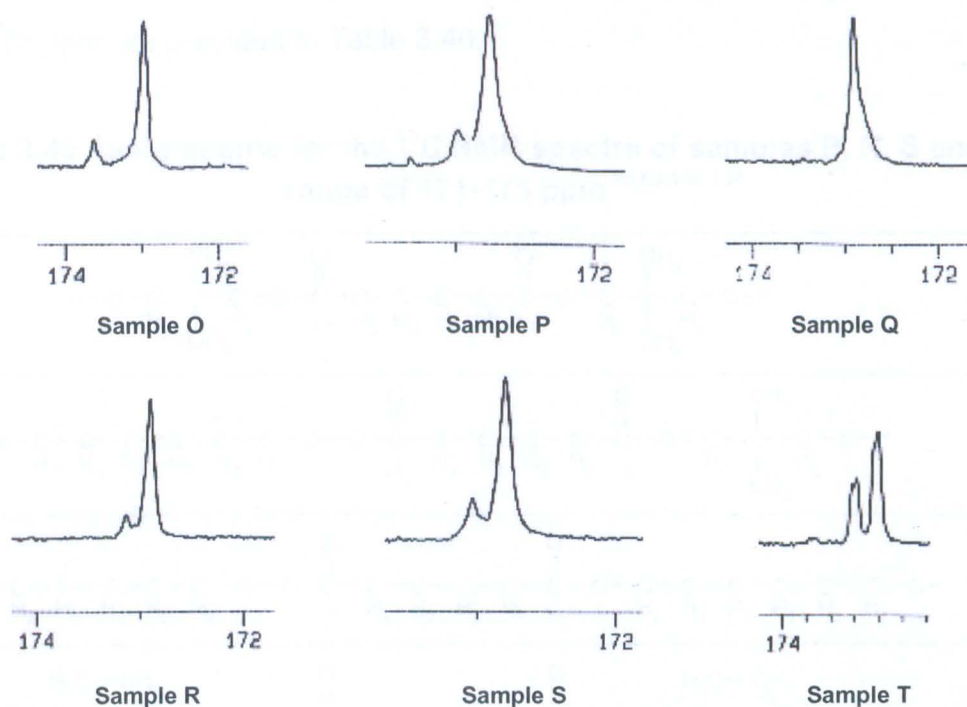


Figure 3.21  $^{13}\text{C}$  NMR spectra in the range of 171-175 ppm

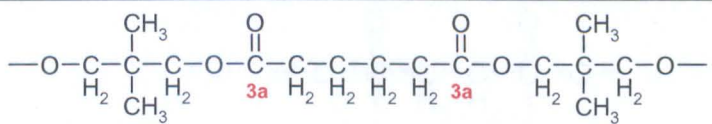
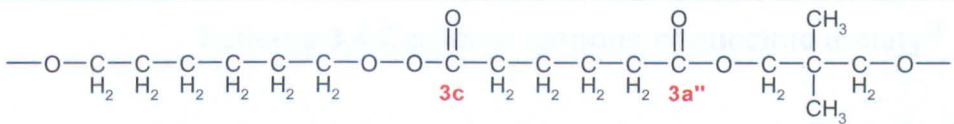
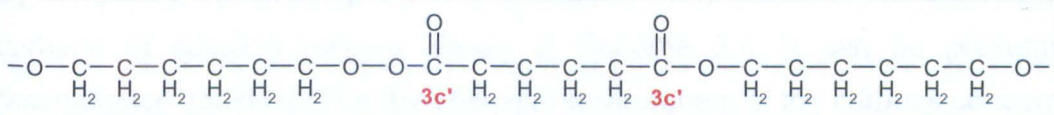
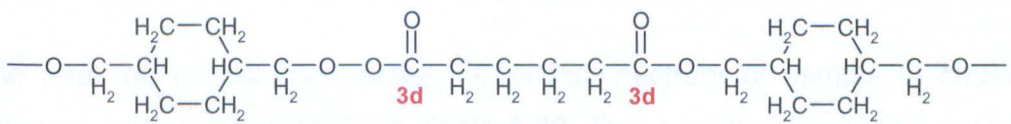
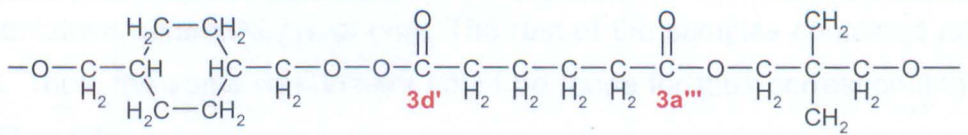
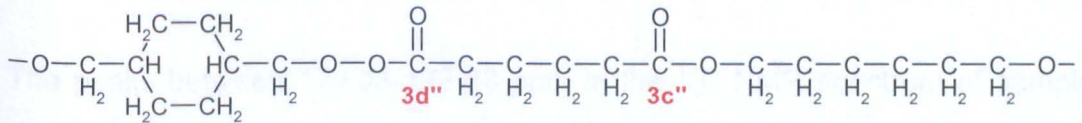
Assignments for the  $^{13}\text{C}$  NMR spectra of samples O and Q in the range of 171-175 ppm are provided in Table 3.39.

Table 3.39 Assignments for the  $^{13}\text{C}$  NMR spectra of samples O and Q in the range of 171-175 ppm<sup>36,60,133,134</sup>

$\text{---O---C} \begin{array}{c} \text{CH}_3 \\   \\ \text{H}_2 \end{array} \text{---C} \begin{array}{c} \text{CH}_3 \\   \\ \text{H}_2 \end{array} \text{---C---O---C} \begin{array}{c} \text{O} \\    \\ \text{3a} \end{array} \text{---C} \begin{array}{c} \text{H}_2 \\   \\ \text{H}_2 \end{array} \text{---C} \begin{array}{c} \text{H}_2 \\   \\ \text{H}_2 \end{array} \text{---C} \begin{array}{c} \text{H}_2 \\   \\ \text{H}_2 \end{array} \text{---C} \begin{array}{c} \text{O} \\    \\ \text{3a} \end{array} \text{---O---C} \begin{array}{c} \text{CH}_3 \\   \\ \text{H}_2 \end{array} \text{---C} \begin{array}{c} \text{CH}_3 \\   \\ \text{H}_2 \end{array} \text{---C---O---}$		3a
$\text{---O---CH}_2 \begin{array}{c} \text{H}_3\text{C---H}_2\text{C---C} \begin{array}{c}   \\ \text{---O---CH}_2 \end{array} \end{array} \text{---CH}_2\text{---O---C} \begin{array}{c} \text{O} \\    \\ \text{3b} \end{array} \text{---C} \begin{array}{c} \text{H}_2 \\   \\ \text{H}_2 \end{array} \text{---C} \begin{array}{c} \text{H}_2 \\   \\ \text{H}_2 \end{array} \text{---C} \begin{array}{c} \text{H}_2 \\   \\ \text{H}_2 \end{array} \text{---C} \begin{array}{c} \text{O} \\    \\ \text{3a}' \end{array} \text{---O---C} \begin{array}{c} \text{CH}_3 \\   \\ \text{H}_2 \end{array} \text{---C} \begin{array}{c} \text{CH}_3 \\   \\ \text{H}_2 \end{array} \text{---C---O---}$		3b-3a'
$\text{---O---CH}_2 \begin{array}{c} \text{H}_3\text{C---H}_2\text{C---C} \begin{array}{c}   \\ \text{---O---CH}_2 \end{array} \end{array} \text{---CH}_2\text{---O---C} \begin{array}{c} \text{O} \\    \\ \text{3b}' \end{array} \text{---C} \begin{array}{c} \text{H}_2 \\   \\ \text{H}_2 \end{array} \text{---C} \begin{array}{c} \text{H}_2 \\   \\ \text{H}_2 \end{array} \text{---C} \begin{array}{c} \text{H}_2 \\   \\ \text{H}_2 \end{array} \text{---C} \begin{array}{c} \text{O} \\    \\ \text{3b}' \end{array} \text{---O---C} \begin{array}{c} \text{H}_2\text{C---O---} \\   \\ \text{H}_2\text{C---O---} \end{array} \text{---C} \begin{array}{c} \text{H}_2\text{C---O---} \\   \\ \text{H}_2\text{C---O---} \end{array} \text{---CH}_2\text{---CH}_3$		3b'
Sample	$\delta$ (PPM)	Assignment
O	172.98-173.63	3a, 3a'-3b, 3b'
Q	172.9	3a

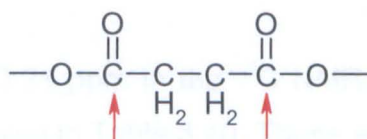
Assignments for the  $^{13}\text{C}$  NMR spectra of samples P, R, S and T (Figure 3.21) in the range of 171-175 ppm are provided in Table 3.40.

**Table 3.40 Assignments for the  $^{13}\text{C}$  NMR spectra of samples P, R, S and T in the range of 171-175 ppm**<sup>36,60,133,134</sup>

	<b>3a</b>	
	<b>3a''-3c</b>	
	<b>3c'</b>	
	<b>3d</b>	
	<b>3d'-3a'''</b>	
	<b>3c''-3d''</b>	
<b>Sample</b>	<b><math>\delta</math> (PPM)</b>	<b>Assignment</b>
<b>P</b>	172.74-172.89	<b>3a, 3a''-3c, 3c'</b>
<b>R</b>	172.86-173.13	<b>3a, 3a''-3c, 3c'</b>
<b>S</b>	172.79-173.03	<b>3a, 3a''-3c, 3c'</b>
<b>T</b>	172.98-173.21	<b>3a, 3a''-3c, 3c', 3d, 3d'-3a''', 3c''-3d''</b>

The  $^{13}\text{C}$  NMR spectra in the range of 171-175 ppm would pertain to  $\text{SP}^2$  carbons neighboring oxygen.<sup>133,134</sup> Signals seen in this frequency range could be due to the carbonyl carbons of adipic moiety. In the  $^{13}\text{C}$  NMR spectra of copolyesters containing similar aliphatic moieties synthesised by Tsai et al<sup>36</sup> and Lozano et al<sup>60</sup>, signals in the same range were assigned to the same carbonyl carbons. Lozano et al<sup>60</sup> characterised a copolyester that contained adipic acid by  $^{13}\text{C}$  NMR and assigned the peaks between 178-

180 ppm to the carbonyl carbon of adipic moiety (p.599). Tsai et al<sup>36</sup> analysed a copolyester that contained succinic acid by <sup>13</sup>C NMR and assigned the peaks between 172.8-173.2 ppm to the carbonyl carbons of succinic residue. The carbonyl carbons of succinic residue are shown in Scheme 3.4.



**Scheme 3.4 Carbonyl carbons of succinic moiety<sup>36</sup>**

By comparing the carbonyl carbons of adipic moiety shown in Table 3.40 and the carbonyl carbons of succinic residue shown in Scheme 3.4, it can be presumed that some resemblance could exist for the chemical environment of the carbons concerned.

The peak at 172.90 ppm in the <sup>13</sup>C NMR spectrum of sample Q could be due to the carbonyl carbons marked 3a in Table 3.39. This assignment could be made since sample Q contained neopentyl glycol only. The rest of the samples contained neopentyl glycol as well. Thus, the same assignment could be made for their corresponding peaks in the <sup>13</sup>C NMR spectra.

The peaks between 172.98-173.63 ppm in the <sup>13</sup>C NMR spectrum of sample O could be due to the carbonyl carbons shown in Table 3.39. These assignments could be made since sample O contained neopentyl glycol and trimethylol propane. It could be seen, from Figure 3.21, that there was a weak signal at 173.63 ppm in the <sup>13</sup>C NMR spectrum of sample O. This signal could not be seen in the same frequency range in the <sup>13</sup>C NMR spectrum of sample Q which did not contain trimethylol propane. Therefore, the rise of this signal in the <sup>13</sup>C NMR spectrum of sample O in the range concerned could be due to the carbonyl carbon of adipic moiety that had reacted with trimethylol propane.

The peaks between 172.74-173.13 ppm in the <sup>13</sup>C NMR spectra of samples P, R and S could be assigned to carbons 3a, 3a'', 3c and 3c' as shown in Table 3.40. These assignments could be made since samples P, R and S contained neopentyl glycol and 1,6 hexanediol. It could be seen, from the <sup>13</sup>C NMR spectra shown Figure 3.21, that samples P, R and S had resulted in similar signals in the range of 171-175 ppm. A weak signal had

emerged between 172.89-173.13 ppm in the  $^{13}\text{C}$  NMR spectra of samples P, R and S. No signal appeared in the same frequency range in the  $^{13}\text{C}$  NMR spectrum of sample Q which did not contain 1,6 hexanediol. Therefore, the rise of this signal in the  $^{13}\text{C}$  NMR spectra of samples P, R and S in the range concerned could be due to the carbonyl carbon of adipic moiety that had reacted with 1,6 hexanediol.

The peaks between 172.98-173.21 ppm in the  $^{13}\text{C}$  NMR spectrum of sample T could be due to the carbonyl carbons shown in Table 3.40. These assignments could be made since sample T contained neopentyl glycol, 1,6 hexanediol and 1,4 cyclohexanedimethanol. It could be seen, from Figure 3.21, that the intensity of the first peak at 172.98 ppm in the  $^{13}\text{C}$  NMR spectrum of sample T had been reduced. The molar content of neopentyl glycol in sample T was lower than the rest of the samples. Therefore, the reduction of the intensity of the said peak in the  $^{13}\text{C}$  NMR spectrum of sample T could be due to availability of less neopentyl glycol moiety in its molecular structure. Moreover, it could be seen, from Figure 3.21, that the intensity of the peak at 173.21 ppm in the spectrum of sample T had been increased. Samples P, R and S did not contain 1,4 cyclohexanedimethanol and had resulted in weaker signals at almost the same frequency. Therefore, the augmentation of the intensity of the signal at 173.21 ppm in the  $^{13}\text{C}$  NMR spectrum of sample T could be due to the carbonyl carbon of adipic moiety that had reacted with 1,4 cyclohexanedimethanol. Similar to the  $^{13}\text{C}$  NMR spectra in the frequency ranges of 24-29 ppm, 33-37 ppm, 62-66 ppm and 164-168 ppm, alterations made to the molecular structure of the saturated polyester resins synthesised could be observed in the  $^{13}\text{C}$  NMR spectra in the range of 171-175 ppm.

### 3.2.2.2 $^1\text{H}$ NMR spectra

In this section, the  $^1\text{H}$  NMR spectra of the synthesised copolyesters are provided, interpreted and discussed. The  $^1\text{H}$  NMR spectra are provided in specific frequency ranges where peaks appeared. These ranges included 0.0-1.3 ppm, 1.3-2.0 ppm, 2.0-2.6 ppm, 3.3-3.7 ppm, 3.8-4.5 ppm, 6.5-7.2 ppm and 8.0-8.5 ppm. As shown in Table 3.21 and with respect to the polyols used, sample Q contained neopentyl glycol only. Beside neopentyl glycol, the rest of the synthesised copolyesters contained additional polyols. Therefore, interpretation of the  $^1\text{H}$  NMR spectra of the other samples was carried out by comparing them with the  $^1\text{H}$  NMR spectrum of sample Q. By doing as such, additional peaks produced

in the  $^1\text{H}$  NMR spectra by the additional polyols could be distinguished. Spectral shift, correlation charts and the results published by the others were also used for interpreting the  $^1\text{H}$  NMR spectra. Feed composition and the hydroxyl values of the copolyester samples that were examined by  $^1\text{H}$  NMR were reviewed in Table 3.21. Parameters of the  $^1\text{H}$  NMR analysis were provided in Table 2.20. The  $^1\text{H}$  NMR spectra of the synthesised copolyesters, in the range of 0.0-1.3 ppm, are shown in Figure 3.22.

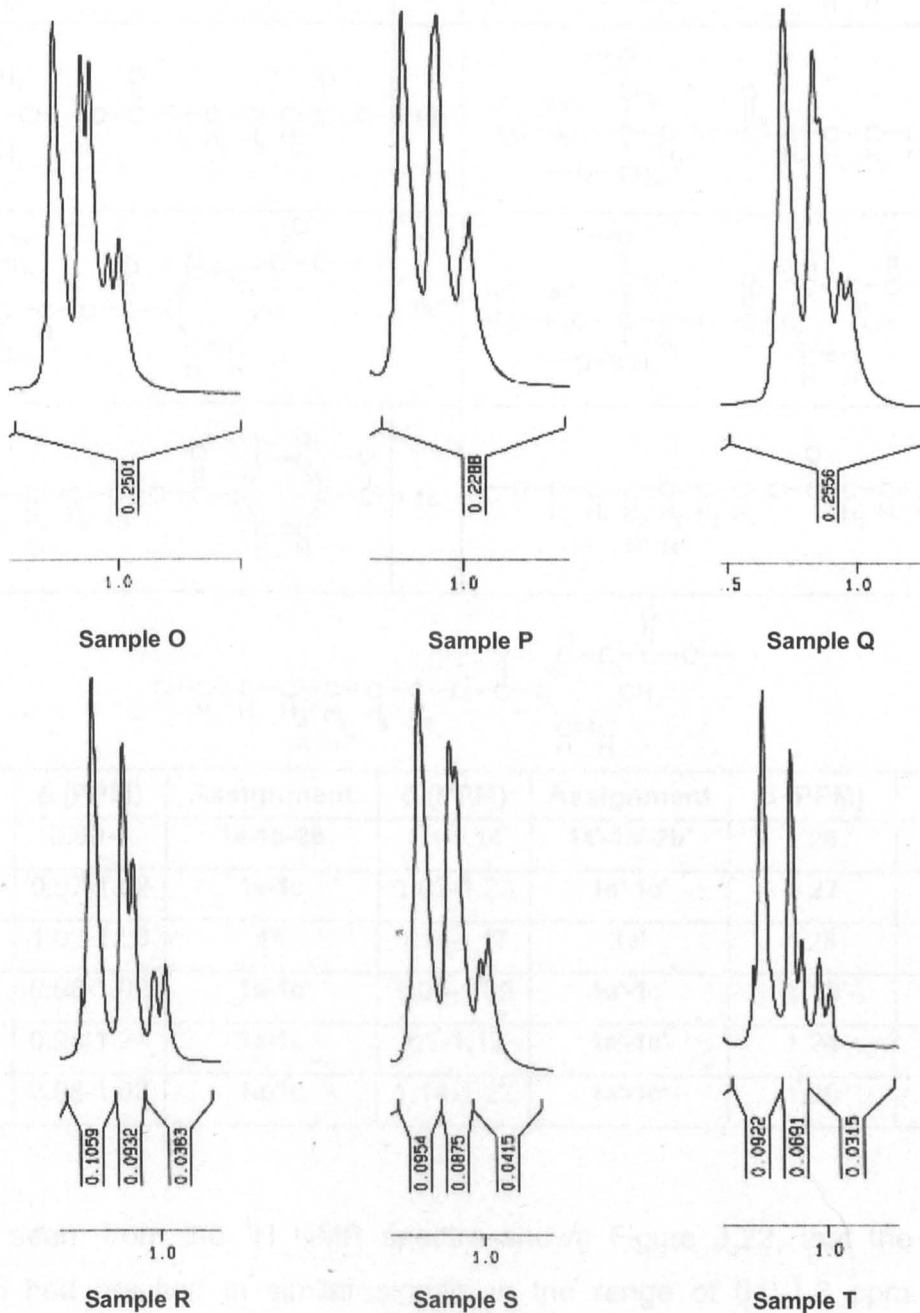
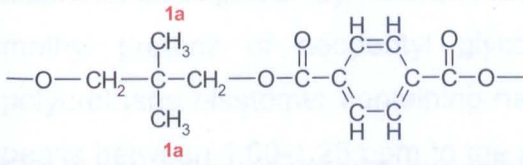
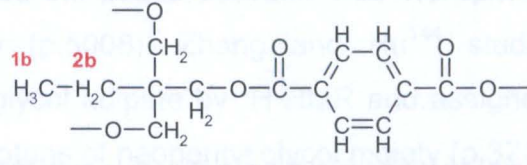
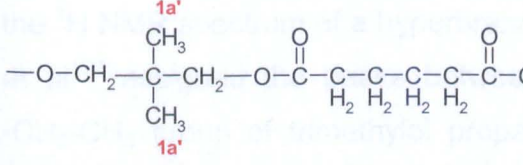
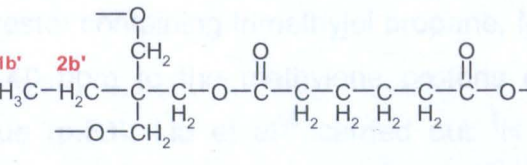
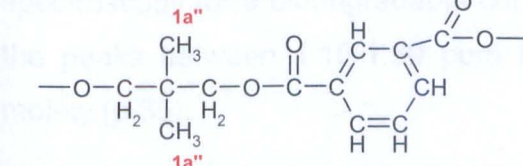
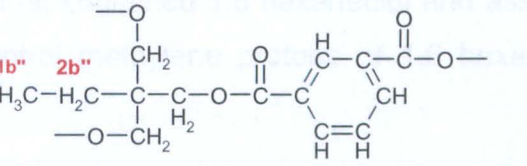
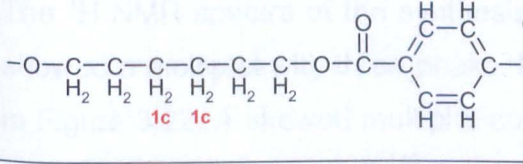
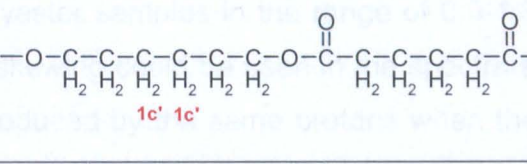
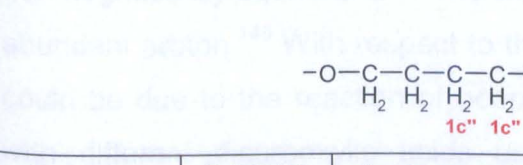


Figure 3.22  $^1\text{H}$  NMR spectra in the range of 0.0-1.3 ppm

Assignments that could be made for the spectra shown in Figure 3.22 are provided in Table 3.41.

**Table 3.41 Assignments for the  $^1\text{H}$  NMR spectra in the range of 0.0-1.3 ppm**<sup>50,104,132,140-144</sup>

	<b>1a</b>		<b>1b</b> <b>2b</b>			
	<b>1a'</b>		<b>1b'</b> <b>2b'</b>			
	<b>1a''</b>		<b>1b''</b> <b>2b''</b>			
	<b>1c</b>		<b>1c'</b>			
	<b>1c''</b>		<b>1c''</b>			
<b>Sample</b>	<b><math>\delta</math> (PPM)</b>	<b>Assignment</b>	<b><math>\delta</math> (PPM)</b>	<b>Assignment</b>	<b><math>\delta</math> (PPM)</b>	<b>Assignment</b>
<b>O</b>	0.99-1	<b>1a-1b-2b</b>	1.1-1.14	<b>1a'-1b'-2b'</b>	1.26	<b>1a''-1b''-2b''</b>
<b>P</b>	0.97-1.02	<b>1a-1c</b>	1.02-1.23	<b>1a'-1c'</b>	1.27	<b>1a''-1c''</b>
<b>Q</b>	1.02-1.06	<b>1a</b>	1.14-1.17	<b>1a'</b>	1.28	<b>1a''</b>
<b>R</b>	0.98-1.02	<b>1a-1c</b>	1.05-1.09	<b>1a'-1c'</b>	1.13	<b>1a''-1c''</b>
<b>S</b>	0.98-1.24	<b>1a-1c</b>	1.1-1.12	<b>1a'-1c'</b>	1.24	<b>1a''-1c''</b>
<b>T</b>	0.98-1.03	<b>1a-1c</b>	1.14-1.22	<b>1a'-1c'</b>	1.25	<b>1a''-1c''</b>

It could be seen, from the  $^1\text{H}$  NMR spectra shown Figure 3.22, that the synthesised copolyesters had resulted in similar signals in the range of 0.0-1.3 ppm. Peaks that appeared in the range of 0.0-1.3 ppm could mainly be due to the methyl protons of neopentyl glycol moiety.<sup>104,140-144</sup> These signals could also be due to the methyl and

methylene protons of trimethylol propane and 1,6 hexanediol residues.<sup>50,132,101,140-142</sup> The protons concerned are shown in Table 3.41. The assignments shown in Table 3.41 could also be made by considering the works of Donovan and Moad<sup>143</sup>, Zhang and Hu<sup>144</sup>, Mishra et al<sup>132</sup> and Liu et al<sup>50</sup>. Donovan and Moad<sup>143</sup> examined a hydroxylated neopentyl glycol isophthalate oligomer by <sup>1</sup>H NMR and assigned the peaks between 1.00-1.3 ppm to the methyl protons of neopentyl glycol moiety (p.5008). Zhang and Hu<sup>144</sup> studied a polyurethane elastomer containing neopentyl glycol adipate by <sup>1</sup>H NMR and assigned the peaks between 1.00-1.25 ppm to the methyl protons of neopentyl glycol moiety (p.3711). In the <sup>1</sup>H NMR spectrum of a hyperbranched polyester containing trimethylol propane, Mishra et al<sup>132</sup> assigned the peaks between 1.10-1.40 ppm to the methylene protons of the -CH<sub>2</sub>-CH<sub>3</sub> group of trimethylol propane residue (p.50). Liu et al<sup>50</sup> carried out <sup>1</sup>H NMR spectroscopy for a biodegradable copolyester that contained 1,6 hexanediol and assigned the peaks between 1.10-1.30 ppm to the central methylene protons of 1,6 hexanediol moiety (p.35).

The <sup>1</sup>H NMR spectra of the synthesised copolyester samples in the range of 0.0-1.3 ppm showed a multiplet with three peaks. Multiplet skewing could be seen in the spectra shown in Figure 3.22. A skewed multiplet could be produced by the same protons when they are not magnetically equivalent.<sup>145</sup> The tallest peak of the multiplet may be caused by the most abundant proton.<sup>145</sup> With respect to the copolyester samples, the skewing of the multiplets could be due to the reaction of neopentyl glycol, trimethylol propane and 1,6 hexanediol with different dicarboxylic acids used. Three dicarboxylic acids were used for the preparation of the copolyesters. These included hexanedioic or adipic acid, isophthalic acid and terephthalic acid. The molar content of terephthalic acid was lower than both adipic acid and isophthalic acid. Therefore, moieties formed as the result of the reaction of neopentyl glycol, trimethylol propane and 1,6 hexanediol with terephthalic acid would have the smallest number in the molecular structure. Based on this, the shortest peaks of the multiplets could be due to the methyl protons of neopentyl glycol terephthalate, methylene protons of trimethylol propane terephthalate and methylene protons of 1,6 hexanediol terephthalate. Correspondingly, the medium height peaks of the multiplets could be due to the methyl protons of neopentyl glycol adipate, methylene protons of trimethylol propane adipate and methylene protons of 1,6 hexanediol adipate. The tallest peaks of the multiplets could be due to the methyl protons of neopentyl glycol isophthalate, methylene protons of trimethylol propane isophthalate and methylene protons of 1,6 hexanediol



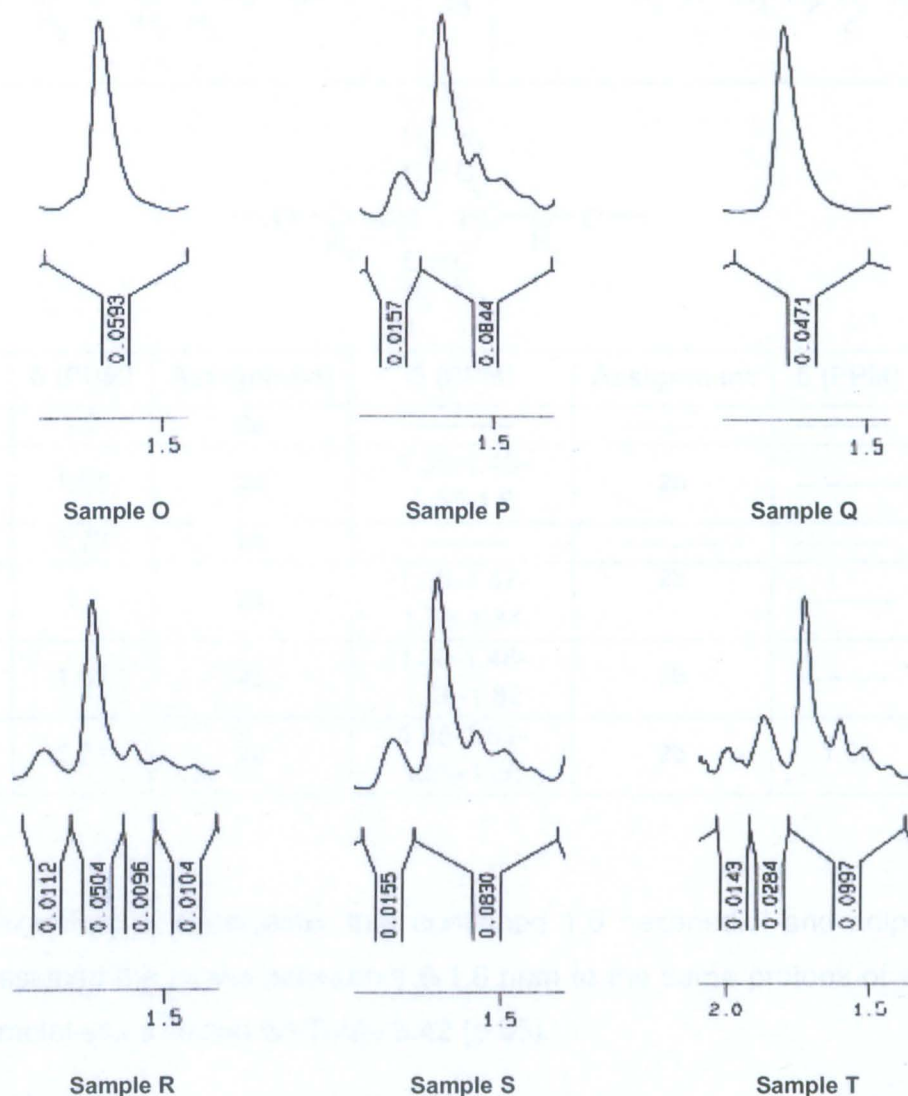
isophthalate. The molar content of isophthalic acid in the copolyester samples was higher than adipic acid.

In the  $^1\text{H}$  NMR spectrum of sample Q in the range of 0.0-1.3 ppm, the first peak of the multiplet could be assigned to the methyl protons of neopentyl glycol terephthalate moiety. These protons are marked 1a in Table 3.41. The second peak of the multiplet could be assigned to the methyl protons of neopentyl glycol adipate. These protons are marked 1a' in Table 3.41. The third peak of the multiplet could be assigned to the methyl protons of neopentyl glycol isophthalate. These protons are marked 1a'' in Table 3.41. These assignments could be made since sample Q contained neopentyl glycol only. The rest of the samples contained neopentyl glycol as well. Thus the same assignment could be made for their corresponding signals in the  $^1\text{H}$  NMR spectra. Signals in the  $^1\text{H}$  NMR spectra of the rest of the samples in the range of 0.0-1.3 ppm was comparable with the spectrum of sample Q. This could imply that the methyl protons of neopentyl glycol moiety could have mostly given rise to the signals seen in the  $^1\text{H}$  NMR spectra of the rest samples in the range concerned. On the other hand, it could also indicate that the peaks produced by the methyl protons of neopentyl glycol moiety could have overlapped the peaks produced by the methylene protons of trimethylol propane and 1,6 hexanediol residues.

In the  $^1\text{H}$  NMR spectrum of sample O in the range of 0.0-1.3 ppm, the first peak of the multiplet could be assigned to protons 1a, 1b and 2b. The second peak of the multiplet could be assigned to protons 1a', 1b' and 2b'. The third peak of the multiplet could be assigned to protons 1a'', 1b'' and 2b''. The said protons are shown in Table 3.41. These assignments could be made since sample O contained neopentyl glycol and trimethylol propane.

In the  $^1\text{H}$  NMR spectra of samples P, R, S and T in the range of 0.0-1.3 ppm, the first peak of the multiplet could be assigned to protons 1a and 1c. The second peak of the multiplet could be assigned to protons 1a' and 1c'. The third peak of the multiplet could be assigned to protons 1a'' and 1c''. The said protons are shown in Table 3.41. These assignments could be made since samples P, R, S and T contained neopentyl glycol and 1,6 hexanediol.

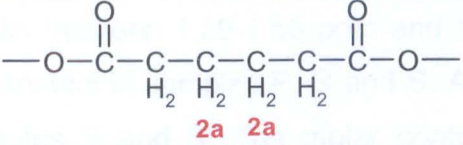
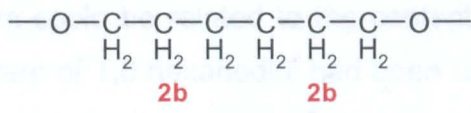
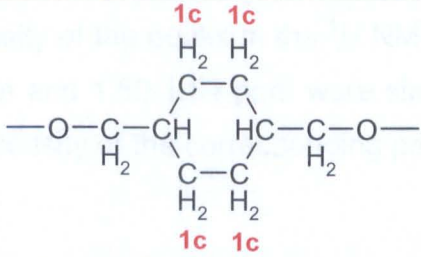
The  $^1\text{H}$  NMR spectra of the synthesised copolyesters, in the range of 1.3-2.0 ppm, are shown in Figure 3.23.



**Figure 3.23**  $^1\text{H}$  NMR spectra in the range of 1.3-2.0 ppm

From the  $^1\text{H}$  NMR spectra shown in Figure 3.23, it could be seen that all the samples had resulted in a stretched peak in the range of 1.62-1.73 ppm. Additional peaks could be seen in the  $^1\text{H}$  NMR spectra of samples P, R, S and T in the ranges of 1.26-1.59 ppm and 1.8-1.86 ppm. Peaks that appeared in the range of 1.62-1.73 ppm could be due to the central methylene protons of adipic moiety.<sup>50,140-142</sup> Peaks that appeared in the range of 1.26-1.59 ppm and 1.8-1.86 ppm could be due to the methylene protons of the residues of 1,6 hexanediol and 1,4 cyclohexanedimethanol as shown in Table 3.42.<sup>50,140-142</sup>

**Table 3.42 Assignments for the  $^1\text{H}$  NMR spectra in the range of 1.3-2.0 ppm**<sup>50,140-142</sup>

			1a				2b
							1c
Sample	$\delta$ (PPM)	Assignment	$\delta$ (PPM)	Assignment	$\delta$ (PPM)	Assignment	
O	1.7	2a	-----	-----	-----	-----	
P	1.66	2a	1.39-1.46- 1.55-1.8	2b	-----	-----	
Q	1.73	2a	-----	-----	-----	-----	
R	1.7	2a	1.39-1.47- 1.58-1.84	2b	-----	-----	
S	1.62	2a	1.39-1.48- 1.56-1.82	2b	-----	-----	
T	1.71	2a	1.28-1.51- 1.59-1.86	2b	1.98	1c	

Liu et al<sup>50</sup> examined a copolyester that contained 1,6 hexanediol and adipic acid by  $^1\text{H}$  NMR and assigned the peaks between 1.6-1.8 ppm to the same protons of adipic and 1,6 hexanediol moieties as shown on Table 3.42 (p.35).

The peak at 1.7 ppm in the  $^1\text{H}$  NMR spectrum of sample O could be assigned to the central methylene protons of adipic moiety. The same assignment could be made for the peak at 1.73 ppm in the  $^1\text{H}$  NMR spectrum of sample Q. In the  $^1\text{H}$  NMR spectra of samples O and Q in the range concerned, apart from the peaks that appeared at 1.7 ppm and 1.73 ppm, no other peaks could be seen.

The  $^1\text{H}$  NMR spectra of samples P, R and S in the range of 1.30-2.00 ppm showed five peaks. The stretched peak between 1.62-1.70 ppm could be assigned to the central methylene protons of adipic moiety. The peaks between 1.39-1.58 ppm and 1.80-1.84 ppm could be assigned to the methylene protons of 1,6 hexanediol that are marked 2b in Table

3.42. This assignment could be made since no peaks appeared in the same range in the  $^1\text{H}$  NMR spectrum of sample Q which did not contain 1,6 hexanediol. The intensity of the peaks between 1.39-1.58 ppm and 1.80-1.84 ppm could be related to the content of 1,6 hexanediol in samples P, R and S. An equal content of 1,6 hexanediol had been used for samples P and S. The molar content of 1,6 hexanediol in sample R was lower than samples P and S. The intensity of the peaks in the  $^1\text{H}$  NMR spectra of samples P and S in the ranges of 1.39-1.58 ppm and 1.80-1.84 ppm were similar. However, it could be seen, from Figure 3.23, that the intensity of the corresponding peaks in the spectrum of sample R had been reduced.

The  $^1\text{H}$  NMR spectrum of sample T in the range of 1.30-2.00 ppm showed six peaks. The stretched peak at 1.71 ppm could be assigned to the central methylene protons of adipic moiety. The peaks between 1.28-1.51 ppm and at 1.86 ppm could be assigned to the methylene protons of 1,6 hexanediol (protons 2b in Table 3.42). In the  $^1\text{H}$  NMR spectrum of sample T in the range concerned, one additional peak could be seen at 1.98 ppm. No peak appeared in the  $^1\text{H}$  NMR spectra of the other samples between 1.9-1.98 ppm. Sample T was the only copolyester that contained 1,4 cyclohexanedimethanol. Therefore, the additional peak at 1.98 ppm in the  $^1\text{H}$  NMR spectrum of sample T could be assigned to the methylene protons on the cycloaliphatic ring of 1,4 cyclohexanedimethanol (protons 1c in Table 3.42).

Modifications made to the molecular structure of the synthesised copolyesters were visible in the  $^1\text{H}$  NMR spectra in the range of 1.3-2.0 ppm. It could be seen, from the  $^1\text{H}$  NMR spectra of samples P, R and S, that exclusive peaks appeared in the ranges of 1.39-1.58 ppm and 1.80-1.84 ppm. As mentioned, these peaks could pertain to the methylene protons of 1,6 hexanediol moiety. Inclusion of 1,4 cyclohexanedimethanol in sample T had also resulted in the rise of a particular peak at 1.98 ppm. On the other hand, no signals could be seen in the said frequency ranges in the  $^1\text{H}$  NMR spectra of samples O and Q which did not contain either 1,6 hexanediol or 1,4 cyclohexanedimethanol.

The  $^1\text{H}$  NMR spectra of the synthesised copolyesters, in the range of 2.00-2.50 ppm, are shown in Figure 3.24.

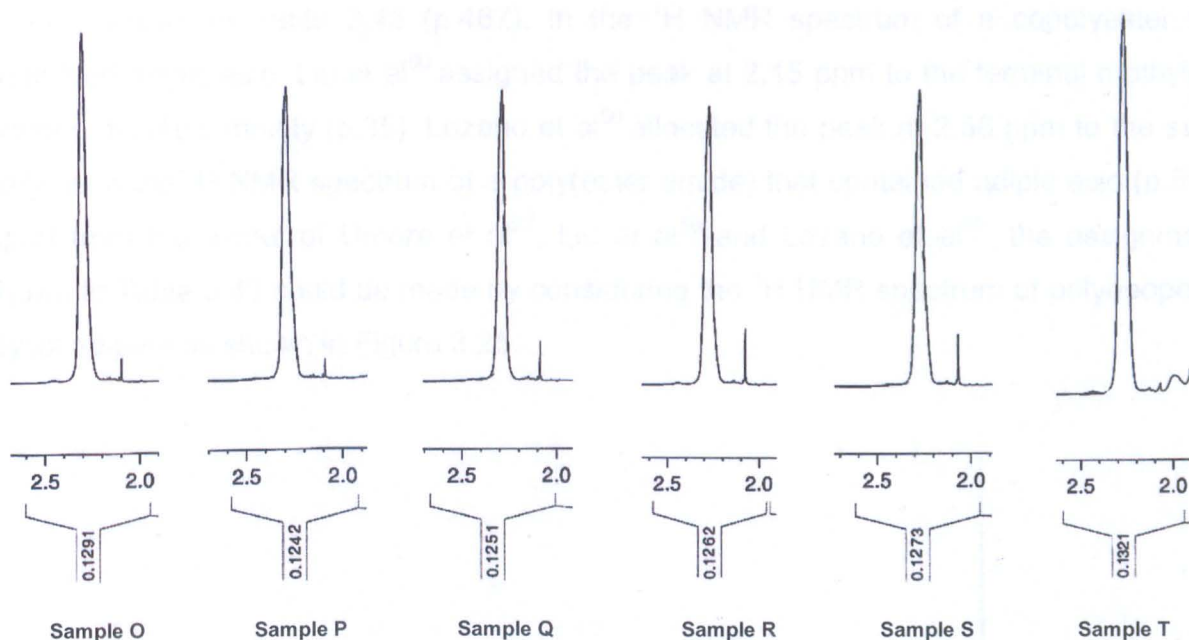


Figure 3.24  $^1\text{H}$  NMR spectra in the range of 2.0-2.5 ppm

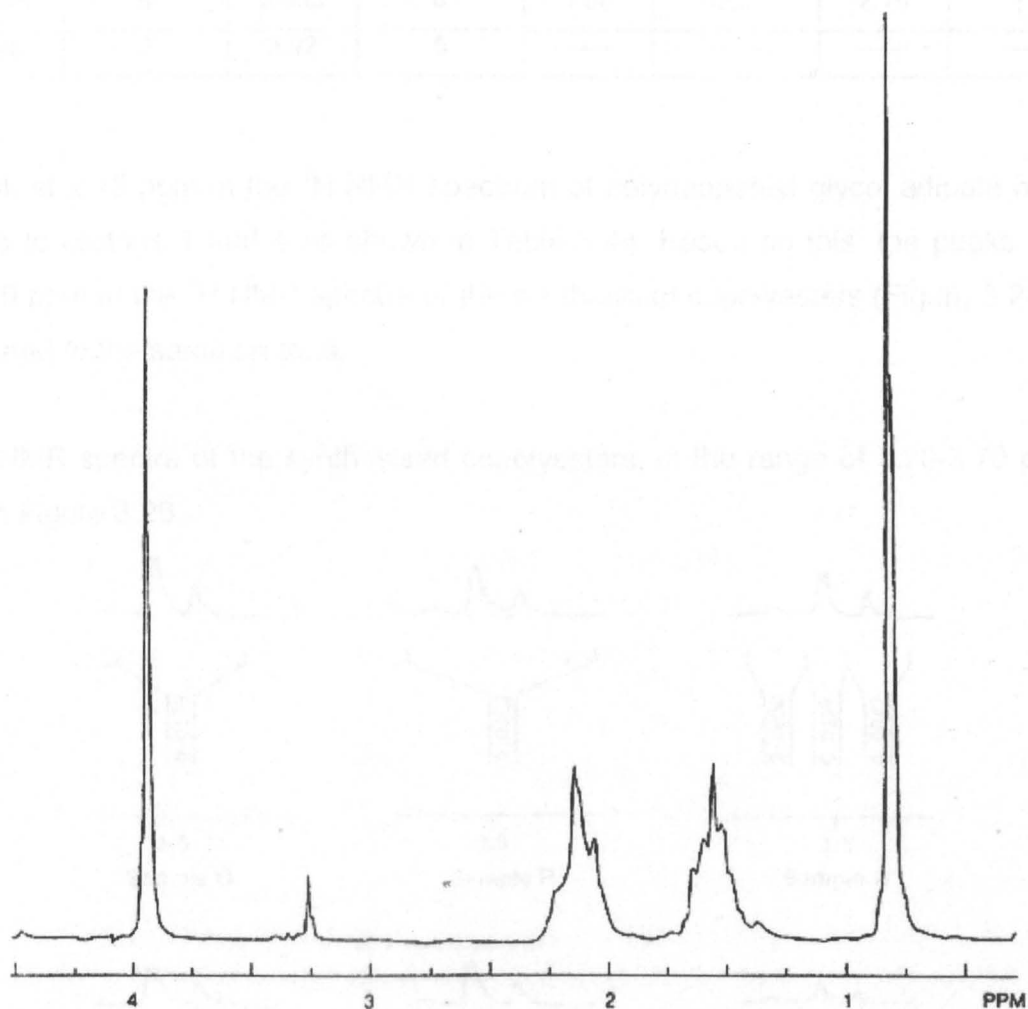
Assignments that could be made for the spectra shown in Figure 3.24 are provided in Table 3.43.

Table 3.43 Assignments for the  $^1\text{H}$  NMR spectra in the range of 2.0-2.5 ppm<sup>27,50,60,99,140-142</sup>

$\text{---O---C(=O)---CH}_2\text{---CH}_2\text{---CH}_2\text{---CH}_2\text{---C(=O)---O---}$		
Sample	$\delta$ (PPM)	Assignment
O	2.293	3a
P	2.290	3a
Q	2.288	3a
R	2.283	3a
S	2.275	3a
T	2.277	3a

It could be seen, from the  $^1\text{H}$  NMR spectra shown Figure 3.24, that all the synthesised copolyesters had resulted in a singlet peak between 2.27-2.29 ppm. This peak could be due to the terminal methylene protons of adipic moiety.<sup>27,50,60,99,140-142</sup> The protons concerned are marked 3a in Table 3.43. The results published by Umare et al<sup>27</sup>, Liu et al<sup>50</sup> and Lozano et al<sup>60</sup> also confirm the assignments shown in Table 3.43. Umare et al<sup>27</sup> examined 1,3 propanediol adipate by  $^1\text{H}$  NMR and assigned the peak at 2.33 ppm to the

protons shown in Table 3.43 (p.467). In the  $^1\text{H}$  NMR spectrum of a copolyester that contained adipic acid, Liu et al<sup>50</sup> assigned the peak at 2.15 ppm to the terminal methylene protons of adipic moiety (p.35). Lozano et al<sup>60</sup> allocated the peak at 2.56 ppm to the same protons in the  $^1\text{H}$  NMR spectrum of a poly(ester amide) that contained adipic acid (p.598). Apart from the works of Umare et al<sup>27</sup>, Liu et al<sup>50</sup> and Lozano et al<sup>60</sup>, the assignments shown in Table 3.43 could be made by considering the  $^1\text{H}$  NMR spectrum of polyneopentyl glycol adipate as shown in Figure 3.25.


**Analysis details**

Nucleus:  $^1\text{H}$ , Frequency: 80MHz, Spectrometer: Bruker WP80,  
 Detection technique: FT-10 pulses, Solvent:  $\text{C}_6\text{D}_6$ , Temperature: 80°C

**Figure 3.25**  $^1\text{H}$  NMR spectrum of polyneopentyl glycol adipate<sup>146</sup>

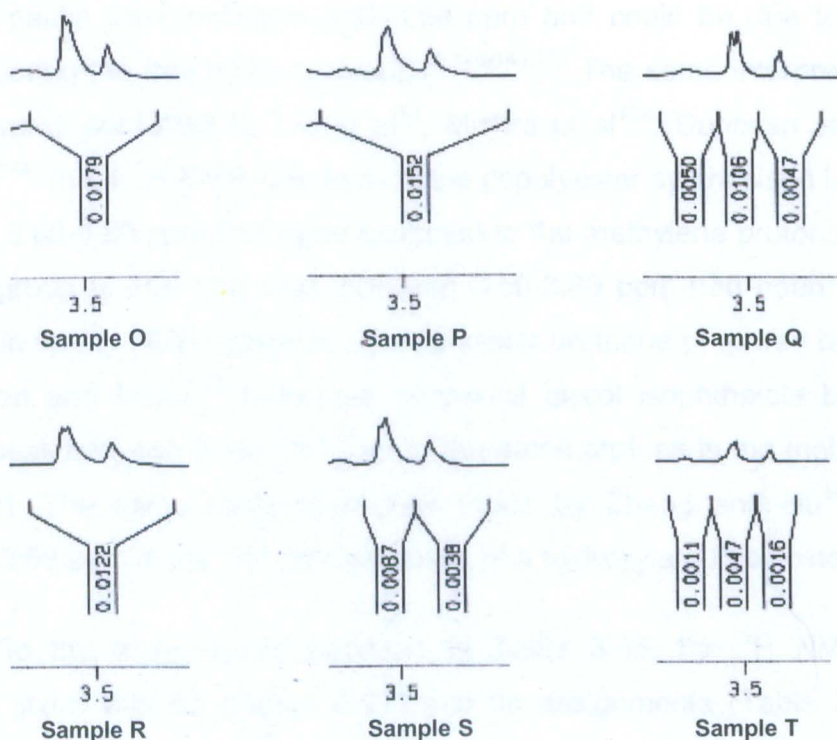
Assignments for the  $^1\text{H}$  NMR spectrum of polyneopentyl glycol adipate are shown in Table 3.44.

**Table 3.44 Assignments for the  $^1\text{H}$  NMR spectrum of polyneopentyl glycol adipate<sup>146</sup>**

$\text{HO}-\underset{\text{H}_2}{\text{C}}-\overset{\text{CH}_3}{\underset{\text{CH}_3}{\text{C}}}-\underset{\text{H}_2}{\text{C}}-\text{O}-\left[ \overset{\text{O}}{\parallel}{\text{C}}-\underset{\text{H}_2}{\text{C}}-\underset{\text{H}_2}{\text{C}}-\underset{\text{H}_2}{\text{C}}-\underset{\text{H}_2}{\text{C}}-\overset{\text{O}}{\parallel}{\text{C}}-\text{O}-\underset{\text{H}_2}{\text{C}}-\overset{\text{CH}_3}{\underset{\text{CH}_3}{\text{C}}}-\underset{\text{H}_2}{\text{C}}-\text{O} \right]_n$							
<b>Analysis details</b>							
Nucleus: $^1\text{H}$ , Frequency: 80MHz, Spectrometer: Bruker WP80, Detection technique: FT-10 pulses, Solvent: $\text{C}_6\text{D}_6$ , Temperature: 80°C							
$\delta$ (PPM)	Assignment	$\delta$ (PPM)	Assignment	$\delta$ (PPM)	Assignment	$\delta$ (PPM)	Assignment
0.845	8	0.863	6	1.58	2,3	2.15	1,4
3.25	9	3.92	5	-----	-----	-----	-----

The peak at 2.15 ppm in the  $^1\text{H}$  NMR spectrum of polyneopentyl glycol adipate had been assigned to protons 1 and 4 as shown in Table 3.44. Based on this, the peaks between 2.27-2.29 ppm in the  $^1\text{H}$  NMR spectra of the synthesised copolyesters (Figure 3.24), could be assigned to the same protons.

The  $^1\text{H}$  NMR spectra of the synthesised copolyesters, in the range of 3.20-3.70 ppm, are shown in Figure 3.26.

**Figure 3.26  $^1\text{H}$  NMR spectra in the range of 3.20-3.70 ppm**

Assignments that could be made for the spectra shown in Figure 3.26 are provided in Table 3.45.

**Table 3.45 Assignments for the  $^1\text{H}$  NMR spectra in the range of 3.20-3.70 ppm**<sup>50,140-143,146</sup>

$\text{HO}-\overset{\text{a}}{\text{CH}_2}-$		<b>a</b>
$\begin{array}{c} \text{CH}_3 \\   \\ -\text{O}-\text{C}-\text{C}-\text{CH}_2-\text{OH} \\   \quad   \\ \text{H}_2 \quad \text{b} \\ \text{CH}_3 \end{array}$		<b>b</b>
Sample	$\delta$ (PPM)	Assignment
O	3.41-3.54-3.56	a
P	3.40-3.54-3.55	a
Q	3.44-3.58-3.59	b
R	3.39-3.53-3.55	a
S	3.40-3.54-3.56	a
T	3.40-3.52-3.54	a

The  $^1\text{H}$  NMR spectra of the copolyester samples in the range of 3.20-3.70 ppm showed two peaks. These peaks were between 3.39-3.59 ppm and could be due to the methylene protons neighboring the free hydroxyl group.<sup>50,140-143,146</sup> The same interpretation had been made in the works published by Liu et al<sup>50</sup>, Mishra et al<sup>132</sup>, Donovan and Moad<sup>143</sup> and Zhang and Hu<sup>144</sup>. In the  $^1\text{H}$  NMR spectrum of the copolyester synthesised by Liu et al<sup>50</sup>, the peak between 3.60-3.80 ppm had been assigned to the methylene protons adjacent to the free hydroxyl group (p.35). The peak between 3.50-3.80 ppm had been assigned to the same protons in the  $^1\text{H}$  NMR spectrum of a polyester urethane prepared by Mishra et al<sup>132</sup> (p.50). Donovan and Moad<sup>143</sup> examined neopentyl glycol isophthalate by  $^1\text{H}$  NMR and assigned the peak between 3.40-3.50 ppm to the same protons in the moiety of neopentyl glycol (p.5008). The same assignment was made by Zhang and Hu<sup>144</sup> for the peak between 3.25-3.50 ppm in the  $^1\text{H}$  NMR spectrum of a hydroxylated polyester (p.3711).

With respect to the assignments provided in Table 3.45, the  $^1\text{H}$  NMR spectrum of polyneopentyl glycol adipate (Figure 3.27) and its assignments (Table 3.44) were also considered. In the  $^1\text{H}$  NMR spectrum of polyneopentyl glycol adipate, the peak at 3.25 ppm had been assigned to the same protons as shown Table 3.44.



In view of the fact that sample Q contained neopentyl glycol only, its peaks in the  $^1\text{H}$  NMR spectra in the range of 3.20-3.70 ppm could be assigned to the terminal methylene protons adjacent to the free hydroxyl end group in the moiety of neopentyl glycol. In addition to neopentyl glycol, the rest of the samples contained either trimethylol propane, 1,6 hexanediol or 1,4 cyclohexanedimethanol. In other words, in the molecular structure of the rest of the copolyesters the residues of the polyols mentioned could contain free hydroxyl end groups. Thus, the peaks that appeared in the  $^1\text{H}$  NMR spectra of the rest of the samples in the range concerned could also be due to the terminal methylene protons of the residues of these additional polyols.

It could be seen, from the spectra shown in Figure 3.26, that the intensity of the peaks of sample O was higher than the rest of the samples. The free hydroxyl content of sample O was higher than the rest of the samples. It could also be seen, in the spectra shown in Figure 3.26, that the intensity of the peaks of sample T was lower than the rest of the samples. The free hydroxyl content of sample T was lower than the rest of the samples. Therefore, the intensity of the peaks in the range of 3.20-3.70 ppm could be related to the free hydroxyl contents of the synthesised copolyesters. The free hydroxyl content of the copolyester samples were reviewed in Table 3.21.

The  $^1\text{H}$  NMR spectra of samples O and Q, in the range of 3.80-4.50 ppm, are shown in Figure 3.27.

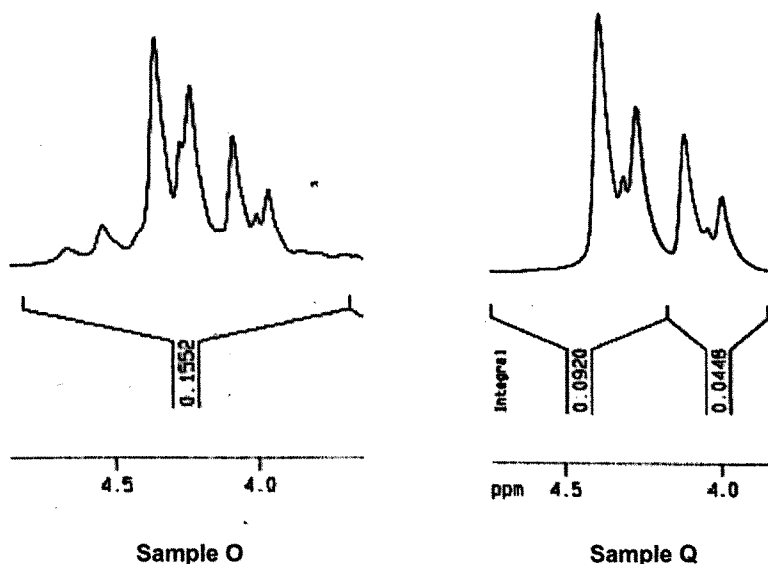
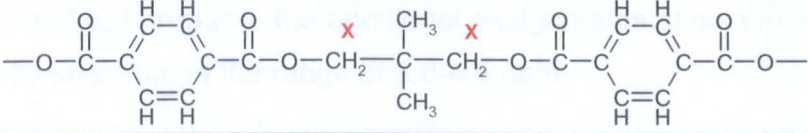
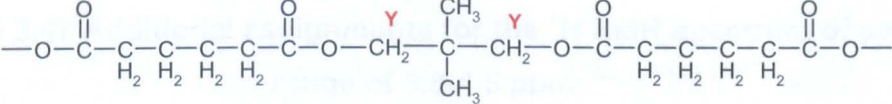
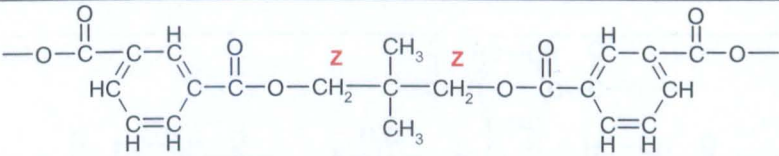
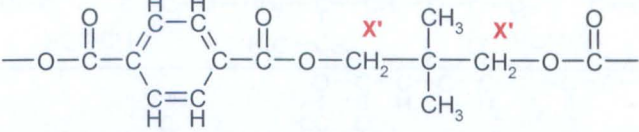
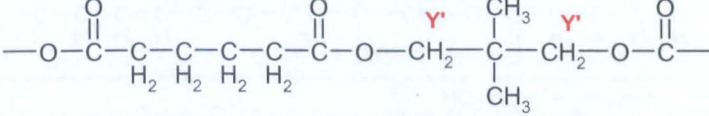
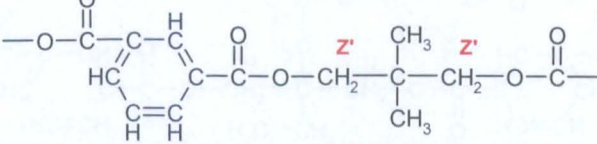


Figure 3.27  $^1\text{H}$  NMR spectra of samples O and Q in the range of 3.8-4.5 ppm

Assignments that could be made for the spectra shown in Figure 3.27 are provided in Table 3.46.

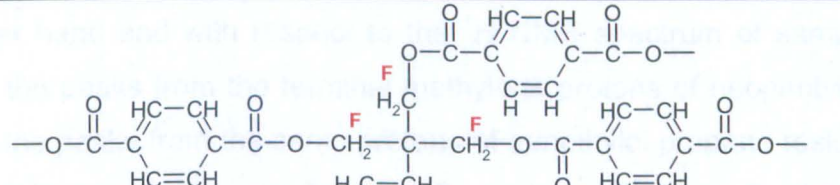
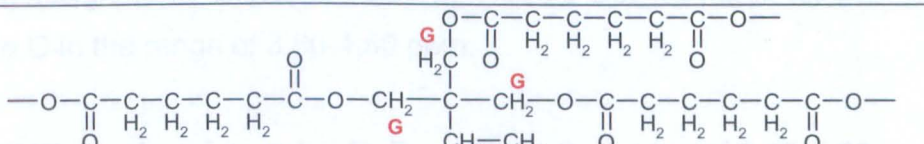
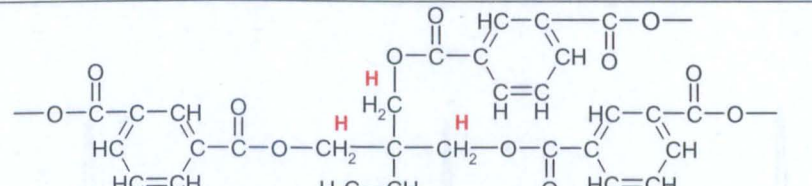
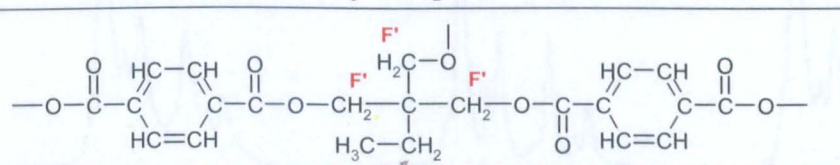
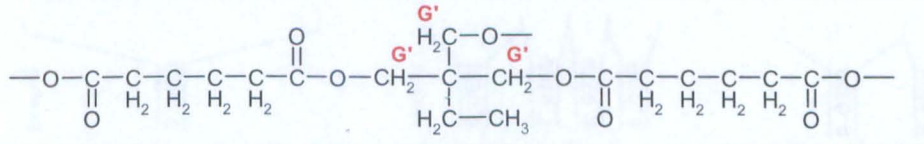
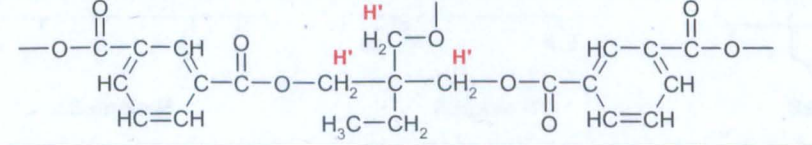
**Table 3.46 Assignments for the  $^1\text{H}$  NMR spectra of samples O and Q in the range of 3.8-4.5 ppm** <sup>135,140-143,146</sup>

		<b>X</b>				
		<b>Y</b>				
		<b>Z</b>				
		<b>X'</b>				
		<b>Y'</b>				
		<b>Z'</b>				
Sample	$\delta$ (PPM)	Assignment	$\delta$ (PPM)	Assignment	$\delta$ (PPM)	Assignment
O	3.96-4.08	X, X'	4.23-4.27	Y, Y'	4.35	Z, Z'
Q	3.99-4.11	X, X'	4.26-4.31	Y, Y'	4.38	Z, Z'

It could be seen, from the  $^1\text{H}$  NMR spectra shown in Figure 3.27, that samples O and Q had resulted in similar peaks in the range of 3.8-4.5 ppm. In general, peaks that appear in the  $^1\text{H}$  NMR spectra in the range concerned could be due to the terminal methylene protons that are bound to oxygen. <sup>140-142,146</sup> It could be seen, from Figure 3.27, that the peaks appeared in the form of a skewed multiplet. The peaks of the copolyester samples had also appeared in the form of a skewed multiplet in the range of 0.0-1.3 ppm. In this regard, Figure 3.23 and Figure 3.24 can be used. The probable cause of multiplet skewing

in the  $^1\text{H}$  NMR spectra of the copolyester samples was explained earlier as the peaks in the range of 0.0-1.3 ppm were interpreted. Based on this, the assignments provided in Table 3.46 could be made for the spectra of samples O and Q in the range of 3.80-4.50 ppm. As shown in Table 3.46, the peaks in the range concerned could be due the terminal methylene protons of neopentyl glycol moiety. Since sample O contained both neopentyl glycol and trimethylol propane, the additional assignments shown in Table 3.47 could also be made for its spectrum in the range of 3.8-4.5 ppm.

**Table 3.47 Additional assignments for the  $^1\text{H}$  NMR spectrum of sample O in the range of 3.8-4.5 ppm** <sup>132,135,140-142</sup>

						F
						G
						H
						F'
						G'
						H'
Sample	$\delta$ (PPM)	Assignment	$\delta$ (PPM)	Assignment	$\delta$ (PPM)	Assignment
O	3.96-4.08	F, F'	4.23-4.27	G, G'	4.35	H, H'

For making the assignments shown in Table 3.46, the interpretation made by Donovan and Moad<sup>143</sup> was also considered. In the work of the said, the peak between 4.00-4.50 ppm in the <sup>1</sup>H NMR spectrum of neopentyl glycol isophthalate had been assigned to the terminal methylene protons adjacent to the ester group in the moiety of neopentyl glycol (p.5008)<sup>143</sup>. The work published by Mishra et al<sup>132</sup> was considered for making the assignments shown in Table 3.47 as well. Mishra et al<sup>132</sup> studied a trimethylol propane containing polyester urethane by <sup>1</sup>H NMR and assigned the peak between 4.00-4.40 ppm to the terminal methylene protons of trimethylol propane residue (p.50). The similarity of the pattern of the peaks in the <sup>1</sup>H NMR spectra of samples O and Q in the range of 3.80-4.50 ppm could indicate that these peaks had been mostly produced by the terminal methylene protons of neopentyl glycol moiety rather than the same protons in the trimethylol propane residue. On the other hand and with respect to the <sup>1</sup>H NMR spectrum of sample O in the range concerned, the peaks from the terminal methylene protons of neopentyl glycol could have overlapped the peaks from the same protons of trimethylol propane residue. Therefore, the additional assignments shown in Table 3.47 could also be made for the <sup>1</sup>H NMR spectrum of sample O in the range of 3.80-4.50 ppm.

The <sup>1</sup>H NMR spectra of samples P, R and S, in the range of 3.80-4.50 ppm, are shown in Figure 3.28

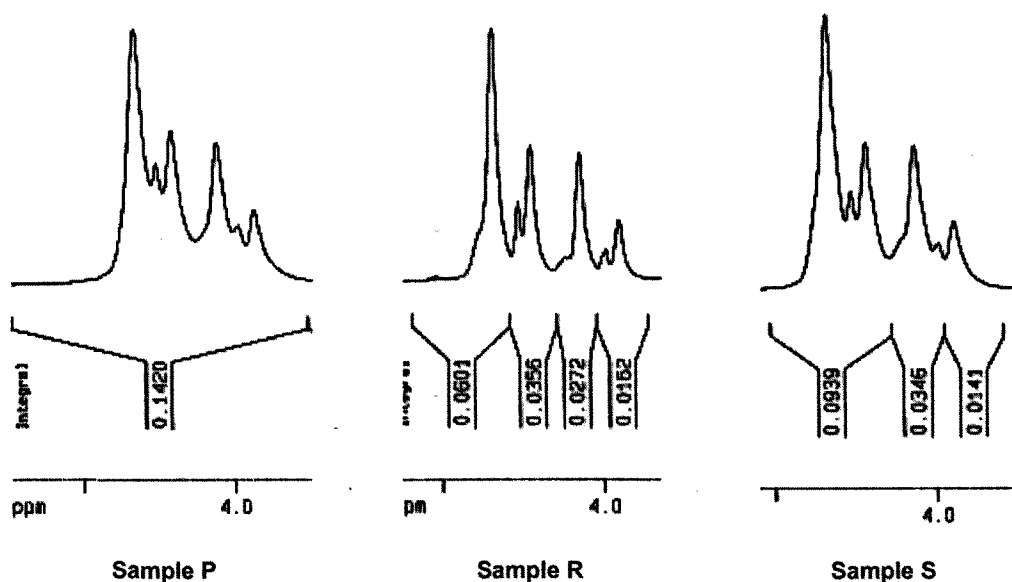
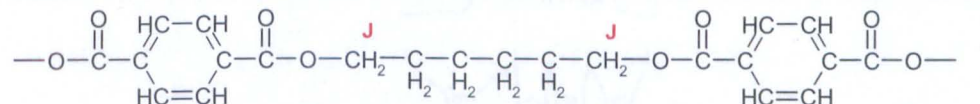
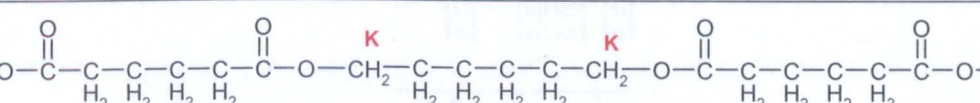
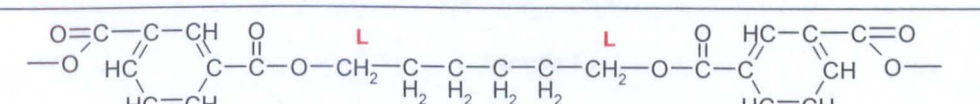
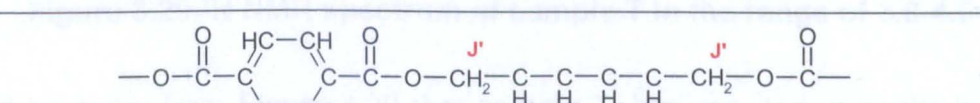
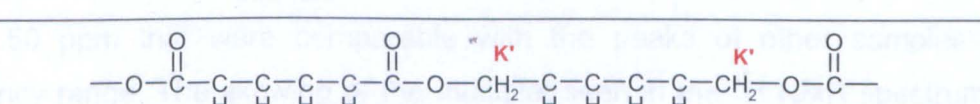
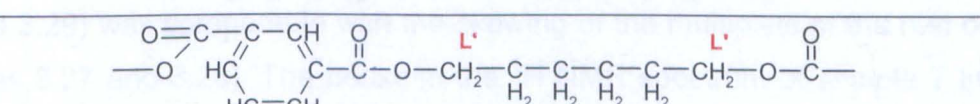


Figure 3.28 <sup>1</sup>H NMR spectra of samples P, R and S in the range of 3.8-4.5 ppm

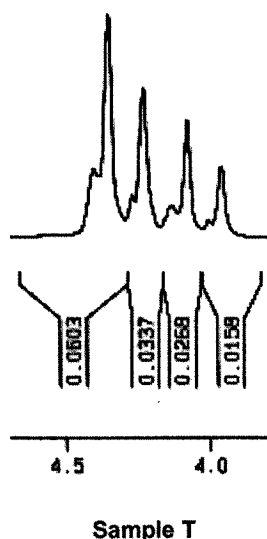
It could be seen, from the  $^1\text{H}$  NMR spectra shown in Figure 3.28, that samples P, R and S had resulted in similar peaks in the range of 3.80-4.50 ppm. It could also be seen, from the  $^1\text{H}$  NMR spectra shown in Figures 3.27 and 3.28, that the peaks produced by samples P, R and S in the range of 3.80-4.50 ppm were comparable with the peaks produced by sample O in the same frequency range. Sample O contained neopentyl glycol only. Samples P, R and S also contained neopentyl glycol. Therefore, the assignments shown in Table 3.46 could also be made for the  $^1\text{H}$  NMR spectra of samples P, R and S in the range of 3.80-4.50 ppm. Samples P, R and S also contained 1,6 hexanediol. Therefore, in addition to the assignments provided in Table 3.46, the assignments that are provided in Table 3.48 as following could also be made for the  $^1\text{H}$  NMR spectra of samples P, R and S in the range of 3.80-4.50 ppm.

**Table 3.48 Additional assignments for the  $^1\text{H}$  NMR spectra of samples P, R and S in the range of 3.8-4.5 ppm** <sup>50,135,140-142</sup>

							J
							K
							L
							J'
							K'
							L'
Sample	$\delta$ (PPM)	Assignment	$\delta$ (PPM)	Assignment	$\delta$ (PPM)	Assignment	
P	3.93-4.06	J, J'	4.20-4.25	K, K'	4.33	L, L'	
R	3.95-4.07	J, J'	4.22-4.26	K, K'	4.34	L, L'	
S	3.94-4.06	J, J'	4.21-4.26	K, K'	4.34	L, L'	

The additional assignments that are provided in Table 3.48 could be made for the  $^1\text{H}$  NMR spectra of samples P, R and S in the range concerned since the peaks produced by the terminal methylene protons of neopentyl glycol moiety could have overlapped the peaks produced the same protons in the residue of 1,6 hexanediol. For making the assignments shown in Table 3.48, the interpretation made in the work published by Liu et al<sup>50</sup> was also considered. Liu et al<sup>50</sup> examined a copolyester that contained 1,6 hexanediol by  $^1\text{H}$  NMR and assigned the peak between 4.00-4.20 ppm to the terminal methylene protons of 1,6 hexanediol residue (p.35).

The  $^1\text{H}$  NMR spectrum of sample T, in the range of 3.80-4.50 ppm, is shown in Figure 3.29

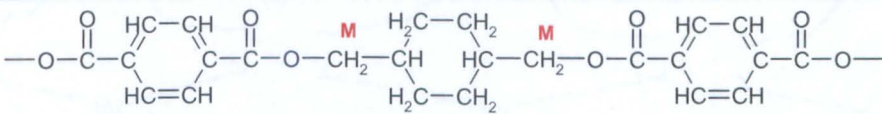
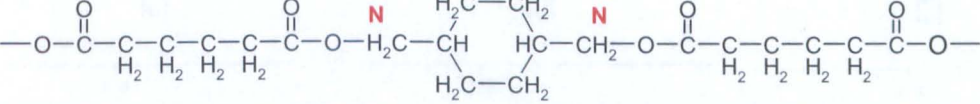
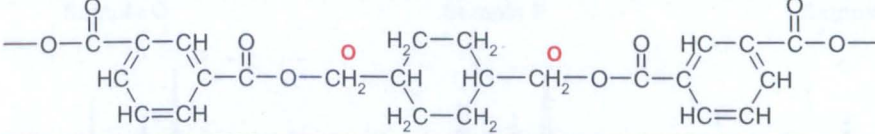
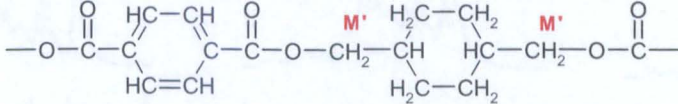
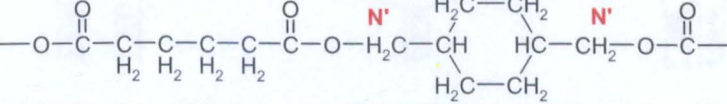
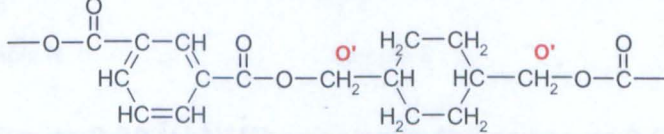


**Figure 3.29  $^1\text{H}$  NMR spectrum of sample T in the range of 3.8-4.5 ppm**

It could be seen, from Figure 3.29 that sample T, had resulted in peaks in the range of 3.80-4.50 ppm that were comparable with the peaks of other samples in the same frequency range. The skewing of the multiplet seen in the  $^1\text{H}$  NMR spectrum of sample T (Figure 3.29) was comparable with the skewing of the multiplets of the rest of the samples (Figures 3.27 and 3.28). The peaks in the  $^1\text{H}$  NMR spectrum of sample T in the range of 3.80-4.50 ppm had risen at the same frequencies as the peaks of the rest of the samples. However, in comparison with the peaks of the rest of the samples in the frequency range concerned, it could be seen, from Figure 3.29, that the intensity and the width of the peaks of sample T had been reduced. Sample T contained three polyols. These included neopentyl glycol, 1,4 cyclohexanedimethanol and 1,6 hexanediol. The rest of the samples contained a maximum of two polyols. The content of neopentyl glycol in sample T was

lower than the rest of the samples. On the other hand, sample T was the only sample in which 1,4 cyclohexanedimethanol had been used. These may have resulted in the reduction of the intensity and the width of the peaks of sample T in the  $^1\text{H}$  NMR spectrum in the range of 3.80-4.50 ppm. Since sample T contained neopentyl glycol and 1,6 hexanediol, the assignments shown in Tables 3.46 and 3.48 could be made for its  $^1\text{H}$  NMR spectrum in the range concerned. Sample T also contained 1,4 cyclohexanedimethanol. Therefore, in addition to the assignments provided in Tables 3.46 and 3.48, the assignments that are provided in Table 3.49 as following could also be made for the  $^1\text{H}$  NMR spectrum of sample T in the range of 3.80-4.50 ppm.

**Table 3.49 Additional assignments for the  $^1\text{H}$  NMR spectrum of sample T in the range of 3.8-4.5 ppm** <sup>52,135,140-142,147</sup>

	M			
	N			
	O			
	M'			
	N'			
	O'			
<b>Sample</b>	<b><math>\delta</math> (PPM)</b>	<b>Assignment</b>	<b><math>\delta</math> (PPM)</b>	<b>Assignment</b>
T	3.96-4.12	M, M', N, N'	4.23-4.27	O, O'

The additional assignments that are provided in Table 3.49 could be made for the  $^1\text{H}$  NMR spectrum of sample T in the range concerned since the peaks produced by the terminal

methylene protons of neopentyl glycol moiety could have overlapped the peaks produced by the same protons in the residue of 1,4 cyclohexanedimethanol. For making the assignments shown in Table 3.49, the assignment made in the work published by Tsai et al<sup>52</sup> was also considered. Tsai et al<sup>52</sup> analysed a copolyester that contained 1,4 cyclohexanedimethanol by <sup>1</sup>H NMR and assigned the peak between 3.80-4.10 ppm to the terminal methylene protons of 1,4 cyclohexanedimethanol moiety (p.73).

The <sup>1</sup>H NMR spectra of the synthesised copolyesters, in the range of 6.50-7.20 ppm, are shown in Figure 3.30.

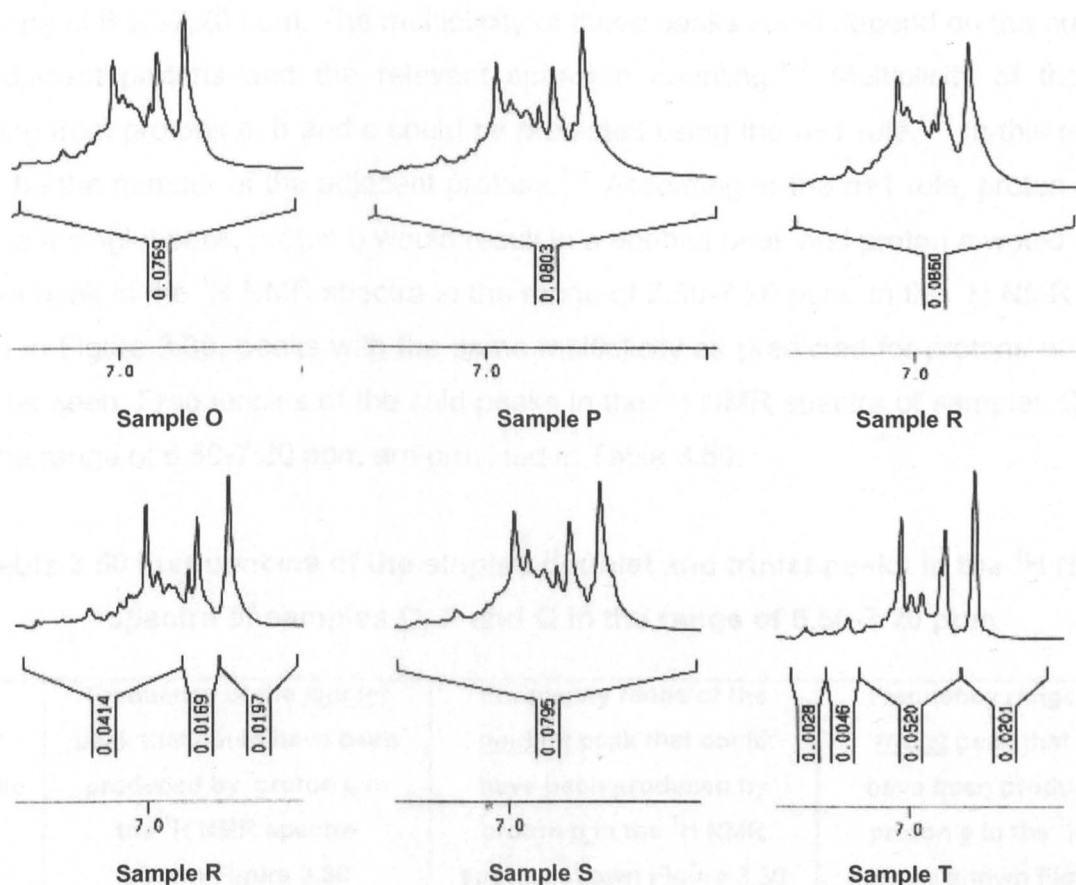
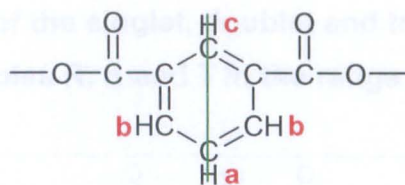


**Figure 3.30** <sup>1</sup>H NMR spectra in the range of 6.5-7.2 ppm

It could be seen, from Figure 3.30, that the synthesised copolyesters had resulted in similar peaks in the range of 6.50-7.20 ppm. The peaks in this particular frequency region could be due to the protons of the benzene ring of isophthalic moiety.<sup>140-142</sup> Protons on the benzene ring of isophthalic moiety that could have given rise to the peaks in the <sup>1</sup>H NMR spectra in the range of 6.50-7.20 ppm are shown in Scheme 3.5.





**Scheme 3.5** Protons that could have given rise to the peaks in the  $^1\text{H}$  NMR spectra in the range of 6.5-7.2 ppm<sup>140-142</sup>

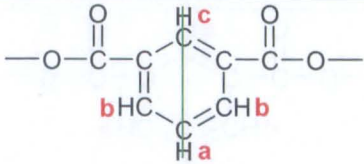
It could be seen, from Scheme 3.5, that on the benzene ring of isophthalic moiety, three protons were of unique chemical environments. These protons are marked a, b and c. Protons a, b and c could have given rise to three exclusive peaks in the  $^1\text{H}$  NMR spectra in the range of 6.50-7.20 ppm. The multiplicity of these peaks could depend on the number of the adjacent protons and the relevant spin-spin coupling.<sup>148</sup> Multiplicity of the peaks resulting from protons a, b and c could be predicted using the  $n+1$  rule.<sup>148</sup> In this regard,  $n$  would be the number of the adjacent protons.<sup>148</sup> According to the  $n+1$  rule, proton c would result in a singlet peak, proton b would result in a doublet peak and proton a would result in a triplet peak in the  $^1\text{H}$  NMR spectra in the range of 6.50-7.20 ppm. In the  $^1\text{H}$  NMR spectra shown in Figure 3.30, peaks with the same multiplicity as predicted for protons a, b and c could be seen. Frequencies of the said peaks in the  $^1\text{H}$  NMR spectra of samples O, P and Q in the range of 6.50-7.20 ppm are provided in Table 3.50.

**Table 3.50** Frequencies of the singlet, doublet and triplet peaks in the  $^1\text{H}$  NMR spectra of samples O, P and Q in the range of 6.50-7.20 ppm

Sample	Frequency of the <b>singlet</b> peak that could have been produced by proton <b>c</b> in the $^1\text{H}$ NMR spectra shown Figure 3.30	Frequency range of the <b>doublet</b> peak that could have been produced by proton <b>b</b> in the $^1\text{H}$ NMR spectra shown Figure 3.30	Frequency range of the <b>triplet</b> peak that could have been produced by proton <b>a</b> in the $^1\text{H}$ NMR spectra shown Figure 3.30
O	6.83 ppm	6.9-6.92 ppm	6.97-6.98-7.01 ppm
P	6.79 ppm	6.84-6.87 ppm	6.98-7.01-7.04 ppm
Q	6.86 ppm	6.92-6.95 ppm	6.97-6.98-7.01 ppm

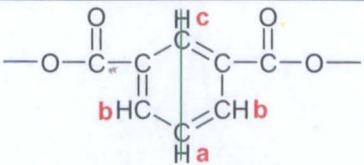
Frequencies of the peaks in the  $^1\text{H}$  NMR spectra of samples R, S and T with the same multiplicity as predicted for protons a, b, and c are provided in Table 3.51 as follows.

**Table 3.51** Frequencies of the singlet, doublet and triplet peaks in the  $^1\text{H}$  NMR spectra of samples R, S and T in the range of 6.50-7.20 ppm

			
Sample	Frequency of the <u>singlet</u> peak that could have been produced by proton <u>c</u> in the $^1\text{H}$ NMR spectra shown Figure 3.30	Frequency range of the <u>doublet</u> peak that could have been produced by proton <u>b</u> in the $^1\text{H}$ NMR spectra shown Figure 3.30	Frequency range of the <u>triplet</u> peak that could have been produced by proton <u>a</u> in the $^1\text{H}$ NMR spectra shown Figure 3.30
R	6.82 ppm	6.88-6.9 ppm	6.94-6.97-7 ppm
S	6.79 ppm	6.89-6.92 ppm	6.95-6.98-7.02 ppm
T	6.83 ppm	6.94-6.96 ppm	6.99-7.01-7.05 ppm

In the  $^1\text{H}$  NMR spectra of the copolyester samples in the range of 6.50-7.20 ppm, peaks that appeared in the frequencies specified in Tables 3.50 and 3.51 could be assigned to protons a, b and c of the isophthalic moiety. In this regard, the assignments that could be made for sample O are provided in Table 3.52.

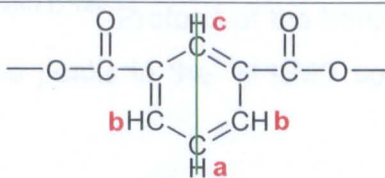
**Table 3.52** Assignments for the  $^1\text{H}$  NMR spectrum of sample O in the range of 6.5-7.2 ppm

						
Sample	$\delta$ (PPM)	Assignment	$\delta$ (PPM)	Assignment	$\delta$ (PPM)	Assignment
O	6.83	c	6.9-6.92	b	6.97-6.98-7.01	a

Based on the frequencies of the singlet, doublet and triplet peaks in the  $^1\text{H}$  NMR spectra in the range of 6.5-7.2 ppm, as specified in Tables 3.50 and 3.51, the assignments provided in Table 3.53 could be made for samples P, Q, R, S, and T.

**Table 3.53 Assignments for the  $^1\text{H}$  NMR spectra of samples P, Q, R, S and T in the range of 6.5-7.2 ppm**

Sample	$\delta$ (PPM)	Assignment	$\delta$ (PPM)	Assignment	$\delta$ (PPM)	Assignment
P	6.79	c	6.84-6.87	b	6.9-6.94-6.97	a
Q	6.86	c	6.92-6.95	b	6.98-7.01-7.04	a
R	6.82	c	6.88-6.9	b	6.94-6.97-7	a
S	6.79	c	6.89-6.92	b	6.95-6.98-7.02	a
T	6.83	c	6.94-6.96	b	6.99-7.01-7.05	a



The  $^1\text{H}$  NMR spectra of the synthesised copolyesters, in the range of 8.00-8.50 ppm, are shown in Figure 3.31.

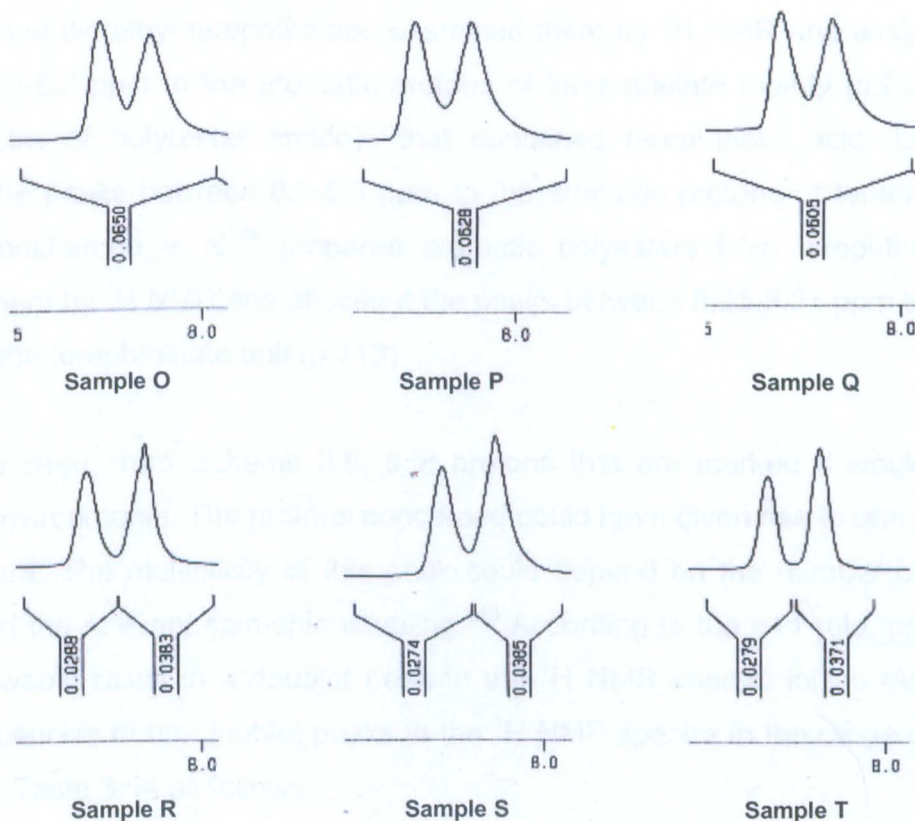
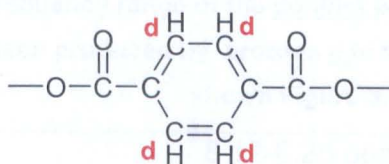


**Figure 3.31  $^1\text{H}$  NMR spectra in the range of 8.0-8.5 ppm**

It could be seen, from the  $^1\text{H}$  NMR spectra shown in Figure 3.31, that the synthesised copolyesters had resulted in similar peaks in the range of 8.0-8.5 ppm. The peaks that appeared in this particular frequency region could be due to the protons on the benzene ring of terephthalic moiety.<sup>31,60,140-142,149</sup> Protons of the benzene ring of terephthalic residue that could have given rise to the peaks in the  $^1\text{H}$  NMR spectra in the range of 8.00-8.50 ppm are shown in Scheme 3.6.

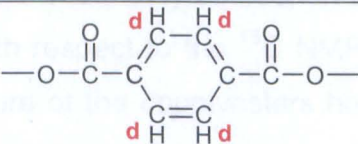


**Scheme 3.6 Protons that could have given rise to the peaks in the  $^1\text{H}$  NMR spectra in the range of 8.0-8.5 ppm**<sup>31,60,140-142,149</sup>

The interpretations made in the works published by Wang et al<sup>31</sup>, Lozano et al<sup>60</sup> and Honkhambe et al<sup>149</sup> also confirm that the peaks that appear in the range of 8.00-8.50 ppm could be due to the protons shown in Scheme 3.6. Wang et al<sup>31</sup> synthesised copolyesters that contained dimethyl terephthalate, examined them by  $^1\text{H}$  NMR and assigned the peak between 8.0-8.3 ppm to the aromatic protons of terephthalate moiety (p.2222). In the  $^1\text{H}$  NMR spectra of poly(ester amide)s that contained terephthalic acid, Lozano et al<sup>60</sup> assigned the peaks between 8.1-8.3 ppm to the aromatic protons of terephthalic residue (p.598). Honkhambe et al<sup>149</sup> prepared aromatic polyesters from terephthaloyl chloride, analysed them by  $^1\text{H}$  NMR and allocated the peaks between 8.25-8.35 ppm to the aromatic protons of the terephthalate unit (p.713)

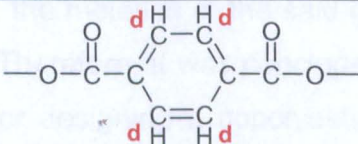
It could be seen, from Scheme 3.6, that protons that are marked d would be of equal chemical environments. The protons concerned could have given rise to one peak in the  $^1\text{H}$  NMR spectra. The multiplicity of this peak could depend on the number of the adjacent protons and the relevant spin-spin coupling.<sup>148</sup> According to the n+1 rule, protons that are marked d would result in a doublet peak in the  $^1\text{H}$  NMR spectra in the range of 8.0-8.5 ppm. Frequencies of the doublet peaks in the  $^1\text{H}$  NMR spectra in the range of 8.0-8.5 ppm provided in Table 3.54 as follows.

**Table 3.54** Frequencies of the doublet peaks in the  $^1\text{H}$  NMR spectra in the range of 8.0-8.5 ppm

	
Sample	Frequency range of the <b>doublet</b> peak that could have been produced by protons <b>d</b> in the $^1\text{H}$ NMR spectra shown Figure 3.31
<b>O</b>	8.12-8.25 ppm
<b>P</b>	8.09-8.22 ppm
<b>Q</b>	8.16-8.29 ppm
<b>R</b>	8.12-8.25 ppm
<b>S</b>	8.11-8.23 ppm
<b>T</b>	8.15-8.27 ppm

In the  $^1\text{H}$  NMR spectra of the copolyester samples in the range of 8.0-8.5 ppm, peaks that appeared in the frequencies specified in Table 3.54 could be assigned to the protons on the benzene ring of terephthalic moiety. In this regard, the assignments shown in Table 3.52 could be made.

**Table 3.55** Assignments for the  $^1\text{H}$  NMR spectra in the range of 8.0-8.5 ppm

		
Sample	$\delta$ (PPM)	Assignment
<b>O</b>	8.12-8.25	<b>d</b>
<b>P</b>	8.09-8.22	<b>d</b>
<b>Q</b>	8.16-8.29	<b>d</b>
<b>R</b>	8.12-8.25	<b>d</b>
<b>S</b>	8.11-8.23	<b>d</b>
<b>T</b>	8.15-8.27	<b>d</b>

No peaks appeared above 8.50 ppm in the  $^1\text{H}$  NMR spectra of the saturated polyester resins synthesised. With respect to the  $^1\text{H}$  NMR spectra, modifications made to the molecular structure of copolyesters could only be seen in the frequency range of 1.30-2.00 ppm. On the other hand and with respect to the  $^{13}\text{C}$  NMR spectra, inclusion of additional moieties to the molecular structure of the copolyesters had resulted in the appearance of exclusive peaks in the frequency ranges of 24-29 ppm, 33-37 ppm, 62-66 ppm, 164-168 ppm and 171-175 ppm. The  $^{13}\text{C}$  NMR spectra of the synthesised copolyesters were provided, interpreted and discussed in Section 3.2.2.1. Based on this, it was concluded that the  $^{13}\text{C}$  NMR analysis was more efficient than the  $^1\text{H}$  NMR analysis for studying the effect of the substitution or inclusion of polyols on the molecular structure of the resulting copolyester. On the whole, by evaluating the  $^{13}\text{C}$  NMR and the  $^1\text{H}$  NMR spectra, it could be concluded that the moieties present in the molecular structure of the synthesised copolyesters were in good agreement with the composition of the feed. For the feed composition of the copolyesters concerned, Table 3.21 can be used.

As mentioned in Section 3.2.2, in order to develop of a novel and standalone coil coating copolyester system, a glass transition temperature between 8-10°C needed to be achieved whilst an adequate degree of flexibility had to be maintained. For this purpose, 1,4 cyclohexanedimethanol and 1,6 hexanediol needed to be employed in the composition of the copolyester. By studying the  $^{13}\text{C}$  NMR and the  $^1\text{H}$  NMR spectra of the resulting copolyester (sample T), it could be seen that the inclusion of 1,4 cyclohexanedimethanol and 1,6 hexanediol in the feed composition had resulted in the rise of exclusive peaks in the said spectra. In other words, the moieties of the said glycols were definitely present in the molecular structure formed. Therefore, it was concluded that an appropriate molecular structure had been envisaged for designing a copolyester that would provide a suitable balance between flexibility, hardness and adhesion as a novel and standalone coil coating polyester resin system.

### 3.2.2.3 FTIR spectra

In this section, the FTIR spectra of the synthesised copolyesters are provided, interpreted and discussed. The feed compositions of the copolyesters that were analysed by FTIR spectroscopy were reviewed in Table 3.21. The parameters of the FTIR analysis were

mentioned in Section 2.4.3. The FTIR spectra of the synthesised copolyesters are shown in Figure 3.32.

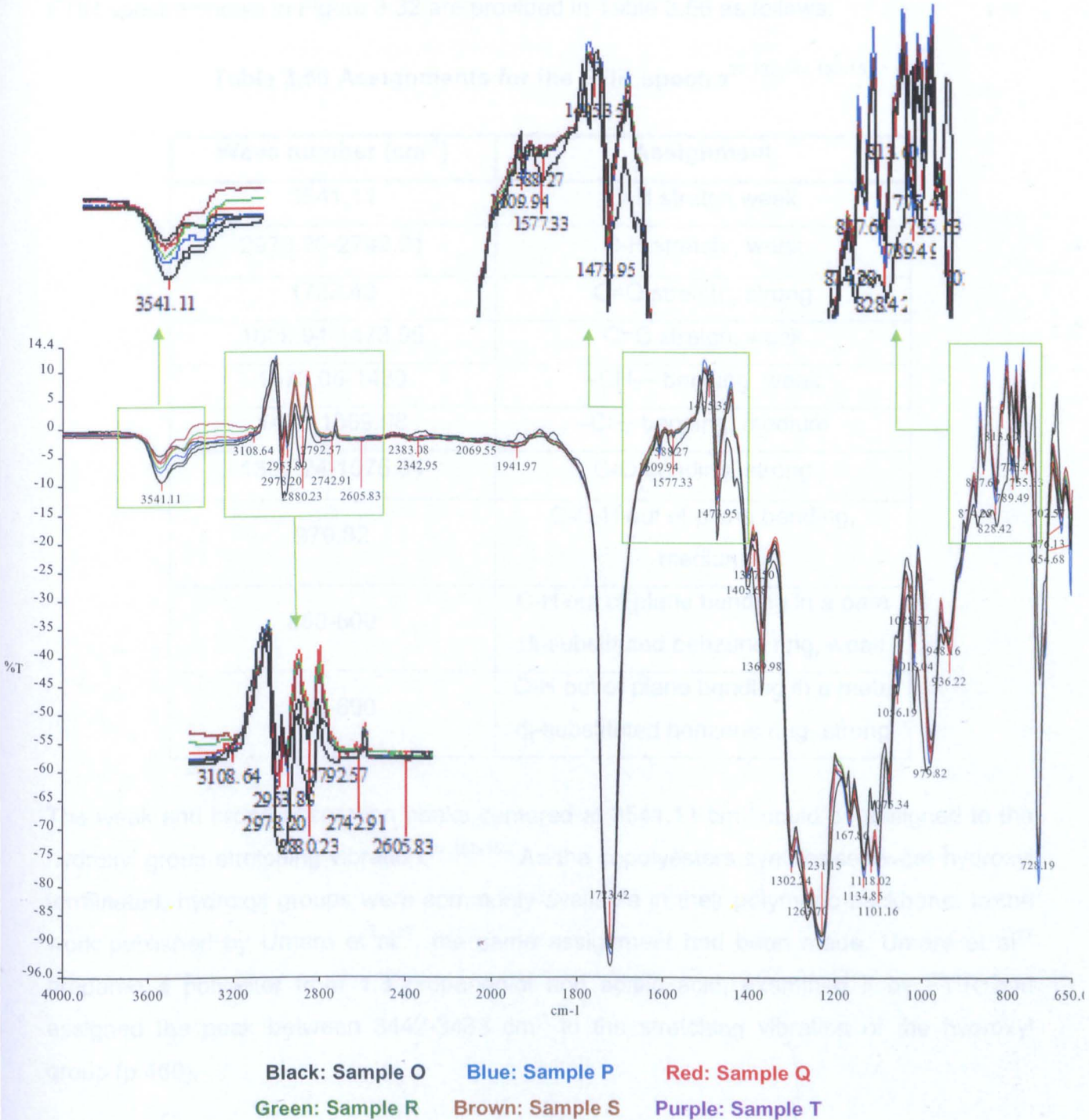


**Figure 3.32 FTIR spectra of the synthesised copolyesters**

It could be seen, from Figure 3.32, that the copolyester samples had resulted in similar absorption peaks in the FTIR spectra. It could also be seen, from Figure 3.32, that the absorption peaks of the samples overlaid each other well. The similarity of the FTIR

absorption peaks could be due to the resemblance of the functional groups of the moieties included in the molecular structure of the samples. Assignments that could be made for the FTIR spectra shown in Figure 3.32 are provided in Table 3.56 as follows.

**Table 3.56 Assignments for the FTIR spectra**<sup>27,132,144,150-153</sup>

Wave number (cm <sup>-1</sup> )	Assignment
3541.11	O-H stretch weak
2978.20-2742.91	C-H stretch , weak
1723.42	C=O stretch , strong
1609.94-1473.95	C=C stretch, weak
1473.05-1430	-CH <sub>2</sub> - bending, weak
1426-1369.98	-CH <sub>3</sub> bending, medium
1302.24-1075.34	C-O bending, strong
979.82	C-O-H out of plane bending, medium
850-800	C-H out of plane bending in a para di-substituted benzene ring, weak
780-690	C-H out of plane bending in a meta di-substituted benzene ring, strong

The weak and broad absorption peaks centered at 3541.11 cm<sup>-1</sup> could be assigned to the hydroxyl group stretching vibration.<sup>27,150-152</sup> As the copolyesters synthesised were hydroxyl terminated, hydroxyl groups were commonly available in their polymeric backbone. In the work published by Umare et al<sup>27</sup>, the same assignment had been made. Umare et al<sup>27</sup> prepared a polyester from 1,3 propanediol and adipic acid, examined it by FTIR and assigned the peak between 3442-3433 cm<sup>-1</sup> to the stretching vibration of the hydroxyl group (p.468).

The weak absorption peaks between 2978.20-2742.91 cm<sup>-1</sup> could be assigned to the stretching of C-H.<sup>27,132,150-152</sup> The same assignment had been made for the absorption peaks between 2800-3000 cm<sup>-1</sup> in the FTIR spectra of different polyesters by Umare et al<sup>27</sup> (p.468) and Mishra et al<sup>132</sup> (p.51).



The strong absorption peaks centered at  $1723.42\text{ cm}^{-1}$  could be assigned to carbonyl (C=O) stretching.<sup>27,144,150-153</sup> These peaks were indicative of the ester linkages that were present in the polymeric backbone of the copolyesters. In the works published by Umare et al<sup>27</sup> (p.468), Zhang and Hu<sup>144</sup> (p.3711) and Tang et al<sup>153</sup> (p.3362), the same assignment had been made for the absorption peaks between  $1738\text{-}1733\text{ cm}^{-1}$  in the FTIR spectra of different polyesters.

The weak absorption peaks within  $1609.94\text{-}1473.95\text{ cm}^{-1}$  could be assigned to C=C stretching.<sup>150-152</sup> Such groups would be in the aromatic rings of isophthalic and terephthalic moieties. Similar contents of isophthalic acid and terephthalic acid had been used in the feed composition of the synthesised copolyesters.

The weak absorption peaks between  $1473.05\text{-}1430\text{ cm}^{-1}$  could be assigned to methylene ( $-\text{CH}_2-$ ) bending.<sup>27,150-152</sup> The same assignment had been made by Umare et al<sup>27</sup> for the absorption peaks between  $1474\text{-}1454\text{ cm}^{-1}$  in the FTIR spectrum of 1,3 propanediol adipate (p.468) In the molecular structure of the polyester resins synthesised, methylene groups would be in the adipic residue and the moieties of the polyols. The polyols concerned include neopentyl glycol, trimethylol propane, 1,6 hexanediol and 1,4 cyclohexanedimethanol. With respect to sample Q which contained neopentyl glycol only, the absorption peaks within  $1473.05\text{-}1430\text{ cm}^{-1}$  could be due to the bending of the methylene groups in the moieties of neopentyl glycol and adipic acid. With respect to sample O which contained neopentyl glycol and trimethylol propane, the peaks between  $1473.05\text{-}1430\text{ cm}^{-1}$  could be due to the bending of the methylene groups in the moieties of neopentyl glycol, trimethylol propane and adipic acid. Samples P, R and S contained neopentyl glycol and 1,6 hexanediol. Therefore, their FTIR absorption peaks within  $1473.05\text{-}1430\text{ cm}^{-1}$  could be due to the bending of the methylene groups in the moieties of neopentyl glycol, 1,6 hexanediol and adipic acid. Sample T contained neopentyl glycol, 1,6 hexanediol, and 1,4 cyclohexanedimethanol. As a result, its absorption peaks within  $1473.05\text{-}1430\text{ cm}^{-1}$  could be due to the bending of the methylene groups in the moieties of neopentyl glycol, 1,6 hexanediol, 1,4 cyclohexanedimethanol and adipic acid.

The absorption peaks between  $1426\text{-}1369.98\text{ cm}^{-1}$  could be due to methyl ( $-\text{CH}_3$ ) bending.<sup>150-152</sup> In the molecular structure of the synthesised copolyesters, methyl groups would be available in the moieties of neopentyl glycol and trimethylol propane. Neopentyl

glycol had been used with different contents in the feed composition of the synthesised copolyesters. Trimethylol propane had only been used in sample O. Thus, the absorption peaks between  $1473.05\text{-}1430\text{ cm}^{-1}$  in the FTIR spectrum of sample O could be due to the methyl groups in the moieties of both neopentyl glycol and trimethylol propane.

The strong absorption peaks between  $1302.24\text{-}1075.34\text{ cm}^{-1}$  could be assigned to the C-O group of the ester linkages.<sup>150-153</sup> Tang et al<sup>153</sup> made the same assignment for the absorption peak at  $1170\text{ cm}^{-1}$  in the FTIR spectrum of a polyester derived from sebacic acid and glycerol.

The absorption peaks centered at  $979.82\text{ cm}^{-1}$  could be due to the carboxyl functionality.<sup>153</sup> Although the copolyesters had been designed with hydroxyl excess and synthesised as such so that the carboxyl functionality would be totally consumed, small traces of unreacted carboxyl functionality could have been present in their molecular structure.

The weak absorption peaks between  $850\text{-}800\text{ cm}^{-1}$  could be due to the out of plane bending of C-H in the meta di-substituted benzene ring.<sup>150-152</sup> With respect to the copolyester samples, the peaks concerned could be due to the C-H in the benzene ring of terephthalic residue. The strong absorption peaks within  $780\text{-}690\text{ cm}^{-1}$  could be due to the out of plane bending of C-H in the meta di-substituted benzene ring.<sup>150-152</sup> The peaks concerned could have been resulted by the C-H in the benzene ring of isophthalic moiety.

On the whole, the absorption peaks that could be seen in the FTIR spectra of the synthesised copolyesters (Figure 3.32) were similar and were due to the regular functional groups present in the molecular structure of the copolyesters. Unlike the  $^{13}\text{C}$  NMR and the  $^1\text{H}$  NMR spectra, the effect of the exclusion or inclusion of polyols on the molecular structure of the resulting copolyester could not be seen in the FTIR spectra.

### **3.2.3 Composition of the saturated polyester resins synthesised and the overall properties of the resulting coil coatings**

For links between the composition and the properties of the saturated polyester resins synthesised, Table 3.57 and Table 3.58 as follows can be used.

**Table 3.57 Composition, glass transition temperature and free hydroxyl content of the synthesised saturated polyester resins**

Sample Component	N	O	P	Q	R*	S	T
Adipic acid	1.78	2.01	2.01	2.01	1.97	1.97	1.97
Isophthalic acid	1.60	2.90	2.90	2.90	2.64	2.64	2.64
Terephthalic acid	2.93	1.45	1.45	1.45	1.75	1.75	1.75
Trimethylol propane	----	1.00	----	----	----	----	----
Neopentyl glycol	3.34	6.16	6.16	7.44	6.63	6.20	4.47
1,6 hexanediol	3.69	----	1.13	----	0.75	1.13	1.13
1,4 cyclohexanedimethanol	----	----	----	----	----	----	1.25
Total moles	13.35	13.52	13.65	13.80	13.71	13.69	13.22
Hydroxyl value (mgKOH/g)	51.68	93.44	67.42	78.37	72.91	69.23	34.88
Glass transition temperature (°C)	-4.20	13.83	1.37	9.24	6.22	2.42	8.27

\*: Formulation of sample R was designed through the combination of the formulations of samples N and Q according to their coil top coating mixing ratio. The relevant calculations were provided in Table 3.12.

**Table 3.58 Properties of the coil coatings derived from the synthesised saturated polyester resins**

Sample Properties	N	O	P	Q	N + Q **	R	S	T	T used as standalone binder in both primer coating and top coating	Coil primer coating and top coating film based on four control polyesters ***
	<b>T-bend</b>									
Cracking radius	0T	2T	0T	1T	0T	0.5T	0T	0T	0T	0T
Adhesion radius	0T	0T	0T	0T	0T	0T	0T	0T	0T	0T
Resistance to MEK solvent (double rubs)	200	150	90	125	140	118	95	200	200	100
Resistance to 15 Joules impact (% pass)	100	100	100	100	100	100	100	100	100	100
Konig pendulum film hardness (seconds @23°C)	20	151	43	126	88	93	55	100	90	77

\*\* : The mixing ratio in the coil top coating was 79.56 (sample Q) / 20.44 (sample T) (m:m).

\*\*\* : Specifications of the control polyesters and their mixing ratios in the coil primer coating and the coil top coating were provided in Section 2.5.2.

As described in Section 3.2.1.3 and shown in Tables 3.57 and 3.58, sample T performed as a novel and standalone binder system for the coil primer coating and the coil top coating. A combination of high flexibility, adequate adhesion, suitable glass transition temperature and chemical resistance was incorporated into sample T through the developmental stages described in Section 3.2.1.3. Being efficiently balanced in terms of the properties mentioned, sample T could be employed as a novel and sole binder system for the coil primer coating and the coil top coating. There was no requirement for employment of additional modifier polyesters in the coil primer coating and the coil top coating when sample T was used. Nowadays, modifier polyesters are commonly used in coil coatings to provide the required balance between hardness and flexibility.

With respect to the composition of the polyester samples shown in Table 3.57, the results of the tests of T-bend and pendulum film hardness for their resulting coil top coatings were discussed in Sections 3.2.1.2 and 3.2.1.3. Therefore, the results of the tests of resistance to MEK solvent, resistance to 15 Joules impact and resistance to salt spray will be discussed in Sections 3.2.3.1, 3.2.3.2 and 3.2.3.3 as follows.

### **3.2.3.1 Resistance of the coil top coating to MEK solvent**

As described in Section 2.5.1.2, this test was carried out for the coil top coatings derived from the polyester resins synthesised for evaluation of the degree of curing. All of the coil coatings prepared from the synthesised polyesters were cured in similar conditions. The curing conditions were described in Sections 2.5.3.5 and 2.5.3.6. The curing agent used for the samples was the same curing agent that had been used for the control polyesters. The amount of the curing agent used for the samples was similar to the amount used for the control polyesters. Details of the curing agent used and its incorporation amount in the coil top coating were provided in Section 1.7.1 and Section 2.5.2. Table 3.57 and Table 3.58 can be used for links between the composition of the polyesters and their resistance to MEK solvent in the coil top coating.

Similar to the results discussed in Section 3.1.3, the outcome indicated that regardless of the hydroxyl content, the hard monomers used in the composition of the polyesters had a considerable effect on the solvent resistance of the resulting coil coating film. Based on the

composition of the synthesised polyesters (Table 3.57), the following conclusions were made regarding the results of the MEK solvent double rub test.

- 1- The coil top coatings derived from samples P and S gave 90 and 95 MEK double rubs respectively. The coil top coatings derived from the rest of the samples gave 100 or over 100 MEK double rubs.
- 2- Regarding the probable increase in the number of MEK double rubs by higher hydroxyl content and consequently higher degree of crosslinking, samples O, Q and R were considered. The hydroxyl contents of the said samples were above 70 mgKOH/g and higher than the rest of the samples shown in Table 3.57. The coil top coatings based on samples O, Q and R gave 150, 125 and 118 MEK double rubs.
- 3- Regarding the probable decrease in the number of MEK double rubs by lower hydroxyl content and consequently lower degree of crosslinking, samples P and S were considered. The hydroxyl contents of the said samples were below 70 mgKOH/g. The coil top coatings based on samples P and S gave 90 and 95 MEK double rubs.
- 4- It could be seen, from Tables 3.57 and 3.58, that regardless of the hydroxyl content, the hard monomers included in the composition of the polyesters affected the MEK solvent resistance of the resulting coil coating. This conclusion was made according to the MEK solvent resistance of the coil top coatings derived from samples N and T. The free hydroxyl content of samples N and T was lower than the rest of the samples shown in Table 3.57. However, the coil top coatings based on samples N and T gave 200 MEK double rubs. The overall content of the aromatic diacids of isophthalic and terephthalic in the composition of sample N was comparable with the rest of the polyesters shown in Table 3.57. However, the content of terephthalic acid included in sample N was almost twice the content of isophthalic acid. The rest of the samples contained more isophthalic acid than terephthalic acid. It has been confirmed that terephthalic acid further increases the mechanical and resistance properties of polyesters in comparison to isophthalic acid.<sup>31,44,61</sup> Therefore, the higher MEK solvent resistance of the coil top coating derived from sample N could be due to the high content of terephthalic moiety in its backbone. The content of isophthalic acid and terephthalic acid in the composition of

sample T was comparable with the rest of the samples excluding sample N. However, 1.25 moles of 1,4 cyclohexanedimethanol had been included in sample T. 1,4 cyclohexanedimethanol had not been included in the composition of the rest of the samples. Therefore, the higher solvent resistance of the coil top coating derived from sample T was due to the presence of 1,4 cyclohexanedimethanol moiety in its molecular structure. Awasthi and Agrawal<sup>56</sup> had also concluded that inclusion of 1,4 cyclohexanedimethanol in the composition of the polyester would result in increased solvent resistance (p.48).

- 5- The MEK solvent resistance of samples S and T indicated that 1,4 cyclohexanedimethanol resulted in a better solvent resistance than neopentyl glycol. The coil top coating based on sample S gave 95 MEK double rubs. On the other hand, the coil top coating based on sample T gave 200 MEK double rubs. The formulation of sample T was designed by modification of the formulation of sample S. As can be seen from Table 3.57, the content of neopentyl glycol was reduced by 1.73 moles and 1.25 moles of 1,4 cyclohexanedimethanol was included. As a result of this modification, the solvent resistance of the coil top coating derived from sample T increased. As shown in Section 3.2.1.3, the inclusion of 1,4 cyclohexanedimethanol in the composition of sample T also resulted in the achievement of undisturbed flexibility, adequate adhesion and the desired glass transition temperature. Therefore, it was concluded that for designing a novel and standalone coil coating polyester system with a combination of the properties mentioned as well as high solvent resistance, the moiety of 1,4 cyclohexanedimethanol should definitely be built into the polyester backbone.

### **3.2.3.2 Resistance of the coil top coating to cracking after deformation by 15 Joules impact**

Table 3.57 and Table 3.58 can be used for links between the composition of the polyesters and their resistance to cracking after deformation by 15 Joules impact. Based on the composition of the synthesised polyesters (Table 3.57), the following conclusions were made with respect to the results of the impact test.

- 1- It could be seen, from the results shown in Table 3.58, that the coil top coatings which passed the T-bend test, also passed the 15 Joules impact test. The T-bend cracking radii of the coil top coatings derived from samples O and Q were 2T and

1T. In other words, these polyester resins were not flexible enough. As concluded in Section 3.1.4, the impact resistance of the coil top coating highly depended on its efficient flexibility. Therefore, the impact resistance of the coil top coatings based on samples O and Q was not satisfactory due to the insufficient flexibility of these saturated polyester resins.

- 2- The insufficient flexibility of sample O was due to the inclusion of trimethylol propane in its composition. As discussed and concluded in Sections 3.1.2 and 3.2.1.2, a branched structure would be achieved for the polyester as a result of the incorporation of trimethylol propane. Therefore, the flexibility of the resulting coil coating film would be weak.
- 3- In Section 3.2.1.3, it was concluded that saturated polyester resins that were prepared from different dicarboxylic acids and neopentyl glycol, could be employed for coil top coatings in combination with saturated polyester resins of high linearity. Examples of such combinations with respect to the synthesised polyesters would be samples N and Q. Formulations of samples N and Q are shown in Table 3.57. It could be seen, from Table 3.58, that the impact resistance of the coil top coating based on the mixture of samples N and Q was satisfactory. On the other hand, the impact resistance of the coil top coating solely derived from sample Q was weak.
- 4- The impact resistance of the coil top coating was significantly improved as 1,6 hexanediol was incorporated in the composition of its base polyester resin. This conclusion was made based on the performances of the coil top coatings derived from samples P and Q. The contents of the dicarboxylic acids of samples P and Q were similar. Sample P contained 6.16 moles of neopentyl glycol and 1.13 moles of 1,6 hexanediol. Sample Q contained 7.44 moles of neopentyl glycol. The impact resistance of the coil top coating resulting from sample P was satisfactory. On the other hand, the impact resistance of the coil top derived from sample Q was weak. Obviously, 1,6 hexanediol had provided further elongation tolerance and flexibility for sample P.
- 5- It could be seen, from Table 3.58, that the resulting coil top coating films of samples R, S and T passed the impact test. The contents of the dicarboxylic acids of the said

samples were similar. Sample R contained 0.75 mole of 1,6 hexanediol and 6.63 moles of neopentyl glycol. Sample S contained 6.20 moles of neopentyl glycol and 1.13 moles of 1,6 hexanediol. Sample T contained 4.47 moles of neopentyl glycol, 1.25 moles of 1,4 cyclohexanedimethanol and 1.13 moles of 1,6 hexanediol. As mentioned, the result of the impact test highly depended on the content of 1,6 hexanediol. As the coil top coatings based on samples R, S and T passed the impact test, it could be concluded that the content of 1,6 hexanediol for such polyester systems should be within 0.75-1.13 moles. Incorporation of 1,6 hexanediol by the amount mentioned, would provide the required flexibility for the resulting coil top coating film and there will be no occurrence of cracking after the 15 Joules impact.

### 3.2.3.3 Resistance to salt spray

As shown and concluded in Sections 3.2.1.3, 3.2.3.1 and 3.2.3.2, the saturated polyester resin synthesised as sample T performed well as a novel and standalone coil primer coating and coil top coating binder system. Thus, a primer coating and a top coating was derived solely from sample T according to the procedures mentioned in Sections 2.5.3.2 and 2.5.3.3. The coatings mentioned were applied on a galvanised steel substrate according to the procedures mentioned in Section 2.5.3.6. The test of resistance to salt spray was carried for the coated panel according to the procedure described in Section 2.5.1.4. The appearance of the galvanised steel panel after completion of the salt spray test cycle is shown in Figure 3.33.



**Figure 3.33 Appearance of the coil top coating film derived from the developed standalone polyester resin system after completion of the salt spray test**



It could be seen, from Figure 3.33, that there were no occurrence of blistering along the X-shaped cuts. In addition, hardly any creeping of rust was present after the 500 hours of exposure. Thus, the resistance of the coil coating to salt spray was satisfactory.

### 3.2.4 Characteristics of the pilot scale and the industrial scale reproductions of the novel and standalone coil coating polyester resin developed

The developed standalone polyester resin system (sample T) was reproduced at the pilot and industrial scales. The polymerisation details of the pilot scale reproduction of sample T was shown in Table 2.16. The polymerisation details of the industrial scale reproduction of sample T was shown in Tables 2.18A and 2.18B. In this regard, the molecular weight characteristics of the pilot scale and the industrial scale reproductions were determined by size exclusion chromatography. The resulting chromatograms are provided and discussed in Section 3.2.4.1. The coil coating film properties of the pilot scale and industrial scale reproductions of sample T are also provided in Section 3.2.4.2.

#### 3.2.4.1 Size exclusion chromatography of the pilot scale and the industrial scale reproductions of sample T

The GPC chromatogram of sample T is shown in Figure 3.34.

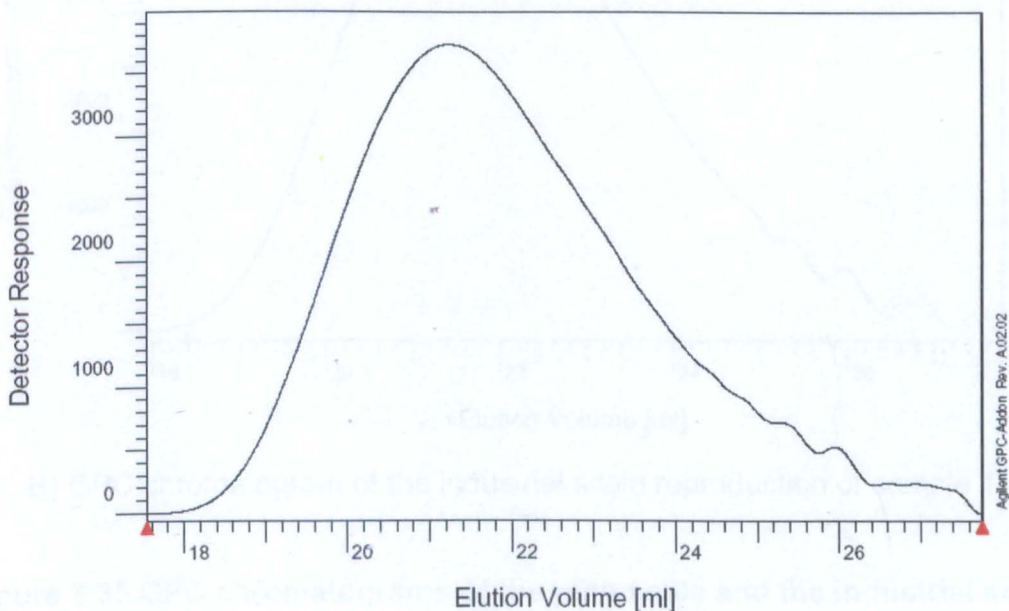
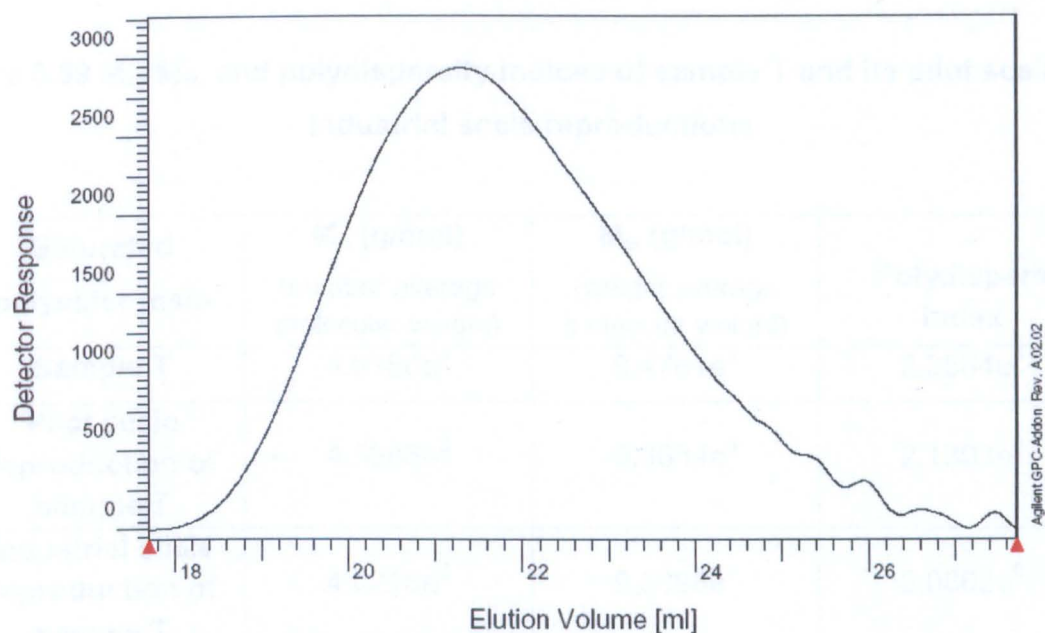
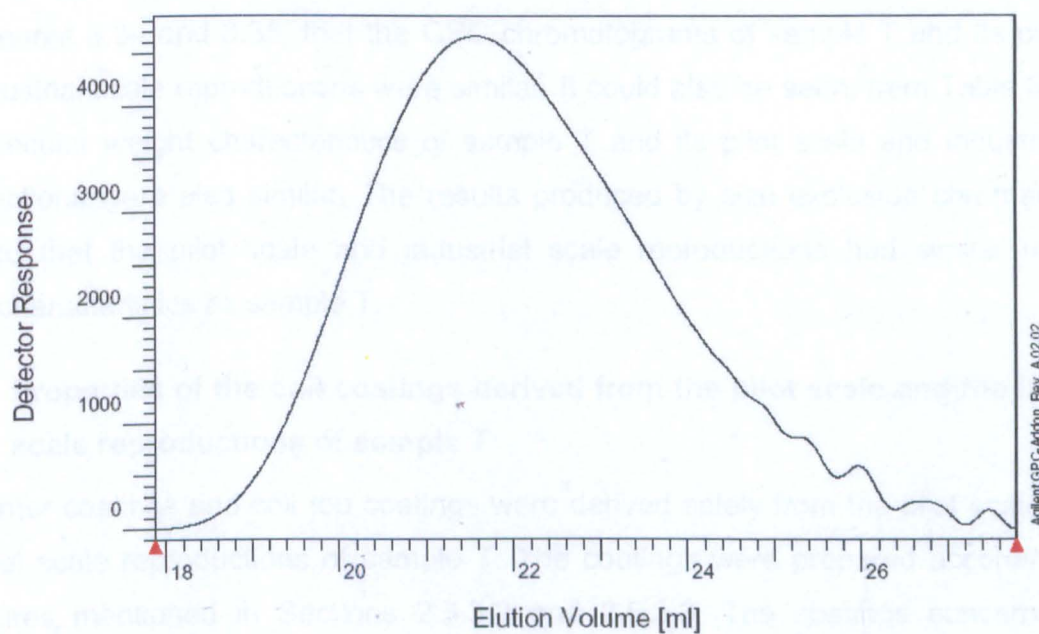


Figure 3.34 GPC chromatogram of sample T

The GPC chromatograms of the pilot scale and the industrial scale reproductions of sample T are shown in Figure 3.35.



A) GPC chromatogram of the pilot scale reproduction of sample T



B) GPC chromatogram of the industrial scale reproduction of sample T

**Figure 3.35 GPC chromatograms of the pilot scale and the industrial scale reproductions of sample T**

The number average molecular weight, the weight average molecular weight and the polydispersity index of sample T and its pilot scale and industrial scale reproductions are shown in Table 3.59.

**Table 3.59  $M_n$ ,  $M_w$ , and polydispersity indices of sample T and its pilot scale and industrial scale reproductions**

<b>Saturated polyester resin</b>	<b><math>M_n</math> (g/mol)</b> (number average molecular weight)	<b><math>M_w</math> (g/mol)</b> (weight average molecular weight)	<b>Polydispersity index</b>
<b>Sample T</b>	4.0180e <sup>3</sup>	9.4761e <sup>3</sup>	2.3584e <sup>0</sup>
<b>Pilot scale reproduction of sample T</b>	4.5386e <sup>3</sup>	9.6684e <sup>3</sup>	2.1303e <sup>0</sup>
<b>Industrial scale reproduction of sample T</b>	4.0216e <sup>3</sup>	9.3898e <sup>3</sup>	2.0862e <sup>0</sup>

The parameters shown in Table 3.59 were determined by the instrument. It could be seen, from Figures 3.34 and 3.35, that the GPC chromatograms of sample T and its pilot scale and industrial scale reproductions were similar. It could also be seen, from Table 3.59, that the molecular weight characteristics of sample T and its pilot scale and industrial scale reproductions were also similar. The results produced by size exclusion chromatography indicated that the pilot scale and industrial scale reproductions had similar molecular weight characteristics as sample T.

#### **3.2.4.2 Properties of the coil coatings derived from the pilot scale and the industrial scale reproductions of sample T**

Coil primer coatings and coil top coatings were derived solely from the pilot scale and the industrial scale reproductions of sample T. The coatings were prepared according to the procedures mentioned in Sections 2.5.3.2 and 2.5.3.3. The coatings concerned were applied on galvanised steel substrates according to the procedure mentioned in Section 2.5.3.6. The resulting coil coating films were tested according to procedures described in Section 2.5.1. The results of the tests are provided in Table 3.60 as follows.

**Table 3.60 Properties of the coil coatings derived from the pilot scale and the industrial scale reproductions of sample T**

<b>Polyester</b> <b>Property</b>	<b>Sample T</b>	<b>Pilot scale reproduction of sample T</b>	<b>Industrial scale reproduction of sample T</b>	<b>Test method</b>
<b>Cracking radius of the T-bend test</b>	0T	0T	0T	ECCA-T7
<b>Adhesion radius of the T-bend test</b>	0T	0T	0T	
<b>Resistance to MEK solvent (double rubs)</b>	200	200	200	ECCA-T11
<b>Resistance to deformation by impact (% pass)</b>	100	100	100	ECCA-T5
<b>Resistance to salt spray</b>	Length of blistering: <3mm	Length of blistering: <3mm	Length of blistering: <3mm	ECCA-T8
	Length of creeping of rust: <3mm	Length of creeping of rust: <3mm	Length of creeping of rust: <3mm	
<b>Konig Pendulum film hardness (seconds @ 23°C)</b>	90	91	93	ISO 1522

The results shown in Table 3.60 indicated that in terms of the coil coating film properties, complete reproducibility had been achieved with the pilot scale and the industrial scale reproductions of sample T as a novel and standalone coil coating polyester resin system.

## CHAPTER 4 - CONCLUSIONS

The main objective of this project was to synthesise and characterise a novel and standalone coil coating saturated polyester resin system with multiple properties. The properties concerned included excellent flexibility, adequate adhesion, high hardness and appropriate chemical resistance. The resin system to be developed was desired to act as a singular binder system in both coil primer coating and coil top coating. Nowadays, a combination of up to five polyester resins have to employed in coil primer coatings and coil top coatings to provide the required flexibility, adhesion, hardness and chemical resistance. Due to the reasons mentioned in Section 1.2, coil coatings have to be extremely flexible and hard. On the whole, research into development of singular polyester systems for coil coatings that would contribute to all the properties required appeared to be limited. One the more relevant published works in this regard was that of Boyes et al<sup>29,107</sup>. In the work concerned, effort was made to develop a polyester system with balanced hardness and flexibility through grafting *p*-hydroxybenzoic acid to a hydroxyl functional polyester. Eventually, the product developed by Boyes et al<sup>29,107</sup> failed to provide the required properties at the rapid coil coating curing process. Through the developmental stages described in Sections 3.1 and 3.2.1, the direct esterification of a combination of specific diols and dicarboxylic acids resulted in a saturated polyester resin system that provided the desired properties. The composition of the novel polyester system developed is shown in Table 4.1.

**Table 4.1 Composition of the novel and standalone coil coating saturated polyester resin system developed**

Dicarboxylic acid	Structure	Moles	Diol	Structure	Moles
Adipic acid		1.96	Neopentyl glycol		4.47
Terephthalic acid		1.75	1,6 hexanediol		1.13
Isophthalic acid		2.63	1,4 cyclohexane - dimethanol		1.25

The novel polyester system developed was used as a replacement for four control polyesters in a coil primer coating and a coil top coating. The coil coating solely derived from the newly developed polyester system provided the same properties previously achieved through employment of four polyester resins. The properties concerned were evaluated through a series of standard coating film tests. These included resistance to cracking on bending, resistance to MEK solvent, resistance to cracking after rapid deformation, resistance to salt spray and pendulum film hardness. The methods of the tests mentioned were described in Section 2.5.1. Basis of selection with respect to the properties desired to be achieved was mentioned in Section 2.5.2. The properties achieved by the coil coatings derived solely from the new polyester system developed (sample T) were shown in Table 3.58.

Polyesters that were synthesised during the early stages of the study provided valuable understanding for designing a standalone coil coating binder system. The early results indicated that in order to develop such a binder, achievement of an optimum balance among flexibility, adhesion and glass transition temperature was critical. Essential and completing knowledge was achieved through the synthesis and characterisation of the products discussed in Section 3.2.1. The new product developed and its precursors were characterised by differential scanning calorimetry,  $^{13}\text{C}$  NMR,  $^1\text{H}$  NMR, FTIR and size exclusion chromatography. The fundamental conclusions that were made as a result of this study included the following;

- 1- Triols such as trimethylol propane could not be included in the composition of the polyester. Inclusion of triols in the composition resulted in the formation of a branched molecular structure. Therefore, the flexibility of the resulting coil top coating film was insufficient to obtain the lowest cracking radius of the T-bend test. The method of the T-bend test or resistance to cracking on bending was described in Section 2.5.1.1. For the achievement of the desired flexibility, only diols had to be employed.
- 2- The aromatic dicarboxylic acids of isophthalic and terephthalic provided the required adhesion for the new polyester. It was concluded that a total of 4.10 to 4.65 moles of the mentioned dicarboxylic acids had to be included in the composition. The molar content mentioned pertained to a feed composition in which a sum total of 13.00-13.50 moles of diols and diacids had been used. In this regard, the appropriate

contents were 2.63-2.90 moles for isophthalic acid and 1.45-1.75 moles for terephthalic acid.

- 3- It was concluded that the solvent resistance of the coil top coating depended on the contents of the aromatic and cycloaliphatic components. In this regard, the contents shown in Table 4.1 for isophthalic acid, terephthalic acid and 1,4 cyclohexane-dimethanol provided the required solvent resistance for the resulting coil top coating film.
- 4- It was concluded that the new polyester had to be designed with low hydroxyl content. It was observed that polyesters with low hydroxyl contents resulted in coil coatings with superior flexibility. In this regard, the saturated polyester resin needed to be designed with a theoretical hydroxyl content of 20-40 mgKOH/g.
- 5- The results produced by differential scanning calorimetry (DSC) confirmed that the glass transition temperature of the saturated polyester resin directly affected the pendulum hardness of the resulting coil top coating film. Augmentation of the glass transition temperature of the saturated polyester resin resulted in increased pendulum film hardness for the coil top coating. On the other hand, the reduction of the glass transition temperature of the saturated polyester resin resulted in the reduction of the pendulum hardness of the resulting coil top coating film. For a detailed discussion pertaining to this matter, Section 3.2.1 can be used.
- 6- It was concluded that for the achievement of the desired pendulum film hardness, a saturated polyester resin with a glass transition temperature between 8-10°C needed to be designed. As mentioned in Section 2.5.2, the König pendulum film hardness of the coil top coating needed to be between 70-100 seconds at 23°C. The method and the instrument used for the determination of the König pendulum film hardness were described in Section 2.5.1.5.
- 7- It was concluded that incorporation of aliphatic moieties to the molecular structure of the polyester resulted in the reduction of the glass transition temperature. With respect to the saturated polyester resins synthesised, this phenomenon was observed when 1,6 hexanediol was employed. As the molar content of 1,6 hexanediol in the feed composition increased, the glass transition temperature of the

resulting saturated polyester resin was reduced. In this regard, the discussion provided in Section 3.2.1.2 can be used.

- 8- It was concluded that in order to achieve the required flexibility, specific contents of the aliphatic hexanedioic (adipic) acid and 1,6 hexanediol had to be included in the composition. With respect to 1,6 hexanediol, inclusion of 1.13 moles sufficed. Regarding adipic acid, a molar content of 1.97-2.01 moles in the feed composition would be adequate.
- 9- It was concluded that in order to compensate for the loss of glass transition temperature as a result of the inclusion of aliphatic moieties, the best approach would be to include an appropriate content of a cycloaliphatic moiety to the molecular structure. Such modification would result in the augmentation of the glass transition temperature without disturbing the flexibility. With respect to the new polyester system developed, inclusion of 1.25 moles of 1,4 cyclohexanedimethanol provided an excellent compromise between glass transition temperature and flexibility. When the composition shown in Table 4.1 was synthesised with 6.20 moles of neopentyl glycol and without the inclusion of 1,4 cyclohexanedimethanol, the glass transition temperature of the resulting polyester was 2.42°C. However, when the molar content of neopentyl glycol was reduced to 4.47 moles and 1,4 cyclohexanedimethanol was incorporated by 1.25 moles, the glass transition temperature of the resulting polyester was 8.27°C. The latter glass transition temperature resulted in the achievement of a König pendulum film hardness of 90 seconds at 23°C. On the other hand, the molar contents of the aliphatic components of adipic acid and 1,6 hexanediol remained unchanged and the flexibility of the polyester resin was maintained. For a detailed discussion in this regard, Section 3.2.1.3 can be used.
- 10- The carbon-13 nuclear magnetic resonance ( $^{13}\text{C}$  NMR) and the proton nuclear magnetic resonance ( $^1\text{H}$  NMR) spectra of the synthesised copolyesters provided valuable information regarding their molecular structure. The copolyesters had been prepared from three dicarboxylic acids and a variety of polyols. Complexity could be seen in the  $^{13}\text{C}$  NMR and the  $^1\text{H}$  NMR spectra. This was due to the effect of different neighbors on each kind of carbon or proton. However, modifications made to the molecular structure of the synthesised copolyesters could be observed and studied



in specific frequency ranges of the  $^{13}\text{C}$  NMR and the  $^1\text{H}$  NMR spectra. Modifications had been made through partial replacement of neopentyl glycol with 1,6 hexanediol and 1,4 cyclohexanedimethanol. Exclusive peaks appeared in specific frequency ranges of the  $^{13}\text{C}$  NMR and the  $^1\text{H}$  NMR spectra that could be due to the carbons and protons in the moieties of 1,6 hexanediol and 1,4 cyclohexanedimethanol. 1,6 hexanediol and 1,4 cyclohexanedimethanol had been included to achieve the desired balance between flexibility and glass transition temperature. From the  $^{13}\text{C}$  NMR and the  $^1\text{H}$  NMR spectra, it could also be concluded that the composition of the new copolyester system and its precursors were in good agreement with those expected from the composition of the feed. The  $^{13}\text{C}$  NMR and the  $^1\text{H}$  NMR spectra of the saturated polyester resins synthesised were provided, interpreted and discussed in Sections 3.2.2.1 and 3.2.2.2.

- 11- It was concluded that the  $^{13}\text{C}$  NMR analysis was more effective than the  $^1\text{H}$  NMR analysis for studying the effect of the substitution of diols on the molecular structure of the resulting polyester. Considering the  $^{13}\text{C}$  NMR spectra, it could be seen that variations of the molecular structure were visible in the form of exclusive peaks in the frequency ranges of 24-29 ppm, 33-37 ppm, 62-66 ppm, 164-168 ppm and 171-175 ppm. On the other hand and with respect to the  $^1\text{H}$  NMR spectra, dissimilarities in the molecular structure could only be seen in the frequency range of 1.30-2.00 ppm.
- 12- Alteration made to the molecular structure of the synthesised copolyesters could not be seen in the Fourier transformed infrared (FTIR) spectra. Overall, the absorption peaks that could be seen in the FTIR spectra of the copolyesters were similar to a great extent and mostly pertained to the functional groups of the moieties included in their molecular structure.
- 13- According to size exclusion chromatography (SEC), the molecular weight characteristics of the pilot scale and the industrial scale reproductions of the standalone coil coating polyester resin system developed were comparable with the initial product synthesised at the lab scale. The relevant chromatograms were provided and discussed in Section 3.2.4.1.

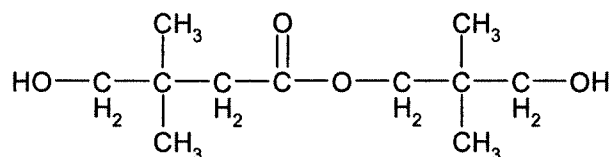
14- The novel and standalone polyester resin system developed for coil primer coatings and coil top coatings was successfully reproduced at the industrial scale. The procedure of synthesis and the polymerisation details pertaining to the industrial scale reproduction were provided in Sections 2.3.4, 2.3.5.1 and 2.3.5.4. For the characteristics, molecular weight attributes, mechanical and chemical resistance properties of the industrial scale reproduction of the invented polyester resin system, Sections 2.3.5.6, 3.2.4.1 and 3.2.4.2 can be used respectively.

## CHAPTER 5 – FUTURE WORK

The market for exterior purposed coated steel coils continues to grow constantly worldwide. The growth in the consumption of coil coatings for outdoor steel sheets has resulted in the demand for improved exterior durability of the coil top coating. Therefore, the augmentation of the exterior durability has become a key requirement for the coil top coating systems.

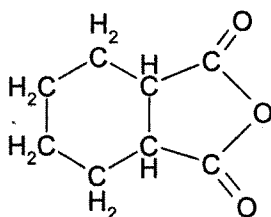
There are three factors which dominantly cause the degradation of coil coatings in outdoor conditions. These include UV radiation, heat and moisture. Coil coatings that are used in outdoor conditions would be subjected to the combined action of UV radiation, moisture and heat. This could result in chemical changes in their polymeric network. These chemical changes often result in the loss of gloss, blistering and cracking.<sup>6</sup> One of the more important factors causing the degradation of coil coatings is high UV radiation. In the majority of the polyester based coil top coatings, additives which absorb UV light are employed to increase the exterior durability of the coating film. The incorporation of these additives results in the augmentation of the exterior durability. However, the exterior durability achieved through the inclusion of UV absorbing additives is often not satisfactory. Santos et al<sup>116</sup> studied the behaviour of polyester and silicone modified polyester coil coatings and concluded that silicone modified polyesters would degrade less than pure polyesters. In spite of this, cost effective pure polyesters can be developed that could provide excellent durability in high UV environments. Inclusion of high contents of moieties with labile  $\beta$  hydrogens in the molecular structure of the polyester results in decreased resistance to UV radiation.<sup>154</sup> Excellent exterior durability can be achieved through minimisation of the content of labile  $\beta$  hydrogens in the polyester. In this regard, the knowledge and experience achieved throughout the course of this project will be employed for the synthesis and characterisation of a standalone coil top coating saturated polyester resin system with high resistance to UV radiation and outdoor conditions. Effort will be made to incorporate the same exceptional and novel properties of the polyester system invented throughout the course of this study to the UV radiation durable polyester system to be developed. In other words, a polyester system is desired to be developed that, apart from high resistance to UV radiation, would simultaneously provide extreme flexibility, excellent adhesion, high film hardness and suitable chemical resistance.

In terms of polyester components, it can be envisaged that isophthalic acid, terephthalic acid, 1,4 cyclohexanedimethanol and 1,4 cyclohexanedicarboxylic acid would provide poor or moderate UV radiation resistance. Isophthalic acid and terephthalic acid contain unsaturated aromatic rings. Although the cyclohexyl rings of 1,4 cyclohexanedimethanol and 1,4 cyclohexanedicarboxylic acid are completely saturated, the presence of labile  $\beta$  hydrogens limits their exterior durability. For molecular structures of the polyacids and the polyols mentioned, Section 1.6 can be used. Throughout the course of this study, it was concluded that exclusion or minimal inclusion of the polyols and the polyacids mentioned would result in the loss of adhesion, chemical resistance and glass transition temperature. However, these losses may be compensated for through the inclusion of a certain polyol and a certain phthalic acid. The polyol concerned in this regard is hydroxy pivalic acid neopentyl glycol ester (HPN). The molecular structure of HPN is shown in Scheme 5.1.



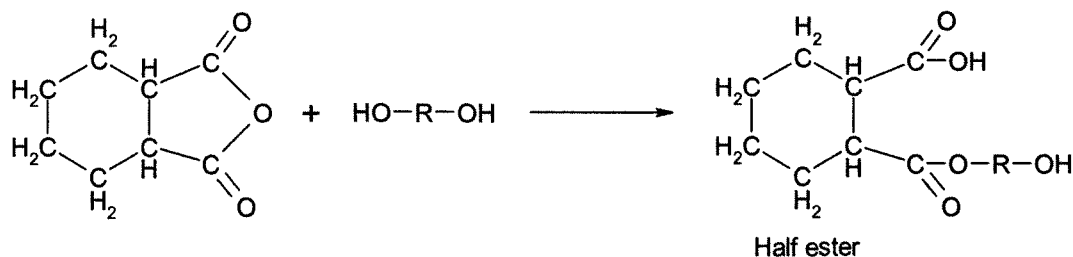
**Scheme 5.1 Molecular structure of hydroxy pivalic acid neopentyl glycol ester<sup>154</sup>**

It can be seen, from Scheme 5.1, that there are no labile  $\beta$  hydrogens in the molecule of HPN. This diol can partly replace 1,4 cyclohexanedimethanol. The exclusion or reduction in the content of 1,4 cyclohexanedimethanol should increase the exterior durability of the polyester resin. On the other hand, it may not be possible to totally eliminate 1,4 cyclohexanedimethanol due to its effect on increasing the glass transition temperature of the polyester resin. A detailed discussion in this regard was provided in Section 3.2.1.3. The effect of the inclusion of HPN on the glass transition temperature will be determined by differential scanning calorimetry. As replacement for isophthalic acid and terephthalic acid, hexahydrophthalic anhydride (HHPA) could be employed. The molecular structure of HHPA is shown in Scheme 5.2.



**Scheme 5.2 Molecular structure of hexahydrophthalic anhydride<sup>155</sup>**

During the synthesis of the polyester, HHPA can react with the hydroxyl functionality of a diol to form a half ester. The scheme for this reaction is shown in the following.



**Scheme 5.3 Reaction of hexahydrophthalic anhydride and a diol**

The half ester could then take part in a direct esterification reaction with a diol. It could be presumed that the inclusion of HHPA in the backbone of the polyester resin and the exclusion of isophthalic acid and terephthalic acid would enhance the UV radiation resistance. However, it cannot be determined whether the same adhesion and solvent resistance properties as achieved by isophthalic acid and terephthalic acid can also be achieved by HHPA. This will be experimentally determined.

In this regard, the formulation shown in Table 5.1 was designed and can be proposed.

**Table 5.1 Proposed formulation for a coil coating polyester resin with enhanced resistance to UV radiation**

Raw Material	Molecular weight	Equivalent weight	Charged weight (g)	Moles	Equivalents hydroxyl ( $e_{OH}$ )	Equivalents acid ( $e_{COOH}$ )	Theoretical weight of liberated water (g)
Adipic Acid	146	73	287.76	1.97	-----	3.943	70.979
HHPA	154.16	77.08	513.59	3.33	-----	6.663	59.967
1,4 cyclohexane dicarboxylic acid	172	86	179.58	1.04	-----	2.088	37.586
1,4 cyclohexane-dimethanol	144	72	89.79	0.62	1.247	-----	-----
Neopentyl glycol	104	52	464.92	4.47	8.941	-----	-----
1,6 Hexandiol	118	59	133.96	1.14	2.271	-----	-----
HPN	204.26	102.13	126.06	0.62	1.234	-----	-----
Sum total			1795.76	13.19	13.693	12.694	168.532

The formulation shown in Table 5.1 was theoretically evaluated according to the method mentioned in Section 2.2 and the following were determined.

Hydroxyl excess ( $e_{OH} / e_{COOH}$ ) = 1.079, Hydroxyl value = 34.42 mgKOH/g,

Yield at acid value 0 = 1627 g, Yield at acid value 10 = 1632 g, Molecular weight at acid value 10 = 2065 g/mol, Average functionality (F) = 1.9243, Degree of reaction at gel point ( $P_{gel}$ ) = 1.0393

In comparison to the novel and standalone coil coating polyester system developed, the same contents of 1,6 hexanediol and adipic acid were included in the proposed formulation. This was done to maintain the same level of flexibility. The content of neopentyl glycol was also maintained. No labile  $\beta$  hydrogens are present in the molecules of neopentyl glycol, 1,6 hexanediol and adipic acid. Isophthalic acid and terephthalic acid were replaced by HHPA and 1,4 cyclohexanedicarboxylic acid. This was done to obtain a polyester resin without the unsaturated aromatic rings in its backbone. The content of 1,4 cyclohexanedimethanol was reduced from 1.25 moles to 0.62 moles. To compensate, 0.62 moles of HPN was included. The reduction of the content of 1,4 cyclohexanedimethanol was due to the presence of labile  $\beta$  hydrogens in its molecule. The proposed formulation was designed to have the same theoretical characteristics as the new product developed throughout the course of the project. The characteristics concerned included hydroxyl excess, hydroxyl value and molecular weight. In the future, the formulation shown in Table 5.1 will be synthesised, characterised by the techniques mentioned in Section 1.8 and its coil top coating film properties will be evaluated. The mechanical properties and the chemical resistance of the resulting coil coating film will be evaluated according to the procedures described in Section 2.5.1. Resistance to UV radiation and exterior durability of the coil top coating film will be evaluated according to the ECCA-T10 test method. Similar to the test methods described in Section 2.5.1, the method for the test of ECCA-T10 has been defined by the European Coil Coating Association. ECCA-T10 is an accelerated weathering test. For this test, coil coated specimens are exposed in a cyclic manner to elements of natural weathering. That is to say light, temperature and water. A particular chamber simulates the weathering conditions mentioned. The chamber concerned is equipped with facilities to provide temperature and humidity. To simulate and accelerate exterior light, UV lamps with specified radiation characteristics are fitted into this chamber.

After the test cycle ends, the loss of gloss and colour changes of the specimen are measured instrumentally and reported as the test result. Limits for the changes in the coating parameters mentioned are often defined by the coil top coating customers. In general, the loss of gloss and discoloration should not be more than 50%.

The formulation proposed in Table 5.1 will probably be a starting point. Its value will depend on the suitability of its glass transition temperature, its performance in terms of meeting the coating film properties specified in Section 2.5.2 as well as its resistance to the accelerated weathering test. If modification towards better properties was needed, changes will be made to the proposed formulation. Further synthesis will be carried out and the products obtained will be characterised by the analytical techniques employed throughout the course of this study. The technical knowledge and experience achieved will also be employed. Based on the capability achieved in terms of the design, synthesis and characterisation of such polymeric binder systems, it is envisaged that a novel and standalone coil top coating saturated polyester resin with excellent flexibility, adequate adhesion, suitable glass transition temperature, sufficient solvent resistance and exceptional exterior durability will be developed in the future.

## REFERENCES

- 1- Husbands, M.J, Standen C.J.S, and Hayward G. *A MANUAL FOR RESINS FOR SURFACE COATINGS VOLUME III*. Second Edition. London, England: SITA Technology Ltd, 1987. 63-68
- 2- Deligny, P, Polyester Resins. *In: P.K.T Oldring (ed.), RESINS OF SURFACE COATINGS VOLUME II Alkyds & Polyesters*. Second Edition. Exeter, UK, John Wiley and Sons Ltd in Association with SITA Technology Ltd, 2000. 119-123
- 3- Goldshmidt, A. and Streitberger H.J.. *BASF HANDBOOK ON Basics of Coating Technology*. Hannover, Germany, Primedia, 2003. 66-70
- 4- Fisher L.A and Hayward G.R. *The Basics of Resin Technology*. [Online]. Oil and Color Chemists' Association.1998. Available from:  
[http://www.occa.org.uk/site/downloads/Mono\\_10.pdf?session=lgmMdl:921CDFA19339107B7EA3C5C002AAD952](http://www.occa.org.uk/site/downloads/Mono_10.pdf?session=lgmMdl:921CDFA19339107B7EA3C5C002AAD952) [Accessed: 08/01/2007]
- 5- Husbands, M.J, C.J.S Standen and Hayward G. *A MANUAL FOR RESINS FOR SURFACE COATINGS VOLUME III*. Second Edition. London, England, SITA Technology Ltd, 1987. p.81
- 6- Malanowski P, Huijser S, Scaltro F, van Benthem R.A.T.M, van der Ven L.G.J, Laven J, and de With G. Molecular mechanism of photolysis and photo oxidation of poly (neopentyl isophthalate). *Polymer*, 2009, **50** , 1358-1368
- 7- Johansson K, and Johansson M. A model study on fatty acid methyl esters as reactive diluents in thermally cured coil coating systems. *Progress in Organic Coatings*, 2006, **55** , 382-387
- 8- Johansson K, and Johansson M. The effect of fatty acid methyl esters on the curing performance and final properties of thermally cured solvent-borne coil coatings. *Progress in Organic Coatings*, 2007, **59** , 146-151
- 9- Oldring, P.K.T, Paint Technology-Some Important Factors. *In: P.K.T Oldring (ed.), RESINS OF SURFACE COATINGS VOLUME II Alkyds & Polyesters*. Second Edition. Exeter, UK: John Wiley and Sons Ltd in Association with SITA Technology Ltd, 2000. p.13
- 10-Goldshmidt, A. and Streitberger H.J. *BASF HANDBOOK ON Basics of Coating Technology*. Hannover, Germany, Primedia, 2003. p.723



- 11-Genevay, J P. The European coil coatings market. *European Coatings JOURNAL*, 09.2008, H1571, p.18
- 12-Rossi S, Deflorian F, and Fiorenza J. Environmental influences on the abrasion resistance of a coil coating system. *Surface Coatings & Technology*, 2007, **201**, 7416-7424
- 13-Souto R.M, Llorente M.L, and Fernandez-Mérida L. Accelerated tests for the evaluation of the corrosion performance of coil-coated steel sheet: EIS under cathodic polarisation. *Progress in Organic Coatings*, 2005, **53**, 71-76
- 14-Goldshmidt, A. and Streitberger H.J.. *BASF HANDBOOK ON Basics of Coating Technology*. Hannover, Germany, Primedia, 2003. pp. 724-727
- 15-European Coil Coating Association, *www.eccacoil.com*, [Online]. European Coil Coating Association. 2007. Available from: <http://www.eccacoil.com/education.asp> [Accessed 08/01/2007]
- 16-R. Drufer, *Article- Coil Coating Part II -The Process*, [Online]. SpecialChem S.A. 2007. Available from : <http://www.specialchem4coatings.com/resources/articles/article.aspx?id=2869> [ Accessed 05/01/2007]
- 17-Becker Industrial Coatings, *Coil Coating Process*, [Online]. Becker Industrial Coatings. 2007. Available from : <http://www.beckers-bic.com/BIC/bicweb.nsf/key/CoilCoatingProcess> [Accessed 05/01/2007]
- 18-Johansson K, and Johansson M. Fatty acid methyl ester as reactive diluents in thermally cured solvent-borne coil coatings-the effect of fatty acid pattern on the curing performance and final properties. *Progress in Organic Coatings*, 2008, **63**, 155-159
- 19- Vayeda R, and Wang J. Adhesion of coatings to sheet metal under plastic deformation. *International Journal of Adhesion & Adhesives*, 2007, **27**, 480-492
- 20-Deflorian F, Fedrizzi L, and Rossi S. Effects of mechanical deformation on the protection properties of coil coating products. *Corrosion Science*, 2000, **42**, 1283-1301
- 21-Jerome C, and Lectome P. Recent advances in the synthesis of aliphatic polyesters by ring-opening polymerisation. *Advanced Drug Delivery Reviews*, 2008, **60**, 1056-1076

- 22- Vahteristo K, Laari A, Haario H, and Solonen A. Estimation of kinetic parameters in neopentyl glycol esterification with propionic acid. *Chemical Engineering Science*, 2008, **63**, 587-598
- 23- Wang D.H, Cheng S.Z.D, and Harris F.W. Synthesis and characterisation of aromatic polyesters containing multiple n-alkyl side chains. *Polymer*, 2008, **49**, 3020-3028
- 24- Husbands, M.J, Standen C.J.S, and Hayward G. *A MANUAL FOR RESINS OF SURFACE COATINGS VOLUME III*. Second Edition. London, England, SITA Technology Ltd, 1987. 67-68
- 25- Deligny, P, Polyester Resins. In: P.K.T Oldring (ed.), *RESINS OF SURFACE COATINGS VOLUME II Alkyds & Polyesters*. Second Edition. Exeter, UK, John Wiley and Sons Ltd in Association with SITA Technology Ltd, 2000.143-145
- 26- Castle, R, Standen C, and Hayward G, An Introduction to Polymer Science. In: P.K.T Oldring, and G. Hayward (eds.), *A MANUAL FOR RESINS FOR SURFACE COATINGS VOLUME I*. Second Edition. London, UK, SITA Technology Ltd, 1987.32-33
- 27- Umare S.S, Chandure A.S, and Pandey R.A. Synthesis, characterization and biodegradable studies of 1,3-propanediol based polyesters. *Polymer Degradation and Stability*, 2007, **92**, 464-479
- 28- Tang J, Zhang Z, Song Z, Chen L, Hou X, and Yao K. Synthesis and characterization of elastic aliphatic polyesters from sebacic acid, glycol and glycerol. *European Polymer Journal*, 2006, **42**, 3360-3366
- 29- Boyes S.G, Chaplin R.P, Davis T.P, Viatos J, and Buxton D.P. Direct esterification of a hydroxyl functional polyester resin with *p*-hydroxybenzoic acid Part A: investigation of the direct esterification reaction scheme and characterisation of products . *Progress in Organic Coatings*, 2000, **39**, 137-143
- 30- Soni R.K., Soam S, and Dutt K. Studies on biodegradability of copolymers of lactic acid, terephthalic acid and ethylene glycol. *Polymer Degradation and Stability*, 2009, **94**, 432-437
- 31- Wang L, Xie Z, Bi X, Wang X, Zhang A, Chen Z, Zhou J, and Feng Z. Preparation and characterization of aliphatic/aromatic copolyesters based on 1,4-cyclohexanedicarboxylic acid. *Polymer Degradation and Stability*, 2006, **91**, 2220-2228
- 32- Goldshmidt, A. and Streitberger H.J.. *BASF HANDBOOK ON Basics of Coating Technology*. Hannover, Germany, Primedia, 2003. 66-70

- 33-Pilati, F, Tosselli M, and Messori M. Principles of Step Polymerisation. *In: D. Sanders (ed.), WATERBORNE AND SOLVENT BASED SATURATED POLYESTERS AND THEIR END USER APPLICATIONS*. London, UK, John Wiley and Sons Ltd in association with SITA Technology Ltd, 1999.15-16
- 34- *Organic Chemistry Portal- Fischer Esterification*, [Online]. 2008. Available from : <http://www.organic-chemistry.org/namedreactions/fischer-esterification.shtm>  
[ Accessed 04/01/2008]
- 35-Husbands, M.J, Standen C.J.S, and Hayward G. *A MANUAL FOR RESINS OF SURFACE COATINGS VOLUME III*. Second Edition. London, England, SITA Technology Ltd, 1987. pp. 153-155
- 36-Tsai C.J. Chang W.C, Chen C.H, Lu H.Y, and Chen M. Synthesis and characterisation of polyesters derived from succinic acid, ethylene glycol and 1,3-propanediol. *European Polymer Journal*, 2008, **44**, 2339-2347
- 37-Ferré T, Franco L, Rodriguez-Galan A, and Puiggali J. Poly(ester amide)s derived from 1,4-butanediol, adipic acid and 6-aminohexanoic acid. Part II: composition changes and fillers. *Polymer*, 2003, **44**, 6139-6152
- 38-Husbands, M.J, Standen C.J.S, and Hayward G. *A MANUAL FOR RESINS OF SURFACE COATINGS VOLUME III*. Second Edition. London, England, SITA Technology Ltd, 1987. p.114
- 39-Pang K, Kotek R, and Tonelli A. Review of conventional and novel polymerization processes for polyesters. *Progress in Polymer Science*, 2006, **31**, 1009-1037
- 40-Pilati, F, Tosselli M, and Messori M. Principles of Step Polymerisation. *In: D. Sanders (ed.), WATERBORNE AND SOLVENT BASED SATURATED POLYESTERS AND THEIR END USER APPLICATIONS*. London, UK, John Wiley and Sons Ltd in association with SITA Technology Ltd, 1999. 6-7
- 41-McKee M.G, Unal S, Wilkes G.L, and Long T.E. Branched polyesters: recent advances in synthesis and performance. *Progress in Polymer Science*, 2005, **30**, 507-539
- 42-Pilati, F, Tosselli M, and Messori M. Principles of Step Polymerisation. *In: D. Sanders (ed.), WATERBORNE AND SOLVENT BASED SATURATED POLYESTERS AND THEIR END USER APPLICATIONS*. London, UK, John Wiley and Sons Ltd in association with SITA Technology Ltd, 1999. 7-8

- 43-Husbands, M.J, Standen C.J.S, and Hayward G. *A MANUAL FOR RESINS OF SURFACE COATINGS VOLUME III*. Second Edition. London, England, SITA Technology Ltd, 1987. 84-86
- 44-Deligny, P, Polyester Resins. In: P.K.T Oldring (ed.), *RESINS OF SURFACE COATINGS VOLUME II Alkyds & Polyesters*. Second Edition. Exeter, UK, John Wiley and Sons Ltd in Association with SITA Technology Ltd, 2000.128-138
- 45-ICIS Chemical Business, *Chemical profile: neopentyl glycol*, [Online]. ICIS Chemical Business. 2006. Available from :  
<http://icischemicalbusiness.com> [Accessed 02/10/2006]
- 46-Grayson, M. and Eckroth D. (eds), *KIRK-OTHMER ENCYCLOPEDIA OF CHEMICAL TECHNOLOGY VOLUME 11*. Third Edition. USA, John Wiley and Sons Inc, 1980. pp. 964-965.
- 47- Weisskopf K. Characterisation of poly(ethylene terephthalate) by gel permeation chromatography. *Journal of Applied Polymer Science*, 1990, **39**, 2141-52
- 48-Yoon K.H, Min B.G, and Park O.O. Effect of multifunctional comonomers on the properties of poly(ethylene terephthalate) copolymers. *Polymer International*, 2002, **51**, 134-9
- 49-Mehdipour-Ataie, S. Soluble, thermally stable poly(ester amide)s derived from terephthalic acid(biscarboxydiphenyl methyl) ester and different diamines. *EUROPEAN POLYMER JOURNAL*, 2005, **41**, 65-71
- 50- Liu C, Qian Z.Y, Gu Y.C, Fan L.Y, Li J, Chao G.T, Jia W.J, and Tu M.J. Synthesis, characterisation, and thermal properties of biodegradable aliphatic copolyester based on  $\epsilon$ -caprolactone, adipic acid, and 1,6 hexanediol. *materials letters*, 2006, **31**, 31-38
- 51- Gesti S, Almontassir A, Casas M.T, and Puiggali J. Molecular packing and crystalline morphologies of biodegradable poly(alkylene dicarboxylate)s derived from 1,6 hexanediol. *polymer*, 2004, **45**, 8845-8861
- 52-Tsai Y, Jheng L.C, and Hung C.Y. Synthesis, properties and enzymatic hydrolysis of biodegradable alicyclic/ aliphatic copolyesters based on 1,3/1,4-cyclohexanedimethanol. *Polymer Degradation and Stability*, 2010, **95**, 72-78
- 53-Sulatha M.S, Purushotham S, and Natarajan U. RMMC simulations of the chain properties of polyester homopolymers from 1,4-cyclohexanedimethanol and 2,2,4,4-tetramethyl-1,3-cyclobutanediol. *polymer*, 2002, **43**, 6295-6305

- 54-Ni H, Dauma J.L, Thiltgen P.R, Soucek M.D, Simonsick W.J, Zhong W, and Skaja A.D. Cycloaliphatic polyester-based high-solids polyurethane coatings II. The effect of difunctional acid. *Progress in Organic Coatings*, 2002, **45**, 49-58
- 55-Eastman Chemical Company, *Eastman CHDM-D Glycol (1,4-Cyclohexanedimethanol)*, [Online]. Eastman Chemical Company. 2007. Available from :  
<http://www.eastman.com/products/producthome.asp?product=71001802&SelectorUrl=%2fProducts%2fproductSelector.htm&ListPath=%2fProducts%2fProductList.htm&sSelectorType=Generic&sCategoryName=&sKeyword=CHDM-D>  
[Accessed 19/01/2007]
- 56-Awasthi S and Agrawal D. Ring-shaped. *European Coatings Journal*, 2008, **02**, 44-48
- 57-Grayson, M. and Eckroth D. (eds), *KIRK-OTHMER ENCYCLOPEDIA OF CHEMICAL TECHNOLOGY VOLUME 11*. Third Edition. USA: John Wiley and Sons Inc, 1980. p.935
- 58-Grayson, op.cit. 946-948
- 59-Danick C. Improving flexibility and impact resistance. *FOCUS ON POWDER COATINGS*, January 2005, 4-5
- 60- Lozano M, Franco L, Rodriguez-Galan A, and Puiggali J. Poly (ester amides)s derived from 1,4-butanediol, adipic acid and 6-aminohexanoic acid Part III : substitution of adipic acid units by terephthalic acid units. *Polymer Degradation and Stability*, 2004, **85**, 595-604
- 61-Muller R.J, Keeberg I, and Deckwer WD, Biodegradation of polyesters containing aromatic constituents. *Journal of Biotechnology*, 2000, 342-346
- 62-Grayson, M. and Eckroth D. (eds), *KIRK-OTHMER ENCYCLOPEDIA OF CHEMICAL TECHNOLOGY VOLUME 11*. Third Edition. USA, John Wiley and Sons Inc, 1980. pp. 758-761.
- 63-Eastman Chemical Company, *Eastman 1,4-CHDA-HP (1,4-Cyclohexanedicarboxylic Acid), High Purity*, [Online]. Eastman Chemical Company. 2007. Available from :  
<http://www.eastman.com/Products/Producthome.htm?product=71001166>  
[Accessed 19/01/2007]
- 64-Heidt P.C, and Elliot M.L. Aliphatic dibasic acid-modified polyesters for thermoset industrial coatings, in : *Proceedings of the Waterborne, High Solids, and Powder Coatings Symposium*, New Orleans, LA, February 1995

- 65-Deligny, P, Polyester Resins. In: P.K.T Oldring (ed.), *RESINS OF SURFACE COATINGS VOLUME II Alkyds & Polyesters*. Second Edition. Exeter, UK, John Wiley and Sons Ltd in Association with SITA Technology Ltd, 2000. p.44
- 66-Oldring, P.K.T, and Tuck N, *RESINS OF SURFACE COATINGS VOLUME III Polyurethanes, Polyamides, Phenoplasts, Aminoplasts, Maleic Resins*. Second Edition. Exeter, UK, John Wiley and Sons Ltd in Association with SITA Technology Ltd, 2001.134-135
- 67-Grayson, M. and Eckroth D. (eds), *KIRK-OTHMER ENCYCLOPEDIA OF CHEMICAL TECHNOLOGY VOLUME 7*. Third Edition. USA: John Wiley and Sons Inc, 1979. 768-772.
- 68-Husbands, M.J, Standen C.J.S, and Hayward G. *A MANUAL FOR RESINS OF SURFACE COATINGS VOLUME III*. Second Edition. London, England, SITA Technology Ltd, 1987. 99-101
- 69-Oldring, P.K.T, and Tuck N, *RESINS OF SURFACE COATINGS VOLUME III Polyurethanes, Polyamides, Phenoplasts, Aminoplasts, Maleic Resins*. Second Edition. Exeter, UK, John Wiley and Sons Ltd in Association with SITA Technology Ltd, 2001. 285-287
- 70-Oldring, op.cit.. 267-268
- 71-Perou A.L, and Vergnaud J.M. Correlation between the State of Cure of a Coil Coating and its Resistance to Liquids. *Polymer Testing*, 1997, **16**, 19-31
- 72-Differential scanning calorimetry-Wikipedia, the free encyclopedia [online].2009 [Accessed 09/07/2009]. Available from:  
[http://en.wikipedia.org/wiki/Differential\\_scanning\\_calorimetry](http://en.wikipedia.org/wiki/Differential_scanning_calorimetry)
- 73-Höhne,G.W.H, Hemminger W.F, and Flammersheim H.J. *Differential Scanning Calorimetry*. Second Edition. Berlin, Germany, Springer, 2003.1-8
- 74-anasys: introduction to DTA & DSC (1) [online], 2009 Available from:  
<http://www.anasys.co.uk/library/dsc1.htm> [Accessed 16/07/2009]
- 75- Höhne,G.W.H, Hemminger W.F, and Flammersheim H.J. *Differential Scanning Calorimetry*. Second Edition. Berlin, Germany, Springer, 2003. 203-205
- 76-Höhne,op.cit.116-118

- 77-Stoye,D, Freitag W, and Beuschel D (eds), *Resins for Coatings: Chemistry, Properties and Applications*. Cincinnati, Ohio, USA, Hanser Gardner Publications, 1996. p.47
- 78- Deligny, P, Polyester Resins. *In: P.K.T Oldring (ed.), RESINS OF SURFACE COATINGS VOLUME II Alkyds & Polyesters*. Second Edition. Exeter, UK, John Wiley and Sons Ltd in Association with SITA Technology Ltd, 2000. p.141
- 79-Pilati, F, Tosselli M, and Messori M, Polyester Design Considerations. *In: D. Sanders (ed.), WATERBORNE AND SOLVENT BASED SATURATED POLYESTERS AND THEIR END USER APPLICATIONS*. London, UK, John Wiley and Sons Ltd in association with SITA Technology Ltd, 1999. p.78
- 80-Pilati, F, Tosselli M, and Messori M, Principles of Step Polymerisation. *In: D. Sanders (ed.), WATERBORNE AND SOLVENT BASED SATURATED POLYESTERS AND THEIR END USER APPLICATIONS*. London, UK, John Wiley and Sons Ltd in association with SITA Technology Ltd, 1999. p.27
- 81-Number average molecular weight-Wikipedia the free encyclopedia, [Online]. 2007. Available from : [http://en.wikipedia.org/wiki/Number\\_average\\_molecular\\_weight](http://en.wikipedia.org/wiki/Number_average_molecular_weight) [ Accessed 21/09/2007]
- 82-How-to Guides - Polymers , [Online]. 2007. Available from : <http://www.waters.com/watersdivision/ContentD.asp?watersit=JDRS-5LTGJR&WT.svl=1> [ Accessed 28/10/2007]
- 83-Missouri University of Science and Technology. *Definitions of Molecular weight*, [Online]. 1995. Available from : <http://web.mst.edu/~WLF/MW/definitions.html> [ Accessed 07/03/2008]
- 84-Weight average molecular weight-Wikipedia the free encyclopedia, [Online]. 2007. Available from : [http://en.wikipedia.org/wiki/Weight\\_average\\_molecular\\_weight](http://en.wikipedia.org/wiki/Weight_average_molecular_weight) [ Accessed 21/09/2007]
- 85-Poydispersity index-Wikipedia the free encyclopedia, [Online]. 2007. Available from : <http://en.wikipedia.org/wiki/Polydispersity> [ Accessed 21/09/2007]
- 86-Defintion of polydisperse - Chemistry Dictionary, [Online]. 2005. Available from : <http://www.chemicool.com/definition/polydisperse> [ Accessed 21/09/2007]
- 87-Size exclusion chromatography - Wikipedia, the free encyclopedia , [Online]. 2008. Available from : [http://en.wikipedia.org/wiki/Gel\\_permeation\\_chromatography#Theory\\_and\\_method](http://en.wikipedia.org/wiki/Gel_permeation_chromatography#Theory_and_method) [Accessed 06/01/2008]
- 88-Viscotek - Separation Theory for the determination of Molecular Weight under Gel Permeation Chromatography, [Online]. 2008. Available from : <http://www.viscotek.com/the-gpc-sep.aspx> [Accessed 08/02/2008]

- 89-Viscotek - *Theory for the determination of Molecular Weight using Gel Permeation Chromatography and Dynamic Light Scattering*, [Online]. 2008. Available from : <http://www.viscotek.com/theory.aspx> [Accessed 08/02/2008]
- 90-University of Colorado, Boulder, Department of Chemistry And Biochemistry, *IR Theory* [Online], 2009, Available from: <http://orgchem.colorado.edu/hndbksupport/irtutor/IRtheory.pdf> [Accessed: 13/07/2009]
- 91-*Infrared spectroscopy - Wikipedia, the free encyclopedia* , [Online]. 2009. Available from : [http://en.wikipedia.org/wiki/Infrared\\_spectroscopy](http://en.wikipedia.org/wiki/Infrared_spectroscopy) [Accessed 09/07/2009]
- 92-Pavia, D.L, Lampan G.M and Kriz G.S. *Introduction To Spectroscopy, A Guide for Students of Organic Chemistry*, Second Edition. Washington, Saunders College, 1996,17-23
- 93-*Infrared Spectroscopy*, [Online]. 2009. Available from : <http://www.cem.msu.edu/~reusch/VirtualText/Spectrpy/InfraRed/infrared.htm> [Accessed 14/07/2009]
- 94-*NMR spectroscopy - Wikipedia, the free encyclopedia* , [Online]. 2009. Available from : [http://en.wikipedia.org/wiki/Nuclear\\_magnetic\\_resonance\\_spectroscopy](http://en.wikipedia.org/wiki/Nuclear_magnetic_resonance_spectroscopy) [Accessed 14/07/2009]
- 95-Mirau, Peter A. *A Practical Guide to Understanding the NMR of Polymers*. New Jersey, John Wiley and Sons, 2005, 2-31
- 96-Pavia, D.L, Lampan G.M and Kriz G.S. *Introduction To Spectroscopy, A Guide for Students of Organic Chemistry*, Second Edition. Washington, Saunders College, 1996, p.119
- 97-Haase, J, and Kozlov M. *The Nuclear Quantum Dance in Pulsed High Field Magnets — IFW Dresden* [online], 2009. Available from: <http://www.ifw-dresden.de/institutes/imw/sections/22/laboratory-for-pulsed-high-magnetic-fields/nmr> [Accessed 14/07/2009]
- 98-Mirau, Peter A. *A Practical Guide to Understanding the NMR of Polymers*. New Jersey, John Wiley and Sons, 2005, p.29
- 99-Mirau, op.cit. p.30
- 100-Pavia, D.L, G.M Lampan G.M and Kriz G.S. *Introduction To Spectroscopy, A Guide for Students of Organic Chemistry*, Second Edition. Washington, Saunders College, 1996,137-142



- 101-Pavia, D.L, Lampan G.M and Kriz G.S. *Introduction To Spectroscopy, A Guide for Students of Organic Chemistry*, Second Edition. Washington, Saunders College, 1996,128-130
- 102- Oh S.J, and Kim B.C. Effects of hydroxyl-group end capping and branching on the physical properties of tailored polyethylene terephthalates. *Journal of Polymer Science Part B: Polymer Physics*, 2001, **39**, 1027-35
- 103-Pham,Q.T, Pétiand R, Waton H, and Llauro-Darricades M.F. *Proton and Carbon NMR Spectra of Polymers*. Fifth Edition. London, UK, Hermes Science Publishing Ltd, 2003. p.207
- 104- Pham,op.cit. p.209
- 105-Pham,op.cit. p.208
- 106-Pham,op.cit. p.210
- 107-Boyes S.G, Chaplin R.P, Davis T.P, Viatos J, and Buxton D.P. Direct esterification of a hydroxyl functional polyester resin with *p*-hydroxybenzoic acid Part B: coating preparation and evaluation. *Progress in Organic Coatings*, 2000, **39**, 145-150
- 108- *Uniqema-a world leader in the manufacture of surfactants and oleochemical derivatives*, [Online]. 2007. Available from :  
<http://www.uniqema.com/irj/servlet/prt/portal/prtroot/com.uniqema.portal.ProductDetailsProject.ProductDetailsComponent?productID=010220> [Accessed 06/03/2007]
- 109- International Organization for Standardization. (1974). ISO 3251:1974. *PAINTS,VARNISHES, PLASTICS, BINDERS FOR PAINTS, POLYMER DISPERSIONS AND CONDENSATION RESINS DETERMINATION OF NON-VOLATILE MATTER CONTENT*. Geneva, ISO
- 110- International Organization for Standardization. (1996). ISO 3682:1996. *BINDERS FOR PAINTS AND VARNISHES, DETERMINATION OF ACID VALUE*. Geneva, ISO
- 111- International Organization for Standardization. (1996). ISO 4629:1996. *BINDERS FOR PAINTS AND VARNISHES, DETERMINATION OF HYDROXYL VALUE*. Geneva, ISO
- 112- International Organization for Standardization. (1974). ISO 2811:1974. *PAINTS VARNISHES AND RELATED PRODUCTS, DETERMINATION OF DENSITY*. Geneva, ISO

- 113- Husbands, M.J, Standen C.J.S, and Hayward G. *A MANUAL FOR RESINS FOR SURFACE COATINGS VOLUME III*. Second Edition. London, England, SITA Technology Ltd, 1987.109-114
- 114- Goldshmidt, A. and Streitberger H.J. *BASF HANDBOOK ON Basics of Coating Technology*. Hannover, Germany, Primedia, 2003. p.52
- 115- Goldshmidt, op.cit.134-137
- 116- Santos D, Costa M.R, and Santos M.T. Performance of polyester and modified polyester coil coatings exposed in different environments with high UV radiation. *Progress in Organic Coatings*, 2007, **58**, 296-302
- 117- Becarria D, Capra A, Bejko I and Carlevaris L. Novel binders for powder coil coating. *FOCUS ON POWDER COATINGS*, June 2007, 2-3
- 118- European Coil Coating Association. (1996). ECCA-T7, 1996. *RESISTANCE TO CRACKING ON BENDING*. Brussels, ECCA.
- 119- European Coil Coating Association. (1999). ECCA-T11, 1999. *M.E.K. SOLVENT RUBBING TEST*. Brussels, ECCA.
- 120- European Coil Coating Association. (1995). ECCA-T5, 1995. *RESISTANCE TO RAPID DEFORMATION*. Brussels, ECCA.
- 121- European Coil Coating Association. (1996). ECCA-T8, 1996. *RESISTANCE TO SALT SPRAY FOG*. Brussels, ECCA
- 122- Goldshmidt, A. and Streitberger H.J. *BASF HANDBOOK ON Basics of Coating Technology*. Hannover, Germany, Primedia, 2003.400-402
- 123- International Organization for Standardization. (2006). ISO 1522:2006. *PAINTS VARNISHES-PENDULUM DAMPING TEST*. Geneva, ISO
- 124- Teknos Oy, [Online].2005. Available from: <http://www.teknos.fi>  
[Accessed: 03/11/2006]
- 125- DSM Coating Resins, [Online].2007. Available from :  
[http://technicaldocuments.dsm.com/dsmDR/DocumentFinder/dcr/relatedDocuments.do?action=getDocFinderRelatedDocumentList&product\\_id=8KEFRuBfkMzsfJXbOu4RjF4Migo6BuTS&activation\\_date=10w%2F1LjnO6oHCeBYryfDePb98XSHF0Qh](http://technicaldocuments.dsm.com/dsmDR/DocumentFinder/dcr/relatedDocuments.do?action=getDocFinderRelatedDocumentList&product_id=8KEFRuBfkMzsfJXbOu4RjF4Migo6BuTS&activation_date=10w%2F1LjnO6oHCeBYryfDePb98XSHF0Qh)  
[Accessed: 03/11/2006]
- 126- CYTEC Industries, [Online].2007. Available from : [http://www.cytec.com/specialty-chemicals/spec\\_pdfs/Cytec%20Automotive%20OEM\\_12.pdf](http://www.cytec.com/specialty-chemicals/spec_pdfs/Cytec%20Automotive%20OEM_12.pdf)  
[Accessed: 05/11/2006]

- 127- Souto R.M, Gonzalez-Garcia Y, Gonzalez S. Evaluation of the corrosion performance of coil-coated steel sheet as studied by scanning electrochemical microscopy. *Corrosion Science*, 2008, **50**, 1637-1643
- 128- Husbands, M.J, Standen C.J.S and Hayward G. *A MANUAL FOR RESINS FOR SURFACE COATINGS VOLUME III*. Second Edition. London, England, SITA Technology Ltd, 1987. p.28
- 129- Deligny, P, Polyester Resins. In: P.K.T Oldring (ed.), *RESINS OF SURFACE COATINGS VOLUME II Alkyds & Polyesters*. Second Edition. Exeter, UK, John Wiley and Sons Ltd in Association with SITA Technology Ltd, 2000. p.163
- 130- Deligny, op.cit. p.162
- 131- Bao C.L, Wang L.S, and Zhang A.Q. Synthesis and properties of waterborne hyperbranched aliphatic polyester clear coats. *Journal of the Taiwan Institute of Chemical Engineers*, 2009, **40**, 174-179
- 132- Mishra A.K, Jena K.K, and Raju K.V.S.N F. Synthesis and characterization of hyperbranched polyester-urethane-urea/ K10-clay hybrid coatings). *Progress in Organic Coatings*, 2009, **64**, 47-56
- 133- Mirau, Peter A. *A Practical Guide to Understanding the NMR of Polymers*. New Jersey, John Wiley and Sons, 2005, p.30
- 134- Pavia, D.L, G.M Lampan and G.S Kriz. *Introduction To Spectroscopy, A Guide for Students of Organic Chemistry*, Second Edition. Washington, Saunders College, 1996, 167-168
- 135- Zagar E, Zigon M, and Podzimek Stepan. Characterization of commercial aliphatic hyperbranched polyesters. *Polymer*, 2006, **47**, 166-175
- 136- Pavia, D.L, Lampan G.M and Kriz G.S. *Introduction To Spectroscopy, A Guide for Students of Organic Chemistry*, Second Edition. Washington, Saunders College, 1996, p.188
- 137- Pavia,op.cit. p.185
- 138-Pham,Q.T, Pétiand R, Waton H, and Llauro-Darricades M.F. *Proton and Carbon NMR Spectra of Polymers*. Fifth Edition. London, UK, Hermes Science Publishing Ltd, 2003. p.194
- 139-Pham,op.cit. p.213

- 140- Pavia, D.L, Lampan G.M and Kriz G.S. *Introduction To Spectroscopy, A Guide for Students of Organic Chemistry*, Second Edition. Washington, Saunders College, 1996, p.130
- 141- Pavia, op.cit. Appendix 2
- 142- Field, L.D, Sternhell S and Kalman J.R. *Organic Structures from Spectra*, Second Edition. Ontario, John Wiley and Sons Canada Ltd, 1995, p.18
- 143- Donovan A.R and Moad G. A novel method for determination of polyester end groups by NMR spectroscopy. *Polymer*, 2005, **46**, 5005-5011
- 144- Zhang J and Hu C.P. Synthesis, characterization and mechanical properties of polyester-based aliphatic polyurethane elastomers containing hyperbranched polyester segments. *European Polymer Journal*, 2008, **44**, 3708-3714
- 145- Pavia, D.L, Lampan G.M and Kriz G.S. *Introduction To Spectroscopy, A Guide for Students of Organic Chemistry*, Second Edition. Washington, Saunders College, 1996, p.149
- 146-Pham,Q.T, Pétiaud R, Waton H, and Llauro-Darricades M.F. *Proton and Carbon NMR Spectra of Polymers*. Fifth Edition. London, UK, Hermes Science Publishing Ltd, 2003. p.187
- 147-Pham,op.cit. p.224
- 148-Pavia, D.L, Lampan G.M and Kriz G.S. *Introduction To Spectroscopy, A Guide for Students of Organic Chemistry*, Second Edition. Washington, Saunders College, 1996,137-142
- 149- Honkhambe P.N, Bhairamadgi N.S, Biyani M.V, Wadgaonkar P.P, and Salunkhe M.M. Synthesis and characterization of new aromatic polyesters containing cardo decahydronaphthalene groups. *European Polymer Journal*, 2010, **46**, 709-718
- 150- Pavia, D.L, Lampan G.M and Kriz G.S. *Introduction To Spectroscopy, A Guide for Students of Organic Chemistry*, Second Edition. Washington, Saunders College, 1996, Appendix 1
- 151- *Infrared Absorption Frequencies* [online].2008. Available from:  
<http://wwwchem.csustan.edu/Tutorials/INFRARED.HTM> [Accessed 25/12/2008]
- 152- Hanson, John. *Infrared Interpretation* [online]. 2008. Available from:  
<http://www2.ups.edu/faculty/hanson/Spectroscopy/IR/IRInterpretation.htm>  
[Accessed 25/12/2008]

- 153- Tang J, Zhang Z, Song Z, Chen L, Hou X and Yao K. Synthesis and characterization of elastic aliphatic polyesters from sebacic acid, glycol and glycerol. *European Polymer Journal*, 2006, **42**, 3360-3366
- 154- Deligny, P, Polyester Resins. In: P.K.T Oldring (ed.), *RESINS OF SURFACE COATINGS VOLUME II Alkyds & Polyesters*. Second Edition. Exeter, UK, John Wiley and Sons Ltd in Association with SITA Technology Ltd, 2000.134-135
- 155- Deligny,op.cit. p.131